Gonçalo Machado Monteiro Ferreira Gonçalves

Licenciado em Ciências da Engenharia Civil

Influence of materials' hygroscopicity in the control of relative humidity and temperature of old buildings

Dissertação para obtenção do Grau de Mestre em
Engenharia Civil – Perfil de Construção

Orientador: Doutor Fernando M. A. Henriques, Professor Catedrático da Faculdade de Ciências e Tecnologia da Universidade Nova de Lisboa

Júri:

Presidente: Professor Doutor Rodrigo M. Gonçalves

Arguente: Professor Doutor Luís G. C. Baltazar

Vogal: Professor Doutor Fernando M. A. Henriques

FACULDADE DE CIÊNCIAS E TECNOLOGIA
UNIVERSIDADE NOVA DE LISBOA

Outubro de 2017

[Influence of materials' hygroscopicity in the control of relative humidity and temperature of old buildings]

Acknowledgments

First of all, I would like to thank to all people in general, who I crossed with in my academic route, and are not mentioned bellow, because, somehow, they helped me to finish this important part of my academic education.

Secondly, I would like to thank to Faculdade de Ciências e Tecnologia and to Nova University of Lisbon (FCT-UNL) for giving me the opportunity to, not only graduate myself and improve my scientific knowledge, but also for allowing me to know many important friends and to experience some remarkable moments.

I would like to thank to *Fraunhofer Institut fur Bauphysic* for making me available a student licence of sotware *Wufi Plus*, that allowed me to make all hygrothermal simulations of the present work and without it I would not have the chance to do it.

I would like to thank to all people who works in Department of Civil Engineer (DEC), from all teachers to all employees that contribute to, every day, increase the good name of the Department and improve the quality of civil engineers of FCT.

I want to thank to my advisor, professor Doctor Fernando Henriques, for have shown to be available to guide me in this last part of the course.

To doctoral researcher Hugo Silva and Engineer Vitor Silva, I would like to truly thank you for having supported me every day and for always shown to be patient and friends. Without you I would not be able to complete this last stage of my graduation.

I have a special thanks to my colleagues and friends, that made this academic route in an unforgettable journey, in special to Rui Ribeiro, João Nobre and Filipe Rodrigues, for have been my closest partners in this long stage of our academic life.

For always supported me, encouraged me to keep focus on my goals and for our special friendship, I would like to deeply thank you, Loubna Kerfah.

I want to thank to all my family, especially to my mother, father and brothers, for allowing me to achieve this important milestone of my life and always motivated me to reach it. To my mother and father, I want to deeply thank you for allowing me to graduate and achieve this outstanding goal, that would be unreachable without your colossal efforts.

Abstract

The comfort of buildings indoor environment and materials durability are severally affected by peaks of temperature and relative humidity (RH) in interior of buildings and therefore they should be controlled and damped.

The presence of people inside buildings as well as artificial illumination and all kind of equipment cause a releasing of moisture to environment, which originates an increment of its relative humidity. The occupants, artificial illumination and equipment also originate a temperature raising depending the occupants' activity and the quantity and power of illumination and equipment.

In order to reach an interior environment with values of relative humidity and temperature that ensure acceptable conditions to human health and materials longevity, it is important to install measures to control them. These measures can be active or passive if, respectively, they intend to remediate the unacceptable values of RH or temperature or if those acceptable values are achieved by installing coating materials capable of control both parameters during all seasons. If the materials are able to control temperature and relative humidity of indoor, so they contribute to improving thermal and hygroscopic inertia of buildings.

Old buildings are characterized by having high thermal inertia and this means that its interior environment has a significant gap in relation to the exterior one, with regard to temperature. However, the temperature also affects relative humidity once both have an inverse relation of proportionality. This makes that it is important to damp relative humidity of old buildings indoor that would not have those values if it did not have high thermal inertia. This fact makes that be important to control relative humidity and temperature of old buildings indoor, preferably using passive measures, to preserve some very important works of art, books or documents, in case of being a museum or an archive.

To control temperature and relative humidity of interior environment it is necessary to choose the best coating materials that can provide to buildings higher hygroscopic and thermal inertia. For that, it is indispensable to make correct materials characterization in order to discover their real behavior and, with base on those characteristics obtained experimentally, they could be properly chosen to be applied in buildings. In consequence of that, in the present dissertation, the materials behavior at different ranges of RH was analyzed as well as the time of exposition to those controlled environments. For that, it was chosen to make the tests of adsorption/desorption isotherm, Moisture Buffering Value (MBV), moisture permeability, thermal conductivity and response time. Additionally, the response of materials to certain interior environment was determined, by making a hygrothermal simulation in transient regime, with recourse to software *Wufi Plus*.

Keywords: Relative humidity, moisture, temperature, hygroscopic inertia, thermal inertia, MBV

Resumo

O conforto do ambiente interior de edifícios e a durabilidade dos materiais podem ser seriamente afectados pelos picos de temperatura e humidade relativa (HR) no interior dos edifícios e, como tal, devem ser controlados e amortecidos.

A presença de pessoas no interior dos edifícios, bem como a iluminação artificial e qualquer tipo de equipamentos, provoca a libertação de vapor de água para o ambiente, que origina o aumento da sua humidade relativa. Os ocupantes, iluminação artificial e os equipamentos também originam o aumento da temperatura, dependendo da actividade das pessoas e da quantidade e potência da iluminação e equipamentos.

De modo a se alcançar condições de ambiente interior com valores de humidade relativa e temperatura que garantam condições aceitáveis para a saúde humana e durabilidade dos materiais, é importante implementar medidas para os controlar. Estas medidas podem ser activas ou passivas se, respectivamente, pretendem remediar valores inaceitáveis de HR ou temperatura ou, se esses valores aceitáveis são alcançados através da instalação de materiais de revestimento capazes de controlar ambos os parâmetros, durante todas as estações do ano. Se os materiais são capazes de controlar a temperatura e humidade relativa do interior, então, eles contribuem para o aumento da inércia térmica e higroscópica dos edifícios.

Os edifícios antigos são caracterizados por terem forte inércia térmica e isso significa que o ambiente interior tem um desfasamento significativo face ao ambiente exterior, no que toca à temperatura. No entanto, a temperatura também afecta a humidade relativa, uma vez que ambos têm uma relação de proporcionalidade inversa. Isto faz com que seja importante amortecer a humidade relativa do interior de edifícios antigos, que não teria esses valores se o edifício não tivesse forte inércia térmica. Este facto faz com que seja importante controlar a humidade relativa e temperatura do interior de edifícios antigos, usando preferencialmente métodos passivos, para preservar algumas obras de arte, livros ou documentos importantes, no caso de se tratar de um museu ou arquivo.

Para controlar a temperatura e humidade relativa do ambiente interior, é necessário escolher os melhores materiais de revestimento, capazes de fornecer ao edifício maior inércia higroscópica e térmica. Para tal, é indispensável realizar-se uma correcta caracterização dos materiais, de forma a descobrir o seu comportamento, o mais real possível, e, com base nessas características obtidas experimentalmente, possam ser devidamente escolhidos para serem aplicados nos edifícios. Como tal, na presente dissertação, foi analisado o comportamento dos materiais em diferentes gamas de humidade relativa, bem como o tempo de exposição dos mesmos nesses ambientes controlados. Assim, foram realizados ensaios de curvas higroscópicas, Moisture Buffering Value (MBV), permeabilidade ao vapor de água, condutibilidade térmica e tempo de reposta. Adicionalmente, foi determinada a resposta dos materiais a um certo ambiente interior, realizando uma simulação higrotérmica, em regime transiente, com recuso ao *software Wufi Plus*.

Palvras-chave: Humidade relativa, humidade, temperatura, inércia higroscópica, inércia térmica, MBV

Contents

List of Figures

List of Tables

List of Acronyms, Materials and Symbols

Symbol	Description	Units
A	Area	m^2
b	Thermal effusivity	$J/(m^2.K.\sqrt{s})$
b_m	Moisture effusivity	$kg/(m^2.Pa.\sqrt{s})$
c_ρ	Specific heat capacity	J/(kg.K)
d	thickness	m
d_H	Active thickness of adsorption	m
$d_{p,1\%}$	Penetration depth	m
D_w	Moisture diffusivity	m^2/s
E_g	Quantity of energy generated	W
E_{in}	Quantity of energy transferred to an element	W
E_{out}	Quantity of energy transferred from an element	W
E_{st}	Stored energy	W
G	Flux of moisture	$kg/(m^2.s)$
g	Moisture flow rate	$kg/(m^2.s)$
$I_{h,d}$	Daily hygroscopic inertia index	$g/(m^3.\%RH)$
MBV	Moisture Buffering Value	$g/(m^2.\%RH)$
m_{dry}	Dry mass	kg
m_w	Mass of water	kg
P_v	Partial pressure of moisture in air	Pa
$P_{v,máx}$	Maximum pressure of moisture in air	Pa
r	Pore's radius	m^3
R	Gases' constant	J/(kg.K)

R^2	Coefficient of determination	-
RH, ϕ	Relative humidity	%
RHS	Relative Humidity Stabilization	-
R_{se}	Exterior surface's thermal resistance	(m².ºC)/W
R_{si}	Interior surface's thermal resistance	(m².ºC)/W
R_T	Thermal resistance	(m².ºC)/W
R_v	Water vapor specific constant	J/(kg.K)
s_d	Equivalent air layer thickness	m
T	Temperature	ºC
t	Time	h
t_p	Time of relative humidity oscillations	h
T_s	Dew point temperature	ºC
TS	Temperature Stabilization	-
u	Moisture content	kg/kg
U	Heat transfer coefficient	W/(m².ºC)
u_h	Critical moisture content	kg/kg
$u_{máx}$	Maximum moisture content	kg/kg
V	Volume	m³
vv	Air velocity	m/s
w	Moisture content	kg/m³
W	Moisture permeance	kg/(m².Pa.s)
w_{cr}	Critical moisture content	kg/m³
w_{sat}	Saturation moisture content	kg/m³
Z	Moisture resistance	(m².s.Pa)/kg
δ	Moisture permeability	kg/(m.s.Pa)
δ_a	Moisture permeability of air	kg/(m.s.Pa)
θ	Contact angle	º
λ	Thermal conductivity	W/(m. ºC)

μ	Moisture resistance factor	-
μ	Damping factor	-
$\boldsymbol{\nu}$	Moisture content in air	kg/m³
$\boldsymbol{\nu}_s$	Saturation limit	kg/m³
ξ	Specific moisture capacity	kg/kg
ρ	Density	kg/m³
ρ_{dry}	Dry density	kg/m³
ρ_w	Water's density	kg/m³
σ	Fluid's surface tension	N/m
ϕ	Delaying factor	-

Acronyms	**Description**
BS	British Standard
DEC	Departamento de Engenharia Civil
EN	European Standard
FCT	Faculdade de Ciências e Tecnologia
HAM	Heat, Air and Moisture
ISO	International Organization for Standardization
JIS	Japanese Industrial Standard
NP	Norma Portuguesa
PAQ	Perceived Air Quality
PD	Percentage of Dissatisfied People
REH	Regulamento do Desempenho Energético dos Edifícios de Habitação
UNL	Universidade Nova de Lisboa

Materials	Description
EA	Finished stucco
M	Recycled cellulose board
N	Projected cellulose coating
NHL	Natural hydraulic lime mortar
O	Wood wool cement board
S	Clayish earth plaster

Chapter 1: Introduction

1.1. Foreword

In the course of the time, buildings tend to be increasingly more waterproof (including the state of water vapor). This is a consequence of using more insulations and walls/floor/ceiling coatings that have almost zero porosity, which do not allow them to adsorb or release any moisture.

The capacity to adsorb moisture makes possible to control interior environment. This behavior of hygroscopic materials allows to control and damp some peaks of relative humidity, adsorbing moisture when RH of interior air is high and releasing moisture when there is lower RH on interior environment.

It is important control the fluctuations of relative humidity and its highest values in order to avoid several problems of occupants and to the building itself. Moisture buffering capacity of coating materials makes possible to control the interior environment and, as consequence, to improve the quality of interior air. The improvement of the quality of air provides better comfort for all occupants and their own health. These coating materials with moisture buffering capacity also extend the materials durability, since they are no longer exposed to extremely high or low relative humidity, which deteriorate them over time.

It is important to choose the best materials to apply as coatings and so to control interior cycles of relative humidity. This capacity to control the relative humidity is known as hygroscopic inertia. In other words, hygroscopic inertia is the resistance of a room or building to change RH. That is, how bigger is hygroscopic inertia, biggest is the resistance of room/building to change a unity of relative humidity. However, not only coatings of walls, floor or ceiling can contribute to improve hygroscopic inertia, once any porous material can adsorb and release moisture. Because of that, it is easy to understand that any textile, book, furniture, carpet, among any other material, since they are porous, contributes to hygroscopic inertia.

1.2. Objectives and scope

The present dissertation belongs to Master in Civil Engineer – Construction Profile of Faculdade de Ciências e Tecnologia – Nova University of Lisbon. The present work looks to characterize the influence of hygroscopicity of coating materials in interior relative humidity (RH) and temperature (T).

First of all, it has to be made a literature review to understand which developments already exist in the area, what set a starting point to be possible to achieve new knowledge.

To better understand the potential of materials to control relative humidity of buildings indoor, it is necessary to know the hygroscopic properties of coating materials. For that, were chosen to make four experimental trials, which perfectly allows to know the hygroscopic behavior of materials. Those tests are Adsorption/Desorption Isotherm, Experiment of classroom, Moisture Permeability and Moisture Buffering Value (MBV).

The choice of materials with good moisture buffering capacity depends how faster they have to respond to fluctuations of relative humidity. In other words, it is important to define the velocity of response that materials have to have to damp and control the RH and temperature inside. Materials with fast adsorption/desorption are good for short cycles of relative humidity changes, as well as materials with slow response are good to long cycles of RH variation. Therefore, was chosen to make a Response Time experimental trial.

To clearly understand the thermal potential of coating materials to control the inside temperature of a building, it was chosen to make a Thermal Conductivity test. However, this test is not the conventional one, since it is made by varying the relative humidity and, as so, the moisture content of samples.

Since experimental trials only allow to know the hygrothermal behavior of a few levels of relative humidity or materials moisture content, it is necessary to know their behavior at any RH or moisture content. Therefore, it is indispensable to propose equations that fit as better as possible to the values of experimental tests and making possible to know the hygrothermal behavior of studied materials at any range of relative humidity or moisture content.

Finally, it is necessary to know how coating materials respond to indoor climate, in transient regime. For that, it was chosen to use *Wufi Plus* software, which is a software that makes hygrothermal analysis of a room in transient regime. For that, after validating the software, the materials used in the present dissertation, as well as its values obtained in experimental trials, were chosen to use as coating of a certain room, to understand the influence they have in control interior temperature and relative humidity.

1.3. Dissertation outline

For better understanding the methodology of the present work and their results, following will be explained in what consists each chapter.

The main divisions are made in seven chapters:

- Chapter 1 is made of a presentation of dissertation, giving a general idea of the studied subjects, as well as its objective and scope;

- Chapter 2 includes a literature review of the previous works, and also includes the essential concepts and physical equations of Heat, Air and Moisture (HAM) behavior of buildings;

- Chapter 3 is a chapter that describes the used materials, as well as all chosen experimental trials;

- Chapter 4 presents the analysis of results of tests made in chapter 3;

- Chapter 5 includes the numerical analysis made for all hygrothermal properties of materials, comparing equations proposed by other works with equations achieved in the present work;

- Chapter 6 contains hygrothermal simulations of a sensivity study with and without some studied materials in the present dissertation, made with software *Wufi Plus*, describing the building's dimensions adopted and the obtained results. In this chapter there also made a verification of MBV obtained experimentally;

- Chapter 7 is the last one, which includes both the main conclusions and proposals to futures works.

All elements located on the present dissertation, that do not have any type of reference, belongs to the archive or were developed by the author.

Chapter 2: Hygrothermal performance of buildings

2.1. Moist air

Water has three different forms in which it can be present in anywhere. Those forms are the liquid one, more known as “water”, vapor form, known as “water vapor” and the solid form, called “ice”. Solid form of water is the one which has the biggest dimensions and vapor form is the one which has the smallest, since each molecule has a diameter of 0.28 nm, approximately. So, this is the reason to why some materials are waterproof, but they are not tight to water vapor. When there is solidification (transition from liquid to solid state), its volume increases, approximately, nine to ten per cent.

Air is composed by water vapor and various other gases, where the main component is Azote (N), followed by Oxygen (O_2) and a small quantity of other gases like Carbon Dioxide (CO_2), Sulfur Dioxide (SO_2), among others, as it can be seen in Figure 2.1.

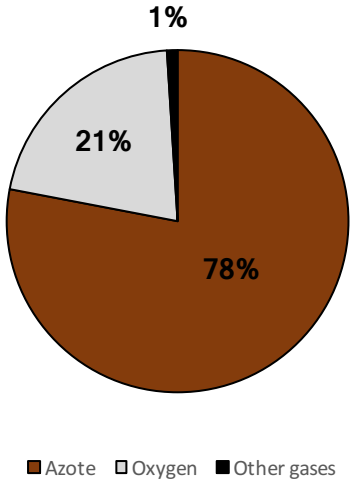

Figure 2.1 – Air constitution

If dry air is assumed as an ideal gas, its partial pressure P_v [Pa] can be represented by the following equation [1]:

$$P_v = R_v * (T + 273{,}15) * \nu \qquad (2\text{-}1)$$

where R_v is the water vapor specific constant [J/(kg.K)] (which takes a constant value of 461,4 J/(kg.K)), T is the air temperature [ºC] and ν is moisture content of the air [kg/m^3].

Partial pressure of moisture in air represents the pressure that moisture would have if it fulfils all the volume occupied by the mass of air that is being analyzed. As it is easy to understand by Equation(2-1), partial pressure of moisture is proportional to temperature and moisture content in air.

The maximum pressure water vapor in air $P_{v,sat}$ [Pa] is achieved when the air becomes saturated and it is exponentially proportional to temperature, as described in Equation(2-2) and Equation(2-3).

$$P_{v,sat} = 610{,}5 * e^{\left(\frac{17{,}269*T}{237{,}3+T}\right)} \quad if\ T > 0\ °C \tag{2-2}$$

$$P_{v,sat} = 610{,}5 * e^{\left(\frac{21{,}875*T}{265{,}5+T}\right)} \quad if\ T \leq 0\ °C \tag{2-3}$$

Both water vapor pressure (partial and saturated) can be related by Equation(2-4), originating Relative Humidity (RH) [%]. When RH is equal to one-hundred per cent it means that the air is saturated and, beyond that point, condensation will start.

$$RH = \frac{P_v}{P_{v,sat}} * 100 = \frac{\nu}{\nu_s} * 100 \tag{2-4}$$

As it possible to see in Equation(2-4), RH can be expressed in terms of moisture content in air ν and saturation limit ν_s [kg/m^3], which represents the maximum moisture concentration allowed in the air, at a certain temperature. The ν_s is calculated by Equation(2-5) and Equation(2-6) [2]:

$$\nu_s = 0{,}6257 * \frac{\left(1{,}098 + \frac{T}{100}\right)^{8{,}02}}{T + 273{,}15} \quad if\ 0°C \leq T \leq 30℃ \tag{2-5}$$

$$\nu_s = 0{,}01016 * \frac{\left(1{,}486 + \frac{T}{100}\right)^{12{,}3}}{T + 273{,}15} \quad if -20℃ \leq T < 0℃ \tag{2-6}$$

The use of a psychrometric diagram is an easy way to correlate partial pressure of water vapor, moisture content in air, temperature and relative humidity (Figure 2.2). This diagram allows to understand the effect of temperature and water vapor concentration (or partial pressure) in RH. The psychrometric diagram allows to see that relative humidity takes lower values with the increasing of temperature, because this increment origin also an increment of saturation limit (as it is easy to understand by Equation(2-5) and Equation(2-6)).

To represent the phenomenon of condensation in terms of temperatures, it was created the concept of dew-point temperature T_s [ºC]. This temperature represents the temperature that, from there beyond, starts condensation, as described by Equation(2-7).

$$T_s = \frac{237{,}3 * (\ln(\phi) + \frac{17{,}269 * T}{237{,}3 + T})}{17{,}269 - (\ln(\phi) + \frac{17{,}269 * T}{237{,}3 + T})} \tag{2-7}$$

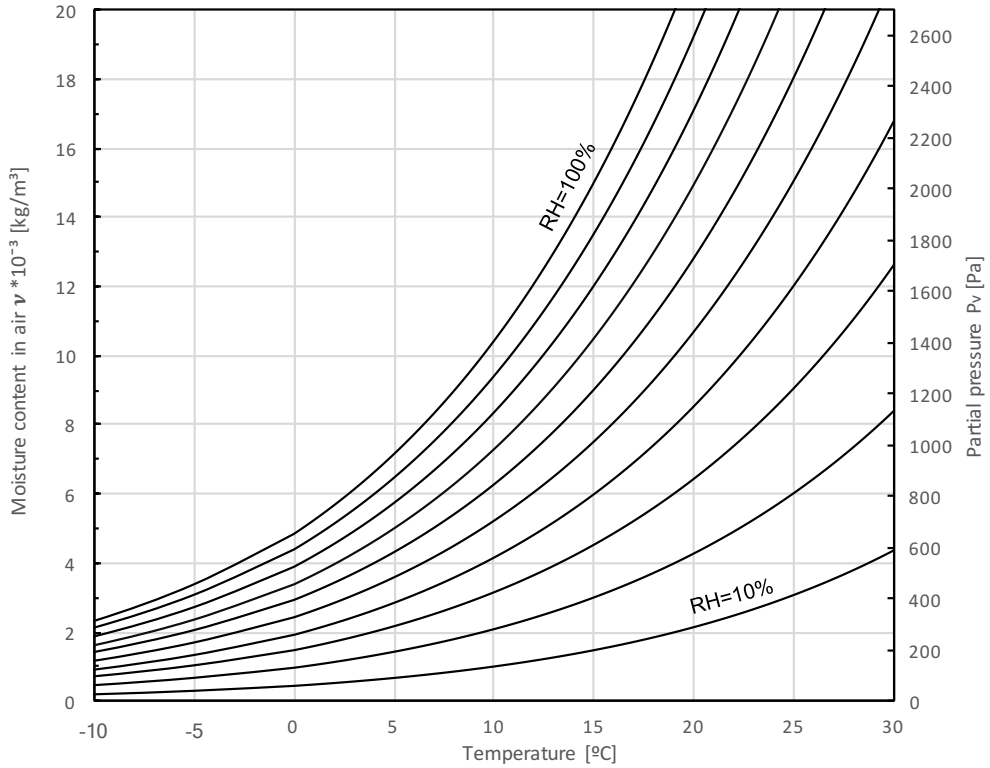

Figure 2.2 – Example of psychrometric diagram

2.2. Hygroscopicity

2.2.1. Moisture transfer

Any material applied in buildings has a certain quantity of moisture, that varies with the moisture content and relative humidity of environment.

Moisture content *u* [kg/kg] of a material is the quantity of water (in any state) m_w [kg] related with the material's dry mass m_{dry} [kg] by the following equation [3]:

$$u = \frac{m_w - m_{dry}}{m_{dry}} \tag{2-8}$$

Moisture content may also be represented as the quantity of water inside a cubic meter of the respective material. This moisture content *w* [kg/m^3] can be achieved by the following two equations:

$$w = \rho_{dry} * u \tag{2-9}$$

where ρ_{dry} is the dry density of material, in kg/m^3.

$$w = \frac{m_w - m_{dry}}{V} \quad (2\text{-}10)$$

where V is the volume of the sample which is being tested, in m^3.

The moisture content of any material can vary between zero and a maximum value, which is particular to each material. The zero value of moisture is, however, impossible to achieve at real cases, being only reached at laboratory domain. Between the zero and maximum moisture content values, there is yet two important values of moisture content, which are the critical moisture content w_{cr} [kg/m^3] and the saturation moisture content w_{sat} [kg/m^3]. The saturation moisture content is the value on which the material is considered full of moisture. However, even when this saturation value is reached at approximately 98% of relative humidity inside the material, there is still some air bubbles which avoid that the material be all filled with water. Therefore, it is considered that it is impossible to achieve values of relative humidity above 98%. Values between 98% and 100% can only be reached with a vacuum process, before material initiate the moisture adsorption process. The critical moisture content is the value that separates the vapor diffusion and the liquid transfer of moisture, that is, it is the value until there is only vapor transfer of moisture and none on liquid form. Therefore, this value beyond, starts interstitial condensation, which is related with pores' radius [1] [4] [5].

The adsorption of moisture is related with pores' radius by Kelvin Law (Equation(2-11)), where it is easy to understand that relative humidity inside pores increases exponentially with the decreasing of pores' radius.

$$RH = e^{\left(-\frac{2*\sigma*\cos(\theta)}{r*\rho_w*R*T}\right)} \quad (2\text{-}11)$$

where σ is the surface tension of the fluid [N/m], θ is the contact angle [º], r is the radius of pores [m], ρ_w is water density [kg/m^3], R is the gases constant [J/(kg.K)] and T is temperature [ºC].

Considering a base case with 20 ºC (which implies a certain value of fluid's surface tension), density of water equals to one thousand kg/m^3 and a contact angle of water of 0 º, therefore, the relation between the pores' radius and the relative humidity inside them is explained by Figure 2.3. This figure has a line that shows at which relative humidity occurs interstitial condensation.

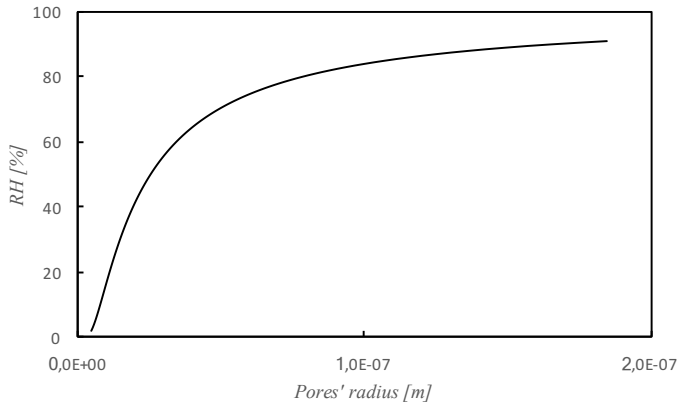

Figure 2.3 – Relation between pores' radius and relative humidity in which occurs interstitial condensation (Kelvin Law)

By Figure 2.3, it is easy to understand that as smaller is the pores' radius, as faster occurs condensation in those pores (at lower relative humidity). In other words, as smaller is the radius of pores, higher are the suction forces exerted by pores and, therefore, faster those material will be saturated.

The adsorption of moisture is divided in different forms, dependent of material's RH. These different forms are shown in Table 2-1

Table 2-1 – Adsorption forms

RH [%]	Adsorption form
0-20	Monomolecular adsorption
20-40	Multi-molecular adsorption
40-98	Condensation

Table 2-1, that is represented by Figure 2.4 [6], shows that condensation begins in pores with the lowest dimensions at 40% of RH [1], but there is no concordance with other authors, who said that the beginning of condensation may be around 50% [7] or even 60% [8] [9] [9] of RH. At low RH (0-20%) the adsorption is made in a single layer of moisture and until begins interstitial condensation, the adsorption is made in multiples layers of moisture. When multi-molecular adsorption happens, the curve is more horizontal than in monomolecular phase in consequence of material starts to be full of water vapor, and then its water vapor permeability decreases. However, when the condensation starts (yet at hygroscopic domain), then the liquid flux begins and consequently the moisture permeability increases. At about 98% of relative humidity begins the capillary domain, when it is considered that the mass transfer only occurs at liquid form and, as so, sorption isotherm becomes almost vertical.

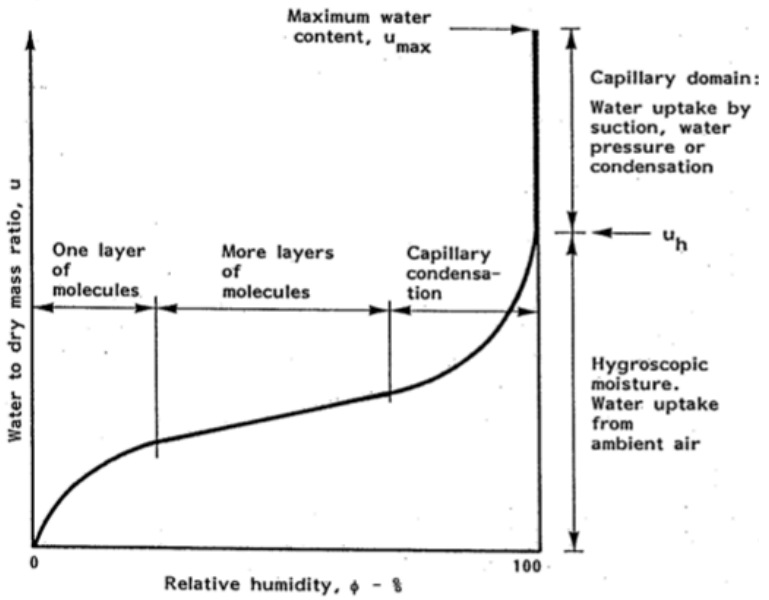

Figure 2.4 – Generical model of a material's sorption isotherm [6]

Where Figure 2.4 has "u_h", is the same value of w_{cr}, explained before. The figure above (Figure 2.4) represents the sorption isotherm most common to construction materials. However, there are many shapes for sorption isotherms, proposed by many authors. Hansen, K. K. [6] presented the most common sorption isotherms (Figure 2.5), after Brunauer, S. *et al.* [10] grouped all sorption isotherms in five different shapes.

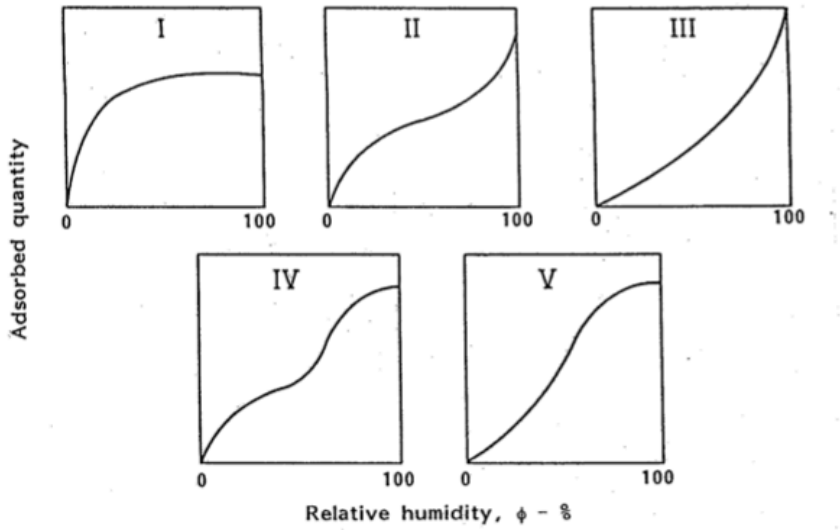

Figure 2.5 – Different shapes of sorption isotherms [6]

The most common porous materials' sorption isotherm follows an "S" shape, represented by the type II curve [6] (Figure 2.5). Lagmuir and BET models are the most known models, however in consequence of some of their limitations, were created new models based on these, that better characterize the adsorption behavior of moisture by porous materials, like models of Lykow or Hansen [5].

Figure 2.4 divided the adsorption process in various phases and domains, which can also be represented by Figure 2.6.

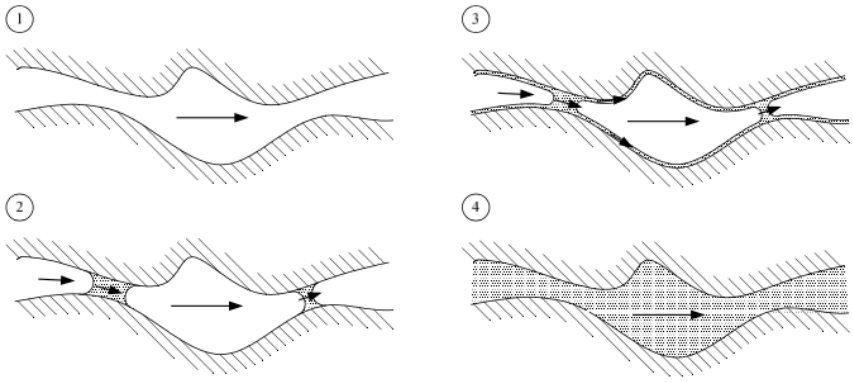

Figure 2.6 - Adsorption phenomenon in their various phases and domains [11]

The phenomenon of adsorption of moisture occurs when partial pressure inside pores is bigger than partial pressure of environment, what makes that moisture be attracted to pore' surfaces. However, when relative humidity of environment is lower than the interstitial one, the moisture tends to leave the pores. This process is called desorption of moisture and it has not a similar behavior to adsorption phenomenon. To this difference between adsorption and desorption isotherm is called hysteresis, which increases with the decreasing of pore radius. The phenomenon of hysteresis is largely majored if materials has ink bottle type pores [12]. These ink bottle type pores are pores which have a higher radius than connection with other pores, that can be observed in Figure 2.7.

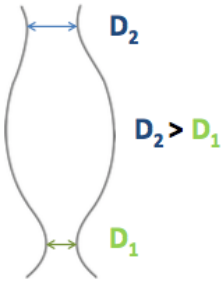

Figure 2.7 – Ink bottle type pores [13]

Ink bottle pores diminish a lot the phenomenon of moisture desorption and originate hysteresis. This happens because the first pore to reach condensation and, as so, a meniscus is the one with D1 diameter of Figure 2.7, and then the same will occur in pore with D2 diameter. However, the interior of ink bottle pores will difficultly be full of moisture, unless the pressure exerted in one of the pore connection is higher than the suction pressure of that pore connection. Those ink bottle pores decrease the desorption process since, if D1 and D2 have different values, some mass transfer will happen between pore with larger radius (D2) to the pore with smaller radius (D1) (Figure 2.8) and, even if there is low pressure to empty larger pores, this pressure may not be low enough to empty the ink bottle pores [14].

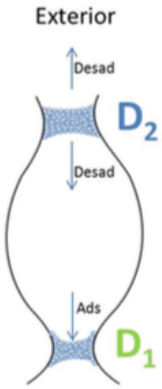

Figure 2.8 – Desorption process in a ink bottle type pore [13]

The phenomenon of hysteresis originates a gap between the adsorption and desorption isotherm (Figure 2.9), what makes that each material has two different isotherms, depending if it is in adsorption or desorption phase. The use of adsorption isotherms of materials without considering the hysteresis phenomenon, leads to an overestimation of buffering capacity of those, and it could underestimate the risk of condensation or mold growth [15]. However, using a mean isotherm between adsorption and desorption' one is a good approximation of the real behavior of materials, if there are not strong variations of boundary conditions [15], as it easy to understand by Figure 2.10.

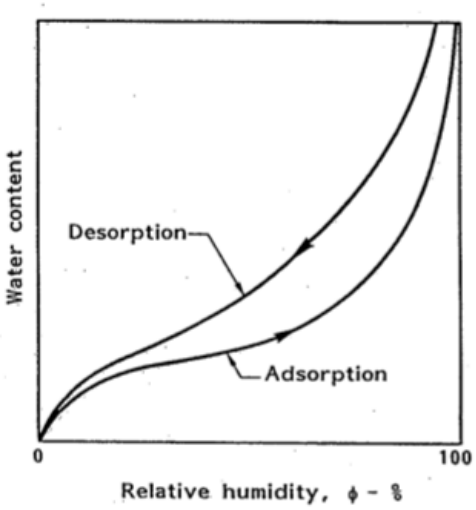

Figure 2.9 – Hysteresis phenomenon [6]

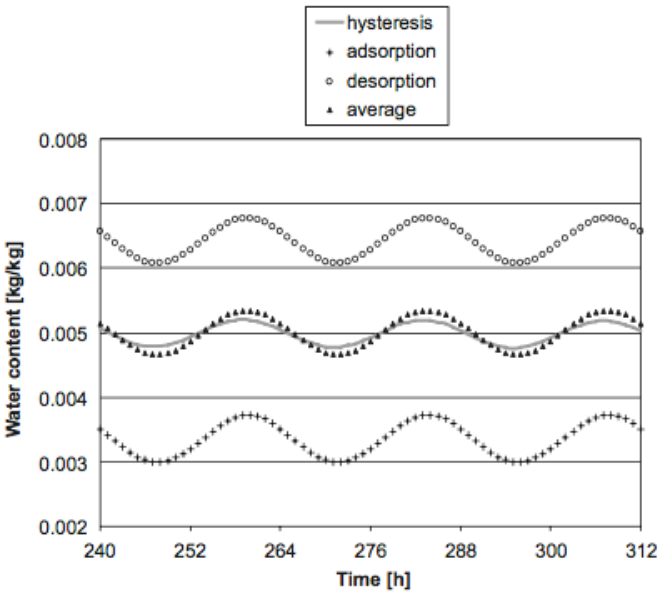

Figure 2.10 – Comparation between mean adsorption/desorption isotherm with hysteresis isotherm [15]

2.2.2. Moisture Permeability

Moisture permeability is the quantity of moisture that a certain material allows to through it when it is subject to some pressure gradients. Moisture diffusion obey to Fick Law (Equation (2-12)), which relates the flux of moisture g [kg/(m^2.s)] with moisture permeability $\boldsymbol{\delta}$ [kg/(m.s.Pa)] and pressure gradient in one direction.

$$g = -\delta * \frac{dP}{dx} \quad (2\text{-}12)$$

Permeability of any material to moisture is directly related with its porosity and pores' radius, since as higher is the porosity, then higher will be its moisture permeability. At the same time, in pores with smaller radius the vapor flux will be reduced, however their interstitial condensation begins at lower relative humidity, then they will have more liquid flux, increasing the global moisture permeability.

The absence of an international standard usually originated very distinguish values of moisture permeability of materials, never producing results within ± 5% of accuracy [16], even if the environment condition would be similar, although the procedure would not be the same, like the air velocity, test's duration, scale's precision, beyond many other conditions. Because of that, latter in time, it was developed an ISO standard [17], which produce more reliable results of moisture permeability.

The moisture permeability values had a lot of uncertainty since the permeability was considered to vary in linear way with relative humidity (RH), which is not true. Therefore, there is a necessity to understand the real behavior of moisture permeability, with RH variation, looking for the most realistic values of moisture permeability [18]. There are two different zones of RH, in which moisture permeability vary in diverse forms [18] [19]:

- **Low relative humidity "dry" zone:** small variations of moisture permeability in function of RH;
- **High relative humidity "wet" zone:** significant increase of moisture permeability with the rise of RH.

To better understand the changes of moisture permeability in function of relative humidity, it was proposed a mathematical function (Equation(2-13)) [19], that showed a good fit to the majority of materials, which originated the graph represented by Figure 2.11.

$$\delta = A * e^{B*\phi} + C \quad (2\text{-}13)$$

where A, B and C are constants and Φ is relative humidity [%].

To continue previous works, four different equations (of various authors) were studied to understand which one has the best fit [20]. Equation(2-13) revealed to be a very good regression of the experimental trials made in [20], however, the best regression to all studied materials was Equation(2-14) [14] [15].

$$\delta = A + B * \phi^{C} \quad (2\text{-}14)$$

The moisture permeability can be related with other parameters, such as moisture resistance factor μ [-] and equivalent air layer thickness s_d [m], which is the fictitious thickness of air which has the same moisture permeability of the analyzed material, that are more common in numerical and computational simulations. Moisture resistance factor is calculated by Equation(2-15) and equivalent air layer thickness is achieved by Equation(2-16).

$$\mu = \frac{\delta_a}{\delta} \quad (2\text{-}15)$$

$$s_d = \mu * d \quad (2\text{-}16)$$

where d [m] is the thickness of sample and δ_a is moisture permeability of air.

To better understand how it is possible to divide the moisture flux in their vapor and liquid forms, it was proposed a separation of total flux in vapor and liquid [22], which, after some mathematical equations and demonstrations, originated the flux division of Figure 2.12.

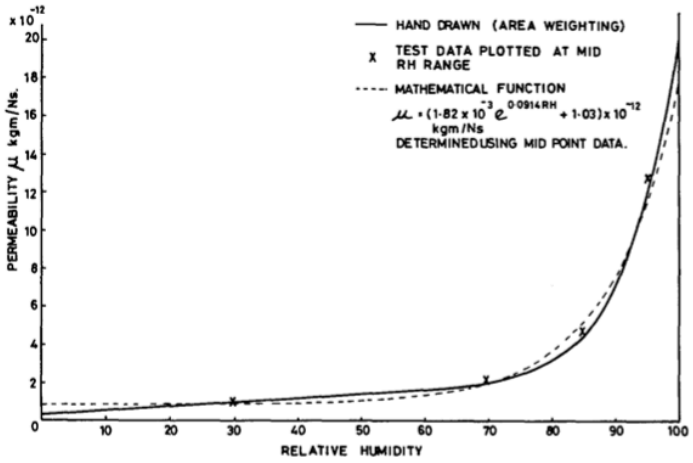

Figure 2.11 – Mathematical function proposed to moisture permeability [19]

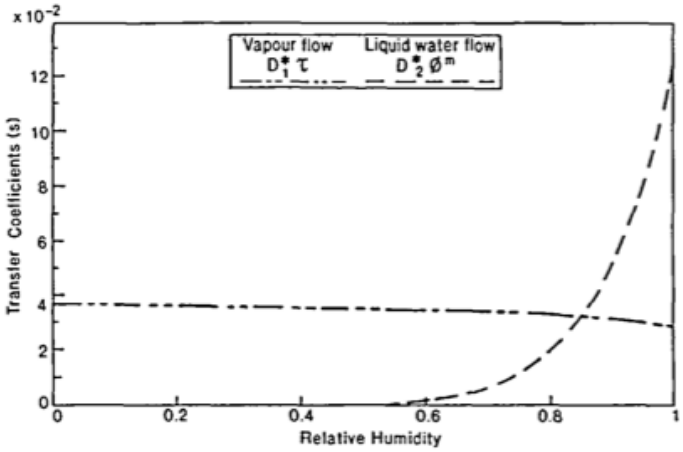

Figure 2.12 – Separation of moisture flux in vapor and liquid form [22]

As it is possible to see in Figure 2.12, the liquid flow of moisture starts for 60% of RH that is the level where the interstitial condensation begins. The liquid flux increases exponentially from 60% of RH beyond, since more pores start to have condensation of water vapor [22] [23]. Figure 2.12 shows that vapor flow slightly decreases with the increasing of relative humidity, since there is less space to moisture, in vapor form, located in pore surfaces. However, it is a good approximation if vapor flow is considered constant at all relative humidity levels, according to Galbraith, G. *et al.* [24]. From various works [22] [23] [25], it was possible to correlate the vapor flow with pressure gradient, in which the vapor flux decreases with the increment of gradient of pressure. However the same does not verify with liquid flux, because it is independent of gradient of pressure [22] [23] [25].

Some works assume that vapor part of moisture permeability of materials is independent of temperature [9]. However, the same article discovered an influence of temperature in liquid phase of moisture permeability, since the increasing of temperature originates a decreasing of surface tension of water and dynamic viscosity of water [26] (Figure 2.13), what makes that the liquid flux increases with temperature.

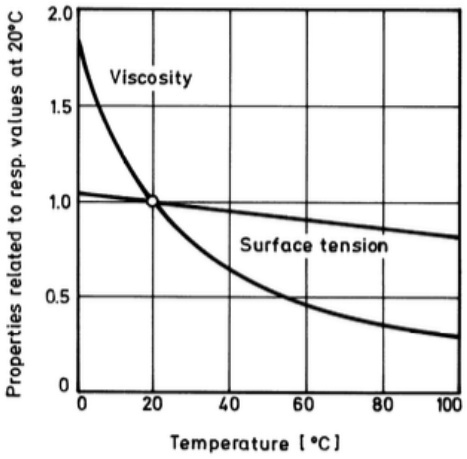

Figure 2.13 – Influence of temperature in viscosity and surface tension of water [26]

The international standard ISO 12572 [17] is the one used to determine the water vapor transmission properties. This standard contemplates the correction of water vapor permeance W [kg/(m^2.Pa.s)] to high permeable materials, which has an equivalent thickness air layer below 0,2 m. This correction is made considering the air between the sample and the salt solution under it (cup test). However, the air above the sample is not considering in the present standard, which can change significantly the results from moisture permeability experimental trial. Therefore, the moisture permeance can also be rectified, considering the air above the sample, which may produce better results [27] [28] [29]. It is important to retain that the values of moisture permeance of a single material may not correspond with its values when applied. In other words, if there is a compound building solution, it should have any type of joints, that there are more permeable to moisture. As so, the moisture diffusion resistance of the global solution is notably lower than the pure material's one, even applied at the same thickness [30]. This fact may improve the building's solution evaporation, but it increases the infiltration of moisture from outside.

Experimental trials made by ISO standard [17] are more reliable when they are made to current materials of construction (plasters, gypsum board, plywood, beyond other materials). Although, Svennberg, K. and Wadso, L. developed a new test, made for highly permeable and lightweight materials [31], which is an test that avoids the problem of the interior surface resistance, as well as it is a really quick method.

ISO 12572 [17] may not be the perfect standard to very moisture tight materials [32], which make that there are a need of further developments to these type of materials.

2.2.3. Moisture Buffering Value (MBV)

Most of methods used to determine the material behavior to moisture adsorption and desorption are usually made at steady-state. Therefore, outcome the necessity of characterize the dynamic behavior of coating materials, determining its capacity to buffer relative humidity of a certain enclosure.

Time, B. [33] studied the influence of changing relative humidity of environment on wood samples weight, at constant temperature. The author studied not only different steps of relative humidity, but also the influence of duration of the exposure of samples to a certain RH. The difference of moisture content between the cycles with a duration of one day and the ones with a week was negligible, meaning that the wood achieved the moisture content equilibrium in less than one day.

Padfield, T. [34] developed a chamber which is capable of measure the buffering capacity of materials, by exposing them to high and low relative humidity cycles. At constant temperature, the cycles of relative humidity are around 10% and 90%, achieved by condensation of water (simulating the air renovation of an enclosure) and evaporation of water (simulating the internal gains of moisture by people, lights, equipment, etc.), respectively. In this work, the concept of penetration depth was used. A big limitation of the proposal method is that until the trial may begin, the equilibrium must be reached, what can take a year or two to achieve it.

Further work improved the concept of penetration depth of moisture, where it is defined as the value where the amplitude of relative humidity in a certain profundity of the element is equal or lower to 1% [35]. The present concept is easier to understand by Figure 2.14, where the dot line represents RH variations. As better is the material's buffering capacity, higher will be its penetration depth, what makes this concept a good parameter to highlight the materials with best moisture buffering capacity.

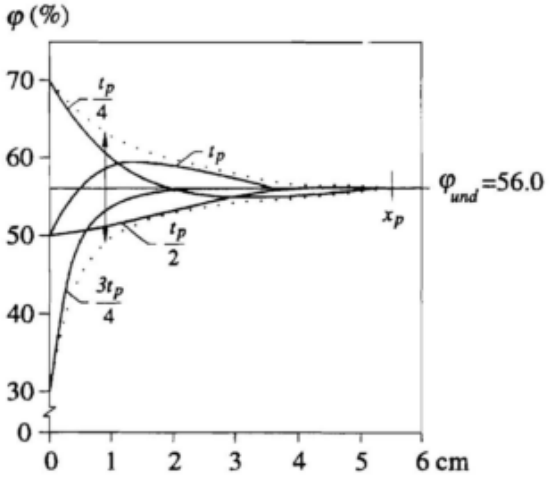

Figure 2.14 – Penetration depth [35]

In 2001, it was made one of the first tests in a room [36], where the materials were situated into the interior elements and then, their moisture buffering capacity was quantified. These results boosted the works made by NORDTEST, which started to make a first workshop in 2003 composed by thirty Nordic and international academics in order to define the best measurements to adopt in the quantification of moisture buffering capacity of materials and constructive systems [37]. In this workshop, the experts were divided in five different working groups, each one working in different scope. The results obtained in [37] originated a final report in which there were made round robin tests, with the main objective of assess the quality of the proposed test method to quantify the moisture buffering capacity of materials and systems [38]. To measure moisture buffering capacity or potential of materials and systems, this NORDTEST report defined four concepts capable to define material's capacity of buffering moisture. These concepts are moisture effusivity, penetration depth, Ideal Moisture Buffering Value (MBV) and Practical MBV. After conclusion of round robin tests, it was defined the ideal experimental trial, which allows anyone to replicate the present test.

Moisture Buffering Value is a value that describes the capability of materials to control peaks of indoor relative humidity. That it, as higher is MBV, better is the ability of materials to adsorb moisture of environment when it is high, and release moisture when there is low relative humidity indoor. As so, the concept of MBV is good indicative of materials potential to buffering humidity and control its peaks, when those are applied in construction with the same thickness [39].

It was developed a similar test experiment to NORDTEST report [38], that classify the response of materials to enclosure RH variation, which is a Japanese Standard (JIS A 1470-1) [40], but, when compared between each other [41], it is possible to understand that both have similar methods and also achieve close results, but Japanese Standard is only applicable to single materials and does not include system's classification.

An inverse approach was made by Dubois, S. and Lebeau, F., with the main intuit of validate MBV experimental trial of NORDTEST [38], by comparing the adsorption an desorption values with a HAM model [42]. The model was capable to predict the dynamic moisture adsorption, with recourse to a DREAM algorithm. Both results (experimental and predicted) were very similar, what makes that both validate each other.

2.3. Hygrothermal behavior of buildings

Interior environment of buildings is function of weather, of materials which make part of construction system and coating materials, interior furniture, books, carpets, beyond others.

It is important to understand how materials can influence the indoor climate, and how they can control indoor RH and temperature, and the consequences that are inherent to these two main concepts.

2.3.1. Thermal and hygric inertia

Thermal inertia

Thermal inertia is defined by the resistance of a certain material, construction system or building to change its temperature. The thermal inertia is mainly function of conduction flux of heat than the other two fluxes of heat (convective and radiation), since it is the heat flux form that goes through the thickness of the respective body.

Thermal inertia allows to have smaller heating and cooling equipment, since it provides to building lower fluctuations of indoor temperature [43]. Thermal inertia affects strongly the necessity of heating buildings situated in cold climates, because it delays the heat flux of warm stations and increases the temperature of indoor, even the climate of outdoor is cold [44]. The thermal inertia of an element is directly proportional to its stored energy E_{st} [W], which is related with the energy to and from the element, E_{in} [W] and E_{out} [W] respectively, and with the generated energy inside the element E_g [W], by the following equation:

$$E_{in} + E_g - E_{out} = E_{st} \tag{2-17}$$

Which eventually becomes the General Heat Conduction Equation:

$$\frac{\partial}{\partial x}\left(\lambda \frac{\partial T}{\partial x}\right) + \frac{\partial}{\partial y}\left(\lambda \frac{\partial T}{\partial y}\right) + \frac{\partial}{\partial z}\left(\lambda \frac{\partial T}{\partial z}\right) + q' = \rho c_\rho \frac{\partial T}{\partial x} \tag{2-18}$$

where λ is thermal conductivity [W/(m.ºC)], q' is the generated energy, ρ density [kg/m^3], c_ρ is specific heat capacity [J/(kg.K)] and T is temperature [ºC].

Equation(2-18) can be simplified, considering that there is no internal energy being generated and that the heat flux only occurs in one direction, and therefore it is obtained the following equation:

$$\frac{\partial}{\partial x}\left(\lambda \frac{\partial T}{\partial x}\right) + q' = \rho c_\rho \frac{\partial T}{\partial x} \tag{2-19}$$

Equation(2-19) allows to understand that the stored energy by an element is directly proportional to its thermal conductivity, density and specific heat capacity. Therefore, the thermal inertia of a building also increases with all these three factors, since it is directly related with the amount of energy that can be stored by its building materials or materials inside it.

Thermal inertia of a building is known by its capacity to damp the amplitude of interior temperature μ, between the maximum and minimum, and to delay the flux of heat φ, making that there is a gap between outside and inside temperatures (Figure 2.15). This gap between both temperature is as bigger as is the thermal inertia of building.

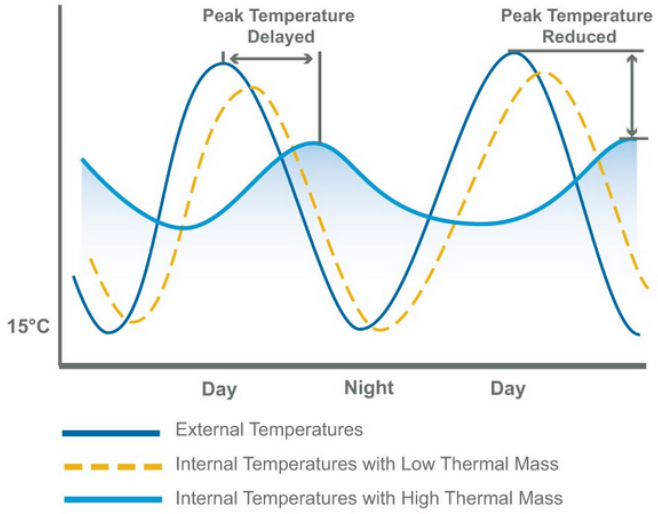

Figure 2.15 – Thermal inertia [45]

Thermal inertia is directly proportional to specific heat capacity c_ρ, density ρ and thermal conductivity λ, once both damp and delay factors are also directly proportional to these three quantities (Equation(2-20) and Equation(2-21)). In consequence of that, it is easy to understand that thermal inertia of a building is as higher as it is its global mass.

$$\mu = e^{-\frac{1}{\lambda}*\sqrt{\frac{\pi}{t}*(\lambda*\rho*c_\rho)}} \tag{2-20}$$

where t is temperature wave time [hours].

$$\varphi = \frac{d}{2*\lambda} * \sqrt{\frac{t}{\pi} * (\lambda * \rho * c_\rho)} \tag{2-21}$$

where d is the thickness of the element [m] and the product of thermal conductivity, density and specific heat capacity originate the concept of admissibility α.

Therefore, it is possible to understand that as higher is the thermal inertia of a building, bigger is the resistance that it offers to change inside's temperature and, as so, there is higher control of interior temperature by building's elements.

Even there is no consensus, the thermal inertia of buildings can be quantified by its specific heat capacity, thermal mass, decrement factor, thermal diffusivity, thermal phase lag, thermal resistance factor, thermal admittance or thermal effusivity [43].

Hygric inertia

With a similar definition of thermal inertia, the hygric inertia is known by the capability of constructive systems, coating materials and all indoor materials in interior of buildings to damp the indoor cycles of relative humidity.

Hygric inertia is function of moisture transfer properties of constructive systems of envelope, since it those constructive systems are much permeable to moisture, then they may not store the desired moisture inside them. The hygric inertia is also function of the materials applied indoor that are capable to adsorb and release moisture.

If the constructive systems of envelope are very tight to moisture, they do not allow the moisture of exterior reaches the interior environment, but they do not also allow that the moisture adsorbed by interior coating transfers to outside. Due to this fact, if moisture cannot be transferred to outside, the good hygroscopic behavior of coating materials is lost in a short period time, since those coating materials remain full of moisture and then they are not capable to adsorb more moisture and control the indoor RH. For that, it is important to establish an optimum point between the moisture tight of constructive systems be good to offer resistance to moisture of outside reaches the interior and also be good to allow that the moisture of indoor coating materials can be transferred to outside.

Itis important to understand how the hygric inertia can damage the thermal inertia of a certain room or building, once the thermal conductivity is much more prejudiced by the increment of moisture than with the increment of temperature [46] [47]. Thermal conductivity varies in linear way with moisture and temperature, in a range between 10 and 40ºC [47] [48], and hygric inertia can affect the thermal comfort of spaces, by dropping the temperature of indoor in 1,5 ºC [49].

The effect of moisture content on thermal conductivity is more relevant in humid climates, but it cannot be despised in drier climates [50]. Also the air exchange rate affects the hygric inertia of a building, since the increment of indoor ventilation originate lower values of hygric inertia [51]

The capability of coating materials to adsorb moisture is function of their porosity and pores' radius, but the capability of these coating materials to contribute to hygric inertia depends of their active thickness of adsorption d_H [m] (Equation(2-22)), which is function of moisture permeability δ, specific moisture content ξ, temperature T and saturation pressure of inside surface $p_{sat,si}$ [44].

$$d_H = \sqrt{\frac{\delta * p_{sat,si} * T}{\pi * \xi}} \tag{2-22}$$

The hygric inertia of some element can be determined by the concept of daily hygroscopic inertia index $I_{h,d}$ [g/(m^3.%RH)] (Equation(2-23)) [29], which is function of MBV of building's materials, and their area, as well as of MBV of objects placed inside which can contribute to buffer relative humidity of indoor, like books, furniture, carpets, etc..

$$I_{h,d} = \frac{\sum_i^n MBV_i * S_i + \sum_j^m MBV_{obj,j}}{N * V * TG} \tag{2-23}$$

where S is the surface of material [-], N is the air exchange rate [h^{-1}], V is the volume of room [m^3] and TG is the vapor production period [h].

This evaluation of hygric inertia by the concept of $I_{h,d}$ is an appropriate form to characterize the hygric inertia of a room and it originates reliable results [52].

It is also possible to characterize the hygric performance of a building without knowing the air exchange rate or the vapor production period of it, and it is possible to achieve by the concept of hygric capacity [g/(m^3.%RH)] that have a similar formula to daily hygroscopic index, and is represented by Equation(2-25) [53].

$$Hygric_{cap.} = \frac{\sum MBV_i * S_i}{V} \quad (2\text{-}24)$$

2.3.2. Condensations

The phenomenon of condensation is characterized by the change of water phase, from vapor state to liquid one.

Condensations may occur at surface, named as superficial condensation, or at the interior of a certain element, named as interior condensation.

Any condensation, superficial or interior, occurs always when the partial pressure of water vapor reaches the saturation pressure of water vapor, which is dependent of temperature. As so, as it is possible to see by Equation(2-4), both pressure can be related with each other, what makes that the condensation starts when relative humidity is equal to 100%.

As it is possible to see in Figure 2.16, relative humidity increases significantly with the reduction of temperature, what shows that for the same partial pressure of water vapor, the saturation pressure increases significantly, which diminishes relative humidity.

With regard to superficial condensations, they are easy to predict, by using a psychrometric diagram or the concept of dew-point temperature. That is, if the inside environment is at a certain temperature (for example, 20ºC), which originates a certain saturation pressure of water vapor, so the air is at around 80% of relative humidity ("A" point of Figure 2.16). If temperature of outside air is significantly lower than 20ºC, and the thermal behavior of construction system is bad enough to originate that its interior surface achieves about 17ºC ("B" point of Figure 2.16), so RH will reach 100% values and, therefore, it will occur superficial condensations.

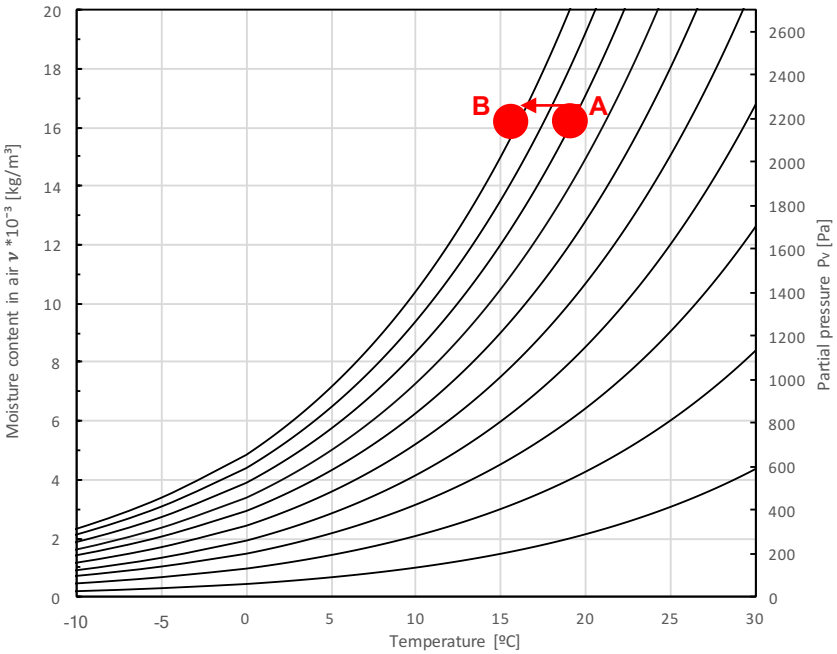

Figure 2.16 – Psychrometric diagram with an example of condensation phenomenon

For condensations that may occur inside any element (denominated of internal condensations), the most usual approach to aim with it is use Glaser method, which relates the partial and saturation

pressures of water vapor over the thickness of the element. Knowing the interior and exterior temperatures of surfaces, and also the heat transfer coefficient of the element U [W/(m^2.ºC)], it is possible to know the temperatures inside it. From the values of temperature, it is possible to calculate the saturation pressure of water vapor and, considering the equilibrium moisture content of the material in analysis, it is also possible to calculate the partial pressure of water vapor. Therefore, as it is visible in Figure 2.17, every time the partial pressure line stays above the saturation one, then will occur condensations.

The Glaser method is an easy handle method to determine interior condensations of an element, however, it has some limitations that does not allow it to consider some important phenomenon:

- Construction system has to have parallel surfaces between each of their elements;
- Moisture content has a fix value which does not allow to consider the hygric behavior of materials;
- Moisture permeability has constant values;
- Does not consider the effects of thermal inertia;
- Makes the analysis in stationary regime.

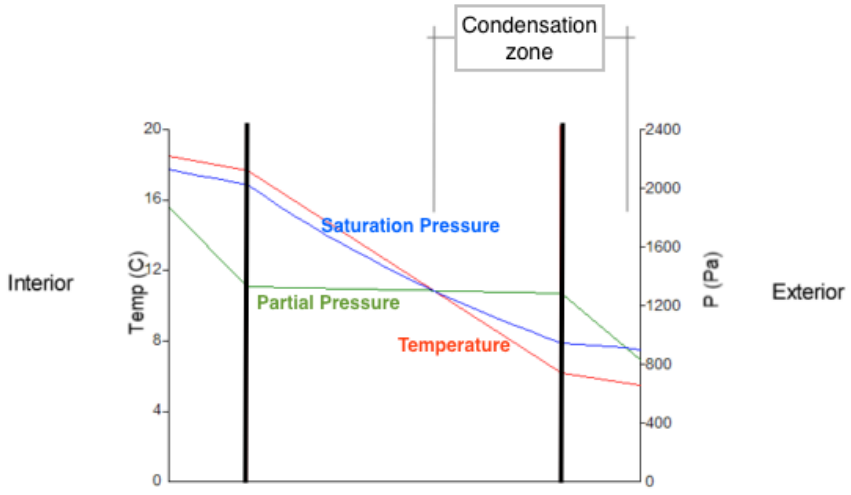

Figure 2.17 – Example of Glaser method for interior condensations (Adapted from [1])

It is important to retain that, as there are more condensation in an element, its thermal conductivity increases, such as the temperature, which brings down the saturation pressure of water vapor and makes that may occur more interior condensations. This phenomenon continuous to develop more and more, until all element has condensation. This process may stop if there would be an increasing of exterior temperature and, as so, begins the evaporation of moisture inside the element.

2.3.3. Consequences of condensations and extreme values of relative humidity

The phenomenon of condensations and extreme values of relative humidity can cause several and irreversible problems to materials, as such to the people which are in surrounding of zones with these problems.

The problems related with relative humidity are not only about high values of RH, but it is also connected with low values of RH. The comfort zone of relative humidity to humans should be between 30% and 60 % of relative humidity [54]. However, other authors suggest that, for human health, the best interval of RH should be around 10% and 50 %[55]. Extremely low values of relative humidity may cause dryness of eyes or skin, as well as dehydration or fatigue [54].

Extremely high values of RH may originate, not only ideal conditions to development of fungi, mold or bacteria, but also the deterioration of materials [56]. From 45-50% of RH beyond, dust mites can develop and, at 60% of RH, starts the development of mold and fungus [54]. With regard to temperature, it has always the perfect values to micro-organisms development, since they grow in a range of 10-35 ºC [55]. Dust mites can originate health problems to humans, and it has a direct relation with RH and temperature (Figure 2.18) [44].

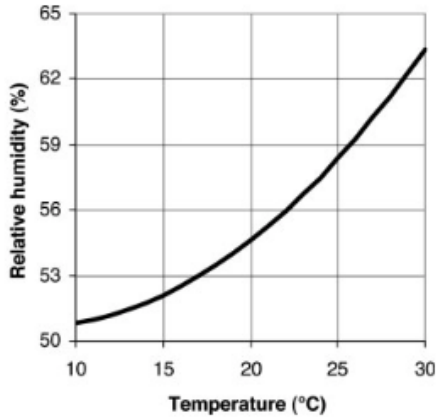

Figure 2.18 – Conditions to development of dust mites [44]

A scientific review composed by 14 different studies discovered that the main family of fungi present in air is *Aspergillus Versicolor*, which does not have a proportional growth with temperature and relative humidity (Figure 2.19) [44].

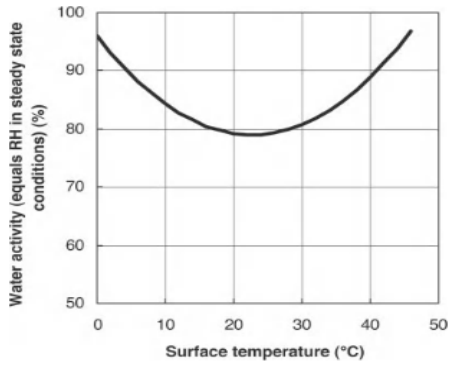

Figure 2.19 – Conditions to development of *Aspergillus Versicolor* [44]

Other work defined the ideal conditions of relative humidity to the development of various problems to human health, referring that the optimum zone to minimize the problem to human health is between 40 and 60% of relative humidity (Figure 2.20) [57].

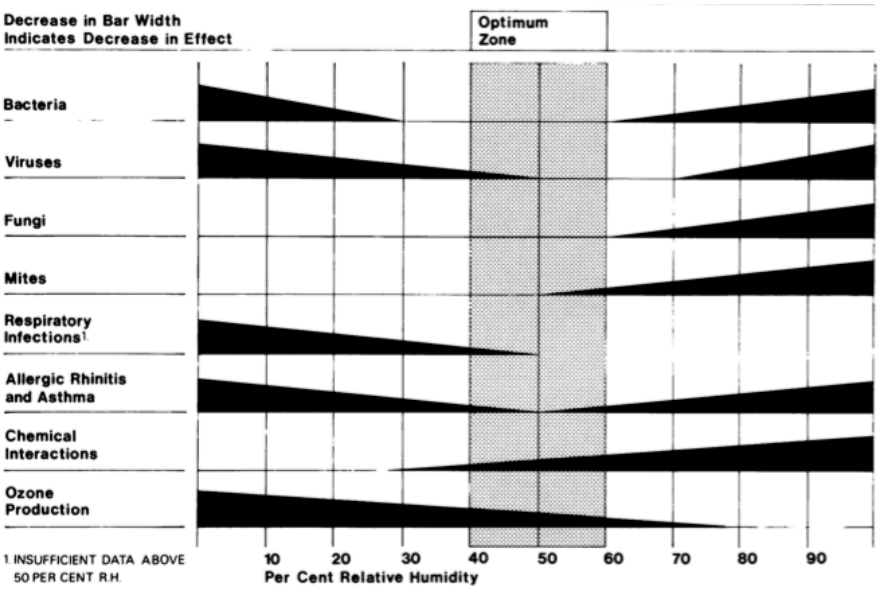

Figure 2.20 – Relative humidity conditons to the development of problems to human health [57]

The grown of mold in building materials can be predicted by a model which relates a mold index with the time that a material takes to reach each level of mold index (from 0 to 5) [58].

If high relative humidity can cause several problems, as the ones shown above, if the condensation is reached (RH=100%), those problems will deeply increase, since at the maximum value of relative humidity, all of the prejudicial micro-organisms are capable to develop.

2.3.4. Processes to lower relative humidity and their consequences

As it was shown in 2.3.3, high RH values can cause several problems to building materials and also to human health. Therefore, it is important to apply processes that allows to lower the RH and, as so, diminish its consequences.

Beside the utilization of hygroscopic materials capable of control the indoor RH, by their ability to adsorb and release moisture from indoor climate, there are five techniques that allows to lower relative humidity [56]:

A. Confine the divisions with moisture production;
B. Dehumidification;
C. Increase temperature of interior environment;
D. Diminish the heat transfer coefficient U of enclosures;
E. Improve ventilation.

Increasing in difficulty of implementation

This type of strategies used to lower relative humidity are also presented on a standard (BS 5250), which proposes some of the above techniques to control relative humidity of interior environment [59].

A. Confine the divisions with water vapor production

The capability of isolate a division which produces moisture is an easy and effective measurement to lower relative humidity. Making that the connection points between the division(s) with production of moisture with the other divisions be tight to moisture makes that RH of the divisions without production of moisture decreases a lot. This happens because, as it is possible to understand by Equation(2-1), partial pressure of water vapor is directly proportional to moisture concentration in air. Therefore, if moisture content in air decreases, the relative humidity of air also decreases (Equation(2-4)).

It is important to refer that this isolation of the divisions with moisture production is made in such a way that allow the occupants to access to divisions with moisture production easily. For example, the divisions with water vapor production are often the bathrooms and kitchen, and they can be isolated with a door that always stay close with the use of a self-closing spring.

B. Dehumidification

This process is equally easy to implement, as easy as increasing temperature of interior environment, and it consists in place a dehumidifier in divisions in which is intending to lower relative humidity.

There is only a need to drain the water collected by dehumidifier.

C. Increase temperature of interior environment

The present process is as easy to implement as dehumidification is, and it just demand the installation of a heating device, which is capable to upper the interior temperature, and then increases the saturation pressure of water vapor (Equation(2-2)), that diminishes relative humidity (Equation(2-4)).

This process of upper the interior temperature has to be made by an electric equipment and not by a gas heater, since it releases moisture over the heating process.

D. Diminish the heat transfer coefficient U of envelope

This technique to lower RH implies a lot of work and nuisance to the building occupants. This decreasing of heat transfer coefficient U [W/(m^2.ºC)] may be done by the reinforcement of thermal insulation (or implementing it as new, if there was not any type of it in building's enclosures), applied by interior, middle or exterior of envelope.

The reinforcement of thermal insulation has a direct impact in thermal resistance R_T [(m^2.ºC)/W] of construction systems (it increases), since verifies an increasing of thickness of thermal insulation (Equation(2-25)). This increment of thermal resistance originates a decreasing of heat transfer coefficient (Equation(2-26)), which means that cross less heat through the enclosures and then the interior environment temperature increases, that originates an increment of saturation pressure of water vapor (Equation(2-2)) and a reduction of relative humidity (Equation(2-4)).

$$R_T = R_{si} + \sum_{i=1}^{n} \frac{d_i}{\lambda_i} + R_{se} \tag{2-25}$$

where R_{si} and R_{se} [(m^2.ºC)/W] are, respectively, the interior and exterior surfaces' thermal resistance and d [m] is the thickness of each material of the construction system.

$$U = \frac{1}{R_T} \tag{2-26}$$

E. Improve ventilation

The ventilation of a building may be done naturally, forced or a mixed of both, also called as hybrid [55].

In case of Portugal, the standard which are commonly used are *Regulamento do Desempenho Energético dos Edifícios de Habitação* REH [60] and NP 1037-1 [61]. In REH the air exchange rate demanded to heating season is 0,4 h^{-1} and 0,6 h^{-1} to cooling station. NP 1037-1 demands air exchange rates of 1 h^{-1} and 4 h^{-1} for main and services compartments, respectively.

The air exchange ratio to avoid mold in a room of 200 m^3 is represented by Figure 2.21, where it is possible to see that the air exchange rate diminishes with the increasing of temperature, once this increment originate lower values of relative humidity [44].

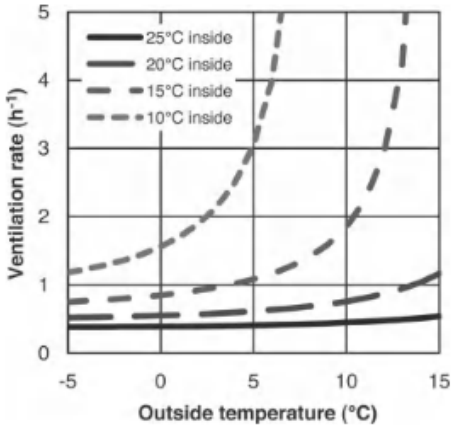

Figure 2.21 – Air exchange rate to avoid mold in a room with 200 m^3[44]

The same authors said that, for the studied case, the minimum value of ventilation rate is about 0,7 h^{-1} [44].

The ventilation design must have into account the fact that the air that comes from outside may be polluted and, as so, there is a necessity to choose equipment capable to reduce the prejudicial consequences of the pollutants [55].

The climate of Lisbon (Figure 2.22), capital of Portugal, shows that there are more moisture content in warm stations than in cold station, since it is situated next to ocean and river, that suffer large evaporation on warm stations and increases the moisture content of the air [1]. Because of that, it is possible to understand that even the ventilation brings warmer air to interior it may have a large quantity of moisture content, so it may be prejudicial to control the indoor RH [62]. Therefore the best recommendations are to make the ventilation and dry the air that becomes from outside, simultaneously to make that the air stays warm and dry which drops considerably the relative humidity values [54] [55].

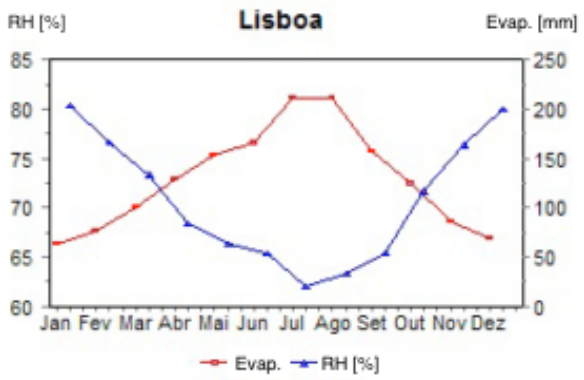

Figure 2.22 – Evaporation and relative humidity in Lisbon (Adapted from [1])

2.3.5. Influence of hygroscopic materials in temperature, relative humidity and air quality

The ability of hygroscopic materials to control the indoor climate is well known and it can be used in benefit of building performance and human health [63].

There are some old buildings, that have high thermal inertia that could have their hygric inertia improved, reducing their inner RH cycles. However, those buildings may achieve an equilibrium between moisture content of materials and the interior environment, even at high values of relative humidity. As so, it is not always recommended to add hygroscopic materials into it [56].

A. Temperature

Hygroscopic materials or coatings can have a direct influence in interior temperature since in cooling season they adsorb moisture from environment, which reduces their enthalpy and therefore makes easier to raise the temperature [64]. These materials may increase the temperature when moisture is adsorbed and they can lower the temperature when releasing moisture to the interior environment [65]. It is possible to increase the temperature in 1 or 2 ºC when hygroscopic materials are used [66], being sometimes 5ºC above to exterior mean, only by the using of these materials [67]. However, the localization of hygroscopic materials may be important in the control of temperature, since if they are installed at coverage zone, they could not produce any influence on temperature [68].

The potential of control the interior temperature may reduce the energy consumption of a building in 2-3% in cold station and 5-30% in warm station [64].

B. Relative humidity

Hygroscopic materials are well known by their ability to buffer moisture of interior environment, being capable of control the RH cycles inside buildings. These materials can be applied as coatings and they can improve the moisture buffering capacity of a regular coating to the double [69]. Hygroscopic materials tend to be dirtier, since humid (or colder) surfaces attract dust and dirtiness [34].

Hygroscopic materials are not only the coating applied in walls, floor or ceiling, but also all materials of interior which are capable to adsorb and release moisture, like furniture, carpets, textiles, books, beyond others [70]. The area of these hygroscopic materials influence the hygric inertia of the room [67], however their best location is not yet well defined [71]. Buffering materials are able to control

relative humidity, which can lead to an significantly energy saving of humidification or dehumidification [68].

As higher is the capability of materials to control the indoor RH, higher will be the hygric inertia of the building [29]. It is possible to predict the impact of this hygric inertia in interior environment by numerical models, which are capable of measure the potential of hygroscopic materials to drop the moisture content of inside [72]. The hygric inertia may also be quantified by the RHS factor (Relative Humidity Stabilization), which is as lower as better is the hygroscopic behavior of the studied element [73].

The potential of a single element to buffer relative humidity can be determined by MBP (Moisture Buffering Potential), which can be calculated by a simple and fast method, that can predict the behavior of material to different scenarios of moisture production [74]. This method is largely better than “effective moisture penetration depth” (EPDM) and “effective capacitance” (EC), since the first one contains time and labor intensive trials and the second one is not much reliable [75].

The effective moisture penetration depth defines the thickness of the hygroscopic materials which is capable of store the moisture adsorbed from interior environment. Although, increasing the thickness of the hygroscopic element beyond its effective moisture penetration depth, which is about 1-2 mm in wood (Figure 2.23) [76] and 50 mm in cellulose panel (Figure 2.24) [77], does not improve its hygroscopic behavior. Many other penetration depths are present in Table 2-2, which was accomplished by work that measured this penetration depth in 24 hours and 360 days’ periods [34].

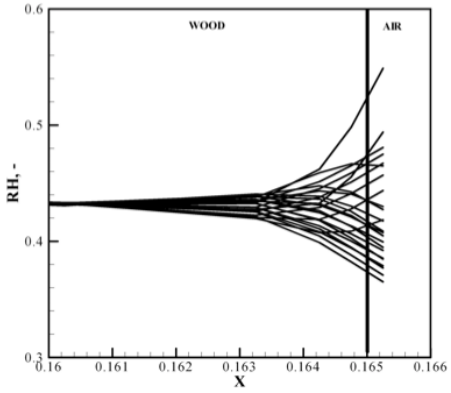

Figure 2.23 – Effective moisture penetration depth of wood [76]

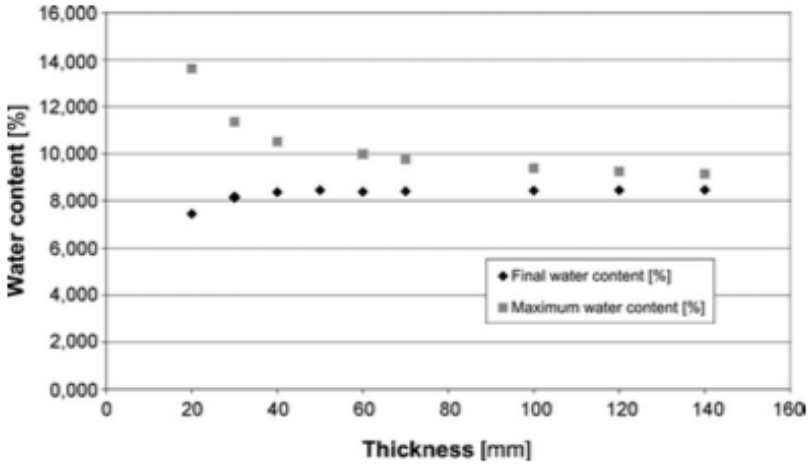

Figure 2.24 – Effective moisture penetration depth of cellulose panel [77]

Table 2-2 – Effective moisture penetration depth of various materials [34]

Material	Effective moisture penetration depth [m]	
	24 hours	360 days
Wool insulation	0,0591	1,12
Wood, radial/tangential	0,002	0,04
Wood, longitudinal	0,0129	0,25
Light clay	0,0054	0,10
Cellular concrete	0,014	0,27
Gypsum board	0,0234	0,44
Cast gypsum	0,034	0,65
Lime plaster	0,0407	0,77
Brick, Falkenlowe	0,0307	0,58

One of the cases that justifies to have thick layers of hygroscopic materials is the cycles that are intended to control have long duration, but it only justifies the implementation of thick coatings if the air exchange rate of the room is low [34]. This because, lower values of air exchange rate originates higher hygric inertia of the room [67] [71] [73], being able of reduce RH from 70 to 50% for 0,5 to 1 h^{-1} air exchange rates [76]. However, it is very difficult to achieve the best hygroscopic behavior of a certain building or room, due the fact that it implies a very low value of air exchange rate, which is not ideal for human health [67].

C. Air quality

The moisture is a parameter which affects the comfort and air quality of indoor. Materials which are hygroscopic and permeable to moisture, may improve the comfort and the perceived indoor air quality, by reducing the phenomenon of condensation and, as so, the mold and micro-organisms growth in interior surfaces of enclosures [63] [68] [76] [78]. The effect of hygroscopic materials, like the wood, can reduce the percentage of dissatisfied people (PD) due to warm respiratory comfort and to perceived air quality (PAQ), since it is possible to reduce these two parameters in 2% and 6 % of PD, respectively, in a room made of wood with two adult persons, comparing with the same room with all coatings covered by an impermeable paint [65].

Hygroscopic materials, as shown before, can control temperature and relative humidity on indoor air. If, for the same level of air pollution, both temperature and relative humidity have higher values, they originate a strongly decreasing of perceived air quality PAQ, which is linearly correlated with the enthalpy of the air (Figure 2.25) [79]. For the same case, it has been concluded that both temperature and relative humidity have a very small impact on perceived of odor intense.

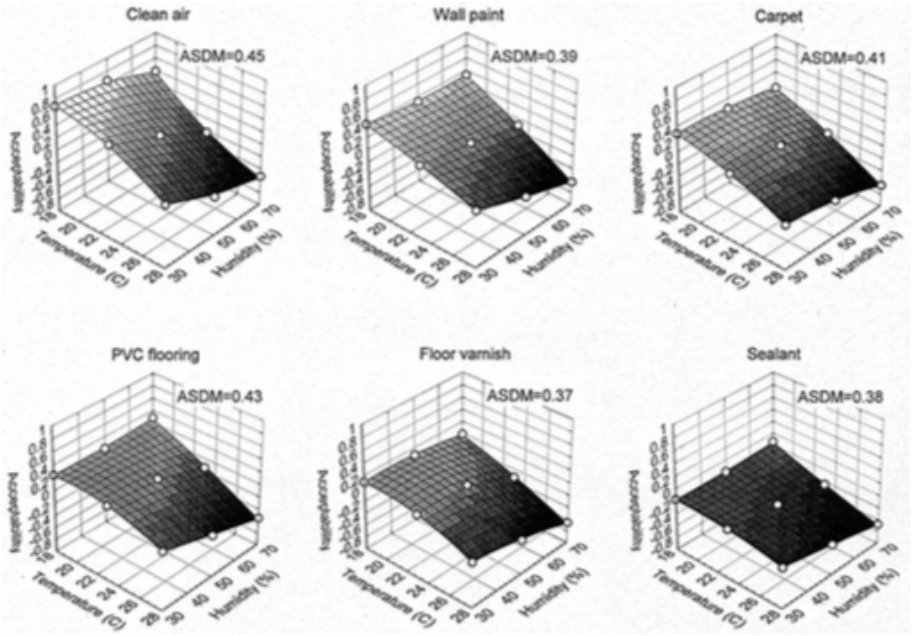

Figure 2.25 – Impact of temperatue and relative humidity on the perceived air quality PAQ [79]

Chapter 3: Methods

3.1. General considerations

In the present chapter is intended to test many hygroscopic materials to different experimental trials that allow to know their hygroscopic characteristics. The chosen tests were adsorption/desorption isotherm, moisture permeability, thermal conductivity depending moisture content, MBV, experiment of classroom and response time. All these tests will allow to understand the ability of the materials to control the indoor climate.

3.2. Materials

To continue the work done in [80], the materials used had to be the same. However, for this experimental campaign it was used just six of those materials. It was only chosen to use some of the materials used in [80], in consequence of the experimental methods focus be the group of hygroscopic coatings.

The coatings hygroscopicity depends on their capacity to regulate the RH of indoor. In other words, those coatings are capable to adsorb moisture when RH of indoor is high and to release moisture to the entourage when its RH is low.

The area of walls is, in most buildings, usually high, makes that their coatings have several consequences in wall thermal and moisture behavior. So, it is very important to choose the best coatings, in way to improve the good behavior of the building and to maintain the interior equilibrium and decrease the oscillation cycles of RH.

In consequence of the past paragraphs, the following six coatings have been chosen to be tested:

- Finished stucco (EA);
- Recycled cellulose boards (M);
- Projected cellulose coating (N);
- Natural hydraulic lime mortar (NHL);
- Wood wool cement board (O);
- Clayish earth plaster (S).

Finished stucco (EA)

The finish stucco is a projected plaster which has a superficial painting that makes these samples less permeable to moisture.

In another work [80], the author made the samples of this material, as it can be seen in Figure 3.1, with the objective of understand the influence of the painting in the behavior of the samples made with this materials.

As stucco is a material known by its high porosity and, therefore, its skill to regulate the interior cycles of relative humidity. So, it seemed to be a good material to subject to hygroscopic experimental trials chosen in the present Master's thesis.

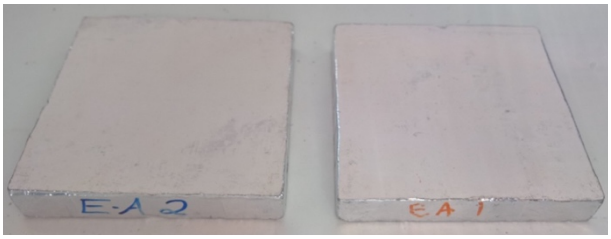

Figure 3.1 – Finished stucco's samples (EA)

Recycled cellulose board (M)

The samples of recycled cellulose board are "Homogeneous, fiber-reinforced gypsum-bound dry construction panels with paper fibers and added non-combustible fibers, made water-repellent at the factory." [81]. These boards are prefabricated, what turned the work a little bit easier, due the fact of it was only necessary to cut them in the dimensions required in each trial's standard, that originated the samples of Figure 3.2. The samples were cut and coated with aluminum tape by Rocha, D. in a previous work [80].

As it is a porous material, so it has a good hygroscopic behavior and then, it has a lot of interest to be analyzed.

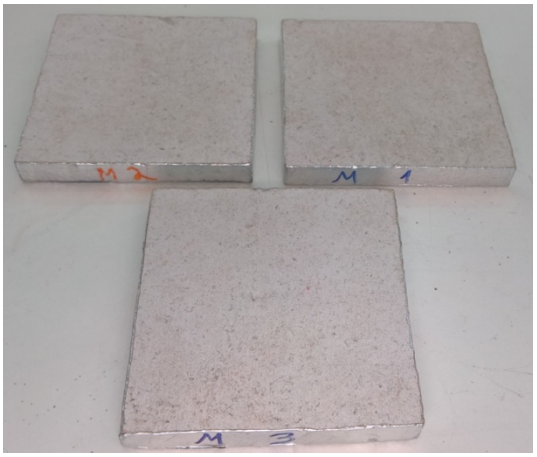

Figure 3.2 – Recycled cellulose board's samples (M)

Projected cellulose coating (N)

Projected cellulose coating is applied to walls and ceilings with the main goal of improving the acoustic behavior. It is applied in areas where reducing reverberation time and noise and improve acoustics is desired.

The solution is from Asona and is named by Sonaspray, with the technical file annexed to the present thesis [82]. This is a prefabricated board, that made that the only thing to worry was cut them in the mandatory dimension, present in each test standard, which originated the samples of Figure 3.3.

Like the previous coating solution (recycled cellulose board), projected cellulose coating contains large quantity of pores with dimension that allows it to be considered a hygroscopic coating. As so, this is one of the chosen material to be tested.

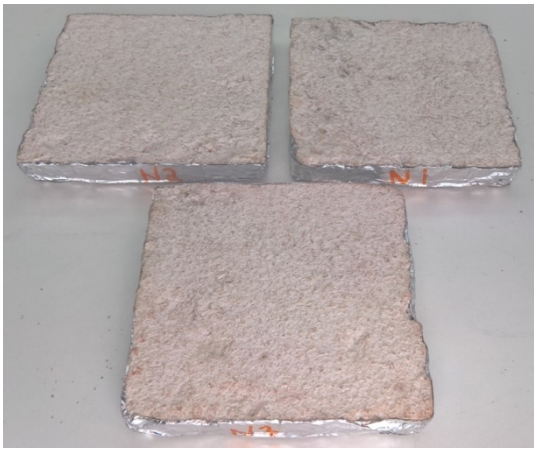

Figure 3.3 – Projected cellulose coating's samples (N)

Natural hydraulic lime mortar (NHL)

This mortar was chosen in order to compare a typical plaster, like natural hydraulic lime mortar (NHL) is, with other coatings, which have good moisture buffering behavior.

The samples made with the present material were made by Rocha, D. [80], and the formulation of samples were based in another Master's thesis [83]. The covering of samples with aluminum tape, as it is possible to see in Figure 3.4, was made in the same previous work. The samples were made with natural hydraulic lime (NHL3.5) and its volumetric trace is 1:3 of binder and sand, respectively.

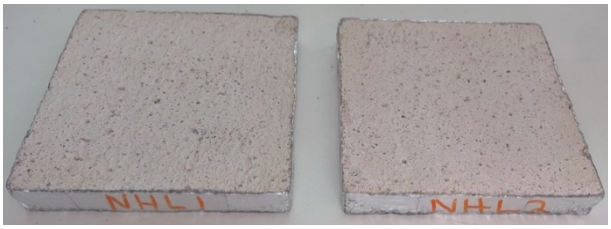

Figure 3.4 – Natural hydraulic lime mortar's samples (NHL)

Wood wool cement board (O)

These panels are products made by three main components. As it is possible to see in Figure 3.5, wood wool cement board is made by:

- 15% calcium carbonate;

- 50% long and strong fir fibers;
- 35% mineral binders.

Figure 3.5 – Wood wool cement board's composition [84]

This material is used on walls and ceilings and it is applied by the interior. It is used to improve the acoustic behavior and, as it is usually applied by the interior and at sight, is required a high fire resistance. Wood wool cement board has the fire resistance needed, as shown in its datasheet [85].

These panels are, such as 0 and 0, prefabricated boards. As so, it was only needed to cut those boards in samples (represented in Figure 3.6), in dimensions that comply the ones present in each trial's standard.

To absorb air sounds, wood wool cement board is highly porous, so it has a potential good hygroscopic behavior. In consequence, this material was one of the chosen material to study.

Figure 3.6 – Wood wool cement board's samples (O)

Clayish earth plaster (S)

The clay soil is characterized by its capacity to retains water, that makes it a high cohesive soil. This type of material improves the hygroscopic behavior of the building, and as it does not need chemical additions, it became a material easy to recycle. Clayish earth is largely used as plaster in consequence of, beyond other characteristics, its low dimensional variation.

The samples made with clayish earth and the NHL samples were the only ones that were not prefabricated and, thus, was necessary make them, which originated the samples of Figure 3.7. These

samples were made by Rocha,D. [80], like Lima *et al.* [86] did, knowing that the samples formation was like E1S2 samples (meaning a ratio binder-aggregate equals to 1:2, respectively).

The only concern about doing the samples of clayish earth was that these had to fulfil the dimensions required in each test's standard.

As it normally retains a lot of water and it is usually classified like a material with good moisture buffering, makes it an interesting material to be tested.

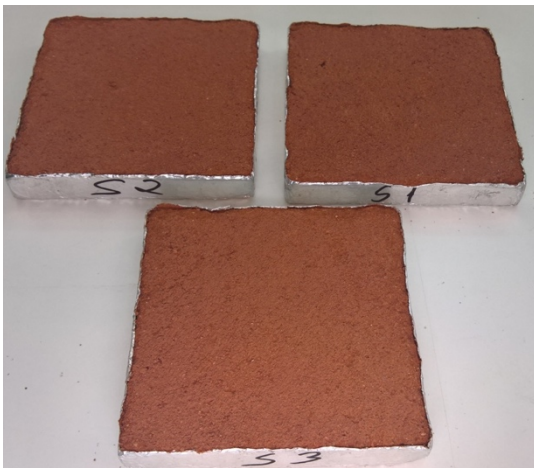

Figure 3.7 – Clayish earth plaster's samples (S)

3.3. Hygroscopic characterization

As understanding the hygroscopic behavior of some coating materials is the main subject of present Master's thesis so, it makes sense that the most of experimental methods focus on hygroscopic properties of those coatings.

The following experiments were made:

- Moisture Buffering Value (MBV)
- Moisture Permeability
- Experiment of classroom
- Adsorption/Desorption Isotherm
- Thermal conductivity
- Response Time

These six tests will give essential information about the behavior of all chosen materials. The experimental trials are made in variable conditions and the moisture values were carefully chosen, looking for representing real situations.

For all experimental trials, except Moisture Permeability one, the face uncovered of samples had to be rough. For example, during the process of making the samples, in the case of clayish earth, five of the six surfaces were in touch with formwork, who brought the fine particles of the plaster to the surfaces.

Therefore, those five surfaces became smoother than the one that was not it touch with anything. As so, this last surface was the only one in contact with air, which replicates very well the only surface of any plaster that is in contact with the environment, in the real application of plaster. In the other three materials (M, N and O), even they are prefabricated, there were always one surface rougher than the other and, as so, this one was the chosen surface to be uncovered.

For Moisture Permeability test, there are two surfaces uncovered where the rough surface is faced to the interior of the cup, because is from where comes the flux (wet cup's trial).

3.3.1. Equipment

For all the tests, there are some equipment associated, both in preconditioning as in trial itself.

All of equipment that were used, fulfilled the respective standard and allowed and all tests have been made following all demands.

Climatic Chamber

The climatic chamber used was Aralab FITOCAL 300 [87], which is a chamber that allows to control temperature, air velocity and relative humidity, make aging or exposure tests, among other many characteristics. These cameras are called of "reach-in" because let the user to reach the interior of the camera, by two front openings filled with a pair of gloves (Figure 3.8).

Figure 3.8 – Climatic chamber

This chamber was used because it can maintain temperature and RH constants, it lets to set a velocity of inside air and allows to make weighing inside chamber, without exposure the samples to (non-desired) ambient moisture. This chamber allows to control the temperature from -45ºC until +180ºC and it is capable of change the inside relative humidity between 10% and 98 %, allowing to set automatic cycles of relative humidity and temperature. The chamber dimension, among all of the remaining characteristics of it, are present at its technical data sheet [87], attached to the present dissertation.

This climatic chamber had different uses, which were the following ones:

- MBV experimental tests;
- Preconditioning of Adsorption/Desorption isotherm samples;
- Preconditioning of Moisture Permeability samples.

Isothermal chamber

Two chambers were built to test the samples at different RH levels. The isothermal behavior presupposes the absence of heat transfer between the interior of chamber and the exterior, and that the interior conditions maintain constant. However, it is not possible to make a chamber with that type of performance, because it would be necessary to isolate them until they have surfaces' thermal conductivity equal to zero, what it is not reachable. Although, to minimize that type of heat exchanges, the room in which these cameras are located, was set to have a temperature near with the inside of the chambers. For that, these chambers were built with Extruded Polystyrene (XPS) in all surfaces but one, that is made of acrylic glass (Figure 3.9). The side made with acrylic glass is the front one and, as so, it was possible to put a pair of gloves in two openings and thus it was possible to work with the samples inside.

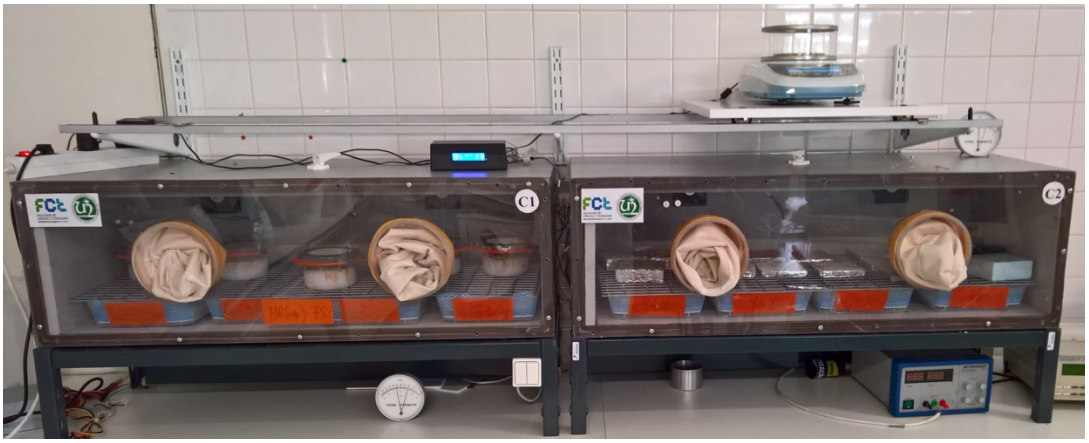

Figure 3.9 – Isothermal chambers

These chambers were made with Extruded Polystyrene (XPS) in consequence it has almost zero porosity, which make it a material who does not adsorb moisture and, as so, makes that the only moisture adsorbed inside the chamber is by the samples being tested.

The two chambers above were used for moisture adsorption, thermal conductivity and response time trials (chamber C2) and for moisture permeability experiments (chamber C1), and they were located side to side.

The sketch of both chambers, with their dimensions, is represented in Figure 3.10.

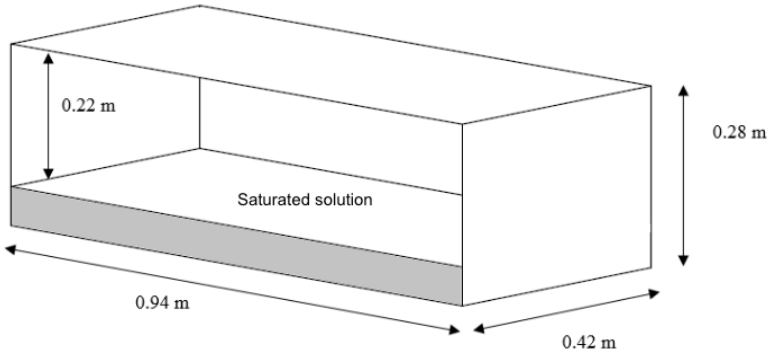

Figure 3.10 – Sketch of isothermal chambers [88]

Sensors

The environment inside the chambers was monitored by four sensors, two in each chamber. The sensors that measured temperature was Thermistor 10K and the ones capable of measure RH were SHT31D. These sensors are capable to output the RH and temperature inside the chambers, like can be seen in Figure 3.11. The sensors allowed to understand if the temperature and relative humidity inside chambers were the intended. These sensors were also used inside classroom, to be possible to obtain the values of relative humidity and temperature over the time, and then relate them with the variation of mass/moisture content of samples.

Figure 3.11 – Sensors used to control relative humidity and temperature

The sensors are also able to record the ambient temperature and RH, in order to try to maintain it as close as possible of standards required temperatures. They make measurements, of both temperature and relative humidity, with an interval of 1 minutes between consecutive measurements.

Scales

As the two isothermal chambers (for moisture permeability, adsorption/desorption isotherm and response time trials) were side by side, there was only one scale above them and it was over two rails that allowed it to move from one chamber to the other (as it can be seen in Figure 3.9) and, therefore, made possible to do both tests with only one scale. The used scale was a KERN PLJ 1200-3A [89] (Figure 3.12) that is characterized by being a high precision scale, capable to weigh materials with 1200 grams in maximum, with a 0,001 grams of precision. This scale is skilled to work in a range of temperature between +5ºC and 35ºC and at a Relative Humidity maximum of 80%.

Figure 3.12 – KERN PLJ 1200-3A scale

The scale in Figure 3.12 was used in almost all experimental trials. It was used in the following tests:

- Moisture Permeability;
- Adsorption/Desorption Isotherm;
- Response Time;
- Experiment of classroom.

Weighing of the MBV trials were carried out using the scale Adam AFP 720 L [90] with an accuracy of 0,001 g, represented in Figure 3.13.

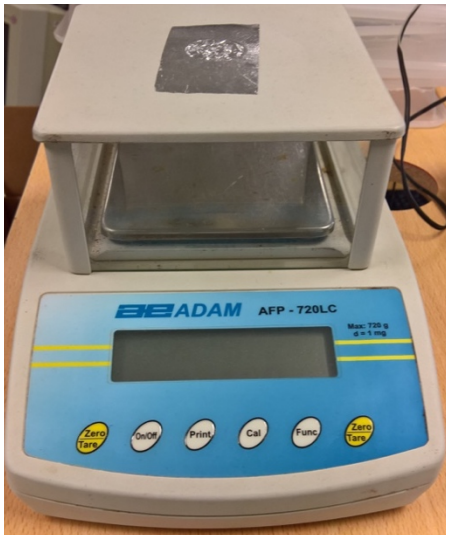

Figure 3.13 – Adam AFP 720 L scale

The scale was used inside the climatic chamber to avoid exposure the samples to relative humidity and temperature of environment when the weighing would be made. This scale (Figure 3.13) has a maximum weight capacity of 720 grams and should be used on a range of temperature between +15ºC and +30ºC, due the fact of being the range in which it provides reliable results.

Airflow equipment

Some standards require that the air velocity must be controlled and, in many of them, there are established extreme values of the air velocity which must be respected. Therefore, there are some equipment able to measure those values, as it is anemometer. It was chosen to use a TA35 Thermal Anemometer [91] that is capable to measure both air velocity and temperature, simultaneously.

As it can be seen in Figure 3.14, this instrument is very light and with small dimensions, what make it an easy handling equipment.

This anemometer is skilled to make the airflow measurements between 0.25 and 20 m/sec, with a precision of 0.01 m/sec, and it is also able to measure the temperature with a minimum and maximum values of 0ºC and +80ºC, respectively.

Figure 3.14 – Anemometer

Thermal conductivity equipment

One of the experimental trials was based in the measurements of thermal conductivity of various samples, at different levels of relative humidity.

This equipment is inserted on hygroscopic characterization since even it measures the thermal behavior of materials, the test chosen for the present work correlates the thermal conductivity of samples with the variation of their equilibrium moisture content.

The equipment used to make the test of thermal conductivity with relative humidity variation was the ISOMET 2104 (Figure 3.15).

The used equipment measures four different parameters:

- Thermal conductivity λ;
- Thermal diffusivity a;
- Volume heat capacity $c\rho$;
- Temperature (ºC).

ISOMET 2104 allows to make measurements with needle probe or with surface probe. The probe utilized was the surface one, which lets to measure quantities between -15 and +50 ºC of environment. Two dissimilar probes were used, where the first one is capable to measure thermal conductivities between 0,04 and 0,3 [W/(m.ºC)] and the from 0,3 to 2,0 [W/(m.ºC)]. The equipment is capable to measure with an uncertain of 0,001 W/(m.ºC).

Figure 3.15 – Thermal conductivity equipment - ISOMET 2104

3.3.2. Adsorption/Desorption Isotherm

Introduction

The adsorption/desorption experiments at isotherm conditions intends to determine the behavior of materials in relation to relative humidity and understand how much moisture those materials are capable to adsorb and release.

The present test is made following the standard ISO 12571 [3], and it is called as adsorption/desorption isotherm since it is made at constant temperature (± 2K).

The only parameter which is calculated on the present test is moisture content of samples, when the equilibrium in mass is achieved. Moisture content of samples can be calculated in u [kg/kg] or w [kg/m^3] by Equation(2-8) and Equation(2-9) respectively.

When desorption process is made, its initial moisture content in equilibrium is assumed as the same of the final moisture content in equilibrium of adsorption phase.

Preparation of samples

As the samples utilized on the present test, were also used in MBV trial (among other two tests), therefore all preparation of samples is explained at MBV test (3.3.5).

The materials used on present experimental trial are recycled cellulose board M, projected cellulose coating N, wood wool cement boar O and clayish earth plaster S, and all samples utilized are represented on Figure 3.35.

However, it is important to refer that the number of samples of each material complies the minimum required in standard, that is three specimens of each material. The mass of samples complies the

minimum required value of 10 grams. All the samples have to be representative of the product applied as construction material, having the same thickness of its real application.

Experimental trial

The test can be made using a desiccator or isothermal chamber, which is the one used in the present work. The used chamber has its specifications in 3.3.1, its dimensions are represented on Figure 3.10 and the whole system of isothermal chamber C2, with the samples inside, is represented in Figure 3.16. The isothermal chamber has to be capable of maintaining relative humidity within ± 5% and temperature within ±0,5ºC over whole test area. The validation of isothermal chamber C2 was made, comparing the values of the expected values of relative humidity with the values measured by sensors inside it (Figure 3.17). Isothermal chamber C2 and the saturated solutions are both validated, due to their almost coincident values of relative humidity. The peaks of relative humidity that occurred inside the chamber, are justified by the fact that the room where the isothermal chamber is inserted has not constant temperature and relative humidity. The sudden dropping of relative humidity is due to the opening of chamber for changing the saturated solution.

Figure 3.16 – Isothermal chamber C2

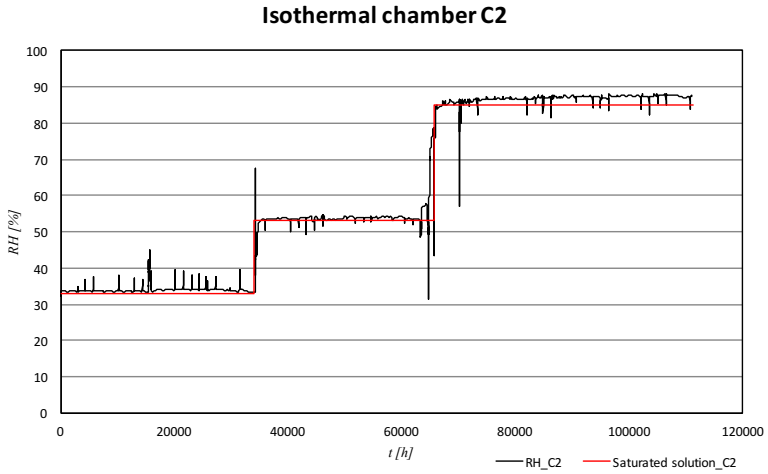

Figure 3.17 – Comparison between expected and real values of relative humidity inside isothermal chamber C2

The tests longs until the equilibrium in mass is reached, which has to be controlled by daily weighing spaced by at least 24 hours, made with a scale with minimum accuracy of ± 0,01%, which could be achieved by scale KERN PLJ 1200-3A (Figure 3.12).

Both adsorption and desorption isotherms are achieved by exposing samples to various environment, with different relative humidity and at same temperature (23 ± 0,5 ºC). The different levels of the relative humidity were 33%, 53%, 75%, 85% and 94% and are accomplished by using hyper saturated salt solutions, as described in Table 3-2. As it can be seen in Figure 3.16, the saturated solutions that conditioned the interior environment were always placed in four trays (Figure 3.28) in order to raise the velocity with which the samples reach equilibrium. The levels of relative humidity are over the minimum required by the standard since it demands at least four different levels of relative humidity.

The present experimental trial, either in adsorption or desorption phase, longs until the following requirement from the standard is achieved:

- Requirement number 1: Change of mass between three consecutive weighing, each made at least 24 hours apart, is less than 0,1 % of the total mass.

However, in this work, it was established an additional requirement, in order to refine the criterion of equilibrium:

- Additional requirement: Change of moisture content between three consecutive weighing, separated from at least 24 hours, should be less than 0,1% of the total moisture content.

3.3.3. Moisture Permeability

Introduction

The moisture permeability of a material is characterized by the ability of porous materials to allow the transfer of moisture through them, when subjected to some gradient of pressure.

To determine the moisture permeability of a certain material, it has to be made an experimental trial, following ISO 12572 [17]. The moisture permeability is function of the dimension of material's pores and its porosity.

To determine moisture flux G [kg/s] which crosses the material, a stopping criterion is established, which is explained later in the present section, and then it is made the mean between the last five changes of mass. To give this value of flux in density of moisture flow rate g [kg/(m^2.s)], it is just necessary to divide the moisture flux by the exposed area of the sample A [m^2], which is the arithmetic mean between both uncovered surfaces.

The value of moisture permeance of material W [kg/(m^2.s.Pa)] can be calculated by dividing the density of moisture flow rate by difference of partial pressure of water vapor Δp_v [Pa] between inside and outside of cup, determined by Equation(3-1).

$$\Delta p_v = \frac{\Delta RH}{100} * 610{,}5 * e^{\frac{17{,}269*T}{237{,}3+T}} \quad (3\text{-}1)$$

where T [ºC] is the temperature inside chamber.

For materials that are highly permeable to moisture, which its moisture diffusion-equivalent air layer thickness is lower than 0,2 m, it is necessary to take in account the effect of the permeability of the air under and above the sample, which in this type of materials affects a lot the moisture permeability of it. If there was not considered the permeability of the air above and under the sample, the moisture permeability of material would be overestimated. The standard of the present test [17] only consider the moisture permeability under the sample (and over the saturated solution). Therefore, other works [27] [28] established the correction of moisture permeability also considering the air above the sample, which makes that the correction of moisture permeance to highly permeable materials should be calculated by Equation(3-2).

$$W = \frac{1}{\frac{A * \Delta p_v}{G} - \frac{1/(67 + 90 * vv)}{\delta_a} - \frac{d_a}{\delta_a}} \quad (3\text{-}2)$$

where vv [m/s] is the air velocity above the sample, d_a [m] is the thickness of air between the sample and the saturated solution (inside cup) and δ_a [kg/(m.s.Pa)] is moisture permeability of air, that can be calculated by Schirmer formula (Equation(3-3)).

$$\delta_a = \frac{0{,}0000231}{R * T} * (\frac{T}{273})^{1{,}81} \quad (3\text{-}3)$$

where R is the constant of gases to water vapor (which takes a constant value of 461,4 J/(kg.K)) and the temperature T is in Kelvin.

The resistance to moisture Z [(m^2.s.Pa)/kg] is the inverse of moisture permeance. When moisture permeance of materials is multipled by the thickness of sample d [m], originates material's moisture permeability δ [kg/(m.s.Pa)] (Equation(3-4)).

$$\delta = W * d \quad (3\text{-}4)$$

To be possible to connect both air and material's moisture permeability, it was created the concept of moisture resistance factor μ [-] which is inversely related with the moisture permeability of material, as it is possible to see by Equation(3-5).

$$\mu = \frac{\delta_a}{\delta} \quad (3\text{-}5)$$

The permeability of a material to moisture can be quantified by the equivalent air layer thickness s_d [m], which represents the thickness of an air layer with the same moisture permeability of the studied material, and it can be calculated by the following two equations:

$$s_d = \mu * d \quad (3\text{-}6)$$

$$s_d = \delta_a * Z \quad (3\text{-}7)$$

Preparation of samples

For this experiment, it is necessary an intense period of preparation, to make sure that the flux of moisture only crosses the sample in one direction.

The materials used were the recycled cellulose board (M), projected cellulose coating (N) and clayish earth plaster (S), represented on Table 3-1, and their information is present in 3.2. All samples have

circular form, in order to adapt to the cup design (Figure 3.18). The dimensions presented in Table 3-1 are result of five measurements of thickness and four measurements of diameter.

Table 3-1 – Moisture permeability samples' dimensions

	Thickness [m]		Diameter [m]	
	Mean	**Standard deviation**	**Mean**	**Standard deviation**
M	0,0127	0,0001	0,0860	0,0001
N	0,0126	0,0001	0,0868	0,0001
S	0,0153	0,0001	0,0828	0,0001

M – Recycled cellulose board; **N –** Projected cellulose coating; **S –** Clayish earth plaster

The samples are introduced on a glass cup, and the sketch of system ready to be tested is represented on Figure 3.18. The test is made with a circular glass cup, which has to resist to corrosion caused by the saturated solution. As the samples' diameter is smaller than the glass ring one, the gap between both, which has to be less or equal to 10% of the cup's interior area, has to be filled with a material tight to moisture. In this case, a mix of beeswax and colophony resin, with a proportion of 1 to 1, was used. The preparation of this mix, implied to dissolve both beeswax and colophony resin in a water bath (Figure 3.19), until it melts and allows to pour it into the cup system.

To prevent that the mix of beeswax and colophony resin sticks to glass ring, it has to be covered by a PVC tape (Figure 3.20 a)). To limit the zone in which is intended to pour the mix, it is used a PVC ring, with 0,125 m of exterior diameter. To avoid that beeswax and colophony resin mix penetrates into the samples, they have to be totally covered by aluminum tape (Figure 3.20 b)), which has to be removed in the circular surfaces, after the mix dry, to allows the moisture flux crosses the samples in the perpendicular direction to these two circular surfaces. All PVC tape, PVC ring and aluminum tape can be seen applied in Figure 3.22 and the system already ready to be tested is shown on Figure 3.24

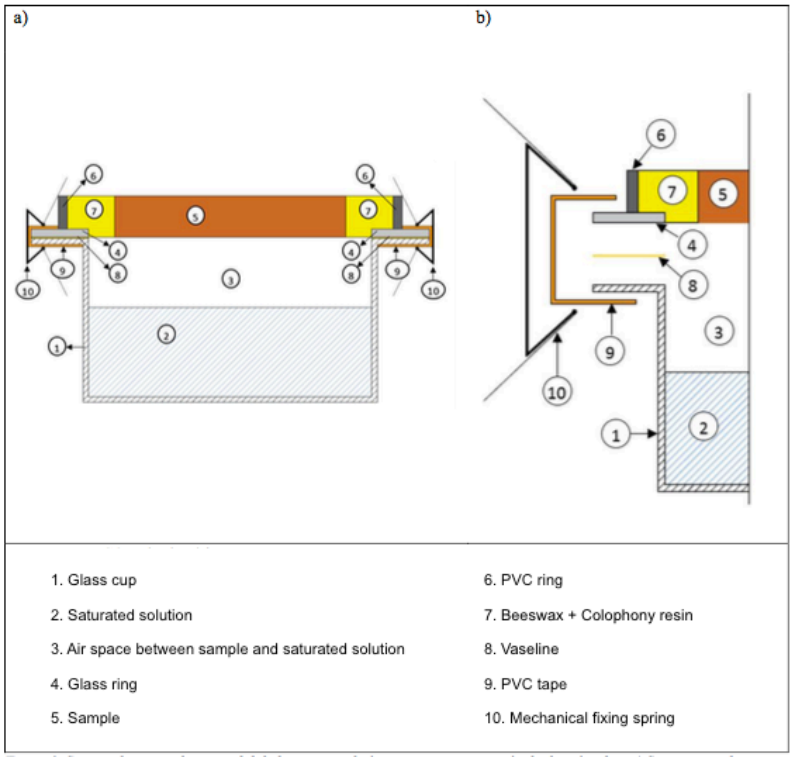

Figure 3.18 – Moisture permeability's cup sketch [88]

Figure 3.19 – Water bath used to melt the mix of beeswax and colophony resin

a) b)

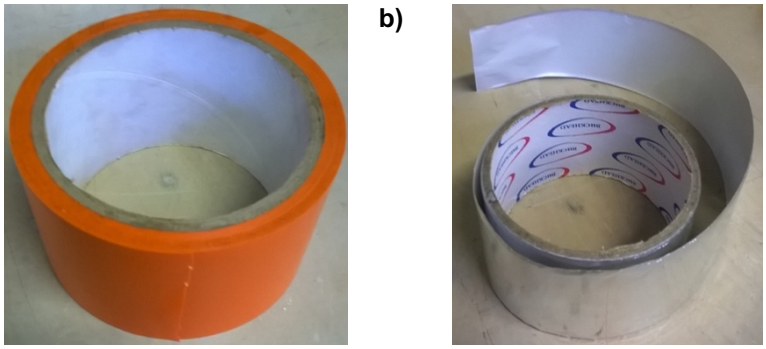

Figure 3.20 – Tapes used on moisture permeability experimental trial

Figure 3.21 – Glass ring covering

Figure 3.22 – Example of the system already covered

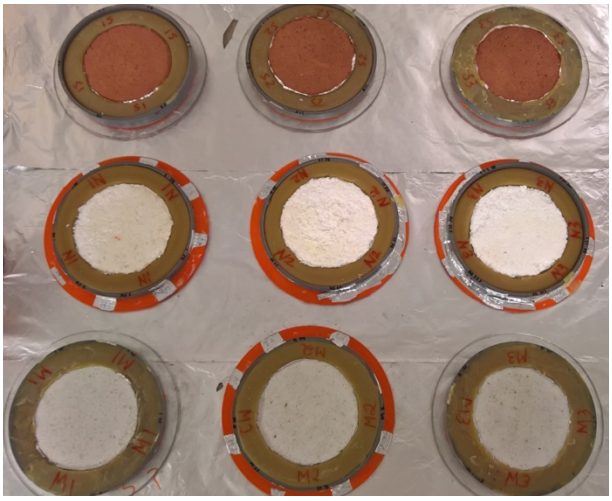

Figure 3.23 – All samples for moisture permeability's experimental trials

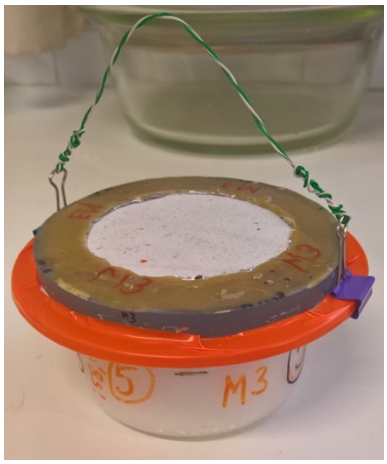

Figure 3.24 – Example of a complete cup system

To avoid some moisture crosses the joint between the glass ring and the cup, as it is visible in Figure 3.18 and Figure 3.24, the joint has to be filled with Vaseline and covered with PVC tape, because both are tight to moisture flux. In order to provide an extra system to make the joint tight to moisture flux, both glass ring and glass cup are pressed against each other by a mechanical fixing spring.

All samples were preconditioned in the climatic chamber at 43% of relative humidity and 23ºC, before the beginning of experiment, which the first level is 33% of RH in chamber and 53% RH inside cup. This value of 43% RH was chosen since it is the mean RH, of the first test, between inside cup and the chamber. It was made only one preconditioning, once all RH levels was followed by each other, giving no space to put the samples again in climatic chamber.

Experimental trial

Moisture permeability tests followed the standard ISO 12572 [17], which forces the utilization of thickness measuring equipment with a minimum precision of ±0,5% or a minimum measurement of 0,1 mm. The test has to use an analytical scale with resolution of 0,001 grams or, for heavier systems, 0,01 grams, which is putted inside isothermal chamber with a removable opening, which allows to make the weighing during the test. The chosen one was KERN PLJ 1200-3A (Figure 3.12), with all of its information presented in 3.3.1, and it was situated above a system trail which allows to move the scale from one isothermal chamber to another (Figure 3.25). The temperature should be maintained at

23±0,5ºC and the relative humidity should be the one of the present level ±3% of RH. Both temperature and relative humidity was always being monitored, using the sensors (Figure 3.11), as explained at 3.3.1.

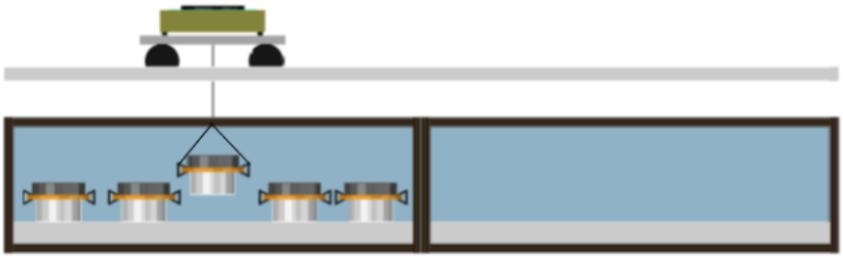

Figure 3.25 – Exemplification of whieghing system [88]

As requested by the standard, the air velocity above the samples were always between 0,2 and 0,3 m/s, measured with airflow equipment (Figure 3.14). This ventilation is made by two fans, which are located in extreme points of the back surface of chamber.

The height of the saturated solution was always bigger than the 15 mm requested in standard, and the gap of air between the sample and the saturated solution was always 20 mm, 5mm more than the minimum accepted. The sketch of cup's system, with the respective dimension, is represented by Figure 3.26.

Samples' dimensions fulfilled all the requirements of the standard.

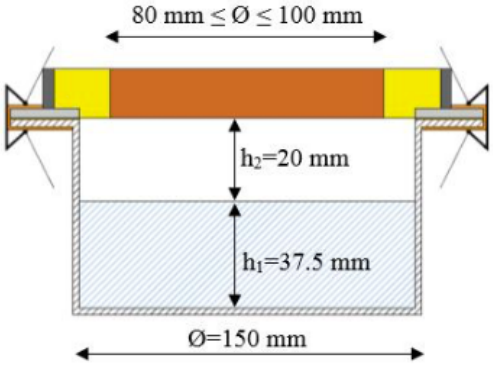

Figure 3.26 – Cup's system sketch with its dimensions [88]

Both inside cup and chamber's relative humidity are achieved by using saturated solutions, which are composed by salt that is hyper saturated with distilled water. These solutions are capable to produce certain values of RH, and all information about the solutions are present in Table 3-2.

Table 3-2 – Salt saturated solutions [17]

Salt		Relative Humidity (at 23ºC) [%]
Name	**Formula**	
Magnesium chloride hexahydrate	$MgCl_2 \cdot 6H_2O$	33%
Magnesium nitrate hexahydrate	$Mg(NO_3)_2 \cdot 6H_2O$	53%
Sodium chloride	$NaCl$	75%
Potassium chloride	KCl	85%
Potassium nitrate	KNO_3	94%

In order to validate both saturation solution and the isothermal chamber, it was made a comparison between the relative humidity that saturation solutions should produce and the relative humidity measured by the sensors and verify if it maintains more and less constant (Figure 3.27).

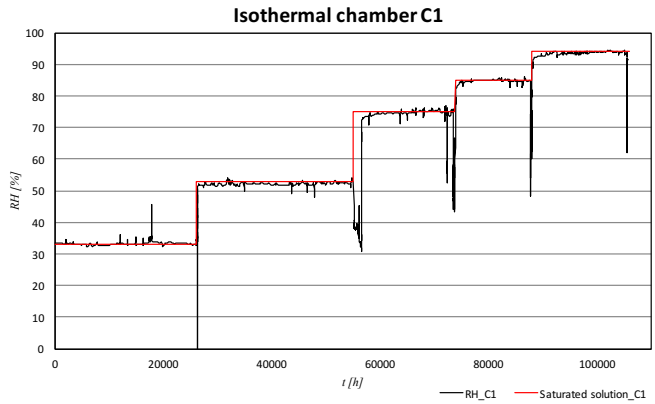

Figure 3.27 – Comparison between expected and real values of realtive humidity inside isothermal chamber C1

The process to validate the saturated solutions and isothermal chamber was made during all moisture permeability tests. By Figure 3.27, it is easy to understand that the saturation solutions produced the expect values and the isothermal chamber was capable to maintain the relative humidity inside. It is important to refer that the peaks of RH, inside each level, is due to the room was not capable to maintain constant values of temperature, and the sudden dropping of RH values is justified by the opening of chamber, to change the level of relative humidity. In conclusion, both saturated solution and isothermal chamber are validated.

There were chosen multiple combinations of relative humidity inside cup and in chamber, in order to fulfil a high range of relative humidity. As so, six different combinations of relative humidity inside and outside cup were used, as described in Table 3-3.

Table 3-3 – Combinations of relative humidity inside and outside cup to moisture permeability tests

Combination number	RH inside cup [%]	RH outside cup [%]	Mean RH [%]
1	53	33	43
2	75	33	54
3	85	33	59
4	85	53	69
5	85	75	80
6	94	85	89,5

It is important to refer that, the higher values of relative humidity were always placed inside cup, since the used sensors to measure relative humidity and temperature are sensible to extreme values of relative humidity and also to simulate the transfer of moisture from indoor to outdoor through the rough surface, which is always faced to the interior of cup.

The saturated solution, that was used to condition the RH of chamber's environment, was placed into four trays (Figure 3.28), with a height of 4 cm to 33% and 53% of relative humidity saturated solution, and of 1,5 cm to the saturated solution utilized to condition RH to 85%, as required from the standard [17].

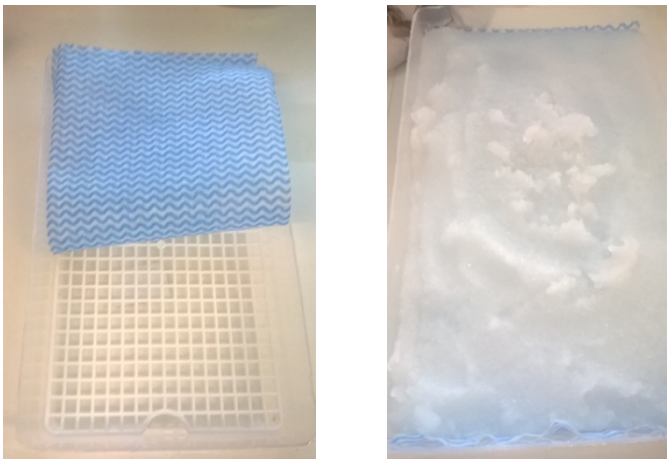

Figure 3.28 – Saturated solution placed into trays

The weighing should be made until one of the three following requirements is achieved:

- Requirement number 1: Five consecutive determinations of change in mass per weighing interval for each test specimen are constant within ± 5% of the mean value for this specimen (or ± 10%, if μ>750000);
- Requirement number 2: Change in weight of the cup assembly exceed 100 times the repeatability of the weighing procedure;
- Requirement number 3: In cup test, the weigh lost achieve half of initial inside saturated solution mass.

The weighing interval between consecutive was, approximately, 24 hours.

The chamber with all samples inside, as well as the trays with saturated solution and all the equipment involved on the present test, are represented in Figure 3.29.

Figure 3.29 – Isothermal chamber C1

3.3.4. Thermal Conductivity

Introduction

As the control of interior temperature of buildings by coating materials is one of the main subjects of the present Master's thesis, makes sense to study the thermal behavior of those materials.

The most usual tests to know the thermal characterization of an element, are based on international or European standards [92] [93] [94] [95], that recommend to make the thermal conductivity measurements at a fix relative humidity and temperature (most usual is 50±10% of RH and 23±1ºC). However, to understand the impact of the moisture content on thermal conductivity and discover how prejudicial is the good moisture hygroscopicity of materials in its thermal conductivity, it is important to measure thermal conductivities in function of RH.

None international standard is already defined to the present test, what makes that the results of thermal conductivity depending on moisture content may not be comparable by different works, due to laboratory conditions and also to the difference of the adopted process.

The experimental trial gives the thermal conductivity of each sample at different relative humidity levels. However, by the adsorption/desorption isotherm trial it is possible to relate the thermal conductivity with moisture content of each material.

Preparation of samples

The used samples were exactly the same of the ones used in adsorption/desorption isotherm experimental trial (3.3.2), because both experiments were made at the same time.

The chosen materials were recycled cellulose board M, projected cellulose coating N, wood wool cement board O and clayish earth plaster S. Each material had three samples, what makes a total of twelve samples to be tested (Figure 3.35).

A single care existed, that was that the surface in which the equipment would be in contact had to be uncovered, in order to does not influence the measurements of thermal conductivity.

Experimental trial

As mentioned above, there is not any international standard to the present experimental trial, what made that a procedure had to be defined. As the main goal is to know the thermal conductivity of the samples at each level of relative humidity, it was important that the samples would reach an equilibrium. For that, and as the present test occurred at the same time of adsorption/desorption isotherm one, with the same samples and in the same chamber, it was decided that the equilibrium proposed in the standard of adsorption/desorption isotherm test [3] totally fulfil the demand of the author. As so, the present test was always made after the equilibrium in moisture content and in mass was achieved (requirements of equilibrium are present in 3.3.2).

Since the utilized apparatus (ISOMET 2104) provide the measurements of thermal conductivity with a single probe, which emits heat to the interior of the samples and measure how much crossed the sample and how much did not, it is important that the samples when being tested be placed above an insulation material (Figure 3.30) to avoid exaggerated heat losses from the surface in touch with insulation. The chosen insulation was extruded polystyrene (XPS) with a considerable thickness (about 30 mm).

Figure 3.30 – Thermal conductiviy measurment

ISOMET 2104 has two probes, that make measurements at different ranges of thermal conductivity (Table 3-4). The choice of which probe would be used to each material was based in previous work's thermal conductivity measurements [80].

Table 3-4 – Thermal conductivity probes' selection

	M	**N**	**O**	**S**
Probe	API 210411	API 210411	API 210411	API 210412
Thermal conductivity range	[0,04 – 0,3]	[0,04 – 0,3]	[0,04 – 0,3]	[0,3 – 2,0]

Both international and European standards of thermal conductivity test at steady-state (ISO 8301 [95] and EN 1946 [92] [93], respectively) recommended, for each sample, at least three measurements and, therefore, there were made three measurements of thermal conductivity for each sample, at each range of relative humidity.

3.3.5. Moisture Buffering Value (MBV)

Introduction

The concept of Moisture Buffering Value, among other concepts (e.g., moisture penetration depth or moisture effusivity), was created by Nordtest researchers [37] [38] with the main goal of better characterize the hygroscopic properties of materials.

The MBV is applicable to homogeneous materials, with a thin stagnant air layer, determined by the air velocity of the chamber/room. This concept is applicable to indoor covering materials, as well as furniture, books, textiles, or every material capable of adsorb moisture.

The Nordtest report divides MBV in two values, one theoretical and one practical. This approach allows to understand how those values varies from each other and how precise are the used experimental method. There are going to be explained both of concepts. First, for knowing theoretical/ideal MBV, it should be known the concept of moisture effusivity (b_m), that is equivalent to thermal effusivity (b). The concept of moisture effusivity intends to represent an increasing or decreasing of moisture content of a certain material, when it is subjected to an abrupt change of surface humidity. In a perfect case, this surface humidity change can be extended to an ambient air humidity change if can be considered that the convective mass exchanges tend to infinity or, in other words, that the air in contact with the material surfaces offer no resistance to moisture exchange. Therefore, moisture effusivity (b_m) is expressed by the following equation:

$$b_m = \sqrt{\frac{\delta * \rho * \xi}{p_{sat}}} \tag{3-8}$$

where δ is the moisture permeability [kg/(m.s.Pa)] from the permeability experimental trial (33%-75%), ρ is materials' density [kg/m^3], ξ is the specific moisture capacity [kg/(kg.RH)] and p_{sat} is the saturation pressure [Pa] which is a pressure associated to the air saturation limit.

As in some heat transfer analysis, it is possible to analyze the materials response to an abrupt change of humidity but it is also possible to know the materials behavior when exposed to harmonic variations. Those variations are represented in Figure 3.31, and are characterized by equal and repeated cycles, with an 8 hours length period as high humidity range and 16 hours length period of low humidity range (always 33% RH).

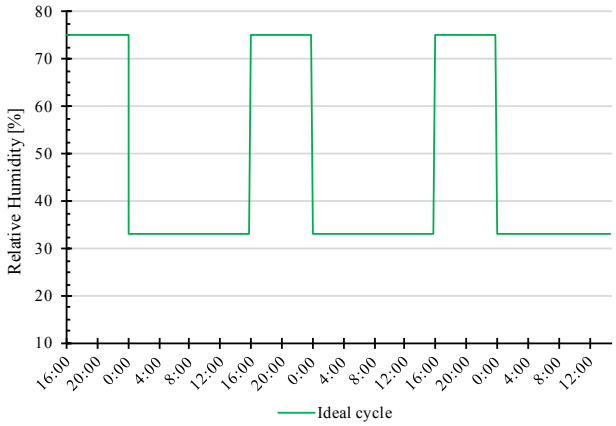

Figure 3.31 – Example of RH variation for MBV

Figure 3.31 only represents one of the four RH variations used on MBV experimental tests. As it is possible to see, it was used a signal function to experimental trials and, therefore it can be evaluated by the Fourier analysis. This analysis allows to predict the moisture flux in function of time and exposure, that throughs some surface of any material. This flux, that it is usually represented by g(t), enables to calculate another important concept: Moisture uptake/release G(t). This new concept is nothing more than the integration of g(t) and is expressed in kg/m^2:

$$\mathbf{G(t)} = \int_0^t g(t)dt = b_m * \Delta p * h(\alpha) * \sqrt{\frac{t_p}{\pi}} \quad [kg/m^2] \tag{3-9}$$

where Δp is the gradient of pressure [Pa], t_p represents adsorption/desorption time [hours] and α is the fraction time where humidity is placed in a high range.

For the chosen case, as periods of high RH has 8 hours of duration in a total of 24 hours (one day), so it makes that α takes a value of 1/3, that results in:

$$\mathbf{h(\alpha)} = \frac{2}{\pi} * \sum_{n=1}^{\infty} \frac{\sin^2(n * \pi * \alpha)}{n^{3/2}}$$
$$\mathbf{h\left(\frac{1}{3}\right)} = 1{,}007 \tag{3-10}$$

therefore, for this condition (α=1/3), G(t) can assume a simplifier equation:

$$\mathbf{G(t)} = 0{,}568 * b_m * \Delta p * t_p{}^{1/2} \quad [kg/m^2] \tag{3-11}$$

As so, Nordtest researchers decided to normalize Moisture uptake/release G(t) to make it to the known ideal Moisture Buffering Value. This normalization consists in divide the Equation(3-11) by the variation of Relative Humidity (RH), that originate ideal MBV:

$$\mathbf{MBV_{ideal}} \approx \frac{G(t)}{\Delta RH} = 0{,}00568 * b_m * p_{sat} * t_p{}^{1/2} \quad [kg/(m^2.\%RH)] \tag{3-12}$$

However, this ideal value is a rough approximation because, when the Equation(3-11) is divided by RH variation, a steady-state is assumed, which does not represent the real cases. However, this is an acceptable approximation and a dynamic analysis will be make later (using the software *Wufi Plus*), in order to fulfill all cases.

The calculation that is used to determine the MBV is the one that Nordtest researchers defined as practical MBV and it is traduced by the mean of difference of mass between adsorption and desorption phases on the stable cycle, per sample area and relative humidity difference of the respective trest, as it is shown in the following equation:

$$\mathbf{MBV_{practical}} = \frac{(m_8 - m_0) + (m_8 - m_{24})}{A * \Delta RH * 2} \quad [g/(m^2.\%RH)] \qquad (3\text{-}13)$$

There is a difference between practical MBV and ideal MBV, because the practical one was made to use in practice and it is relatively easy to calculate.

It is important to understand that the air in contact with the uncovered surface always influence the MBV because it offers some resistance to convective exchanges by the air to the sample's surface, and vice-versa. It is also good to know that ideal MBV and practical MBV will take similar values if the samples are composed by homogeneous material and if their thickness are equal or bigger than the penetration depth [38].

Moisture Buffering Value trial is divided in two periods, one of high RH and other of low RH. The high period of RH has an eight hours duration and intends to simulate presence of people at office, since it is the average working schedule of most people. Another example that MBV intends to simulate is a bedroom, because like working schedule, most people usually sleep eight hours per day. As such, MBV has a high RH period, with a duration of eight hours that simulate the human presence in a certain room, and a low RH period, with a sixteen hours duration, that simulate the absence of people.

The Moisture Buffering Value allows to understand the materials capacity to adsorb and store moisture present in the air when it is high, and, in other case, their capacity to release moisture when the moisture is low, in a dynamic cycle.

There are needed, at least, three samples of each material and those should be pre-conditioned at 50±5 % of Relative Humidity and 23±0,5 ºC, until two consecutives weighing, spaced by 24 hours, differs from each other less than 0,1% of the sample's mass.

For certify that the climatic chamber would work as the expected, Rocha, D. [80] monitored it with a RH and temperature sensors, obtaining the graphic represented in Figure 3.32.

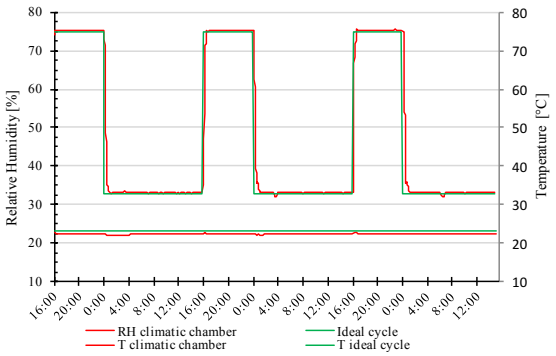

Figure 3.32 – Comparison between theoretical and practical cycles of RH and temperature of climatic chamber

As it is possible to see in Figure 3.32, the climatic chamber has a good behavior, having its theoretical and practical cycles of relative humidity and temperature almost coincident.

The MBV of materials can be classified by their ability to adsorb and release moisture of environment in five different levels, as shown in Figure 3.33.

$MBV_{practical}$ class	Minimum MBV level	Maximum MBV level
	[g/(m² % RH) @ 8/16h]	
Negligible	0	0.2
Limited	0.2	0.5
Moderate	0.5	1.0
Good	1.0	2.0
Excellent	2.0	...

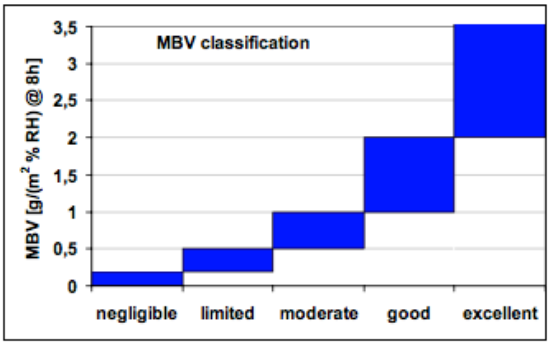

Figure 3.33 – MBV classification [38]

Preparation of samples

Moisture Buffering Value experiments were made to understand the capacity of coating materials to adsorb and release moisture. Then, it was chosen to use all the materials described in 3.2, except EA and NHL, due they all have a good hygroscopic behavior. In consequence, as Nordtest protocol [38] required, had to be prepared three samples of each material, in a total of twelve.

Both preparation of samples and the tests themselves always followed the protocol of Nordtest [38].

The shape and size of samples are not imposed, but it is recommended a rectangular shape and a minimum area of 0,01 m^2. The area should be determined with an accuracy of 1%.

The samples must have a similar thickness with their practical use, as a construction material, and it had to be bigger or equal to the penetration depth. For recycled cellulose board (M), projected cellulose coating (N) and wood wool cement board (O), as they were prefabricated, it was not necessary to choose a depth. However, as clayish earth plaster (S) were made by Rocha, D. [80], it was indispensable to select a depth, according to the regular thickness of clayish earth as a construction material. So, the selected thickness to each material (medium values), and that was equal to all samples of the same material, is placed in Table 3-5.

Table 3-5 – Thickness of samples

	Area [m^2]		Thickness [m]	
	Mean	Standard deviation	Mean	Standard deviation
M	0,01037	0,00025	0,01263	0,00000
N	0,01038	0,00018	0,01392	0,00078
O	0,01021	0,00009	0,02961	0,00056
S	0,01000	0,00000	0,01500	0,00000

M – Recycled cellulose board; **N –** Projected cellulose coating; **O –** Wood wool cement board; **S –** Clayish earth plaster

To limit the moisture exchanges to only one surface, it was needed to impermeabilities the samples. As so, the used vapor barrier had to be tight to moisture, as aluminum tape is. Thus, five of the six

sample surfaces were covered by aluminum tape (Figure 3.34), and the one surface uncovered had to be rough. The aluminum tape is used because it is tight to moisture and it has an excellent hydrophobia behavior [78].

Figure 3.34 – Samples' covering with aluminum tape

All of the used samples are represented in Figure 3.35, and they were used not only in MBV experimental trials, but also in the tests of adsorption/desorption isotherm, thermal conductivity and response time.

Figure 3.35 – Samples used on experimental trials of MBV, adsorption/desorption isotherm, thermal conductivity and response time

Experimental trials

The experiments followed Nordtest protocol [38], uding three different relative humidity ranges of the low humidity cycle, meanwhile the high humidity cycle maintained constant in all of three tests. Therefore, it was chosen to make the test at other ranges of low and high humidity, that are represented on Table 3-6, in order to understand how does the interval of relative humidity affects MBV:

Table 3-6 – RH range used in MBV trials

MBV number	Low RH (%)	High RH (%)
1	33	75
2	50	75
3	60	75

For each cycle of MBV, the temperature should be 23±0,5 ºC and the RH changes between the high and low values should be made in a smaller period than thirty minutes. These exchanges fulfilled the thirty minutes period, like it is possible to see in Figure 3.32.

The Nordtest protocol [38] required that the air velocity inside the chamber should stay between 0,05 and 0,1 m/s. The measurements with an anemometer (Figure 3.14) showed that the air velocity inside climatic chamber complied these standard values.

The tests began with the cycling exposure of samples to high and low relative humidity (8 hours in high RH and 16 hours in low RH) until occurs the two following conditions:

- Requirement number 1: Mass change between the last three cycles is less or equal to 5% in mass;
- Requirement number 2: Difference between adsorption and desorption mass change, of each cycle, is less or equal to 5% in mass.

It was made one weighing on every transition between the high and low RH cycles. In other words, before the constant mass was achieved, there were made two weighing in each day.

When the above requirements occurred, the final cycle was made. At the final cycle, five weighing more than the normal cycle were made, being that these were spaced from each other by one hour and half, except the gap between the last two, that was one hour.

With the weighing made at the final cycle, it was possible to calculate the practical MBV by Equation(3-13), knowing that for every samples of every materials the considered exposed area was 0,01 m^2, in consequence of the samples had quadrangular form, with each side equals to 0,1 m.

3.3.6. Experiment of classroom

Introduction

The ability of materials to control the indoor relative humidity and temperature is directly related to their ability to adsorb and release moisture from it. This ability of materials to control interior environment can be determined by experimental trials and then extrapolated to a real application. However, experimental trials are made with controlled environment and usually in a steady state, not considering the dynamic changes of interior climate. Therefore, it is important to understand the real response of coating materials when exposed to real room in use.

The response of materials to real climate of indoor can be determined by their moisture content variations, that represents the exchanges of moisture with environment. For that, the values of moisture content may be determined by Equation(2-8) [kg/kg - %] or Equation(2-10) [kg/m^3].

Preparation of samples

The chosen samples for the present test were made in a way of having the response of materials with different characteristics. For that, two samples of each material were chosen. The materials utilized in the present experimental trial were finished stucco EA, recycled cellulose board M, projected cellulose coating N, natural hydraulic lime mortar NHL and clayish earth plaster S, that are represented in Figure 3.36.

Figure 3.36 – All samples used on experiment of classroom

In Table 3-7 is possible to see the geometric characteristics of the selected samples.

Table 3-7 – Dimension of samples used in experiment of classroom

	Area [m^2]		Thickness [m]	
	Mean	**Standard deviation**	**Mean**	**Standard deviation**
EA	0,0108	9,2E-05	0,0169	1,2E-04
M	0,0100	7,1E-06	0,0126	4,8E-05
N	0,0101	2,3E-04	0,0288	6,2E-04
NHL	0,0108	2,3E-05	0,0154	2,3E-04
S	0,0101	1,4E-04	0,0304	3,5E-04

EA – Finished stucco; **M –** Recycled cellulose board; **N –** Projected cellulose coating; **NHL –** Natural hydraulic lime mortar; **S –** Clayish earth plaster

As it is possible to see in Figure 3.36, the samples have five of their six surfaces covered by aluminum tape, which make that the exchanges of moisture, between samples and interior environment are only made by the uncovered surface.

Experimental trial

The present experimental trial intends to quantify not only the response of coating materials to a real indoor environment, but also to understand how does relative humidity varies in time.

To the present test, the samples were placed in a classroom (Figure 3.37), which has variations of relative humidity, temperature, moisture production and air exchange rate. The temperature inside classroom varies over the day, according to the temperature of exterior. The moisture production varies according the number of people inside the room, as well as the artificial illumination and equipment. Relative humidity can vary with moisture content of air and its temperature, which are two parameters that change along the day. The air exchange rate has dynamic behavior, since it depends of opening windows and doors, that varies over a day. The chosen classroom was the one with longer period of classes and people inside it, over a day, in order to increment the variations of materials' moisture content. The class is placed in Department of Civil Engineer (DEC) of Faculdade de Ciências e Tecnologia – Nova University of Lisbon, and it has a rectangular form, with an area of 11x6,55 m^2, and a height of 3 m.

Figure 3.37 – Classroom

To be possible to understand how the samples respond to indoor environment, they were weight right before and after the classes period, every day. Therefore, the samples were weight, every day at 09h30±30 minutes and 18h30±30 minutes. Dry mass of materials could not be determined due to external factors to the present work. However, as the samples were pre-conditioned during a week at 53% of relative humidity, in climatic chamber (Figure 3.8), the reference mass was the mass quantified at 53% of RH, after the pre-conditioning period. Thus, the moisture content of materials was always determined considering the reference mass determined after the pre-conditioning period.

The environment of classroom was monitored by sensors (Figure 3.11) and the weighing of samples were made with KERN PLJ 1200-3A scale [89] (Figure 3.12), and both have all of their characteristics presented on 3.3.1.

The period of the test was chosen in order to be highly representative of a real indoor environment of a building and, as so, the classroom test was made during two and half months.

3.3.7. Response Time

Introduction

The time that a material takes to achieve its equilibrium is difficult to quantify in cyclic experimental trials, like MBV, and it is intrinsic to each material. This time is an important factor to the choice of coating materials, since materials that are quicker to reach the equilibrium, are good to short cycles of relative humidity. However, instead of short cycles, can be necessary to damp long cycles of relative

humidity. That is, the ability of coating materials to adsorb moisture from the environment in summer and release it back only in winter can be very important to buildings.

The present experimental trial does not have any standard and it just limits itself to see how much time does a certain sample takes to achieve the equilibrium moisture content, by measuring its mass.

Preparation of samples

The used samples were the same of other tests (MBV, adsorption/desorption isotherm and thermal conductivity) and, because of that, all the procedure of their preparation can be seen in 3.3.5.

Experimental trial

As mentioned above, the present experimental trial does not have any international standard. However, this test has a similar form to the adsorption/desorption isotherm one, once it looks for understand how much time do the materials take to adsorb/release moisture from environment and achieve their equilibrium.

The test was made in isothermal chamber C1 (Figure 3.29), that guarantees that the relative humidity inside maintains almost constant (Figure 3.27).

The tests consist in, after the samples achieve the equilibrium at 33% of relative humidity (it does not count to test), the environment is changed to 75% of RH and then, the time that materials take to reach the equilibrium is measured. After this equilibrium be achieved, the environment is changed to 33% of RH, and again the time in which the samples take to achieve their equilibrium is quantified. It is important to refer that the test was made at 23 $\pm$ 0,5ºC.

The test longs until two requirements are fulfilled. These two are the requirements of adsorption/desorption isotherm experimental trial and they are the following:

- Requirement number 1: Change of mass between three consecutive weighing, each made at least 24 hours apart, is less than 0,1 % of the total mass;
- Additional requirement: Change of moisture content between three consecutive weighing, separated from, at least, 24 hours, is less than 0,1% of the total moisture content.

The test consists in making more weighing in the beginning, in order to represent better the part of the curve that is more vertical, due to the process of adsorption or desorption be faster on that section. For that, the weighing made in this test are spaced by different time intervals, represented on Table 3-8.

Table 3-8 – Time interval of successive weighing of response time test

Time range [h]	Time interval between successive weighing [h]
$0 \leq h \leq 9$	1
$24 \leq h \leq 32$	4
$32 \leq h \leq$ end of test	24

3.3.8. Use of materials

Although there is a large quantity of experimental trials, there were not used all materials in all tests. This because the classroom's test was the one that last more and, due the fact that there were a limited number of samples of some materials, it was not possible to use all materials in all experimental trials. Therefore, the table below (Table 3-9) shows in which test was used each of the chosen materials for the present dissertation, described (above) on this chapter.

The following table shows the utilization of materials in the tests, in order to synthetizes the present chapter:

Table 3-9 – Use of materials

Experimental trial	Materials					
	EA	***M***	***N***	***NHL***	***O***	***S***
MBV	-	✓	✓	-	✓	✓
Moisture Permeability	-	✓	✓	-	-	✓
Experiment of classroom	✓	✓	✓	✓	-	✓
Adsorption/Desorption Isotherm	-	✓	✓	-	✓	✓
Thermal Conductivity	-	✓	✓	-	✓	✓
Response Time	-	✓	✓	-	✓	✓

Chapter 4: Analysis of results

4.1. General considerations

One of the main materials characteristics that affects the ability of materials to control indoor relative humidity and temperature is the porosity and it should be known for the chosen materials of the present work. However, porosity has already been calculated in a previous work by Rocha,D. [80], for some of the same samples used on the present dissertation, and those values of porosity are placed in Table 4-1.

Table 4-1 – Density and porosity (adapted from [80])

	Density [kg/m^3]		Porosity [%]	
	Mean	Standard deviation	Mean	Standard deviation
M	1038,91	34,34	55,06	1,51
N	183,35	13,93	83,15	1,52
O	879,35	11,76	51,57	1,03
S	2027,17	52,41	11,44	4,84

M – Recycled cellulose board; **N –** Projected cellulose coating; **O –** Wood wool cement board; **S –** Clayish earth plaster

4.2. Adsorption/Desorption Isotherm

The process of adsorption and desorption of moisture by coating materials is related with the porosity and pores dimensions of materials. As so, the porosity was calculated in [80] (Table 4-1) for the same samples used in this work and, due to some problems on pores size's apparatus, it was not possible to know the size of pores.

As it is possible to see in Table 4-1, projected cellulose coating (N) is the material that eventually will have less hysteresis, because is the one that have more porosity and maybe higher pores dimensions and so it has bigger evaporation of moisture. In the same way, it is expected that clayish earth plaster (S) have the biggest influence of hysteresis phenomenon because it is the material, among all studied, that has less porosity and, as so, less evaporation.

The results of adsorption/desorption isotherm test are present in Table 4-2 and Table 4-3.

It was chosen to present the results of moisture content by *u* [kg/kg - %] (Table 4-2) and *w* [kg/m^3] (Table 4-3) because *u* is the most common way to represent moisture content and so to compare with other results. It was chosen to present moisture content also by *w* because it is an easier way to understand how much kilogram of moisture is inside of one cubic meter of some coating, and also because it is the parameter that can be inputted on the software of hygrothermal simulation, used in Chapter 6.

The values present in Table 4-2 originate the charts of Figure 4.1 to Figure 4.4.

Table 4-2 – Moisture content of adsorption/desorption isotherm in *u* [kg/kg - %]

	RH [%]	Moisture content *u* [kg/kg - %]							
		M		N		O		S	
		Mean	Standard deviation	Mean	Standard deviation	Mean	Standard deviation	Mean	Standard deviation
Adsorption	33%	0,81	0,025	2,57	0,099	3,00	0,081	0,38	0,010
	53%	1,08	0,031	4,00	0,160	3,60	0,084	0,53	0,011
	75%	1,61	0,048	7,18	0,244	4,89	0,119	0,84	0,007
	85%	1,81	0,034	8,85	0,313	5,25	0,104	0,94	0,012
	94%	2,28	0,021	12,18	0,398	6,38	0,098	1,22	0,012
Desorption	85%	1,97	0,026	9,12	0,310	5,88	0,099	0,96	0,014
	75%	1,69	0,030	6,95	0,242	5,38	0,089	0,78	0,011
	53%	1,22	0,031	4,15	0,139	4,32	0,081	0,46	0,011
	33%	0,84	0,029	2,38	0,090	3,30	0,084	0,22	0,015

M – Recycled cellulose board; **N –** Projected cellulose coating; **O –** Wood wool cement board; **S –** Clayish earth plaster

Table 4-3 – Moisture content of adsorption/desorption isotherm in *w* [kg/m^3]

	RH [%]	Moisture content *w* [kg/m^3]							
		M		N		O		S	
		Mean	Standard deviation	Mean	Standard deviation	Mean	Standard deviation	Mean	Standard deviation
Adsorption	33%	9,26	0,288	5,06	0,195	14,17	0,384	8,05	0,214
	53%	12,34	0,351	7,87	0,314	17,03	0,397	11,43	0,242
	75%	18,41	0,552	14,12	0,479	23,14	0,563	17,91	0,145
	85%	20,62	0,387	17,39	0,616	24,82	0,491	20,13	0,252
	94%	26,00	0,241	23,93	0,783	30,17	0,465	26,15	0,267
Desorption	85%	22,49	0,299	17,93	0,610	27,81	0,470	20,52	0,302
	75%	19,25	0,341	13,66	0,476	25,43	0,421	16,78	0,230
	53%	13,90	0,359	8,16	0,274	20,44	0,383	9,88	0,239
	33%	9,58	0,332	4,68	0,178	15,60	0,397	4,74	0,327

M – Recycled cellulose board; **N –** Projected cellulose coating; **O –** Wood wool cement board; **S –** Clayish earth plaster

Equation(4-1) allows to convert moisture content from *u* [kg/kg - %] to *w* [kg/m^3].

$$w = \rho_{dry} * \frac{u}{100} \quad (4\text{-}1)$$

where ρ_{dry} is dry density [kg/m^3].

The values of Table 4-2 and Table 4-3 are expressed in graphs, represented by Figure 4.1 to Figure 4.4. In these figures are represented the experimental values of moisture content in equilibrium, obtained by present dissertation's experimental trials, as well as the same graphs obtained to the same materials, made by Rocha, D., in a previous work [80]. Even both experiments were made with the same samples, the results may be different since the tests of the present dissertation had the RH conditioned by hyper saturated salty solutions and the experiments made in the previous work were made inside a climatic chamber. It is also important to refer that both experiments were made with different scales.

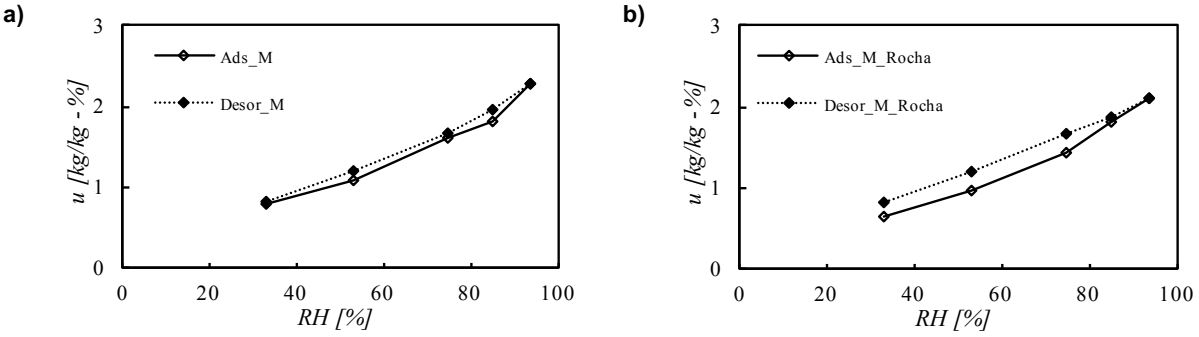

Figure 4.1 – Adsorption and desorption isotherm of recycled cellulose board (M)

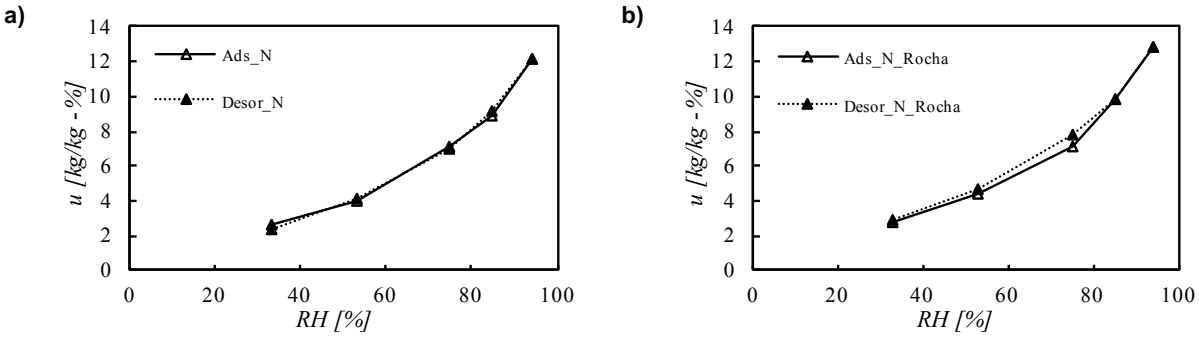

Figure 4.2 - Adsorption and desorption isotherm of projected cellulose coating (N)

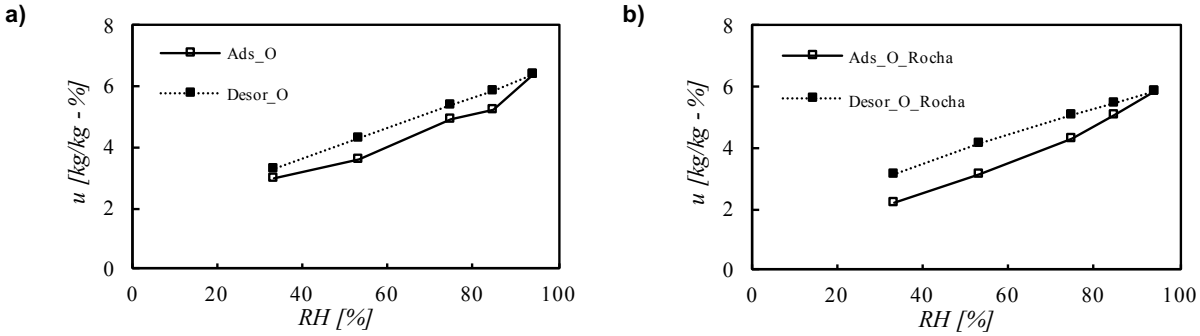

Figure 4.3 – Adsorption and desorption isotherms of wood wool cement board (O)

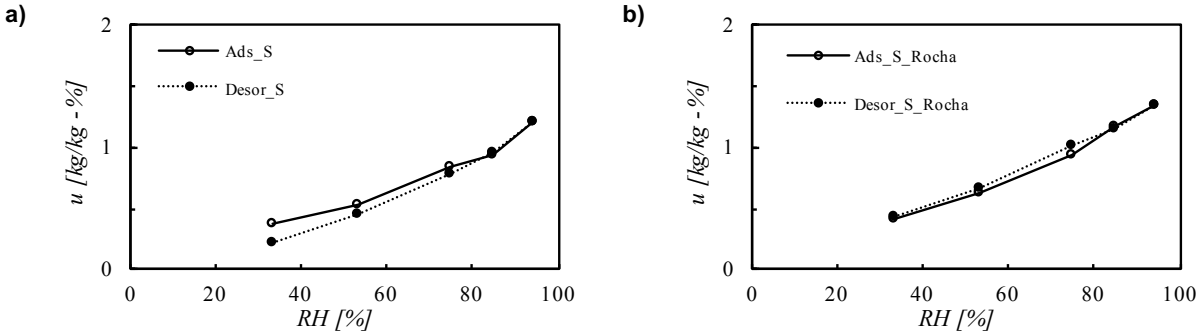

Figure 4.4 – Adsorption and desorption isotherms of clayish earth plaster (S)

As expected, projected cellulose coating (N) (Figure 4.2) has almost none hysteresis because it has a large percentage of porosity, which allows it quick evaporation. It is easy to understand that N should have large pores, what makes that the suction forces inside those be low and so facilitates the evaporation process.

From Figure 4.1 and Figure 4.3 it is clear that recycled cellulose board (M) has less hysteresis than wood wool cement board (O), although it is not a big difference, justified by recycled cellulose board's porosity is bigger than wood wool cement board one.

Clayish earth plaster (S) has an unexpected behavior, as it is possible to see in Figure 4.4, since it has the desorption isotherm bellow the adsorption one. It should be the opposite, since hysteresis phenomenon makes that remains more moisture inside of material, and not that releases more moisture than the initial moisture content. This behavior is not easy to explain and it suggests that happened some experimental errors and it could be influenced by the material have organic matter

that can influence both adsorption and desorption phenomenon. Therefore, it is recommended a repetition of this experiment for clayish earth plaster (S).

It is possible to see by all Figure 4.1 to Figure 4.4 that the values of moisture content in equilibrium obtained in present and previous works are similar, once both tests were made with the same samples. This behavior was the expected, except the desorption isotherm of clayish earth plaster S (Figure 4.4), since the one obtained in the present work reveled to have an unexpected behavior.

To compare all materials and conclude which one adsorb more moisture, the adsorption isotherms of all materials, that were obtained in the experimental trials of the present work, were placed in same graph (Figure 4.5).

Figure 4.5 shows that projected cellulose coating (N) is the material which adsorb more moisture and wood wool cement board (O) follows it at the lower relative humidity, since they are the materials which have more slope.

Recycled cellulose board (M) and clayish earth plaster (S) are the materials which adsorb less moisture due to having lower porosity (Table 4-1) among all materials. The fact of S has really low moisture content is the same: having few porosity (Table 4-1).

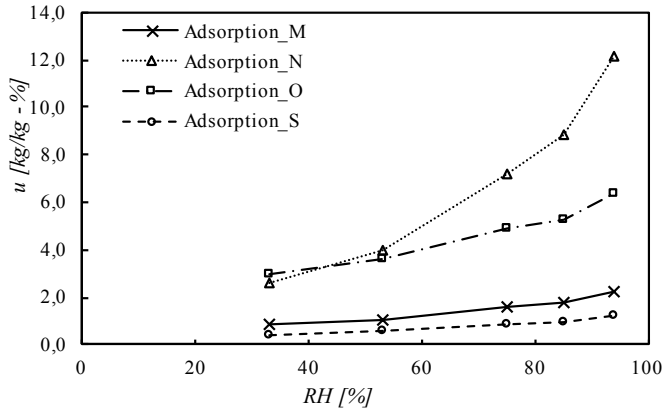

Figure 4.5 – All materials' adsorption/desorption isotherms

4.3. Moisture Permeability

The present experimental trial allows to understand how tight materials are to moisture. Moisture permeability is directly related with dimension of materials' pores. In other words, larger pores can originate higher moisture permeability.

The mean values of moisture permeability of all materials are placed in Table 4-4 and those values originate three different graphs, represented by Figure 4.6 to Figure 4.8, each one for one of the three materials studied in the present test. In all figure, there are placed graphs with moisture resistance factor at all RH ranges, in order to present the results in values that are related with moisture permeability of air, as it is possible to see by Equation(3-5). The values of moisture resistance factor are placed in Table 4-5.

Table 4-4 – Moisture permeability values of all materials

RH [%]			Moisture Permeability δ [kg/(m.s.Pa)] *10^{-11}					
			M		N		S	
Cup	Chamber	Mean	Mean	Standard Deviation	Mean	Standard Deviation	Mean	Standard Deviation
53	33	43	1,16	0,05	9,94	1,80	1,09	0,11
75	33	54	1,34	0,19	9,85	0,99	1,49	0,29
85	33	59	1,30	0,21	8,74	1,47	1,35	0,30
85	53	69	1,14	0,06	7,52	1,10	1,35	0,31
85	75	80	1,74	0,09	9,93	1,83	3,00	0,28
94	85	89,5	2,76	0,16	16,4	1,11	5,77	0,31

M – Recycled cellulose board; **N –** Projected cellulose coating; **S –** Clayish earth plaster

Table 4-5 – Moisture resistance factor of all materials, at all ranges of relative humidity

Mean RH [%]	Moisture resistance factor μ [-]					
	M		N		S	
	Mean	Standard Deviation	Mean	Standard Deviation	Mean	Standard Deviation
43%	16,89	0,55	2,01	0,31	18,11	1,37
54%	14,82	1,61	2,00	0,16	13,52	2,15
59%	15,29	1,88	2,29	0,34	14,92	2,37
69%	17,25	0,69	2,64	0,34	14,97	2,48
80%	11,28	0,45	2,02	0,33	6,56	0,49
89,5%	7,11	0,34	1,20	0,07	3,40	0,15

M – Recycled cellulose board; **N –** Projected cellulose coating; **S –** Clayish earth plaster

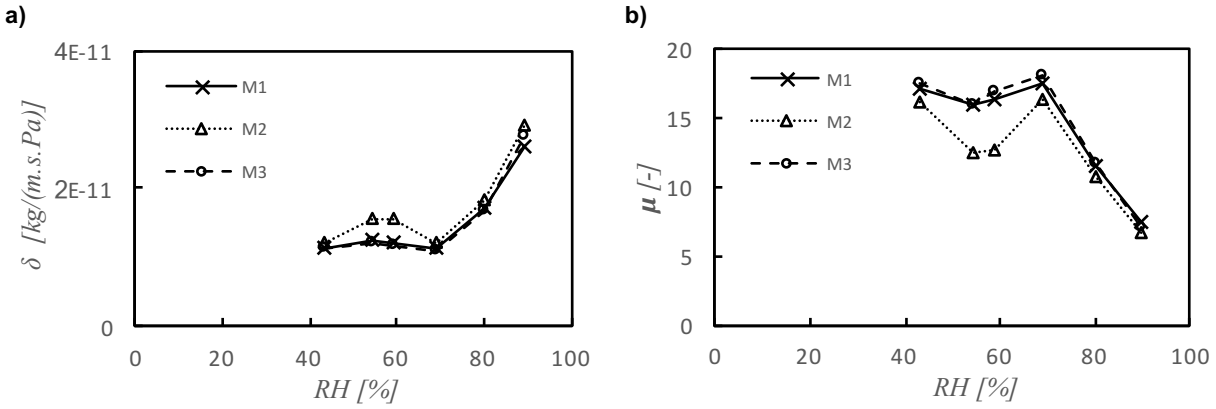

Figure 4.6 – Moisture permeability and moisture resistance factor of recycled cellulose board (M)

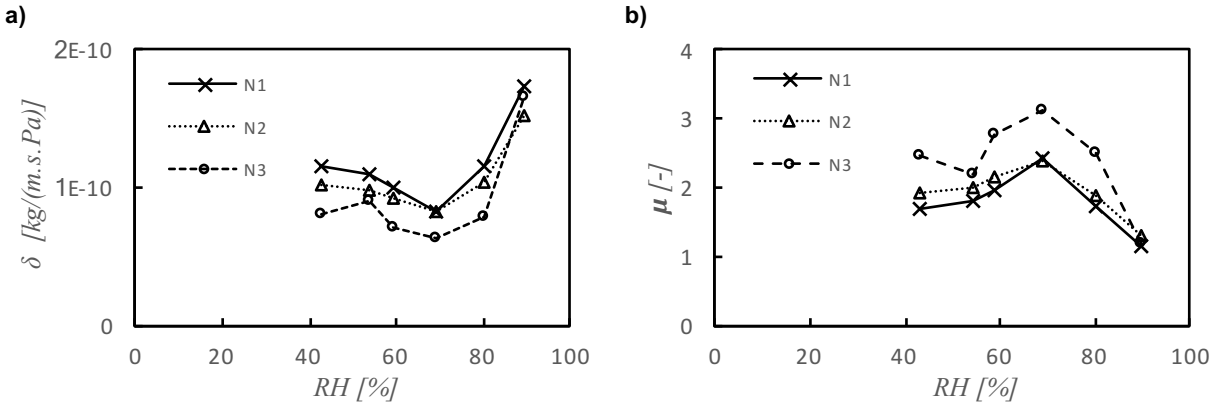

Figure 4.7 – Moisture permeability and moisture resistance factor of projected cellulose coating (N)

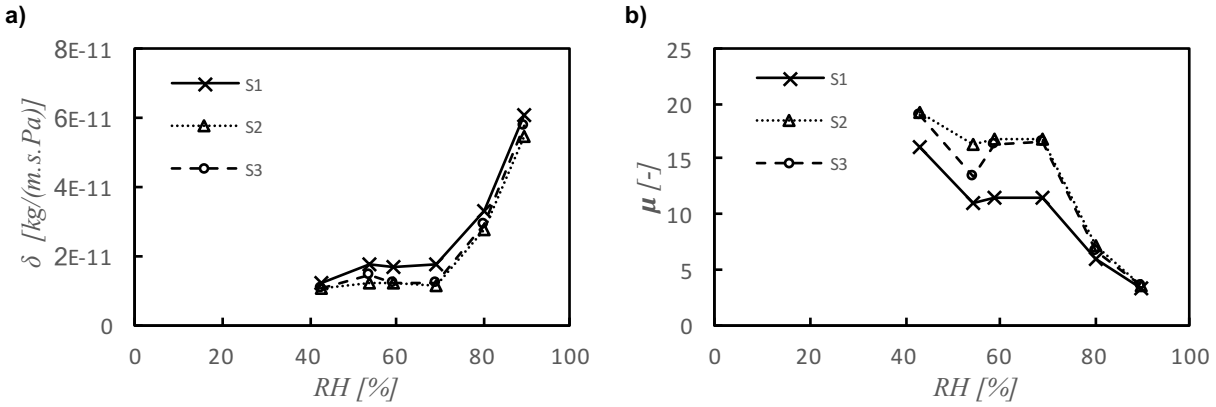

Figure 4.8 – Moisture permeability and moisture resistance factor of clayish earth plaster (S)

The graphs of moisture permeability of all materials (represented by Figure 4.6 to Figure 4.8) were placed together in a single graph (Figure 4.9), in order to be easier to compare all between each other.

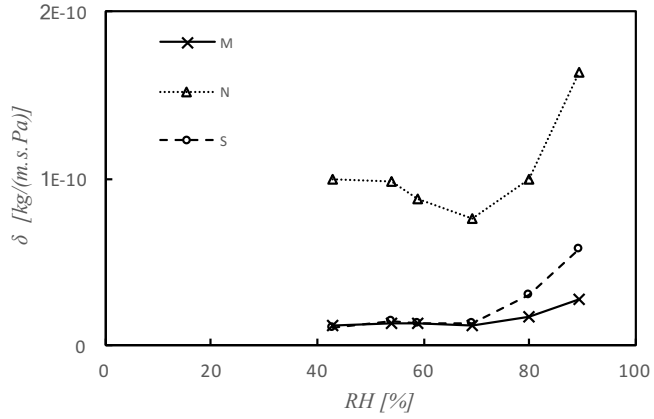

Figure 4.9 – All materials' moisture permeability

As it is possible to conclude by Table 4-1 and Table 4-4, higher porosity generates larger moisture permeability. An example of this is that, for any relative humidity, projected cellulose coating (N) is always the material with higher moisture permeability, because it is the one with biggest porosity. However, the material with lower porosity – clayish earth plaster (S) – is not always the material with

the lowest moisture permeability. This suggests that clayish earth plaster has lower dimension of pores than recycled cellulose board, which makes that clayish earth plaster's interstitial condensation begins at lower RH than recycled cellulose board one. As liquid flux increases then the global permeability to moisture will increase, and its division in vapor and liquid flux is explained later in the present chapter. The fact of the liquid flux increments the global permeability to moisture of materials justifies that clayish earth plaster (S) is more permeable to moisture than the recycled cellulose board (M), even S has less porosity than M. As it is possible to see by Table 4-7, even M has higher permeability to moisture at the first level of relative humidity (43% RH) than S, at the next level of RH (54 %), S already has higher permeability to moisture than M, that is a consequence of liquid flux.

The values of moisture resistance factor of all materials, presented in Figure 4.6 to Figure 4.8, shows an inverse behavior when compared with moisture permeability graphs. This happens due to the formula of moisture resistance factor, represented by Equation(3-5), which shows that moisture permeability and moisture resistance factor are inversely proportional related between each other. The values of moisture resistance factor of all materials were reunited in the same graph, Figure 4.10, in order to be able to compare them between each other. In the same graph are represented the values of equivalent air layer thickness of all materials, which have the same development with relative humidity increment of moisture resistance factor. The values of equivalent air layer thickness have similar behavior of moisture resistance one, since equivalent air layer thickness is directly proportional related with moisture resistance factor, like it is possible to see by Equation(3-6). The values of equivalent air layer thickness, that originate Figure 4.10, are placed in Table 4-6.

Table 4-6 – Equivalent air layer thickness of all materials, at all ranges of relative humidity

Mean RH [%]	Equivalent air layer thickness [m]					
	M		N		S	
	Mean	Standard Deviation	Mean	Standard Deviation	Mean	Standard Deviation
43%	0,214	0,009	0,025	0,004	0,229	0,014
54%	0,188	0,022	0,025	0,002	0,171	0,025
59%	0,194	0,025	0,029	0,004	0,188	0,027
69%	0,218	0,010	0,033	0,004	0,189	0,028
80%	0,143	0,007	0,025	0,002	0,100	0,009
89,5%	0,109	0,005	0,018	0,001	0,052	0,003

M – Recycled cellulose board; **N –** Projected cellulose coating; **S –** Clayish earth plaster

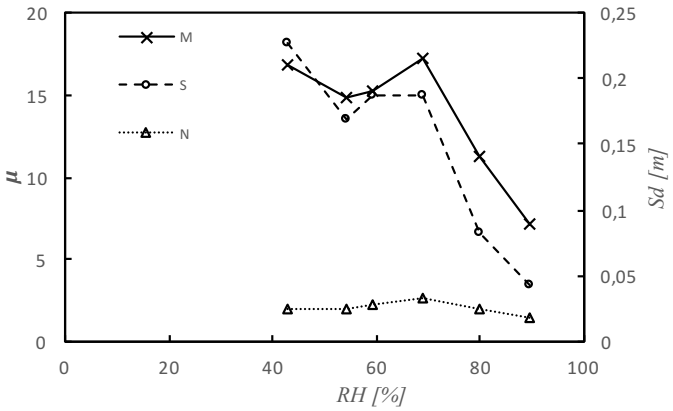

Figure 4.10 – Moisture resistance factor and equivalent air layer thickness of all materials

Separation of moisture flux in vapor and liquid forms

The separation of moisture flux into vapor and liquid forms is based in previous works [22] [23] [24] [25]. These works shown that the best equation to traduces the differential permeability of the generality of material takes the form of Equation(2-14). With this equation it is possible to assume that the "A" coefficient is the permeability to moisture in vapor form, and the rest of equation is the moisture permeability in liquid form [24], as shown in Equation(4-2).

$$g = -\delta * \Delta p_v = \left(\delta_{vapor} + \delta_{liquid}\right) * \Delta p_v = (A + B * \phi^C) * \Delta p_v \qquad (4\text{-}2)$$

It is known that the vapor form of moisture flux is not constant and decreases with the increment of relative humidity, as shown in Figure 2.12. However, it is a good approximation to consider that the vapor form of moisture flux is constant with RH [24], and it takes the value of coefficient "A" of Equation(2-14).

To find the best coefficients of Equation(2-14) for all three materials used in present work, a numerical analysis had to be made, making a non-linear regression of the experimental results, obtained by the test of moisture permeability made in the present dissertation. The numerical analysis, as well as all of its procedure, is explained in a forward chapter (5.2). The coefficients obtained in those non-linear regressions originated the values of liquid and vapor fluxes of moisture, placed in Table 4-7.

Table 4-7 – Flux division of all materials

Mean RH [%]	**Moisture Permeability δ [kg/(m.s.Pa)]**								
	M			**N**			**S**		
	Vapor (*10^{-11})	**Liquid (*10^{-13})**	**Both (*10^{-11})**	**Vapor (*10^{-11})**	**Liquid (*10^{-13})**	**Both (*10^{-11})**	**Vapor (*10^{-11})**	**Liquid (*10^{-13})**	**Both (*10^{-11})**
43	1,22	0,05	1,22	9,04	0,0002	9,04	1,19	0,63	1,20
54	1,22	0,62	1,22	9,04	0,0176	9,04	1,19	4,91	1,24
59	1,22	1,63	1,23	9,04	0,113	9,04	1,19	10,9	1,30
69	1,22	9,03	1,31	9,04	3,07	9,07	1,19	44,4	1,64
80	1,22	45,4	1,67	9,04	69,3	9,74	1,19	168	2,87
89,5	1,22	155	2,77	9,04	737	16,4	1,19	460	5,79

M – Recycled cellulose board; **N** – Projected cellulose coating; **S** – Clayish earth plaster

The Figure 4.11 shows the relation between porosity and vapor flux of moisture. As so, projected cellulose coating (N) is the material with higher porosity, what makes it the material with larger vapor flux (around 9E-11). Clayish earth plaster (S) is the material with less porosity and, as so, it is the material with less vapor flux (around 1,20E-11). However, as explain before, even S has less porosity to flux vapor than recycled cellulose board (M), S has a much bigger permeability to moisture, from 54% of relative humidity beyond, than M (as it is possible to see on Table 4-7).

The fact of recycled cellulose board M (Figure 4.11a)) and projected cellulose coating N (Figure 4.11b)) have sometimes the moisture permeability, obtained by experimental trials, lower that its division in liquid and vapor forms. This happens because, while considering the vapor form of moisture flux constant be a good approximation [24], the real vapor form of moisture flux decreases with relative humidity, which makes that there is an overestimation of the vapor form of moisture flux, although it is small.

The division of moisture flux in liquid and vapor forms allows to understand the reason because the moisture permeability have a few decreasing, until about 70% of RH, like it happens a little in recycled cellulose board M (Figure 4.11a)), but is more pronounced in projected cellulose coating N (Figure 4.11b)). This is justified by the vapor form of moisture permeability decreases with relative humidity and, in both cases, liquid form of moisture flux starts at high values of relative humidity, more pronounced in projected cellulose coating N (Figure 4.11b)), maybe suggested by its high dimensions of pores. This does not happen in clayish earth plaster S (Figure 4.11c)) because it may have low dimensions of pores, what makes that its interstitial condensation begins early, as well as its liquid form of moisture flux.

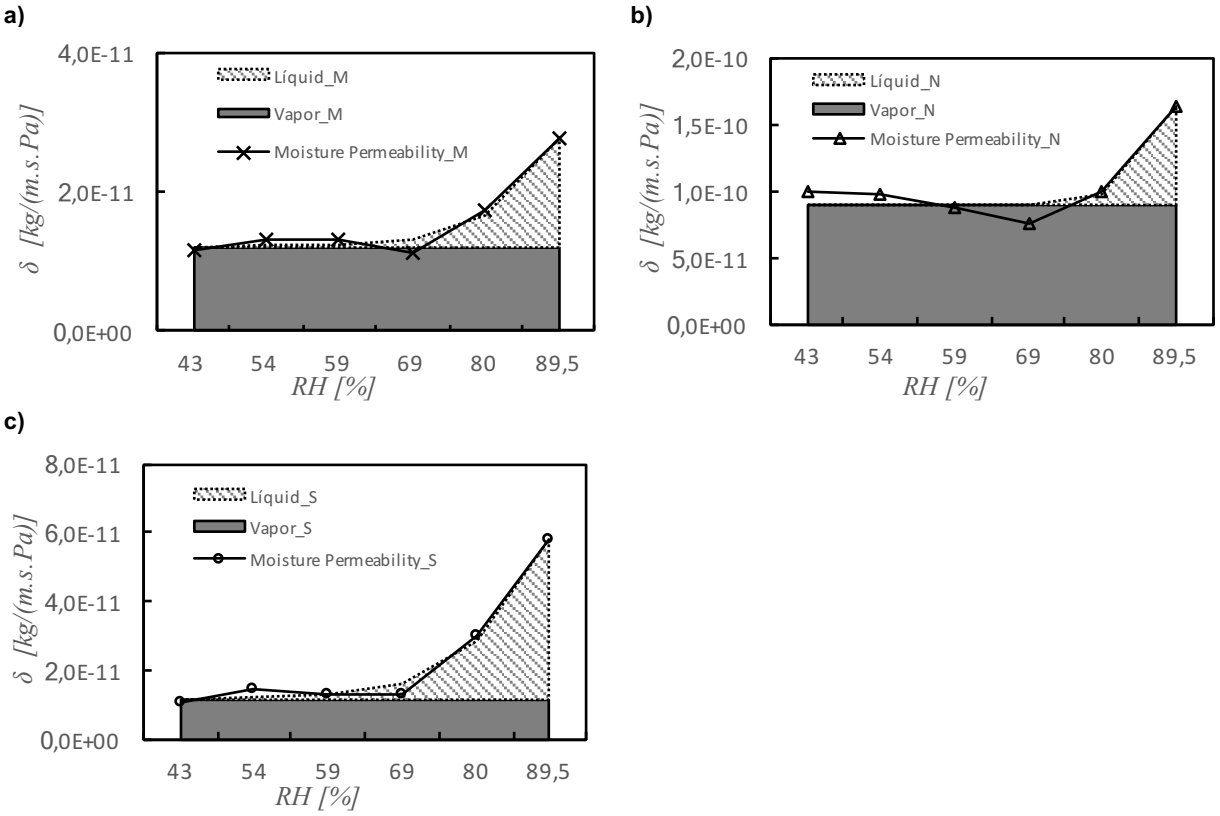

Figure 4.11 – Flux division of moisture permeability, for all materials

4.4. Thermal Conductivity

The present experimental trial was made to verify the influence of moisture content in thermal conductivity of materials. With the increment of moisture content, the pores so far filled with air, which has low thermal conductivity, are going to be gradually occupied by water in any form that will raise thermal conductivity of material.

From Table 4-8, it is possible to understand that, inside any relative humidity level, the thermal conductivity increases with density and with decreasing of porosity (see values at Table 4-1). This fact makes that clayish earth plaster (S) has the highest value of thermal conductivity and projected cellulose coating (N) the lowest.

During the experiment, both fans of isothermal chamber were switched off.

Table 4-8 – Thermal conductivity of all materials

RH [%]	Thermal conductivity λ [W/(m.ºC)]							
	M		N		O		S	
	Mean	Standard Deviation	Mean	Standard Deviation	Mean	Standard Deviation	Mean	Standard Deviation
33%	0,291	0,002	0,065	0,001	0,082	0,006	0,974	0,013
53%	0,289	0,003	0,069	0,002	0,083	0,004	0,984	0,022
75%	0,295	0,006	0,077	0,002	0,086	0,005	1,047	0,019
85%	0,306	0,005	0,080	0,002	0,091	0,007	1,110	0,009
94%	0,311	0,006	0,085	0,002	0,095	0,009	1,148	0,030

M – Recycled cellulose board; **N –** Projected cellulose coating; **O –** Wood wool cement board; **S –** Clayish earth plaster

The Table 4-8 originates the graphs represented by Figure 4.12. All graphs show that the materials' behavior, regarding the uptake of moisture, is the expected. This is, all graphs allow to understand that more moisture inside of samples' pores implies that thermal conductivity raises. However, recycled cellulose board (M) has thermal conductivity at 53% of relative humidity lower than at 33% of RH, maybe justified by the fact that the sequence of thermal conductivity measurements may have been different on those two levels of RH.

As it is possible to see by Figure 4.12 c), the values of thermal conductivity between the three samples of wood wool cement board (O) have significant discrepancy and the sample O3 have a strange behavior of thermal conductivity with variation of relative humidity. These two characteristics are justified by the fact that wood wool cement board (O) be much heterogeneous and anisotropic.

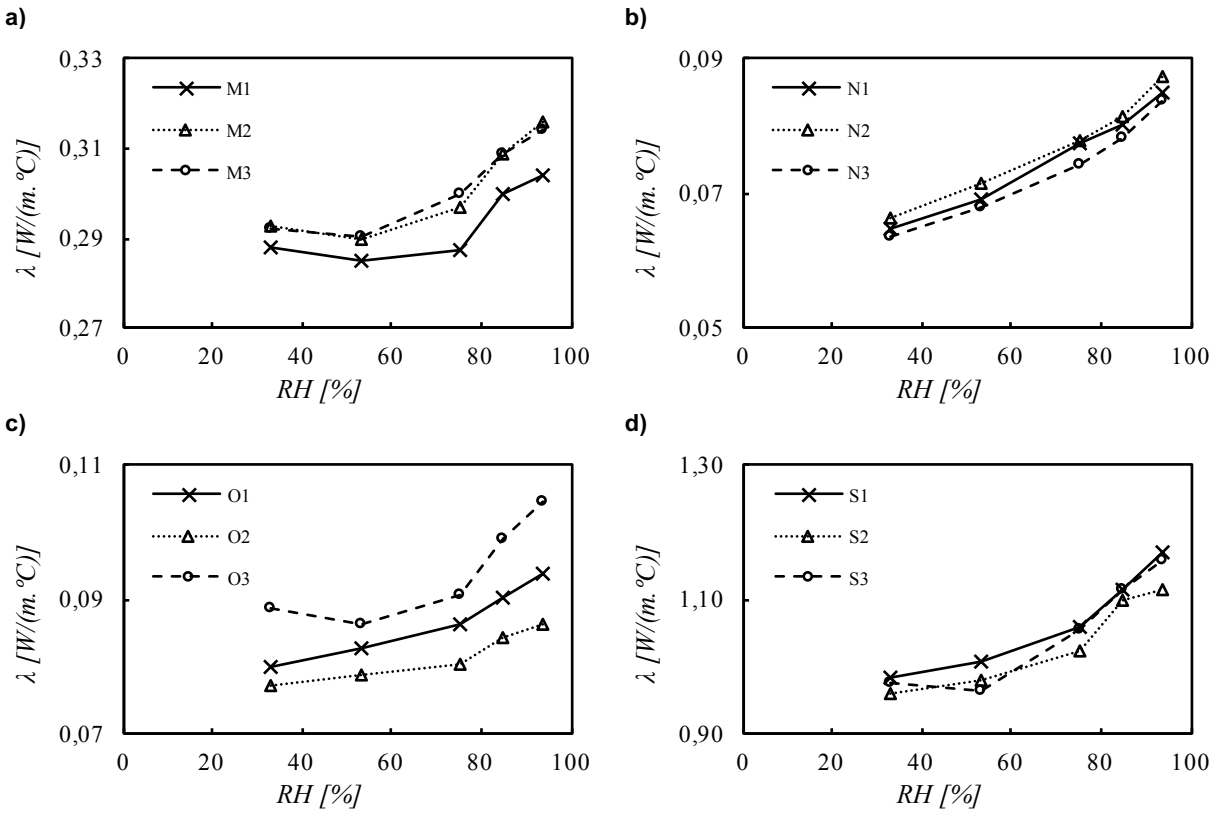

Figure 4.12 – Thermal conductivity of all materials

In order to compare the values of all materials between each other, it was chosen to put all thermal conductivity values in the same graph with the mean values of each material, represented by Figure 4.13. There is a clearly difference between projected cellulose coating (N) and wood wool cement board (O), comparing with the other two materials. This is an outcome of its low values of density and porosity (Table 4-1). The values of porosity and density are equally the reason to clayish earth plaster (S) have the biggest values of thermal conductivity and to recycled cellulose board (M) be the second highest value of thermal conductivity.

Projected cellulose coating N (Figure 4.12 b)) and wood wool cement board O (Figure 4.12 c)) have a negligence increment of thermal conductivity with relative humidity, with increments of, in maximum, 0,03 W/(m.ºC). This suggests that both materials may have high dimension of pores that make that they take a long time to reach interstitial condensation, what makes that pores still be filled with a good portion of air, which causes a negligible increment of thermal.

Recycled cellulose board M (Figure 4.12 a)) and clayish earth plaster S (Figure 4.12 d)) have a more significant increment of thermal conductivity with RH, 0,10 and 0,25 W/(m.ºC), respectively. This suggests that it has low values of pores dimensions which originates early interstitial condensation, as well as liquid form of moisture flux, as it can be seen in Figure 4.11. Therefore, pores will be filled almost with no air, what makes that their thermal conductivity increases significantly with relative humidity.

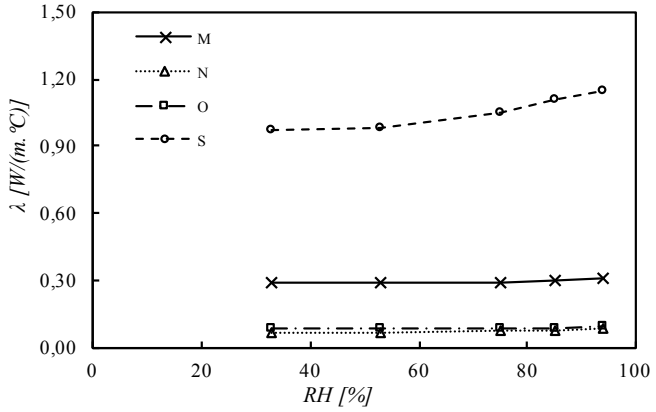

Figure 4.13 – Thermal conductivity of all materials

4.5. Moisture Buffering Value (MBV)

4.5.1. MBV at 33% - 75% RH

The cycle 33% - 75% RH is to be the one analyzed in more detail, since it is present in Nordtest protocol, allowing the comparison with other experiments.

It is known that MBV is a single value and it can be calculated by Equation(3-13). However, the present trial use to define various values of mass difference in final cycle of test, calculated by Equation(3-13) but changing the weighing of 8 hours to the weighing of each hour in which exists a weighing. These values of change of mass, that originates various mass differences during the final cycle.

At 8 hours, in final cycle, the MBV can be calculated and their values for all materials are placed in Table 4-9. Therefore, the MBV is calculated with the weighing of 0, 8 and 24 hours of the final cycle, as described in Equation(3-13), and all graphs that shows the evolution of mass difference with time and also the MBV, which is the highest value of mass difference of each line, are represented in Figure 4.14.

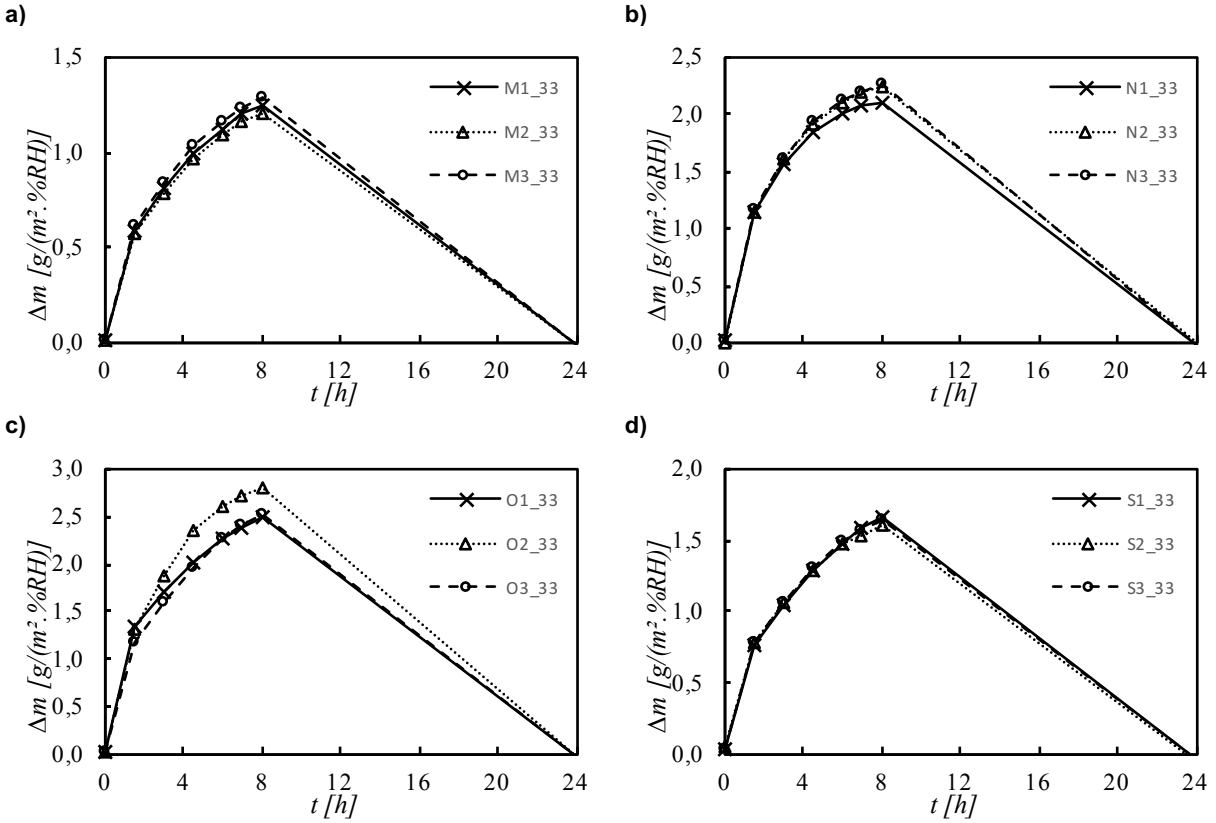

Figure 4.14 – MBV of all materials, at the range of 33%-75% of RH

All materials were placed in the same graph, represented in Figure 4.15 in order to make a comparison between them. It is important to refer that the lines represented in Figure 4.15 contain the mean values of the three samples of each material, represented in Figure 4.14.

As it is possible to see in Figure 4.15, wood wool cement board O (Figure 4.14c)) is the material with the highest value of MBV. Although it is not the material with the highest value of porosity, from the analysis of Figure 3.35 it is possible to conclude that wood wool cement board is a material with big dimensions of pores which can be a justification for it be the material with the highest value of MBV. Another reason to wood wool cement board O has the best MBV is the fact of the samples of this material have, approximately, 30 mm of thickness, which is, at least, the double of thickness of recycled cellulose board M, projected cellulose coating N and clayish earth plaster S. As so, wood wool cement board O has more pores to be filled, as its equilibrium moisture at 75% of RH is the second highest value, as it is possible to see in Figure 4.5, which makes that it reaches interstitial condensation later, making that its velocity to adsorb moisture maintains constant.

Projected cellulose coating N (Figure 4.14b)) has the second highest value of MBV, as it can be seen in Figure 4.15, due to it is the material with the top value of porosity. It should be the material with best MBV, since it is the material with highest value of equilibrium moisture at 75% of RH (Figure 4.5) and the one with fastest response to RH variations, as is described in Figure 4.28, however it has about half of the thickness of O, which make that N have its pores filled of moisture in a faster way. This is a justification of its initial inclination of the graph, and it reaches almost a horizontal line due to its inability to adsorb more moisture. Therefore, it is possible to conclude that projected cellulose coating N is a good coating material to control short cycles of relative humidity inside, because it reacts quickly

to RH variations, however it has not a good behavior to long cycles, because it reaches interstitial condensation early.

Clayish earth plaster S is the material with the lowest value of porosity (Table 4-1) and from Figure 3.35 it looks to have low values of pores dimensions. Both these two facts should imply that it would be the material with lower MBV, because it would be the material that adsorb moisture in slowest way and quantity. However, recycled cellulose board M is the material with lowest MBV (Figure 4.15). This may be justified by the fact that, as clayish earth plaster S is composed by clay that have a mineralogical composition that improves its adsorption and desorption behavior [86] and also increases the response time of clayish earth plaster S is higher than recycled cellulose board M one. This phenomenon is better explained at 4.7.

It is important to refer that MBV lines of M, N and S tend to an equilibrium (Figure 4.15), meanwhile MBV line for material O looks to be far from a horizontal position. This fact makes that wood wool cement board O is the material with best control of long cycles of RH changes. However, as mentioned before, wood wool cement board O have, at least, the double of thickness of all other three materials, which may influence a lot these Moisture Buffering Values.

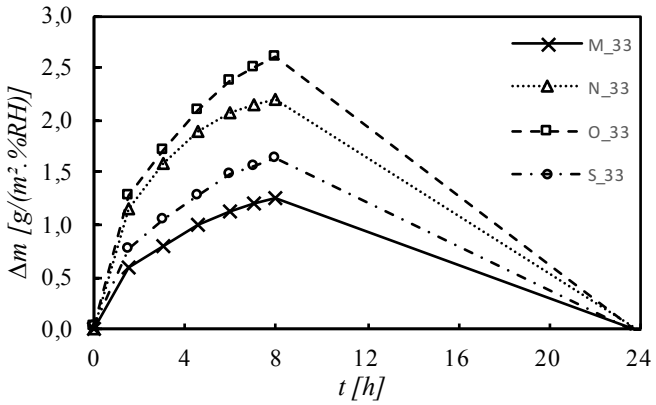

Figure 4.15 – MBV of all materials

4.5.2. Influence of MBV interval

To understand how the interval between the high and low values of RH affects the MBV, two more intervals were tested, where the high value of relative humidity was the same of the main test (75% of RH) and the lowest value of RH was 50% and 60%, as shown in Table 3-6.

Both two new ranges of relative humidity originated MBV placed on Table 4-9. This table originated the four graphs represented in Figure 4.16 that are a comparison between MBV of all ranges of relative humidity for each material. At the same four figures, it is placed next to MBV graphs, the graphs that shows the evolution of moisture content *u* [kg/kg - %] in final cycle to facilitate the understanding of MBV.

Table 4-9 – MBV of all materials of all relative humidity ranges

RH [%]	MBV [g/(m^2.%RH)]							
	M		N		O		S	
	Mean	Standard deviation	Mean	Standard deviation	Mean	Standard deviation	Mean	Standard deviation
33%-75%	1,2	0,04	2,2	0,08	2,6	0,17	1,6	0,02
50%-75%	1,2	0,02	2,4	0,09	2,3	0,15	1,7	0,02
60%-75%	1,1	0,02	2,4	0,11	2,2	0,17	1,8	0,05

M – Recycled cellulose board; **N –** Projected cellulose coating; **O –** Wood wool cement board; **S –** Clayish earth plaster

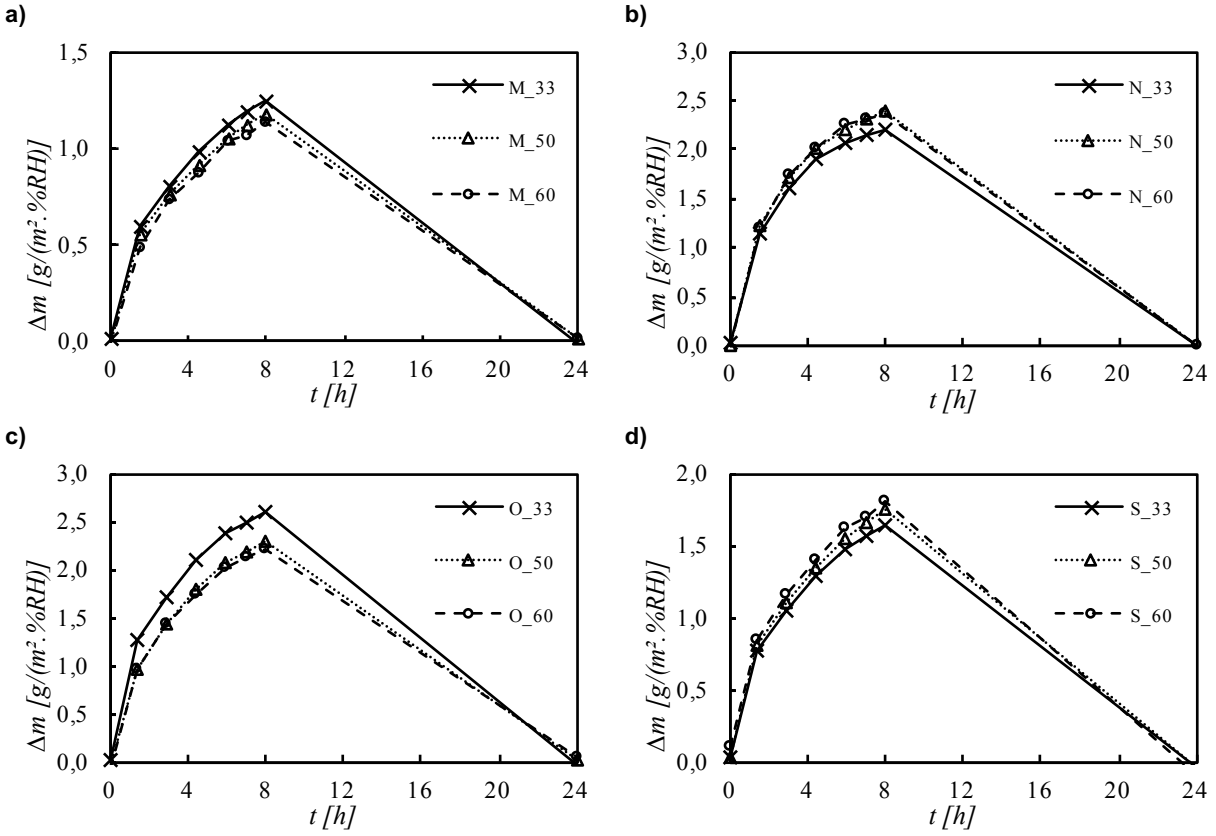

Figure 4.16 –MBV of all materials at all RH ranges

The expected results of MBV for all RH ranges would make that MBV of 33%-75% RH range would be the highest value since it has the highest gap between the high and low values of RH that cause higher mass variation. It is easy to understand that a sample which is placed in an environment that drops its RH value from 75% to 33%, has higher mass variation, due to releasing moisture to environment, than if it would be placed in an environment that drops it RH from 75% to 50 or 60%. This behavior happens in recycled cellulose board M (Figure 4.16a)) and in wood wool cement board O (Figure 4.16c)). However, in other two materials (N and S), the same does not verifies, since it is not the range of 35%-75% of relative humidity that have the highest MBV, as it can be seen in graphs b) and d) of Figure 4.16. This behavior can be explained by their adsorption/desorption isotherms have an exponential, as it is visible in Figure 4.2 and Figure 4.4, that makes that their variation of equilibrium moisture content is much more pronounced from 50 % and 60% to 75% of RH and the variation between 33% and 50% or 60% of RH is less pronounced, since this section of adsorption/desorption isotherm more horizontal. This can be justified by equation of MBV, represented by Equation(3-13) and again written bellow (Equation(4-3)), to make it easier to understand the explanation.

$$\mathbf{MBV_{practical}} = \frac{1/2 * [(m_8 - m_0) + (m_8 - m_{24})]}{A * \Delta RH} \; [g/(m^2.\%RH)] \qquad (4\text{-}3)$$

As referred before, the ranges of relative humidity, that originates the highest gap between the high and low value of RH, should produce higher MBV, since as higher the difference of mass is, higher should be MBV, as it is easy to understand by Equation(4-3). However, as lower is the gap between high and low value of relative humidity, lower will be ΔRH of Equation(4-3), which increases the value of MBV. To better understand the impact that mass variation and RH variation have in MBV, both values are presented in Table 4-10, for all materials and relative humidity ranges, knowing that Δm represents the mean value of mass variation, between the adsorption and desorption phases, and ΔRH represent the difference between the high and low values of relative humidity.

Table 4-10 – MBV of all RH ranges for all materials

		Relative humidity range						Units
		33% - 75%		50% - 75%		60% - 75%		
		Mean	Standard deviation	Mean	Standard deviation	Mean	Standard deviation	
M	**Δm**	0,523	0,02	0,294	0,01	0,171	0,00	[g]
	ΔRH	42	0,00	25	0,00	15	0,00	[%]
	MBV	**1,2**	0,04	**1,2**	0,02	**1,1**	0,02	[g/(m^2.%RH)]
N	**Δm**	0,925	0,03	0,596	0,02	0,354	0,02	[g]
	ΔRH	42	0,00	25	0,00	15	0,00	[%]
	MBV	**2,2**	0,08	**2,4**	0,09	**2,4**	0,11	[g/(m^2.%RH)]
O	**Δm**	1,092	0,07	0,578	0,04	0,332	0,03	[g]
	ΔRH	42	0,00	25	0,00	15	0,00	[%]
	MBV	**2,6**	0,17	**2,3**	0,15	**2,2**	0,17	[g/(m^2.%RH)]
S	**Δm**	0,689	0,01	0,437	0,01	0,270	0,01	[g]
	ΔRH	42	0,00	25	0,00	15	0,00	[%]
	MBV	**1,6**	0,02	**1,7**	0,02	**1,8**	0,05	[g/(m^2.%RH)]

M – Recycled cellulose board; **N –** Projected cellulose coating; **O –** Wood wool cement board; **S –** Clayish earth plaster

As it is possible to see in Table 4-10, both relative humidity and the mean between the difference of mass of adsorption and desorption phases decreases from the range of 33%-75% RH to 50%-75%, and the same verifies between the range of RH of 50%-75% to the range of 60%-75%.

In order to understand how changes the gradient of mass and gradient of relative humidity affects MBV, it was made the Table 4-11, that compares the RH range of 33%-75% with 50%-75% and the range of 50%-75% with 60%-75%, for all four materials. For that, it was made a quotient between the gradient of mass (obtained by the mean of mass variation in adsorption and desorption phases) of RH range with higher gap, between the high and low values of relative humidity, with the range of lower gap (first line of each material of Table 4-11). The same was made to the variation of mean relative humidity, making a quotient between the highest value of RH mean with the lowest value of RH mean, originating the second line of each material of Table 4-11. These two quotients give a value that represents how much lower is the gradient of mass or gradient of relative humidity, of the range with lower gap of RH, comparing with the range of RH with bigger gap. The third line of each material of

Table 4-11 represents the difference between MBV of RH's range with higher gap and the MBV of RH's range with lower gap. Therefore, a negative value of this third line implies that MBV decreased, and a positive value means that MBV increased.

Therefore, by Table 4-11, it is possible to understand that when the quotient between both gradient of mass, of different RH ranges has higher values than the quotient of both mean relative humidity, of different RH ranges, so the MBV will decrease, from the range with bigger gap of RH to the range with lower gap of relative humidity. This is justified by Equation(4-3), since the gradient of mass is placed in numerator and the gradient of relative humidity in denominator. This is the justification to projected cellulose coating N and clayish earth plaster S have the range of 50%-75% of relative humidity with the highest MBV.

Table 4-11 – Comparison of MBV between different RH ranges

		Relative humidity range		**Units**
		i = 33% - 75%	**i = 50% - 75%**	
		j = 50% – 75%	**j = 60% – 75%**	
M	$\Delta m_i / \Delta m_j$	1,776	1,722	[-]
	$\Delta RH_i / \Delta RH_j$	1,680	1,667	[-]
	$MBV_j – MBV_i$	**-0,07**	**-0,04**	[g/(m^2.%RH)]
N	$\Delta m_i / \Delta m_j$	1,550	1,687	[-]
	$\Delta RH_i / \Delta RH_j$	1,680	1,667	[-]
	$MBV_j – MBV_i$	**0,18**	**-0,03**	[g/(m^2.%RH)]
O	$\Delta m_i / \Delta m_j$	1,889	1,744	[-]
	$\Delta RH_i / \Delta RH_j$	1,680	1,667	[-]
	$MBV_j – MBV_i$	**-0,29**	**-0,10**	[g/(m^2.%RH)]
S	$\Delta m_i - \Delta m_j$	1,575	1,620	[g]
	$\Delta RH_i - \Delta RH_j$	1,680	1,667	[g]
	$MBV_j – MBV_i$	**0,11**	**-0,05**	[g/(m^2.%RH)]

M – Recycled cellulose board; **N –** Projected cellulose coating; **O –** Wood wool cement board; **S –** Clayish earth plaster

4.5.3. Classification of MBV

Nordtest report [38] classified the capacity of materials to buffer moisture of indoor, according to their MBV (Figure 3.33) obtained from MBV test with range of 33%-75% RH.

Therefore, the classification of all four materials used on the present work is represented on Figure 4.17.

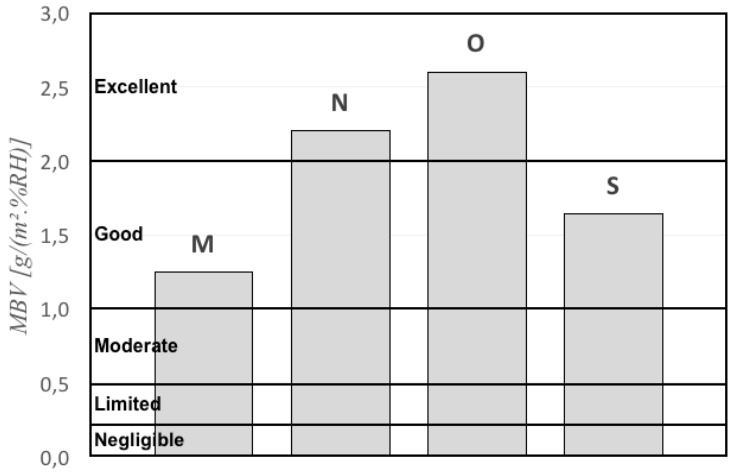

Figure 4.17 – Classification of MBV of all materials

As it is possible to understand, the intervals defined by Nordtest protocol to the MBV classification (Figure 3.33) are represented in Figure 4.17. As so, recycled cellulose board M and clayish earth plaster S are classified as good materials to buffer moisture of indoor and projected cellulose coating N and wood wool cement board O are classified as excellent materials to buffer moisture of indoor.

4.6. Experiment of classroom

The present experimental trial was made to understand the response of coating materials when exposed to real indoor environment. For that, it is important to quantify the variation of materials' mass and correlate it with parameters of indoor climate. It is also important to understand how relative humidity of indoor varies, according to different parameters.

4.6.1. Response of materials

The response of materials to environment of the chosen classroom was quantified by the variation of mass of all materials. The response of materials was analyzed with variations of both relative humidity and temperature of indoor climate.

The mass variation of each material was compared with the changes of temperature and relative humidity of indoor in different graphs in order to understand how their mass changes are affect by temperature and relative humidity, separately. For that, in every figure of the present section, are placed two graphs, where the a) graph represents the variations in time of moisture content of a certain material and relative humidity changes of the room and b) graph represents the variations in time of moisture content of the same material and temperature of the room. The dependence between the variation of materials' mass with changes of temperature and relative humidity was analyzed and it was achieved by coefficient of determination (R^2) of a linear regression made to the data of materials' mass (in Y-axis) and temperature/RH (in X-axis). This coefficient of determination may have values between zero and one, where one represents the perfect fitting of linear-regression to data. The values of the coefficient of determination (R^2) of all materials are placed in all graphs of Figure 4.23

and Figure 4.24, for the correlation between moisture content variations with temperature and relative humidity, respectively.

First of all, it is important to analyze the behavior of finished stucco (EA) when exposed to a dynamic climate. As it is possible to see in Figure 4.18, finished stucco has very small variations of moisture content, once it only has a variation between its maximum and minimum values of moisture content of less than 0,05 [kg/kg - %]. Even knowing that stucco is made of plaster, which is a good hygroscopic material, it has low variations of moisture content due to its superficial painting, that covers its pores and makes it much less permeable to moisture.

From graph a) of Figure 4.18, it is possible to see that moisture content variations, of finished stucco, are very correlated with relative humidity, having a directly proportional relation. In other words, it is possible to see that the increment of moisture content of finished stucco is connected to an increment of relative humidity, in the same period of time. The same verifies in case of moisture content decreasing. The same does not verifies with temperature, once there is no visible relation between temperature changes and variations of finished stucco's moisture content, as it can be seen at graph b) of Figure 4.18. It seems to not exist any type of relation between variations of moisture content and temperature, since the increment of temperature originates, sometimes, the increasing of moisture content of EA but, in other cases, the increment of temperature leads to a decreasing of moisture content.

a) **b)**

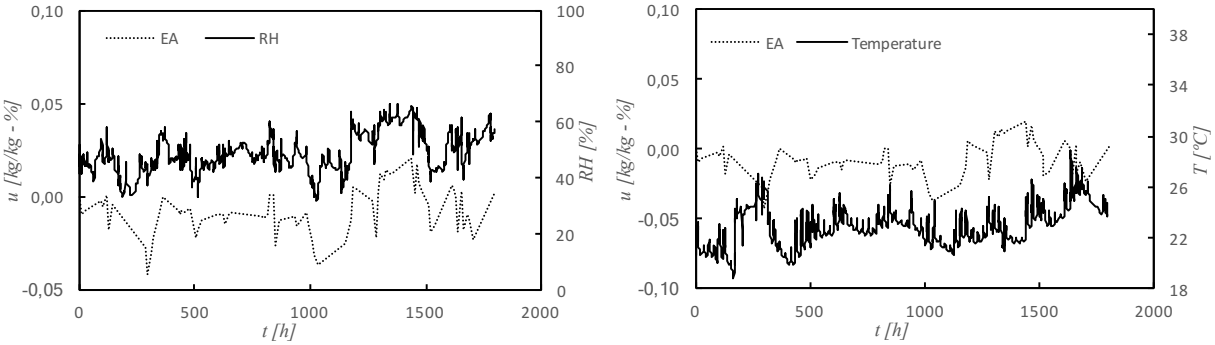

Figure 4.18 – Variations of moisture content of finished stucco (EA) and classroom's relative humidity and temperature

As it is possible to conclude by sections 4.5, 4.2 and 4.7, recycled cellulose board (M) is frequently one of the worse materials, beyond the studied in present work, to buffer moisture of indoor. This fact reflects on the low difference between the highest and lowest values of moisture content in the present test, as it can be seen in Figure 4.19.

From graph a) of Figure 4.19, it is possible to conclude that both temperature and moisture content's variation have a directly proportional relation, since the both changes of moisture content, of recycled cellulose board (M), and relative humidity varies in similar way. That is, when moisture content increases, relative humidity also increases, and when moisture content decreases, relative humidity also lower its values. From graph b) of Figure 4.19, it is possible to see no relation between recycled cellulose board's moisture content variations and changes of temperature, once the sudden variations of moisture content are not followed by sudden variations of temperature and also the increment of temperature leads both increase and decrease of moisture content of recycled cellulose board (M).

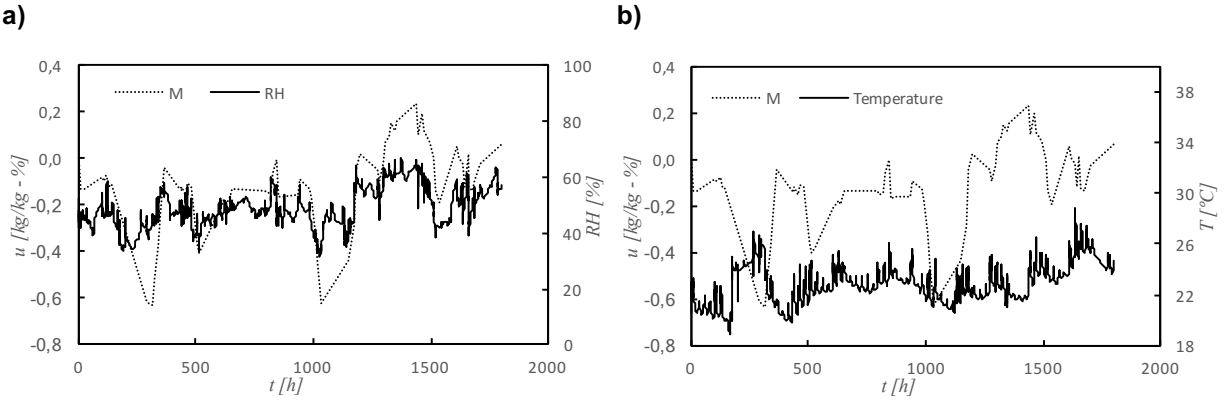

Figure 4.19 – Variations of moisture content of recycled cellulose board (M) and classroom's relative humidity and temperature

From all materials studied in the present test, projected cellulose coating is clearly the material with higher difference between the extreme values of moisture content, almost reaching 2,5 [kg/kg - %], as it can be seen in Figure 4.20.

Moisture content variations of projected cellulose coating (N) have a highly correlation with changes of relative humidity of climate, as shown in graph a) of Figure 4.20, once the increment of relative humidity causes increasing of moisture content of N. The same verifies with the decreasing of moisture content and relative humidity. It is important to refer that as more abrupt be the change of relative humidity, then the variation of moisture content of N will be made, also, in a more sudden way. Therefore, it is valid to conclude that changes of moisture content and relative humidity have a strong directly proportional relation between each other. In case of temperature, the same does not verifies, once variations of moisture content and changes of temperature do not have either directly or inversely proportional relation between each other. As it is possible to see by graph b) of Figure 4.20, the increment of temperature sometimes leads to an increment of projected cellulose coating's moisture content but, in other cases, it causes a decreasing of moisture content of N.

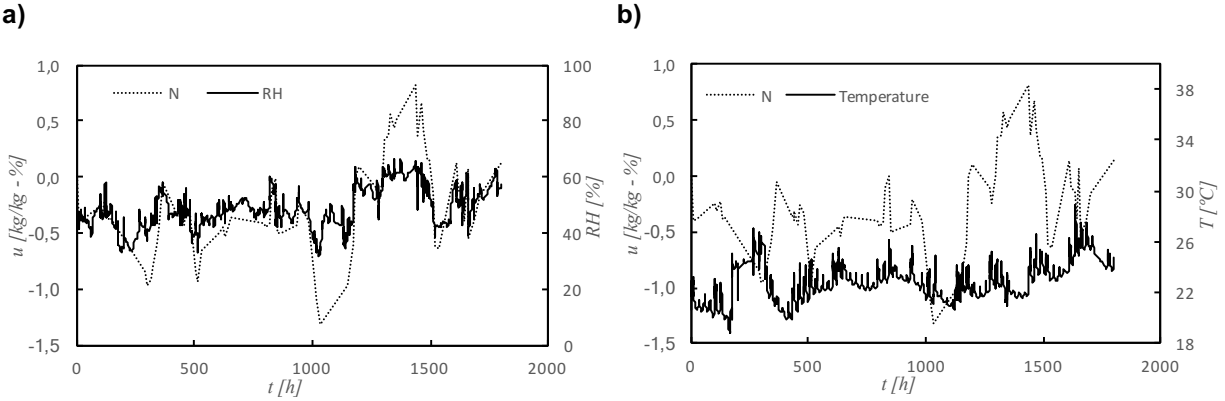

Figure 4.20 – Variations of moisture content of projected cellulose coating (N) and classroom's relative humidity and temperature

Natural hydraulic lime mortar (NHL) was not studied in any other test, besides the classroom one, which makes that there is not any more information about it. However, it is known that this material is a regular mortar, composed by natural hydraulic lime, aggregate and water. This material has a similar value of difference between the extreme values of moisture content (about 0,9 kg/kg - %), to recycled cellulose board (M), what makes that it probably does not have a big capacity to buffer humidity of indoor.

As it is possible to see by graph a) of Figure 4.21, it seems to not exists a big correlation between moisture content and RH, once the values of moisture content, for example, decrease from the beginning of test until 1000 hours, and the values of relative humidity varies in similar cycles, around a constant value, in the same time period. Therefore, it is correct to assume that relative humidity and moisture content of natural hydraulic lime mortar do not have any correlation between each other, either in a direct or inverse way, as it is possible to see by graph b) of Figure 4.21 In other way, temperature and moisture content seems to have a good relation between each other, once the increment of temperature originates a decreasing of natural hydraulic lime mortar's moisture content and an increment of moisture content of NHL is caused by a decreasing of temperature. In this way, it is correct to assume that both moisture content and temperature have an inversely proportional relation, for natural hydraulic lime mortar (NHL). This can be justified by the fact of, as NHL is a mortar, it has more water in its constitution than the other materials, which may evaporate a significantly with the increment of temperature, what originates a reduction of its moisture content.

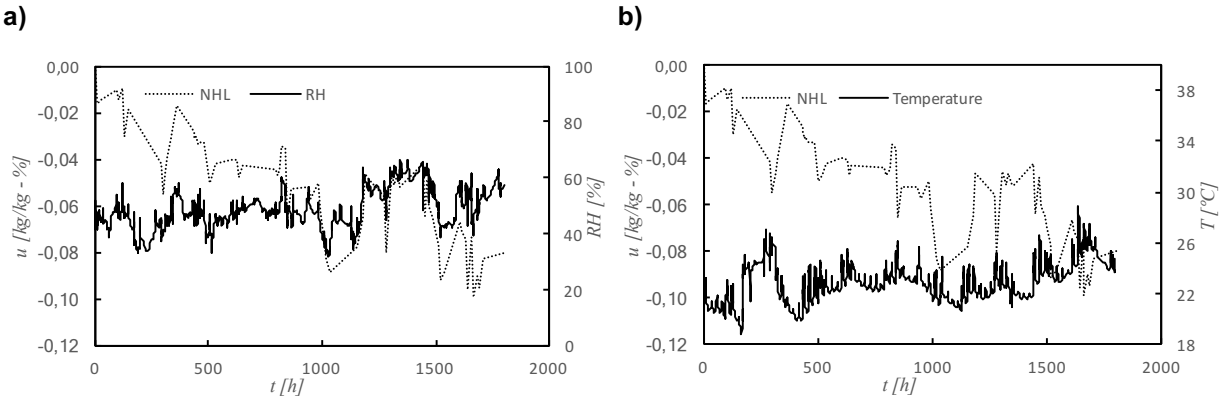

Figure 4.21 – Variations of moisture content of natural hydraulic lime mortar (NHL) and classroom's relative humidity and temperature

Clayish earth plaster (S), beside the present test, was studied in other experimental trials of the present work (4.5, 4.2 and 4.7), and all shown that S responds in slow way to climate changes of relative humidity. However, it seems to exist a relation between moisture content of S and relative humidity of environment, as it can be seen in graph a) of Figure 4.22, since an increment or decrease of relative humidity causes a, increasing or decreasing of moisture content of clayish earth plaster (S), respectively. Therefore, for clayish earth plaster, moisture content and relative humidity have a directly proportional relation between each other. In other way, for temperature changes, the moisture content of clayish earth plaster does not vary always in the same form. That is, an increment of temperature sometimes produces an increment of moisture content of S but, in other cases, it leads to a decrement of clayish earth plaster's moisture content.

In order to understand exactly how does moisture content of all materials varies with changes of relative humidity and temperature of indoor then the values of coefficient of determination (R^2) between variations of moisture content and relative humidity or temperature were calculated. For that, for each material, there were created two graphs for each material, where one compares changes of materials moisture content and changes of relative humidity of indoor and the other compares the variation of moisture content with temperature of indoor. Therefore, the graphs that compares moisture content with temperature, for all materials, are represented on Figure 4.23. In same form, the graphs which compares the variations of moisture content and relative humidity changes, for all materials, are placed on Figure 4.24.

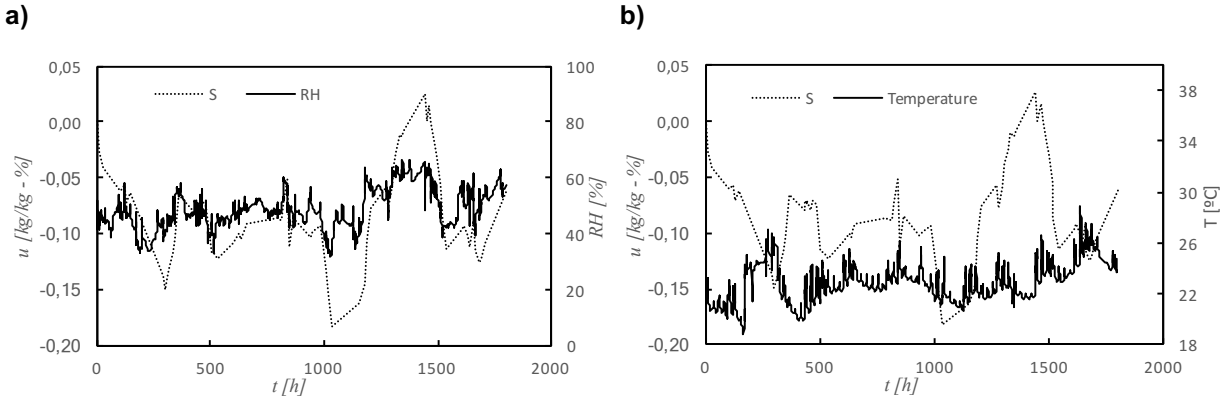

Figure 4.22 – Variations of moisture content of clayish earth plaster (S) and classroom's relative humidity and temperature

As mentioned before, from Figure 4.23 it is possible to conclude that the only material which has a good correlation between its moisture content and the temperature of interior climate is natural hydraulic lime mortar NHL (graph d) Figure 4.23). All other four materials, as concluded before, have almost their coefficient of determination (R^2) equals to zero, meaning that their moisture content variation and temperature changes do not have any proportional correlation, either directly or inversely.

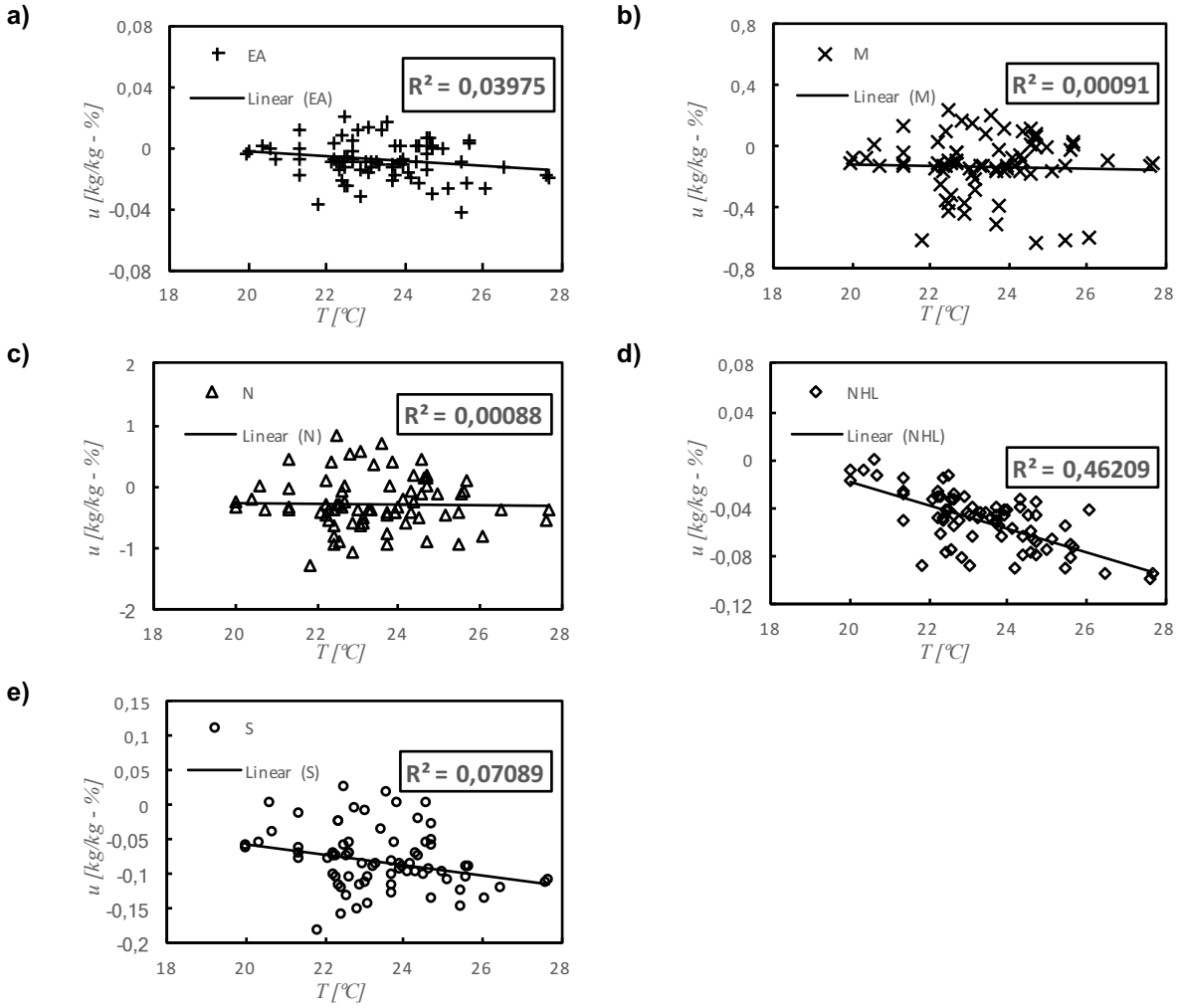

Figure 4.23 – Correlation between material moisture content and temperature of classroom, for all materials

From Figure 4.24, it is possible to confirm that finished stucco EA (graph a)), recycled cellulose board M (graph b)), projected cellulose coating N (graph c)) and clayish earth plaster S (graph e)) have acceptable correlation between their moisture content and relative humidity of environment. This means that, for all these four materials, an increment of relative humidity of environment leads to an increment of moisture content of materials, making that both parameters have a directly proportional relation. It is important to refer that materials like finished stucco (EA) and projected cellulose coating (N) have high values of R^2, probably justified by the fact that both materials have a quick response to climate changes, as it can be seen in 4.7. By the results of the experimental trial of response time (4.7), it is possible to conclude that as faster is the response time of materials, higher will be the R^2 of correlation between their moisture content with relative humidity, excepting for finished stucco EA and natural hydraulic lime mortar NHL, because they were not tested to their response time. It is important to refer that the low value of R^2 of natural hydraulic lime mortar NHL (graph d) of Figure 4.24) is justified by its high value of correlation between its moisture content and temperature, as it can be seen in graph d) of Figure 4.23.

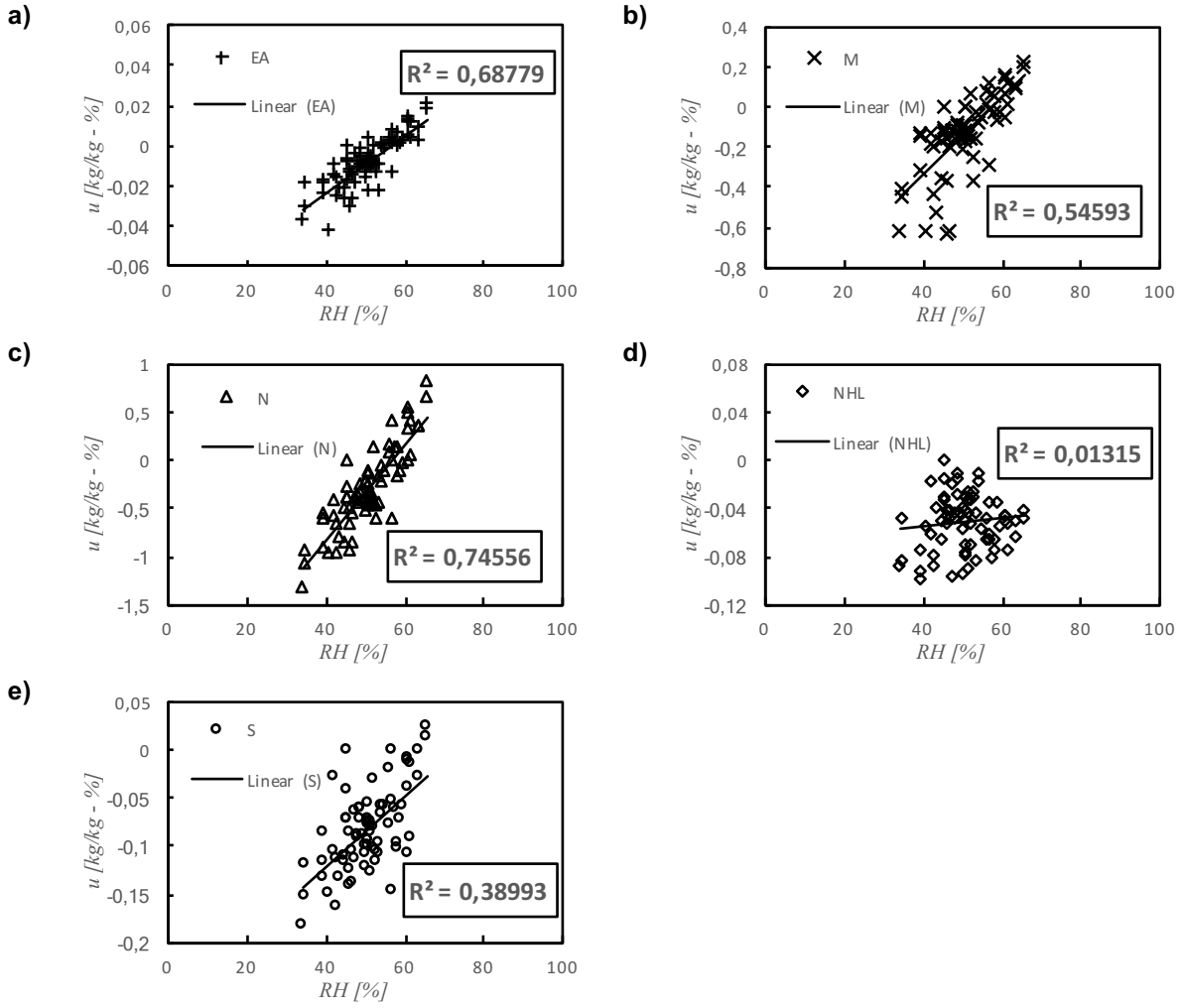

Figure 4.24 – Correlation between material moisture content and relative humidity of classroom, for all materials

4.6.2. Relative humidity of environment

As concluded on previous section (4.6.1), the majority of materials have a moisture content's variation that is directly proportional to relative humidity, with good values of their coefficients of determination (R^2). Therefore, it seemed to be important to understand how the relative humidity of interior's climate varies, in function of other parameters.

Over all test duration, the temperature and relative humidity of the room were monitored at every ten minutes. As it can be seen on Equation(2-5), the saturation limit (ν_s) just need the values of temperature to be determined and, as the temperature was monitored during all experimental trial, it can be determined. From Equation(2-4) it is possible to determine the values of moisture content in air (ν), once the values of relative humidity and saturation limit are known.

As it is possible to see by Figure 2.2, relative humidity varies with moisture content in air (ν) and with temperature, what makes interesting to analyze with which of both parameters the relative humidity varies more. For that, relative humidity was placed in the same graph with temperature and moisture content in air (ν) in Figure 4.25 and Figure 4.26, and both coefficient of determination (R^2) were determined, by making a linear regression of the data. Those values of R^2 are placed in graphs b) of both figures, in order to be easy to understand how relative humidity are correlated with temperature and moisture content in air.

From Figure 4.25 it is possible to understand that relative humidity has low correlation with temperature, even knowing that they are related with each other (Figure 2.2), once the coefficient of determination (R^2) of the linear regression of the data, composed by relative humidity and temperature, has values near to zero (graph b) of Figure 4.25).

From Figure 4.26 it is possible to prove that relative humidity is much related with moisture content in air, since the increment of moisture content in air leads to an increasing of relative humidity values, and a reduction of relative humidity is caused by the decreasing of moisture content in air, as it would be expected (Figure 2.2). Therefore, it is correct to affirm that both relative humidity and moisture content in air have a directly proportional relation. Both two parameters are much correlated with each other, and the R^2 of the linear regression, between relative humidity and moisture content in air's data, has a high value.

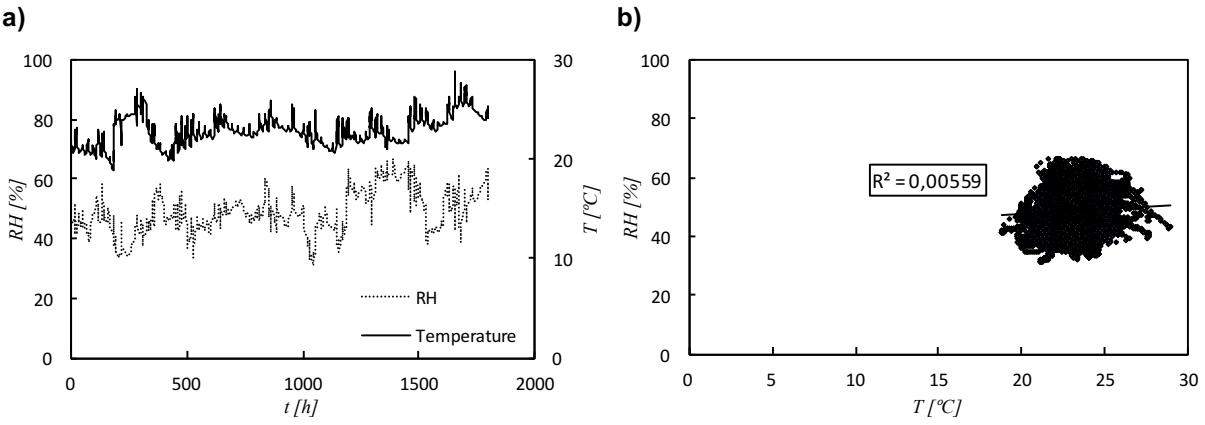

Figure 4.25 – Correlation between relative humidity and temperature of classroom

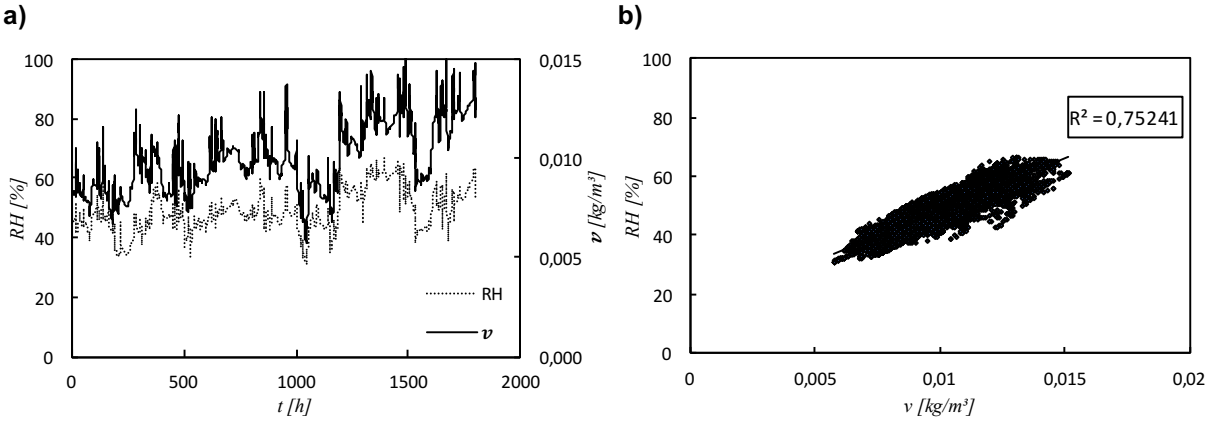

Figure 4.26 – Correlation between relative humidity and moisture content in air of classroom

In consequence of the conclusions of the present section, it is possible to affirm that a correct air exchange rate or dehumidification of interior climate is much more efficient to control relative humidity of indoor than controlling its temperature.

4.7. Response Time

This experimental trial looks to understand how fast the coating materials respond to indoor relative humidity variations.

The present test is directly related with adsorption/desorption isotherm one, since it is a variation of that test. While in adsorption/desorption isotherm experimental trial, the main goal is to understand the maximum capacity of each material to adsorb and release moisture, recording materials moisture content of equilibrium, in the response time test the main objective is to understand the velocity in which the materials respond to indoor changes of relative humidity. As so, the results of the present test are present in percentage of moisture content variation, compared with initial moisture content of both adsorption and desorption tests. For that, the graphs of Figure 4.27 consider that the zero of adsorption curve is the initial moisture content of this adsorption phase and the zero of desorption curve is the value of the final moisture content of desorption phase.

The present experimental trial originated two curves for each material, one for adsorption phase and another to desorption phase. The mean between the three samples of each material is utilized and represented on all four graphs, for all four materials.

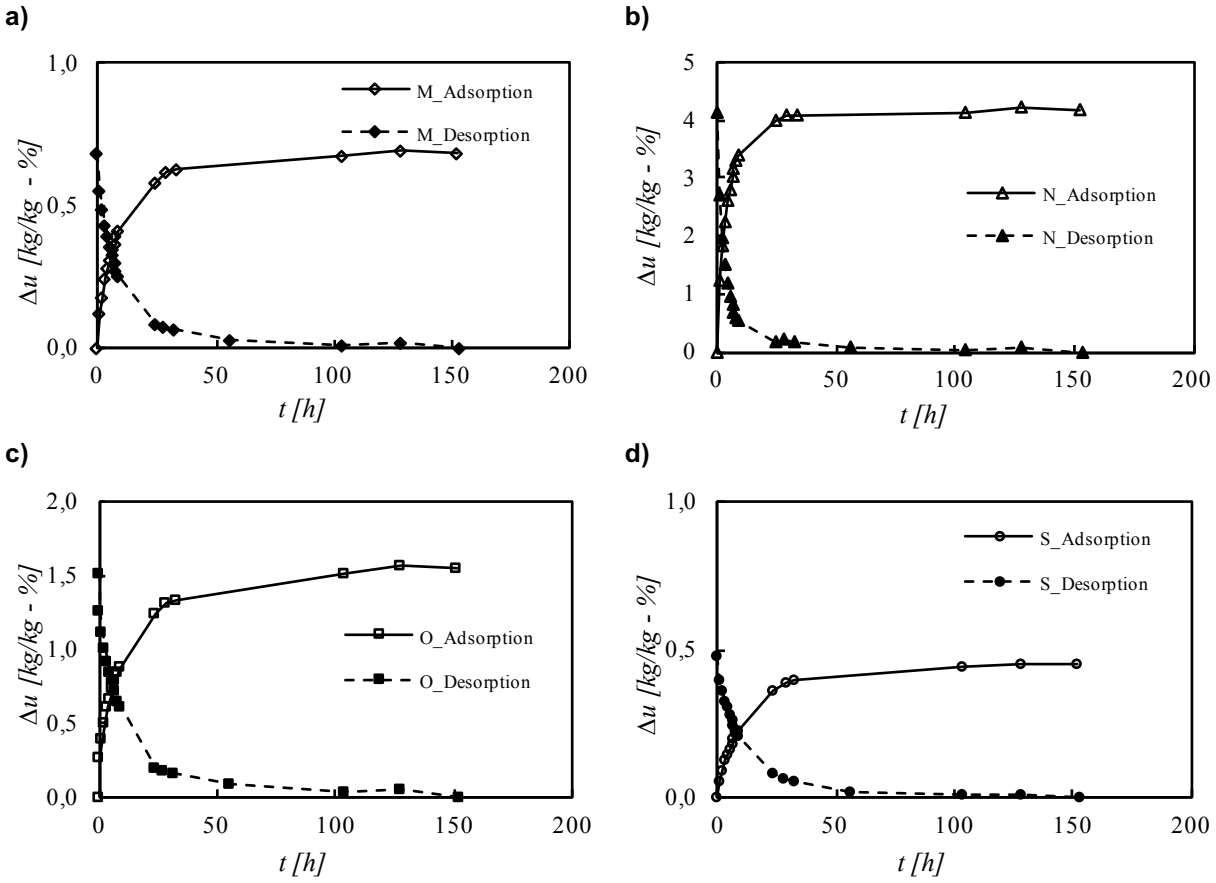

Figure 4.27 – Response time of all materials

As it is possible to understand by all figures above, projected cellulose coating N (Figure 4.27 b)) is the fastest material to respond to RH changes of environment, since it has an almost vertical line in first 9 hours of test, and it adsorb/release more than 3 [kg/kg - %] of moisture content, in relation with the initial moisture content, in such a short period of time.

The material with the slowest behavior is clearly clayish earth plaster S (Figure 4.27 d)), since it adsorb/release just about 0,2 [kg/kg - %] above its initial moisture content. Its lines' section of adsorption and desorption in first 9 hours is far from being horizontal, however it has lower slope than all other material, as it is possible to see in Figure 4.27.

From graphs a) and c) of Figure 4.27 it is clear that wood wool cement board (O) has quicker response than recycled cellulose board (M), since it achieves almost the double of variation of moisture content of the variation of moisture content of M, in the same period of time.

To better understand the response time of each material, it was made an analysis in first 9 hours of test, due to be the time interval in which occurs more development of adsorption and desorption curves. For that, was created a concept of adsorption/desorption velocity [(kg/kg - %)/h], which is similar to the concept of sorptivity [96], and relates the variation of moisture content in first 9 hours with the time gap (same 9 hours). This made that a velocity for adsorption and desorption phases was achieved, and a mean between both was made, in order to be easy to compare all materials. The results of this concept of adsorption/desorption velocity are presented in Table 4-12. By this same table, it is possible to understand that making a mean between both adsorption and desorption velocities does not represent a big error, once both phases have similar values of velocity.

Table 4-12 – Adsorption/desorption velocity of all materials

		Moisture content variation Δu [kg/kg - %]		Response velocity [(kg/kg - %)/h]	
		Mean	Standard deviation	-	Mean
M	**Adsorption**	0,69	0,03	0,076	**0,076**
	Desorption	0,68	0,04	0,075	
N	**Adsorption**	4,19	0,09	0,465	**0,461**
	Desorption	4,11	0,20	0,457	
O	**Adsorption**	1,55	0,08	0,173	**0,171**
	Desorption	1,52	0,09	0,169	
S	**Adsorption**	0,45	0,01	0,050	**0,051**
	Desorption	0,47	0,03	0,053	

M – Recycled cellulose board; **N –** Projected cellulose coating; **O –** Wood wool cement board; **S –** Clayish earth plaster

As mentioned before, from Table 4-12, it is easy to understand that projected cellulose coating N is the material with fastest response to RH changes, and clayish earth plaster is the slowest. The second-fastest material to respond to relative humidity changes of indoor is wood wool cement board O (Figure 4.27 c)), with almost the double of adsorption/desorption velocity of recycled cellulose board M (Figure 4.27 a)). These results are explained, first of all, by materials' porosity (Table 4-1), since the material with higher value of porosity, N, is the one with better response to environment changes of RH. The same verifies for the material with lower porosity, S, that makes it the material with slower response to changes of relative humidity of indoor. However, as it is possible to see by Table 4-1, M has higher value of porosity than O, however both values are very similar. In this case, the material with highest porosity does not have the higher adsorption/desorption velocity, and it even has less than half of velocity than wood wool cement board. This suggests that wood wool cement board O may have higher dimension of pores than recycled cellulose board M. This difference between the dimension of pores of two materials may originate that the one with bigger dimensions of pores adsorb moisture always at the same velocity, once it takes long time have its pores filled with water, and makes that the material with lower pores' dimensions have its pores filled with water faster, what reduces it adsorption/desorption velocity.

It is important to conclude that projected cellulose coating N is a really good coating material to control short relative humidity cycles, but if the cycles of RH changes are longer, the best material to control RH of inside is clayish earth plaster S, since it respond slowly to relative humidity changes. This slow response of coating materials can be important to control relative humidity between seasons of year, like adsorb moisture in summer, and only releases it in winter.

In order to be easier to understand the velocities in which all four materials respond to relative humidity changes, the values of mean velocity in first 9 hours, between adsorption and desorption phase of each material, were placed in the same graph (Figure 4.28) with the values of moisture content variation and not the absolute values of moisture content. The inclination of each curve is the value of adsorption/desorption mean velocity, represented in the last column of Table 4-12.

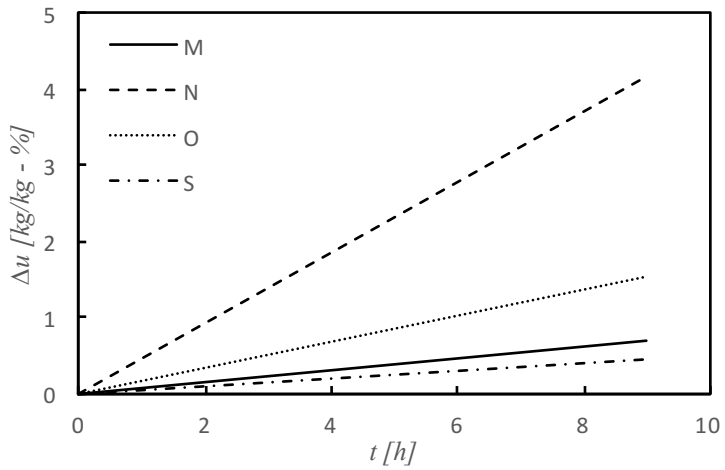

Figure 4.28 – Comparison between moisture content changes of all materials in first 9 hours of response time test

4.8. Chapter synthesis

Porosity and pores' dimension are determinant characteristics of materials, with regard of their behavior to control moisture and temperature of interior climate. These two physics characteristics of materials influence the quantity of moisture that a certain coating material is capable to adsorb or release, as well as the velocity in which it is made. These two materials' characteristics also influence the thermal behavior of the element. Therefore, it is right to say that as higher are porosity and pores' dimension, better will be the coating material to control cycles of relative humidity inside and provide an improvement of hygric inertia. It is also possible to affirm that as bigger are porosity and dimensions of pores, lower will be the variations of materials thermal behavior with the increment of moisture content and so, the effect of relative humidity in thermal inertia of buildings will be less pronounced

From experimental trials and their results analysis, it was possible to conclude that as higher are heterogeneity, porosity and pores' dimensions of materials, more discrepant the results will be (which implies higher values of standard deviation), and so, when the results are treated by their mean, then the attached error by using it, will be higher.

From MBV experimental trial, it was possible to understand that the hysteresis of materials has an important role in the control of relative humidity indoor, by coating materials. This because, as higher is the hysteresis of material, more difficult will be its desorption phenomenon. Therefore, as it releases less moisture, the numerator of MBV will take lower values, what makes that it will have also lower moisture buffering value (MBV). Also the velocity of response takes an strong effect on the MBV, since the both parameters are directly related with each other, except for clayish earth plaster (S) that is the material with slowest response to environment but it does not have the lower MBV.

With increment of relative humidity, the moisture content of materials will also increase, what makes that pores have more moisture inside. The expected behavior of materials would be that their moisture permeability would decrease, in consequence of there would be less air space to the flux of vapor form of moisture. And this verifies until, approximately, 60 % of relative humidity. However, materials' moisture permeability does not decrease indefinitely with increment of relative humidity, once the interstitial condensation brings the liquid flux of moisture, which increases exponentially with higher values of RH. Therefore, it is important to understand that even if materials are very low permeable to moisture, at dry conditions, they can turn into materials with significantly higher values of moisture permeability, if they are subject to high values of relative humidity.

The hygric inertia is a subjective concept, once it depends of the cycles and peaks of relative humidity that are intended to be damped. Therefore, the concept of response time of materials is a crucial physical characteristic with regard to understand which cycles and peaks of relative humidity that can be controlled by them. Therefore, the material which responds quickly to relative humidity changes of indoor is not always the best material to provide the intended hygric inertia, in case of the need to control long cycles of relative humidity changes.

Chapter 5: Numerical Analysis

5.1. General considerations

Experimental trials allow to understand the behavior of materials and some of their physical characteristics, achieved by some sample which are tested. However, experimental trials only allow to know those behavior and physical characteristics of materials at a limited number of environment conditions, even making an intense experimental analysis. Therefore, the results obtained by tests is limited to some environmental conditions, like temperature, relative humidity, air velocity, beyond others, being the behavior of materials at all other conditions, which were not tested, unknown. To be possible to know the behavior of materials at other ranges of temperature, RH, air velocity, or many other variables, it is necessary to make a numerical analysis. The numerical analysis consists, in this case, in making non-linear regressions of data obtained experimentally and chose the coefficients of regression's equations that produce a better fitting of these equations to the results achieved by experimental trials. The non-linear regressions of all tests were made with DataFit 9 curve fitting, developed by Oakdale Engineering, that allow to make linear and non-linear regressions.

5.1. Adsorption/Desorption Isotherm

5.1.1. Adsorption/desorption equations

The experimental trial of adsorption/desorption isotherm allowed to know the values of equilibrium moisture content of all four studied materials, for different relative humidity. The ranges of RH in which the equilibrium moisture content is known are 33%, 53%, 75%, 85% and 94%. However, the values of materials' equilibrium moisture content, at non-studied ranges of relative humidity, are unknown, which brings the necessity to make non-linear regression of experimental results.

Following will be presented the most common equations of moisture content of materials, in function of indoor relative humidity. These mathematical models will be presented with regard to when they were created and they are evolutions from each other, with the main goal of represent better the adsorption and desorption behavior of materials. All of main considerations and characteristics of equations are explained bellow [5] [6], and the equations itself are placed on Table 5-1.

Langmuir [97] assumed that there is only monomolecular adsorption and that all pores, of same material, have similar dimensions. He proposed the equation placed in first line of Table 5-1, where A is the quantity of moisture in a single layer and B is a coefficient proportional to temperature.

Lykow [98] proposed three equations. The first one (second line of Table 5-1) is able to know the moisture content of a material at any value of relative humidity, in a range between 35% and 94% of

RH. Lykow's second equation (third line of Table 5-1) is capable to determine the equilibrium moisture content of a material at any value of relative humidity higher than 10% and lower than 90%. Coefficients G and H, of this second equation of Lykow, are inherent to each material and are dependent of temperature. The third (and last) equation of Lykow (forth line of Table 5-1) is based in Posnow's formula and allows to know the equilibrium moisture content at a range of RH between 30 and 100%. The coefficient u_h is the maximum quantity of moisture of a material that is due to hygroscopicity and B is a factor that depends of temperature. This third equation of Lykow requires that the values of relative humidity be in fraction, and not in percentage.

Freisleben Hansen [99] proposed two equations. The first equation (fifth line of Table 5-1) is made to know the equilibrium moisture content at a range of relative humidity of 20% to 98%, and it demands that RH values be in fraction. The second equation (in last line of Table 5-1) is able to determine the equilibrium moisture content of materials, bellow 95% of relative humidity.

In the present work, a non-linear regression of experimental results was made, using DataFit 9, and an equation was achieved. However, between the almost 300 equations of DataFit 9, the best regression reached was equal to the second one of Hansen (last line of Table 5-1).

As some equations just work with relative humidity in fraction, and not in percentage, all equations coefficients (placed on Table 5-2) were obtained by working with experimental results in function of relative humidity in fraction. However, the graphs of all equations have the axis of RH in percentage, this because it is the most common form to present relative humidity.

All non-linear regressions were made with all experimental results of the three samples of each material, however the Figure 5.1 to Figure 5.4 only presents the mean values of experimental results in order to simplify the graphs, which would be much confused if they have the values of all samples' experimental results.

Table 5-1 – Equations of moisture content

	Equation	Limitations
Langmuir	$\frac{A * B * \phi}{1 + B * \phi}$	-
Lykow (1)	$A + B * \phi^2$	-
Lykow (2)	$\frac{G * \phi}{H - \phi}$	-
Lykow (3)	$u_h * (1 - \frac{\ln(\phi)}{d})^{-1}$ $\quad d = \frac{1}{u_h * B}$	RH has to be in fraction
Hansen (1)	$u_h * (1 - \frac{\ln(\phi)}{A})^{-1/n}$	RH has to be in fraction and it only fits to moisture content in *u* [kg/kg - %]
Hansen (2)	$\frac{\phi}{A * \phi^2 + B * \phi + C}$	RH has to be in fraction

Table 5-2 – Coefficients of all adsorption/desorption equations, for all materials

		M		N		O		S	
		Ads.	**Desor.**	**Ads.**	**Desor.**	**Ads.**	**Desor.**	**Ads.**	**Desor.**
Langmuir	**A**	1071,16	75,40	7130,15	1264,17	20,30	13,26	1031,75	125,53
	B	2,09E-03	3,19E-02	1,50E-03	8,53E-03	0,44	0,95	1,13E-03	8,99E-03
Lykow (1)	**A**	0,58	0,67	0,83	0,73	2,47	3,06	0,25	0,09
	B	1,83	1,82	11,97	12,18	4,22	3,89	1,05	1,25
Lykow (2)	**G**	10,83	68,19	7,49	7,33	1,98E+18	1,55E+17	2,41	0,99
	H	5,65	29,86	1,53	1,51	2,97E+17	2,16E+16	2,88	1,71
Lykow (3)	**B**	0,81	0,69	0,28	0,28	0,19	0,14	1,80	2,43
	u_h	2,52	2,53	15,40	15,56	6,64	6,76	1,39	1,52
Hansen (1)	**A**	0,26	0,73	0,27	0,32	0,18	1,91	0,29	1,26
	n	1,41	0,85	0,92	0,83	2,24	0,65	1,19	0,36
	u_h	2,63	2,50	15,13	15,03	7,25	6,69	1,42	1,38
Hansen (2)	**A**	-0,87	-0,46	-0,18	-0,15	-0,28	-0,09	-1,62	-0,06
	B	1,11	0,62	0,14	0,10	0,41	0,19	1,89	-0,92
	C	0,14	0,24	0,10	0,12	3,80E-03	0,05	0,43	1,69

M – Recycled cellulose board; **N –** Projected cellulose coating; **O –** Wood wool cement board; **S –** Clayish earth plaster

Graphs a), b), c), d), e), f) of Figure 5.1 to Figure 5.4 represent, respectively, equations of Langmuir, Lykow (1), Lykow (2), Lykow (3), Hansen (1) and Hansen (2), represented on Table 5-1.

The only equation that does not represents so well the experimental data is the Langmuir one (graph a) of Figure 5.1 to Figure 5.4) since it has almost always a linear behavior of moisture content with the increment of relative humidity, which is not true. This may be justified by the fact that, as mentioned before, it considers that the adsorption is made only in a monolayer, which it is not the real behavior of adsorption phenomenon of any material. The second equation of Lykow, represented by graph c) represents also the relation between moisture content and relative humidity with linear correlation for recycled cellulose board M (Figure 5.1) and wood wool cement board O (Figure 5.3), which does not represent the real behavior of materials.

Lykow (1), Lykow (3), Hansen(1) and Hansen (2) have a good fitting to experimental results and also represents truly the evolution of material moisture content with increment of relative humidity, as it is possible to see by graphs b), d), e) and f) of Figure 5.1 to Figure 5.4.

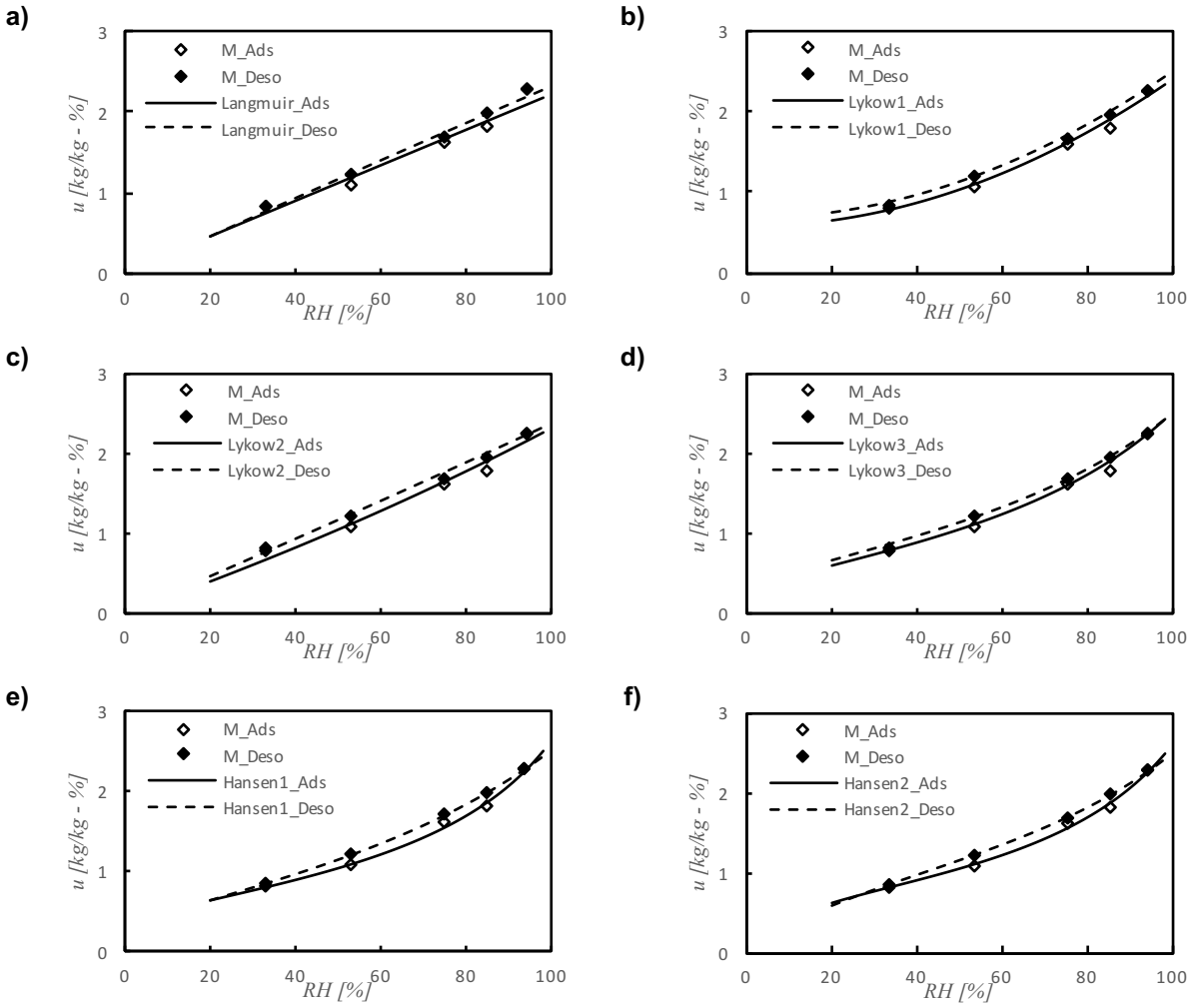

Figure 5.1 – All non-linear regressions of moisture content of recycled cellulose board (M)

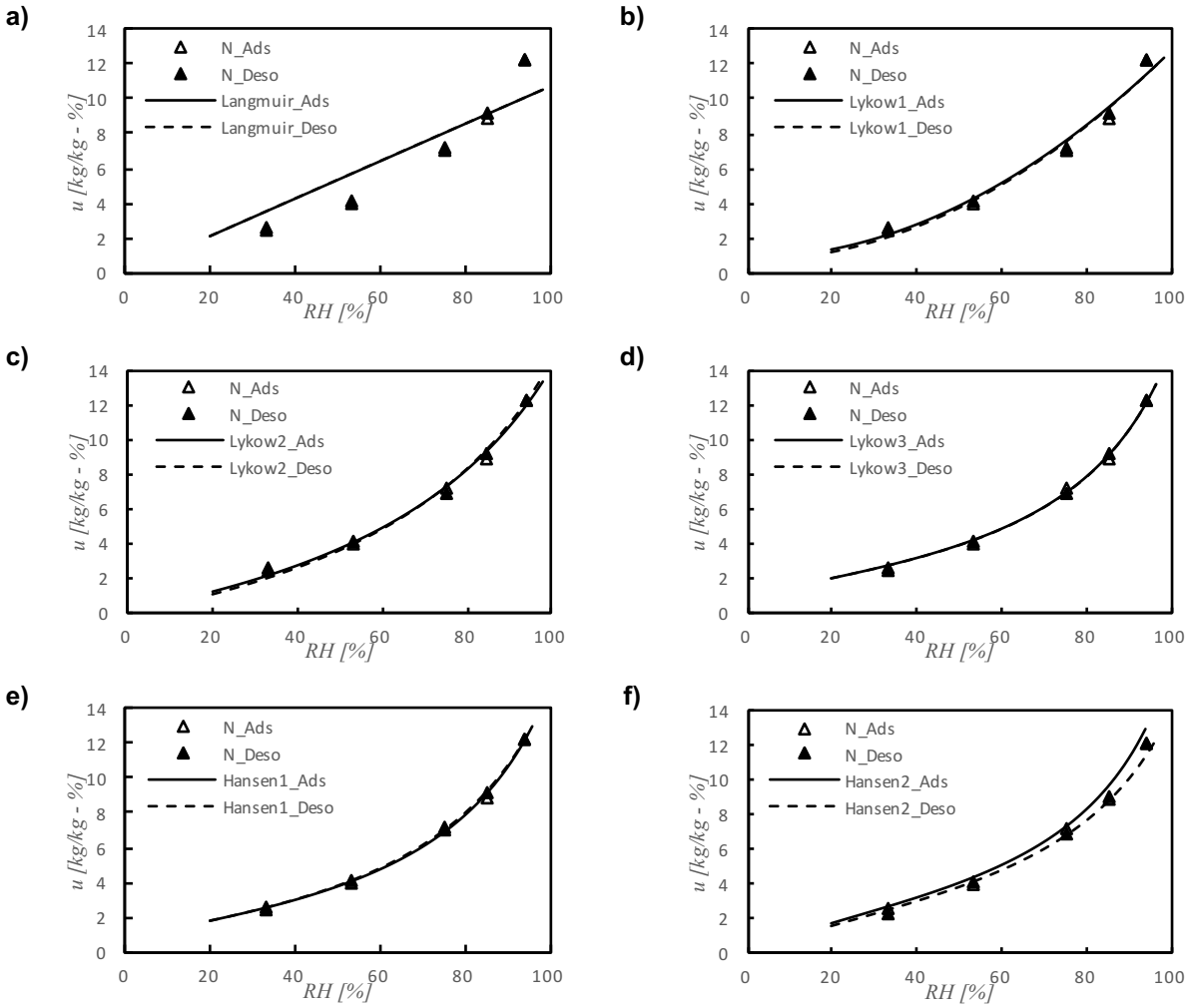

Figure 5.2 – All non-linear regressions of moisture content of projected cellulose coating (N)

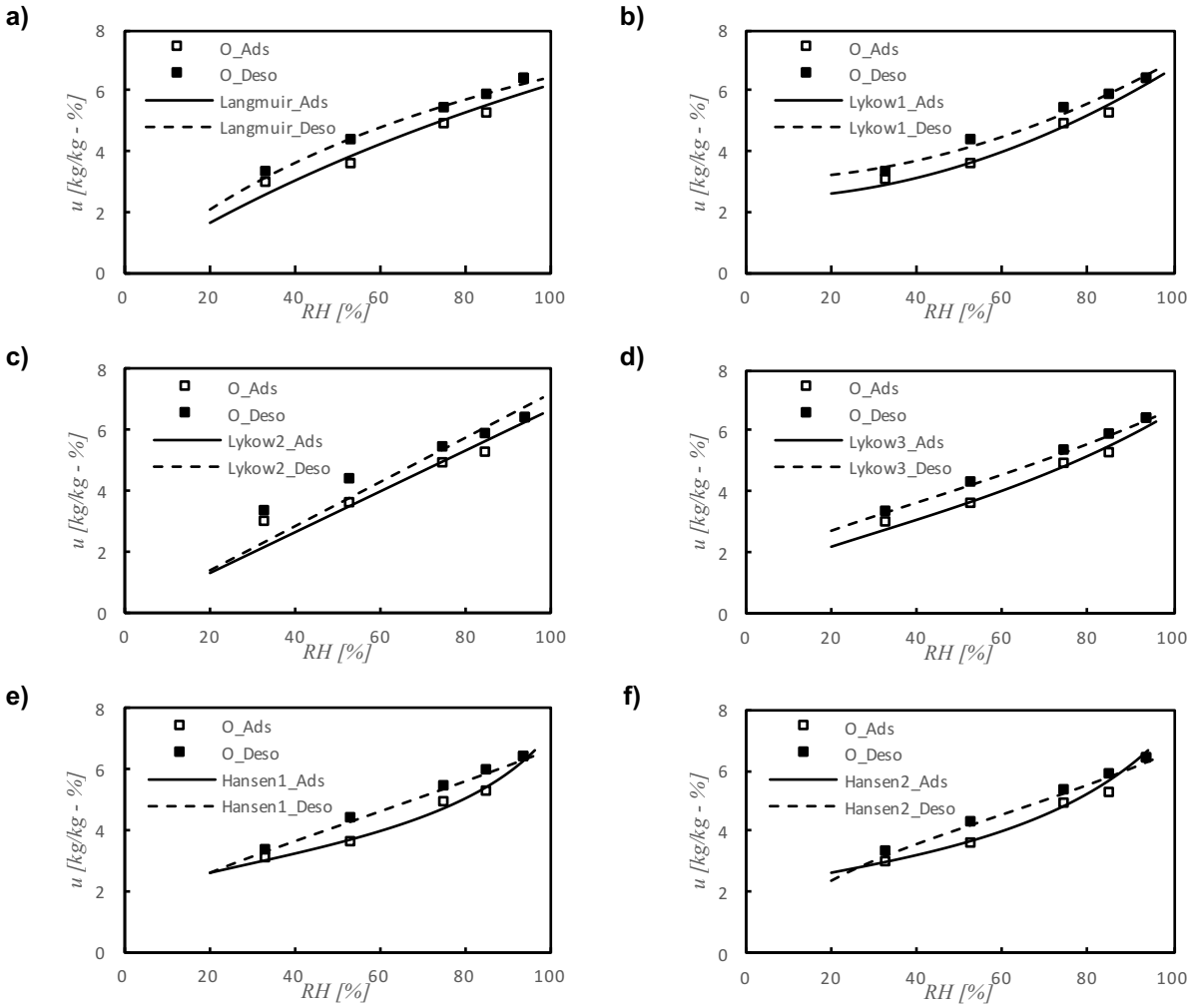

Figure 5.3 – All non-linear regressions of moisture content of wood wool cement board (O)

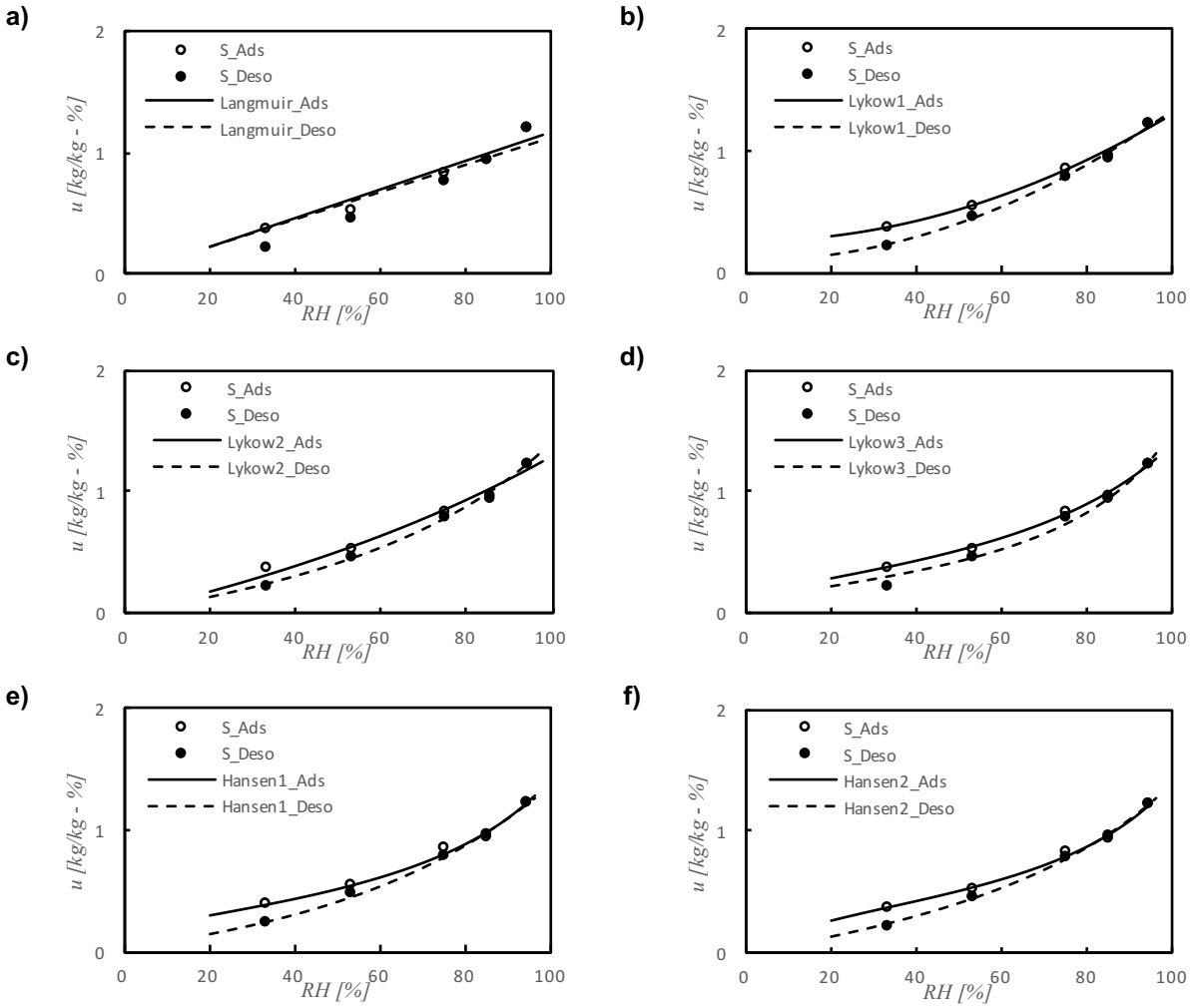

Figure 5.4 – All non-linear regressions of moisture content of clayish earth plaster (S)

The fitting of the non-linear regressions to data obtained experimentally, can be evaluated by the concept of coefficient of determination (R^2), which can take values from 0 to 1, being zero the worse fitting scenario and 1 is the perfect fitting scenario, and the values of this R^2, for all non-linear regressions and all materials, are placed in Table 5-3. With R^2 it is possible to understand the goodness of fit mathematically, once it measures the proximity between the experimental data and the curves of regression, but it does not make a physical consideration of it. Therefore, it is possible to have non-linear regressions with high value of coefficient of determination, placed in Table 5-3, but that does not represent the real behavior of materials.

Table 5-3 - Coefficient of determination (R^2) of all adsorption/desorption equations, for all materials

Equation	R^2							
	M		N		O		S	
	Ads.	Desor.	Ads.	Desor.	Ads.	Desor.	Ads.	Desor.
Langmuir	0,953	0,985	0,844	0,842	0,923	0,985	0,939	0,884
Lykow (1)	0,985	0,996	0,973	0,977	0,980	0,980	0,984	0,995
Lykow (2)	0,961	0,986	0,986	0,991	0,880	0,783	0,972	0,997
Lykow (3)	0,989	0,997	0,993	0,995	0,971	0,995	0,991	0,986
Hansen (1)	0,992	0,998	0,993	0,996	0,986	0,995	0,992	0,997
Hansen (2)	0,992	0,998	0,994	0,996	0,985	0,996	0,992	0,997

M – Recycled cellulose board; **N –** Projected cellulose coating; **O –** Wood wool cement board; **S –** Clayish earth plaster

These values of R^2 just confirms the goodness of fit of non-linear regressions, confirming that Langmuir and Lykow (2) have a not so good fitting (line one and three of Table 5-3) and that the other four non-linear regressions produce good fitting to experimental results (line two, four, five and six of Table 5-3). From Table 5-3 it is also possible to conclude that both Hansen's equations produce the best values of moisture content with relative humidity variations, once they have R^2, for all materials, near to one. Therefore, this two Hansen's equations are the ones that allow to know the moisture content of a certain material in any relative humidity of indoor, even it be a range of RH that was not tested. This confirms the tendency of various authors that, in majority, use the first equation of Hansen (fifth line of Table 5-1) to characterize the adsorption and desorption behavior of materials, in function of relative humidity [3] [26] [77] [94] [100].

It is important to refer that, for example, the equation of Langmuir is able to produce a good mathematical fitting to wood wool cement board, since it causes a coefficient of determination of 0,923 (Table 5-3), however as it is possible to see in Figure 5.3 a) this equation does not produce a real behavior of equilibrium moisture content with the increment of RH. Therefore, it is important to have a good mathematical fitting, but it has to represent the real behavior of materials from the physical point of view.

By Table 5-3 it is possible to conclude that all equations are able to fit both adsorption and desorption phases, what make that all of them can reproduce correctly the real behavior of adsorption and desorption of material, since they consider the phenomenon of hysteresis.

5.1.2. Specific moisture capacity ξ

The specific moisture capacity is an index that allows to understand the ability of materials to adsorb and store moisture, as well as to release it. More specifically, specific moisture capacity represents the quantity of moisture adsorbed or released by a certain material, per unit of mass and relative humidity, and it has a similar meaning to specific heat capacity [1].

This quantity of specific moisture capacity is obtained by making the derivative of adsorption/desorption equation (that traduces moisture content variation with relative humidity), in function of relative humidity. As the most used equation by other authors [3] [26] [77] [94] [100], and also it is the best regression equation for the experimental results of the present work (see in 5.1), is Hansen's equation (Equation(5-1)), therefore, the specific moisture capacity will be determined in function of it.

$$u = u_h * (1 - \frac{ln(\phi)}{A})^{-1/n} \quad (5\text{-}1)$$

Specific moisture capacity ξ can be determined in mass or volume [44] and, since the present work treats frequently the data in values of mass, then specific moisture capacity it will always be in mass.

As referred above, specific moisture capacity is obtained by making the variation of adsorption/desorption phenomenon equations with relative humidity, which originates the following formula:

$$\xi_u = \frac{du}{d\phi} = \frac{u_h}{n * A * \phi} * [1 - \frac{ln(\phi)}{A}]^{-1-\frac{1}{n}} \quad (5\text{-}2)$$

where A, n and u_h are constants that are place in Table 5-2, for all materials.

The most usual form to characterize specific moisture capacity of materials Is to characterize it at various values of relative humidity, but only for adsorption process [26] [77]. Therefore, the represented values of specific moisture capacity are only made to adsorption phase, since the values of desorption phase are unusual and difficult to interpret.

To be possible to represent the values of specific moisture capacity, as it can be seen by Equation(5-2), three coefficients are needed. Although, those coefficients were already being determined, and they are placed in fifth line of Table 5-2, for all materials.

The graphs of specific moisture capacity of recycled cellulose board M, projected cellulose coating N, wood wool cement board O and clayish earth plaster S are represented by Figure 5.5.

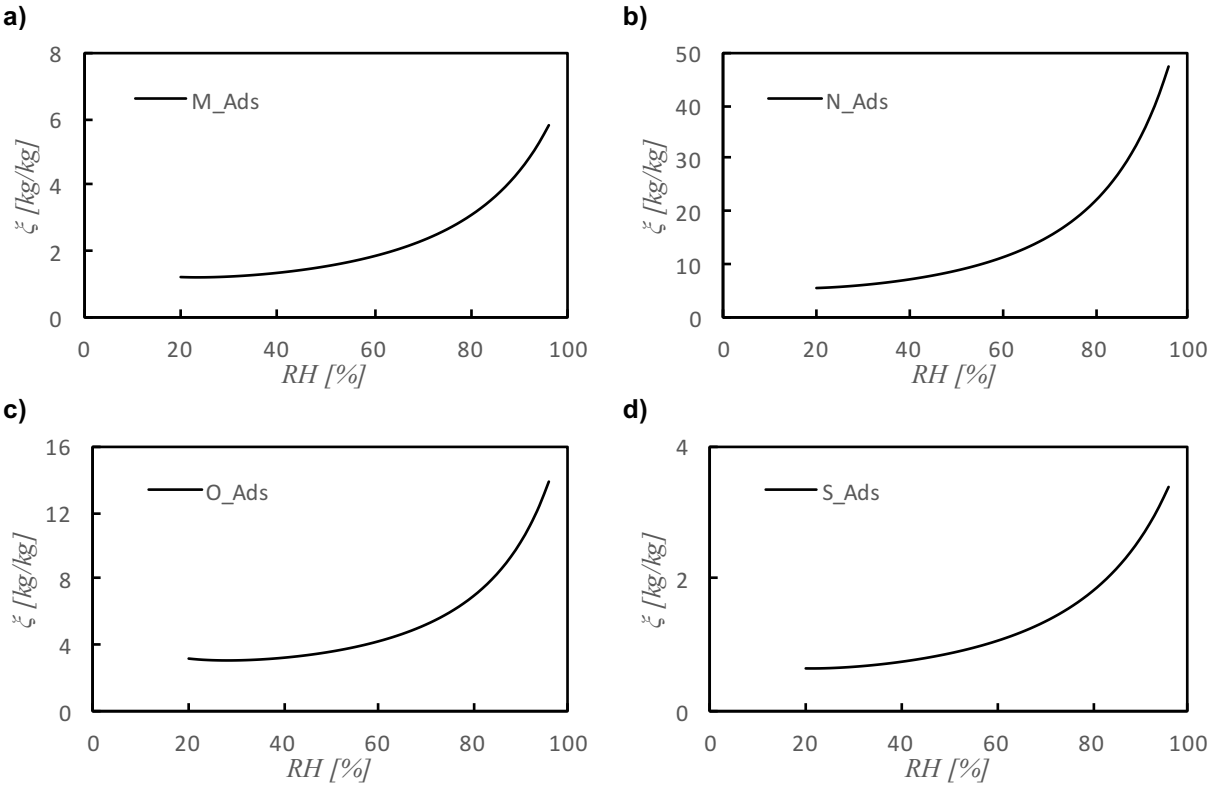

Figure 5.5 – Specific moisture capacity of all materials

In order to compare all materials' specific moisture capacity, all of their curves were placed in the same graph, represented by Figure 5.6.

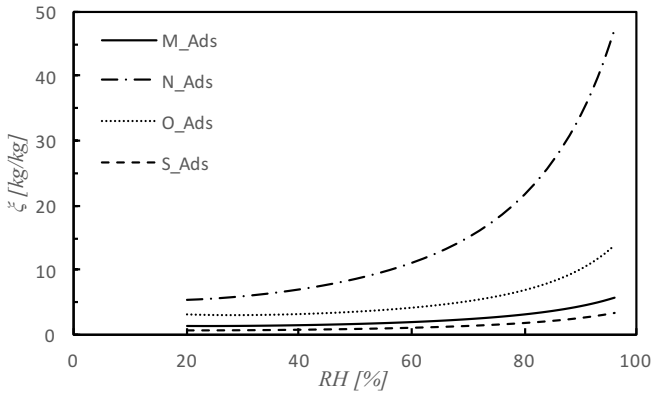

Figure 5.6 – Specific moisture capacity of all materials together

From Figure 5.6 it is possible to conclude that specific moisture capacity ξ follows the behavior of adsorption/desorption phenomenon, having similar curves to adsorption/desorption ones (Figure 4.5), once the values of ξ depend a lot of adsorption phenomenon. However, specific moisture capacity is not related with MBV, once the arrangement of specific moisture capacity curves (Figure 5.6) is different from MBV one (Figure 4.15).

5.2. Moisture Permeability

As shown in 3.3.3, the experiments of moisture permeability were made at 6 different combination of relative humidity inside and outside cup, at mean values of RH of 43%, 54%, 59%, 69%, 80% and 89,5%.

The values of permeability depending relative humidity that were not tested are unknown, but the non-linear regressions will originate a very good prediction of those values.

Four different equations of various authors were studied(Table 5-4) [20], in which the equation 3 reveled to produce the most reliable results beyond all four equations [20] [21].

Table 5-4 – Equations of moisture permeability [20]

Equation number	Authors	Equation	Limitations
1	Various	$A + B * e^{C*\phi}$	RH in %
2	Burch	$e^{A+B*\phi}$	RH in %
3	Galbraith and McLean	$A + B * \phi^{C}$	RH in fraction
4	Richards	$e^{A+B*\phi+C*\phi^2}$	RH in %

Besides all four equations of Table 5-4, it was also developed, in the present work, an equation which fits the best way to all four materials. After testing almost 300 non-linear regressions to experimental results of all materials, the equation which fitted better was Equation(5-3).

$$\frac{1}{A + B * \phi + C * \phi^2} \quad (5\text{-}3)$$

where A, B and C are constant values and ϕ [%] is relative humidity. This equation, from here beyond, is going to be called as Equation 5.

The regressions were made using all values of three samples of each material, as it can be seen on Figure 5.7 to Figure 5.9, in order to do not accumulate errors by using only the mean values.

The coefficients obtained by DataFit 9 that showed to be the best ones to fit to all equations to all materials, are placed in
Table 5-5.

Table 5-5 – Coefficients of all equations of moisture permeability, for all materials

	Equation		M	N	S
1	$A + B * e^{(C*\phi)}$	**A**	1,21E-11	9,00E-11	1,13E-11
		B	1,58E-16	1,14E-19	3,84E-15
		C	0,13	0,23	0,11
2	$e^{(A+B*\phi)}$	**A**	-26,35	-23,79	-28,10
		B	2,14E-02	1,19E-02	0,05
3	$A + B * \phi^{(C)}$	**A**	1,22E-11	9,04E-11	1,19E-11
		B	5,20E-11	7,62E-10	1,25E-10
		C	10,92	21,07	8,98
4	$e^{(A+B*\phi+C*\phi^2)}$	**A**	-22,98	-20,00	-22,57
		B	-8,03E-02	-0,11	-0,10
		C	7,29E-04	8,65E-04	1,04E-03
5	$\frac{1}{A + B * \phi + C * \phi^2}$	**A**	-1,92E+10	-1,73E+10	1,29E+11
		B	3,90E+09	9,60E+08	-4,20E+08
		C	-3,66E+07	-7,79E+06	-9,24E+06

M – Recycled cellulose board; **N –** Projected cellulose coating; **S –** Clayish earth plaster

Graphs a), b), c) and d) of Figure 5.7 to Figure 5.9 represent equations 1, 2, 3 and 4 of Table 5-5, respectively, as graph e) of all these figures represents Equation(5-3) and equation 5 of Table 5-5.

As referred above, the equation represented on graph c) of Figure 5.7 to Figure 5.9, showed to be the best equation to represent moisture permeability of the majority of materials [20]. However, it is important to understand how do all equations fit to experimental results of moisture permeability, for all materials. For knowing how a certain equation really adjusts to experimental data, the coefficient of determination (R^2) is used. This coefficient relates the data obtained by the equation with the data obtained experimentally, and, as closer be both results, higher will be R^2, in a maximum value of 1. If the results obtained by equation are too far from the results of experimental trials, R^2 can takes values as low as zero. From DataFit 9, which was the utilized program to make all the non-linear regressions that have originated all five equations and their coefficients, it was possible to achieve the coefficient of determination (R^2) for all equations and materials, and the results are represented on Table 5-6. As it is possible to see by the same table, equation 3 is the one which produces better results, although

equations 1 and 5 also produce very good fitting results. The only equation that produces worse results is equation 2, and it is the only that should be rejected.

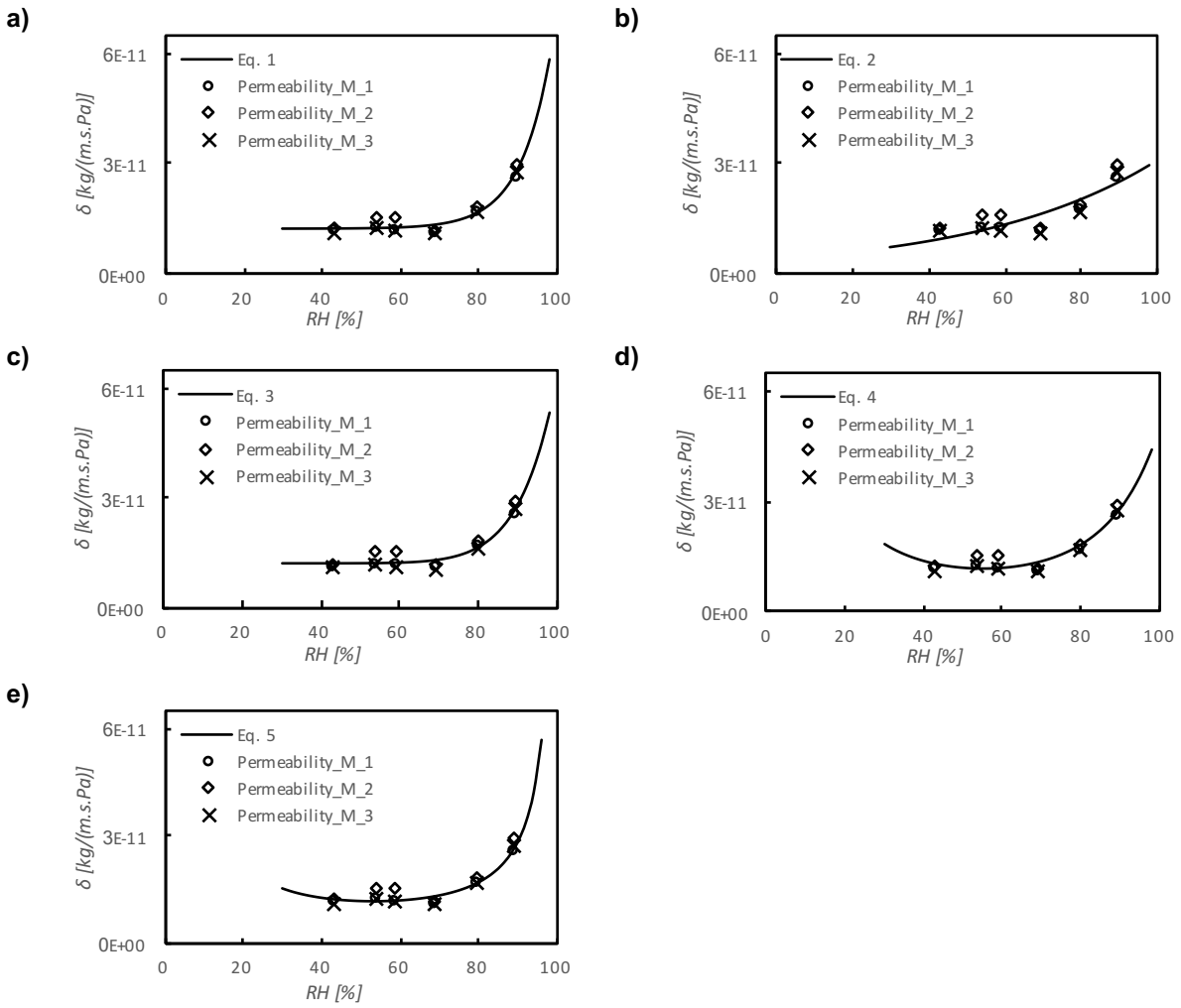

Figure 5.7 – All non-linear regressions of moisture permeability of recycled cellulose board (M)

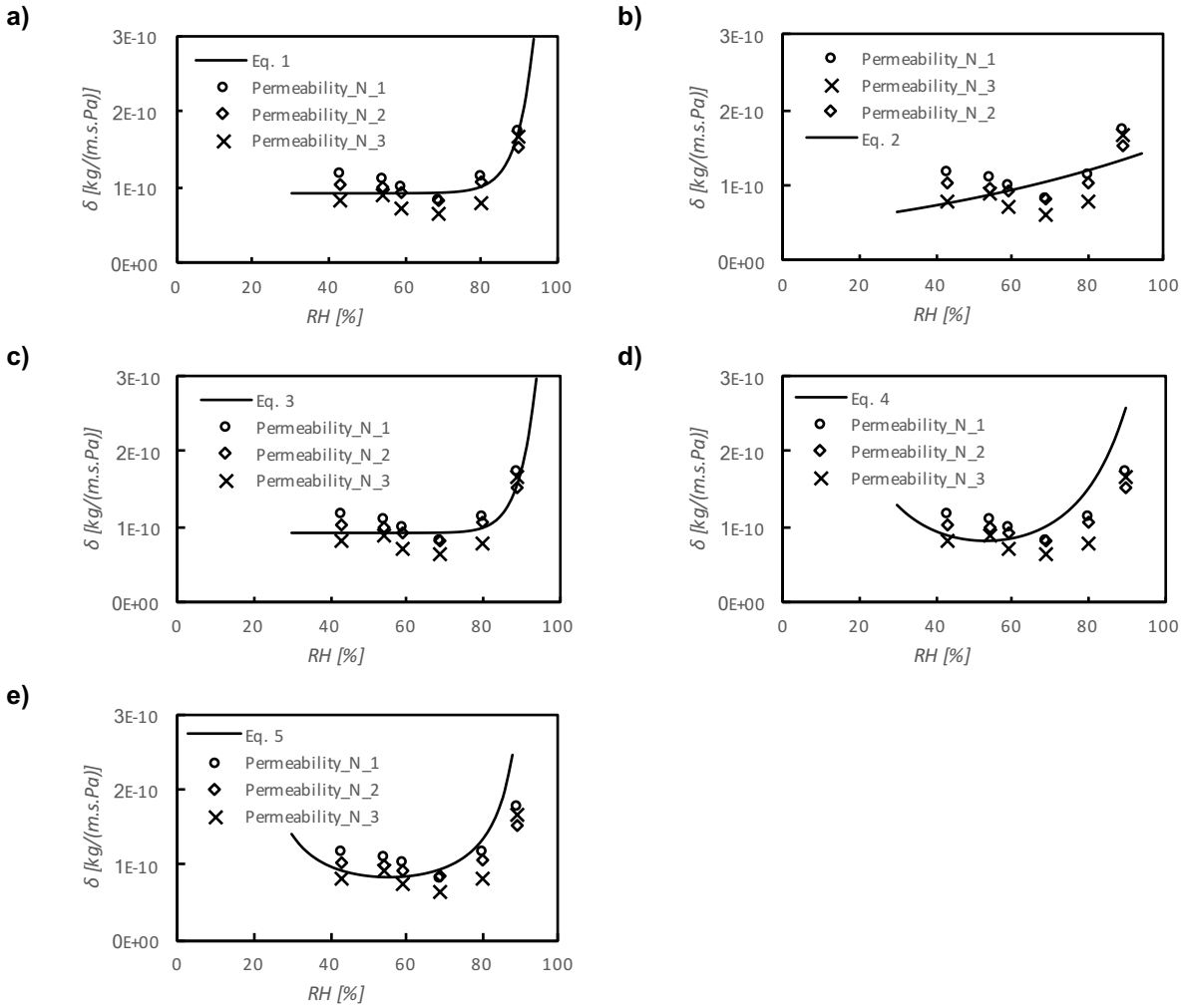

Figure 5.8 – All non-linear regressions of moisture permeability of projected cellulose coating (N)

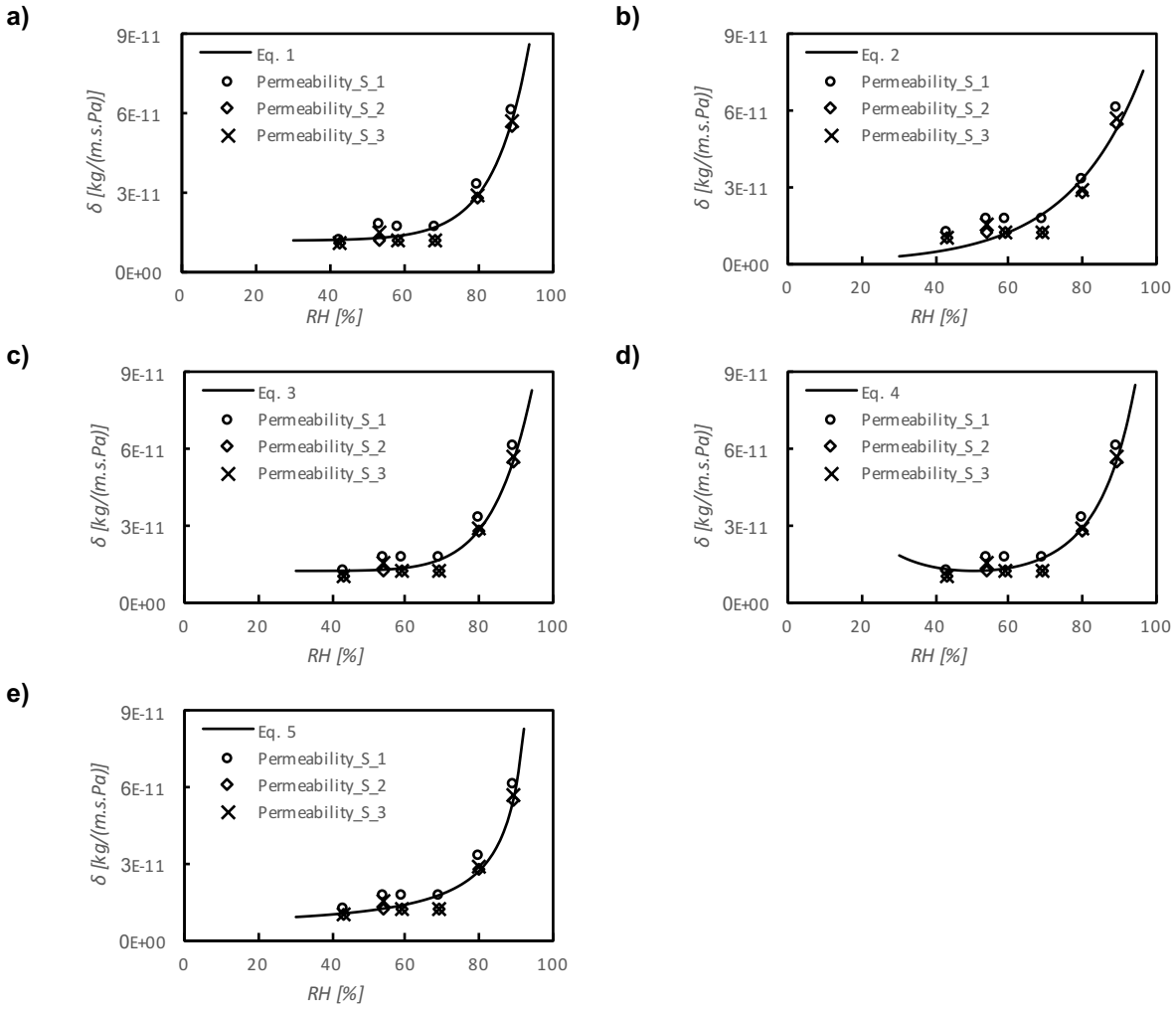

Figure 5.9 – All non-linear regressions of moisture permeability of clayish earth plaster (S)

The results from present work follow the previous ones, once equation 3 is the one which represents better all coating materials moisture permeability (as it is possible to see by graph c) of Figure 5.7 to Figure 5.9) and, as so, it is the one that allows to know better any value of moisture permeability of materials, even at a range of relative humidity that was not tested.

Table 5-6 – Coefficient of determination (R^2) of all moisture permeability equations, for all materials

Equation	R^2		
	M	**N**	**S**
1	0,930	0,783	0,970
2	0,730	0,344	0,907
3	0,932	0,784	0,971
4	0,904	0,764	0,968
5	0,921	0,764	0,968

M – Recycled cellulose board; **N –** Projected cellulose coating;
S – Clayish earth plaster

5.3. Thermal Conductivity

The test of thermal conductivity was made varying the moisture content of samples. The measurements of thermal conductivity were made only when adsorption/desorption isotherm experimental trial stopped, which allowed to relate the thermal conductivity of samples with equilibrium moisture content, at a certain relative humidity.

A previous work [4] already defined a relation between thermal conductivity of materials and moisture content, being the most general equation the number one of Table 5-7. Other work [5] proposed another equation (number two of Table 5-7), that is also applied to many materials.

With the need of find a better equation that represents well the studied materials of the present dissertation, a non-linear regression was made for each material, with DataFit 9, which selected the best equation (number three of Table 5-7), from among almost 300.

Table 5-7 – Equations of thermal conductivity

	Equation
1	$A + B * u$
2	$A + B * u + C * u^2$
3	$A + B * \frac{\ln(u)}{u} + \frac{C}{u}$

The coefficients that revealed to be the best ones to fit to experimental results, for each material, are placed in Table 5-8.

Table 5-8 – Coefficients of all equations of thermal conductivity, for all materials

Equation		**M**	**N**	**O**	**S**
1	**A**	0,27	6,07E-02	6,94E-02	0,88
	B	0,02	2,09E-03	3,88E-03	0,22
2	**A**	0,29	0,06	8,02E-02	0,90
	B	-1,08E-02	3,42E-03	-1,12E-03	0,16
	C	8,57E-03	-9,05E-05	5,38E-04	4,15E-0,2
3	**A**	0,41	0,11	0,17	1,61
	B	-0,12	-0,10	-0,29	-0,27
	C	-0,12	-0,01	0,05	-0,51

M – Recycled cellulose board; **N –** Projected cellulose coating;
O – Wood wool cement board; **S –** Clayish earth plaster

The equations of Table 5-7, with the coefficients of Table 5-8, originate non-linear regressions for recycled cellulose board M (Figure 5.10), projected cellulose coating N (Figure 5.11), wood wool cement board O (Figure 5.12) and for clayish earth plaster S (Figure 5.13). The graph a), b) and c) of all Figure 5.10 to Figure 5.13, represent equation 1, 2 and 3 of Table 5-7, respectively.

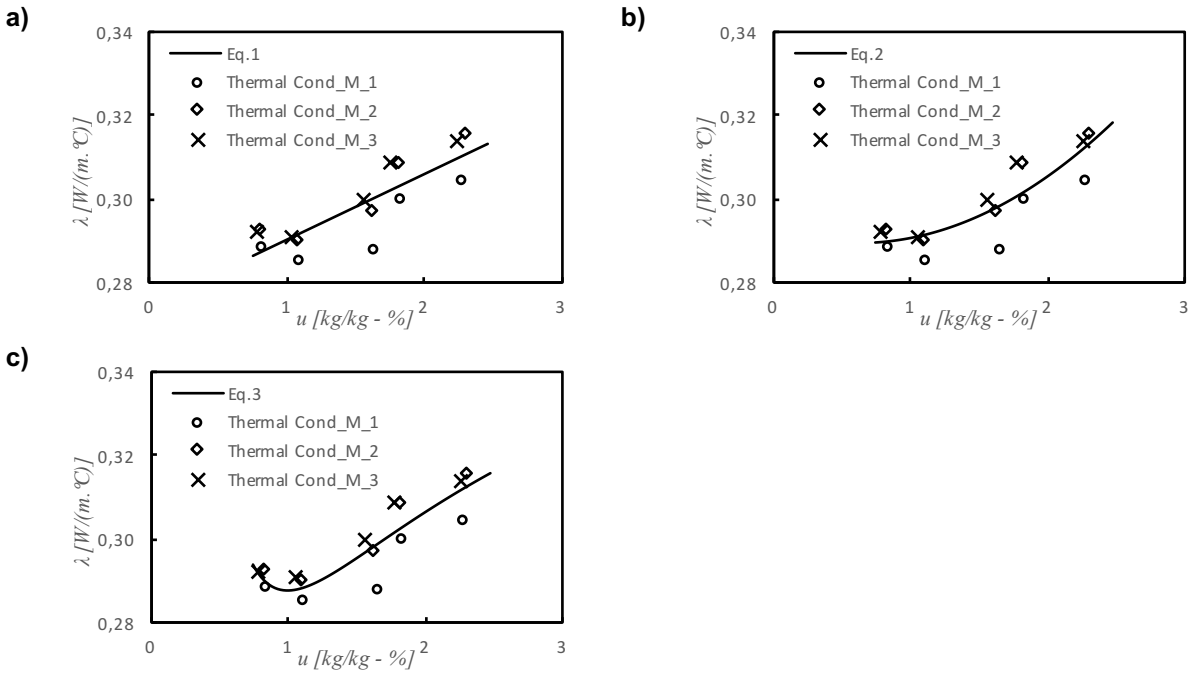

Figure 5.10 – All non-linear regressions of thermal conductivity of recycled cellulose board (M)

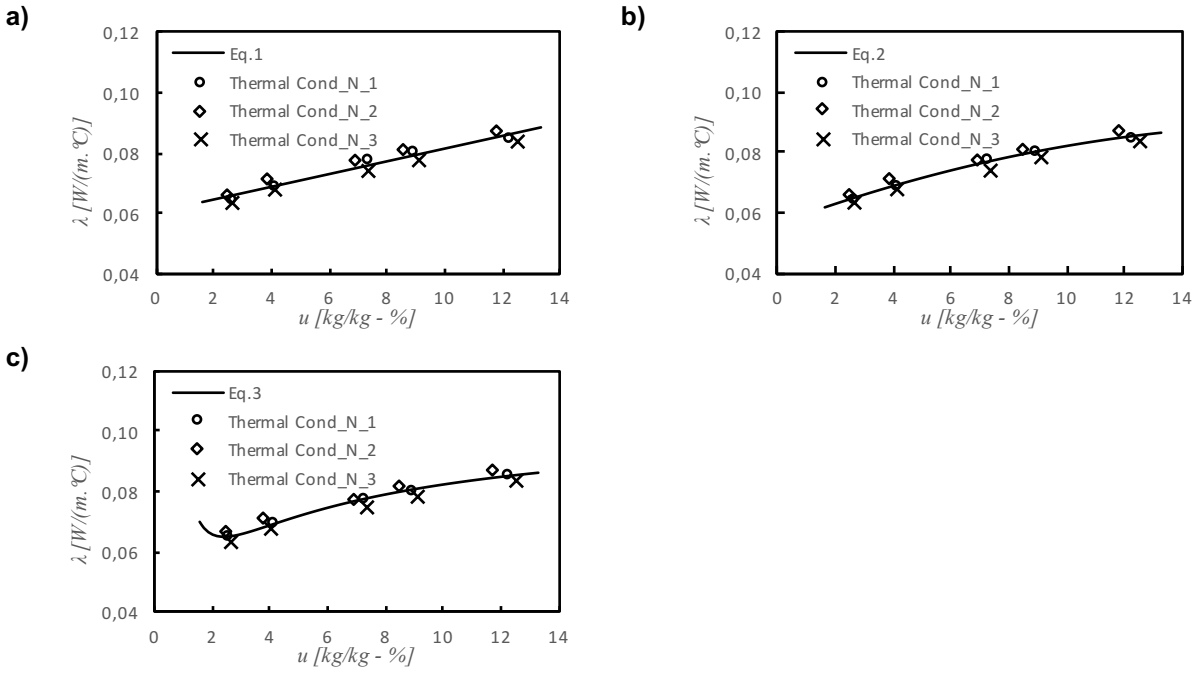

Figure 5.11 – All non-linear regressions of thermal conductivity of projected cellulose coating (N)

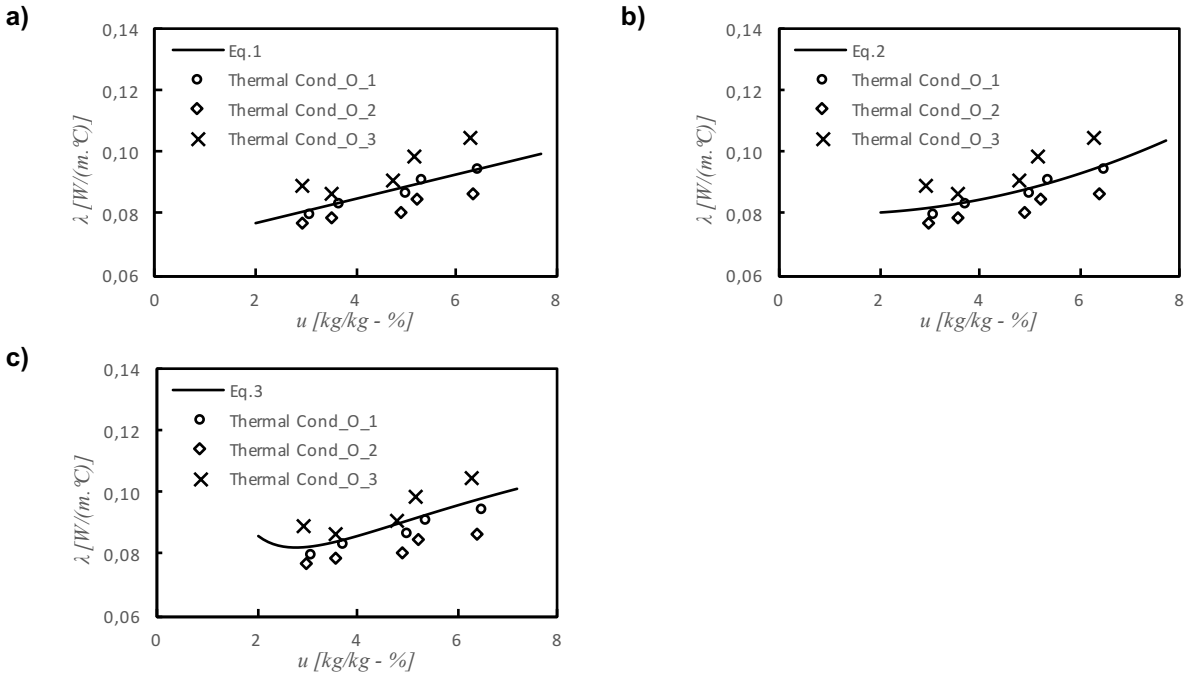

Figure 5.12 – All non-linear regressions of thermal conductivity of wood wool cement board (O)

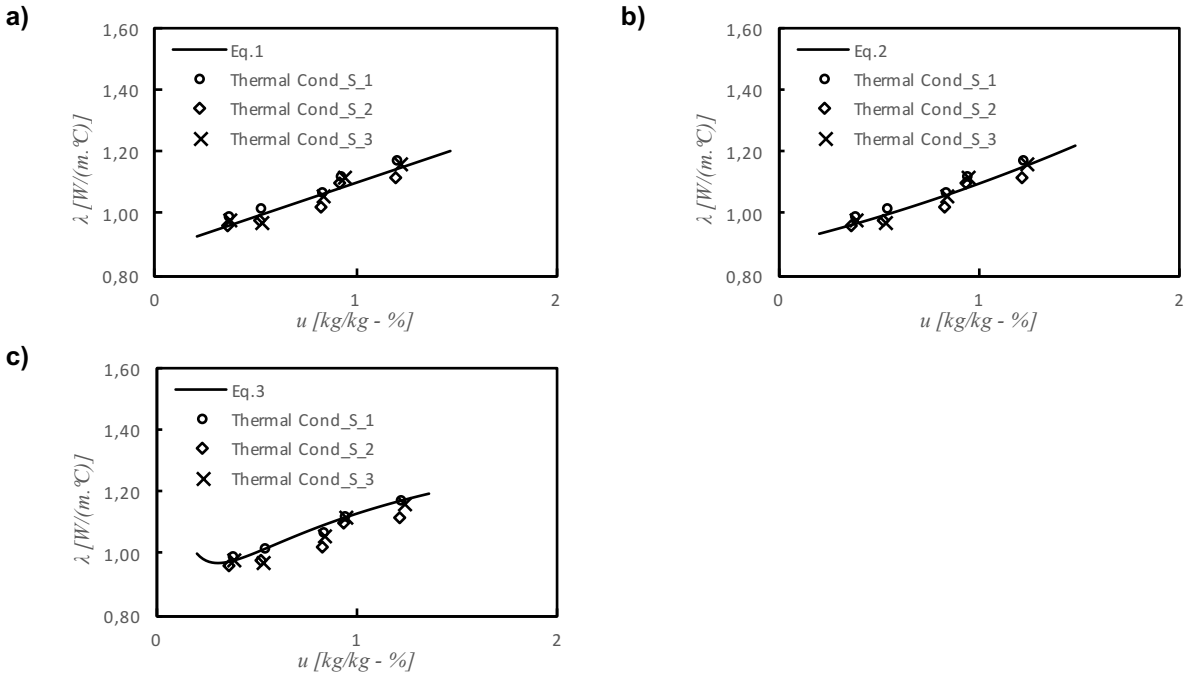

Figure 5.13 – All non-linear regressions of thermal conductivity of clayish earth plaster (S)

As it is possible to see at Figure 5.10 to Figure 5.13, the data obtained by the tests have considerable different values, dependent of the heterogeneity of samples, as well as the response time of materials and also due to the fact that measurements of thermal conductivity of same material's samples are spaced by, about, 10 minutes from each other, what increment their moisture content and so their thermal conductivity. This considerable standard deviation of experimental results clearly affects the goof fitting of non-linear regressions, making that the coefficient of determination (R^2), for all material, takes not so good values, as it can be seen by Table 5-9. From the values of R^2 (Table 5-9) and from

the clear discrepancy between experimental results, it is possible to conclude that the fitting of all non-linear regressions, for recycled cellulose board M (Figure 5.10) and wood wool cement board O (Figure 5.12), is bad.

Table 5-9 – Coefficient of determination (R^2) of all thermal conductivity equation, for all materials

Equation	R^2			
	M	**N**	**O**	**S**
1	0,685	0,928	0,403	0,907
2	0,725	0,942	0,411	0,909
3	0,755	0,940	0,421	0,922

M – Recycled cellulose board; **N –** Projected cellulose coating;
O – Wood wool cement board; **S –** Clayish earth plaster

From all Figure 5.10 to Figure 5.13, and also from Table 5-9, it is possible to conclude that the equation which fits better to all experimental results of thermal conductivity depending of moisture content, for all materials, is equation 3 of Table 5-7. It is important to remind that this equation 3 was achieved in the present dissertation, and, as so, it can improve the approach of numerical models to experimental results, in future works. It is important to refer that even equation 3 has the highest values of R^2 for all materials, it does not represent physically well the behavior of thermal conductivity at low values of equilibrium moisture content of materials, since it decreases with the increment of equilibrium moisture content, which is not the real behavior of materials' thermal conductivity.

Even equation 3 of Table 5-7 exhibits the best fitting results, both equation 1 and 2 (presented on the same table) also produce very acceptable fitting results.

5.4. Moisture Buffering Value (MBV)

To deeply understand all materials' potential to control relative humidity of indoor, it is not only necessary to calculate Moisture Buffering Value. To reach the truly knowledge, it is needed also to know the values of effective moisture penetration depth and the ideal MBV, that allows to compare its results with the results of practical MBV.

5.4.1. Ideal MBV

The concept of ideal MBV was defined by Nordtest report [38], and it was made to compare the real value of MBV (the practical one), with a theoretical value of it, in ideal conditions.

The value of ideal MBV can be calculated by Equation(3-12), which depend of saturation pressure, the time of a complete cycle of MBV and moisture effusivity. This last, can be calculated by Equation(3-8), and it needs the values of moisture permeability and specific moisture capacity at the mean relative humidity of MBV test, which is 54% (mean between 75% and 33% of RH). However, in present work, moisture permeability was only determined to recycled cellulose board (M), projected cellulose coating (N) and clayish earth plaster (S), which makes that the ideal MBV only can be determined for these three materials. In the present work, the experimental trial at the range of 33% and 75% of relative humidity was made and originated the values of moisture permeability, to all three materials, placed in

second line of Table 4-4. For wood wool cement board (O), as it was not tested in experiment of moisture permeability, it was used the ideal moisture resistance factor achieved in 6.3, for mean RH of 54%, that can be related with moisture permeability by Equation(3-5).

Specific moisture capacity is calculated by Equation(5-2), and originated the results, for all materials, presented on first line of Table 5-10. Therefore, knowing that the saturation pressure can be calculated by Equation(2-2), at a temperature of 23ºC, then, the achieved values of moisture effusivity (b_m) are placed on the second line of Table 5-10. As so, the values of ideal MBV can be calculated by Equation(3-12), considering that t_p [h] is equal to the total duration of MBV test, which is 24 hours. Thus, the obtained values of ideal MBV are placed on the third line of Table 5-10, as well as a comparison between it and the practical MBV, at 33%-75% range of relative humidity.

Table 5-10 – Ideal MBV

		M	**N**	**O**	**S**
Specific moisture capacity ξ [kg/kg]		1,34E-11	9,85E-11	3,88E-11	1,48E-11
Moisture effusivity b_m [kg/(m^2.Pa.s$^{1/2}$)]		2,99E-06	8,04E-06	6,26E-06	3,24E-06
MBV [g/(m^2.%RH)]	**Ideal**	**1,4**	**3,8**	**3,0**	**1,5**
	Practical	1,2	2,2	2,6	1,6
	Variation [%]	11,9%	42,2%	12,41%	6,7%

M – Recycled cellulose board; **N –** Projected cellulose coating; **O** – Wood wool cement board; **S –** Clayish earth plaster

As it is possible to see in Table 5-10, recycled cellulose board (M), wood wool cement board (O) and clayish earth plaster (S) have close values of ideal and practical MBV, while projected cellulose coating (N) has a big discrepancy between both ideal and practical MBV. This may be justified by the fact that, as N has high values of porosity it has a high potential behavior with regard to buffer humidity of indoor. However, as the behavior of materials is frequently overestimated in laboratory or theoretical analysis, the practical MBV of projected cellulose coating (N) is almost half of the ideal one. However, looks to exist a recurrent overestimation of MBV for some materials, as shown by Table 5-11 [29].

Table 5-11 – Comparison between ideal and practical MBV of Ramos, N. [29]

		GC	**GP**	**GT**
MBV [g/(m^2.%RH)]	**Ideal**	**1,3**	**0,76**	**1,1**
	Practical	0,75	0,72	0,47
	Variation [%]	41,41%	5,26%	56,88%

GC – Plasterboard; **GP –** Projected plaster; **GT –** Plaster and lime mortar

5.4.2. Penetration depth

The effective moisture penetration depth (EMPD) is a concept develop in Nordtest report, and it is valid only for semi-infinite materials [38]. This concept traduces the active thickness of a material that is used to control relative humidity of environment.

Penetration depth involves many tests, since it needs the value of moisture permeability δ, value of specific moisture capacity ξ_u, which includes adsorption/desorption isotherm test, and the time period of MBV's experimental trial t_p [s], as it is possible to see by Equation(5-4) and Equation(5-5).

$$d_{p,1\%} = 4{,}61 * \sqrt{\frac{D_w * t_p}{\pi}} \tag{5-4}$$

$$D_w = \frac{\delta * p_{sat}}{\rho * \xi_u} \tag{5-5}$$

The penetration depth is achieved when the variation of moisture content inside material, at a certain depth, is only 1% of the variation of moisture content in the surface of the material.

The concept of moisture diffusivity D_w [m^2/s] relates moisture permeability of material, which has all values to all RH ranges, for all materials, in Table 4-4, as well as the saturation pressure (calculated by Equation(2-2), at 23ºC), the density of materials and their specific moisture capacity ξ_u.

In order to fulfil values of penetration depth to all the range of relative humidity, there will be used a non-linear regression of moisture permeability. From 5.2, it was concluded that the best equation to represent the values of moisture permeability, obtained experimentally, is Hansen (1) (third line of Table 5-4), which provides a very good approximation of moisture permeability experimental values, as it can be seen in graph c) of Figure 5.7 to Figure 5.9. However, as wood wool cement board (O) was not tested to its moisture permeability, there will be no value of it of penetration depth.

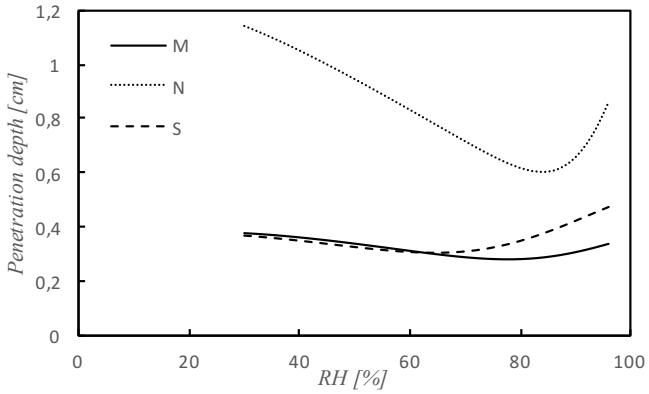

Figure 5.14 – Variation of penetration depth with relative humidity, of all materials

From Figure 5.14 it is possible to understand that penetration depth varies a lot with moisture permeability, as expected, because moisture permeability has directly relation with penetration depth (Equation(5-4) and Equation(5-5)), since moisture permeability tends to lower until about 70% of RH, as it can be seen in Figure 4.6 to Figure 4.8, and raises from that point beyond. This is justified by the beginning of interstitial condensation in all materials.

From Figure 5.14 it is possible to conclude that projected cellulose coating (N) is the one with more penetration depth, due to its higher porosity, and clayish earth plaster (S) has higher penetration depth than recycled cellulose board (M), even M having higher porosity than S. This occurs because, as clayish earth plaster has lower porosity than recycled cellulose board, it will have more liquid form of moisture flux than M, which makes that penetration depth increases more than M one, from 70% of relative humidity beyond.

As the used concept of penetration depth was proposed by Nordtest protocol [38], therefore, the value of penetration depth may be calculated for the mean value of relative humidity between 75% and 33%, which is 54% of RH. As mentioned before in the present section, the value of moisture resistance factor of wood wool cement board (O) was predicted in 6.3, and it makes possible to know the

moisture permeability of O at 54% of mean RH. Therefore, it is also possible to determine the penetration depth of wood wool cement board (O) at 54% RH and it is placed in Table 5-12, as well as the penetration depth of all other three materials at this range of relative humidity.

Table 5-12 – Penetration depth at 54% of relative humidity, for all materials

	M	**N**	**O**	**S**
Penetration depth [cm]	0,33	0,90	0,74	0,32

M – Recycled cellulose board; **N –** Projected cellulose coating; **O** – Wood wool cement board; **S –** Clayish earth plaster

As it is possible to see on Table 3-5 and Table 5-12, penetration depth of recycled cellulose board (M), projected cellulose coating (N), wood wool cement board (O) and clayish earth (S) is lower than the thickness of all samples. This makes that it is not viable to use these coating materials with higher thickness than they actually have, since their active thickness that is capable to adsorb and release moisture from environment is lower than the real thickness. From Table 5-12 it is possible to understand that, considering that the mean relative humidity of a building interior environment always takes the value of 54%, if recycled cellulose board (M), projected cellulose coating (N), wood wool cement board (O) and clayish earth plaster (S) are only applied to buffer the humidity of inside, then there is no benefit that they have higher thicknesses than 0.33, 0.90, 0.74 and 0.32 cm, respectively.

5.5. Response time

The ability of materials to adsorb and release moisture from environment can be quantified by exposing them to some climates with different levels of relative humidity, and measure the maximum quantity of moisture that they can adsorb or release. However, the time in which the materials respond to environment changes is not considered on those tests. For that, it is important to analyze the behavior of materials, in function of time, and understand how do the existent equations of sorption kinetics can fit to the data obtained experimentally.

The analysis of the best sorption kinetics was already made in other works [80] [101], yet some of these equations will be analyzed in the present work in order to understand how do they fit to the materials used on the present dissertation. All equations referred bellow, even if they were not analyzed on the present work, are placed in Table 5-13, knowing that the time (t) is in hours.

One of the first used equations to represent the adsorption and desorption phenomenon, by coating materials, was the Lagergren isotherm [102], created in 1898, that is a first-order equation. However, the Lagergren isotherm does not fit so well to the building materials.

In 1918, Langmuir [103] defined a sorption kinetic capable of represent well the adsorption phenomenon to the majority materials, which have a shape of their adsorption isotherm similar to the Type I of Figure 2.5.

The equation of Langmuir can be rearranged and, by applying grand canonical ensemble in a statistical physics approach, it originated the equation of Hill [104]. Although Hill's equation is similar to the Langmuir one, it is more powerful than the equation of Langmuir [105]. The equation of Hill is one of the best equations of sorption kinetic, and it usually produces very small errors to the experimental data [106].

As the majority of existent kinetic sorption equations were of first order, then emerged a need to develop a new model, capable to represent a larger range of building materials, in what concerns to

their moisture adsorption and desorption behavior. Therefore, it was developed a model for analysis of sorption kinetics, known by pseudo-second-order model, developed by Ho and Mckay [107].

As some building materials were not well represented by the pseudo-second-order model, developed by Ho and Mckay, it is necessary to generalize this previous model, which gives origin to a general form, possible to be adapted to any material. This general equation may originate an initial sorption rate (h) and also the time to reach 50% of equilibrium moisture content of materials ($t_{0,5}$) [101].

In order to understand which are the equation that better represents the behavior of adsorption and desorption in function of time of the used materials on the present work, a non-linear regression of the experimental results was made by using the software DataFit 9. This non-linear analysis was made for all four materials, and it originated an equation, beyond almost 300, designated by Gonçalves.

It is important to refer that these sorption kinetic equations have a big limitation to their real application. This limitation consists in the fact that these equations only consider the variation of time, not contemplating the values of relative humidity of environment. Therefore, the equations of sorption kinetics cannot be applied in real cases, since the relative humidity of climate has not a constant value. So that the sorption kinetics can be applied in a real case, their coefficients would have to be obtained at all of the relative humidity levels, which is not very sensible to achieve.

Table 5-13 – All equations of sorption kinetic equations

Name	Equation		Parameters
	Adsorption	Desorption	
Lagergren [102]	$\log(w_{eq} - w) = \log(w_{eq}) - \frac{K_1 * t}{2{,}303}$	$w = w_{eq} + (w_i - w_{eq}) * e^{-D_1 * t}$	w_{eq}=moisture content at equilibrium w_i = initial moisture content K_1 and D_1 = constants
Langmuir [103]	$w = w_{eq} * \frac{t/\tau}{1 + t/\tau}$		w_{eq}=moisture content at equilibrium τ = characteristic time
Hill [104]	$w = w_{eq} * \frac{t^n}{H + t^n}$	$w = w_i - w_{eq} * \frac{t^n}{H + t^n}$	w_i = initial moisture content w_{eq}=moisture content at equilibrium H and n = constants
2nd order [107]	$\frac{1}{w_{eq} - w} = \frac{1}{w_{eq}} + K_2 * t$	$\frac{1}{w_{eq} - w} = \frac{1}{w_{eq} - w_i} + D_2 * t$	w_i = initial moisture content w_{eq}=moisture content at equilibrium D_2 and K_2 = constants
General [101]	$\frac{dw}{dt} = K_n * (w_{eq} - w)^n$ $h = K_n * w_{eq}^n$ $\quad$ $t_{0,5} = \frac{2^{n-1} - 1}{(n-1) K_n * w_{eq}^{n-1}}$, $(if\ n > 1)$		w_{eq}=moisture content at equilibrium K, h and n = constants
Gonçalves	$w = \frac{A * t}{B + t}$	$w = w_i - \frac{A * t}{B + t}$	A and B = constants

The chosen equations to use on the present work was the pseudo-second-order, Hill and Gonçalves, due to reveled to be the best equation to represent the sorption kinetic of materials, in previous works.

The non-linear regressions of the experimental results were made, for all chosen equations and for all materials, using the software DataFit 9, which originated the coefficients placed on Table 5-14. Those coefficients originated the graphs for recycled cellulose board (M), projected cellulose coating (N), wood wool cement board (O) and clayish earth plaster (S), represented by Figure 5.15 to Figure 5.18, respectively. The coefficients placed in Table 5-14 were achieved by making the non-linear

regressions to the absolute value of moisture content in both adsorption and desorption phases. However, as the section 5.5 represented the values of moisture content in terms of variation compared with initial moisture content in adsorption phase and compared with the last moisture content of desorption phase, therefore the non-linear regressions obtained on the present chapter was also made in moisture content variation.

Table 5-14 – Coefficients of all equations of sorption kinetic for all materials

Equation			M	N	O	S
2^{nd} order	Ads.	K_2	0,74	0,14	0,45	0,48
		w_{eq}	1,45	6,51	4,57	0,66
	Desor.	w_i	1,51	6,56	4,80	0,66
		D_2	-0,24	-0,14	-0,10	-0,26
		w_{eq}	0,81	2,31	3,22	0,16
Hill	Ads.	H	0,95	0,99	0,71	2,39
		n	0,38	0,74	0,25	0,51
		w_{eq}	1,77	6,79	5,89	0,81
	Desor.	H	6,28	2,01	7,20	9,86
		w_i	1,50	6,49	4,79	0,65
		n	1,04	1,18	1,04	1,12
		w_{eq}	0,69	4,11	1,55	0,48
Gonçalves	Ads.	A	1,45	6,51	4,57	0,66
		B	0,94	1,11	0,48	3,15
	Desor.	A	0,70	4,24	1,58	0,50
		B	5,83	1,67	6,65	7,80
		w_i	1,51	6,56	4,80	0,66

M – Recycled cellulose board; **N –** Projected cellulose coating; **O –** Wood wool cement board; **S –** Clayish earth plaster

The first main conclusion to retain is that the equations of pseudo-second-order and the one developed in the present work (Gonçalves) are always coincident, even knowing that both have different forms, as it is possible to see by Table 5-13. This fact makes that the equation developed in the present work (Gonçalves) does not bring any advantage to the accuracy of non-linear regression, when compared with pseudo second-order model, but the new model brings the main advantage of having a simplifier form than the pseudo second-order model, as it is possible to see in Table 5-13.

It is possible to see that, all three equations of sorption kinetic have a really good fitting to experimental data of all materials, as it is possible to see by Figure 5.15 to Figure 5.18.

It is possible to see, in all figures, that all three chosen models represent well the phase of desorption of moisture, for all materials, since all equations are almost overlapped and show to have a really good fitting to the experimental data, as it is possible to see on Figure 5.15 to Figure 5.18.

As referred previously, the pseudo-second-order model, developed by Ho and Mckay, does not represent well some building materials, and this verifies to the used materials in the present work, since it does not represent so well the adsorption data of recycled cellulose board M (Figure 5.15),

wood wool cement board O (Figure 5.17) and clayish earth plaster S (Figure 5.18). Therefore, knowing that the pseudo-second-order and new models present similar values of sorption kinetic, also the equation developed in the present work does not represent much well the data of tests of M, O and S.

It is correct to conclude that all analyzed models represent well the materials with really fast response to changes of relative humidity, since all of them have a good fitting to the experimental results of projected cellulose coating N (Figure 5.16), for both adsorption and desorption phenomenon.

The regressions produced by the chosen models are not influenced by the type of materials, except the case of being a material that has a quick response to environment changes, because the fitting of the models seemed to be the same, independently the nature of material, since the error that they produce, comparing to the experimental data, is similar, for recycled cellulose board M (Figure 5.15), wood wool cement board O (Figure 5.17) and clayish earth plaster S (Figure 5.18).

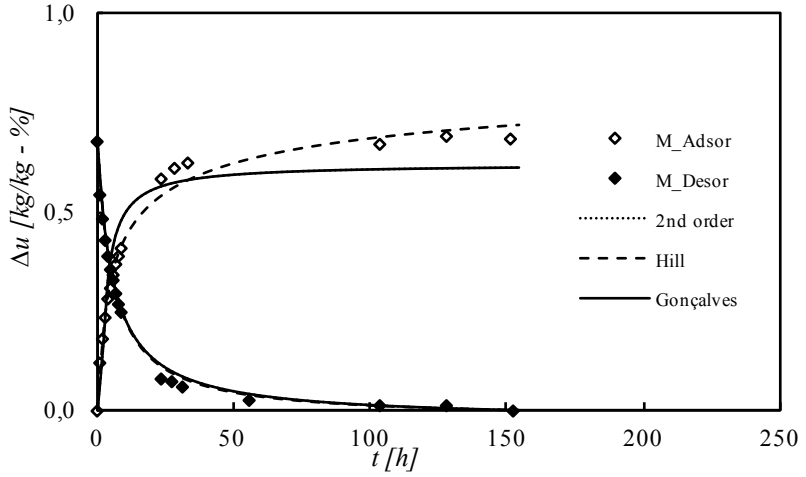

Figure 5.15 – All equations of sorption kinetic applied to response time test, for recycled cellulose board (M)

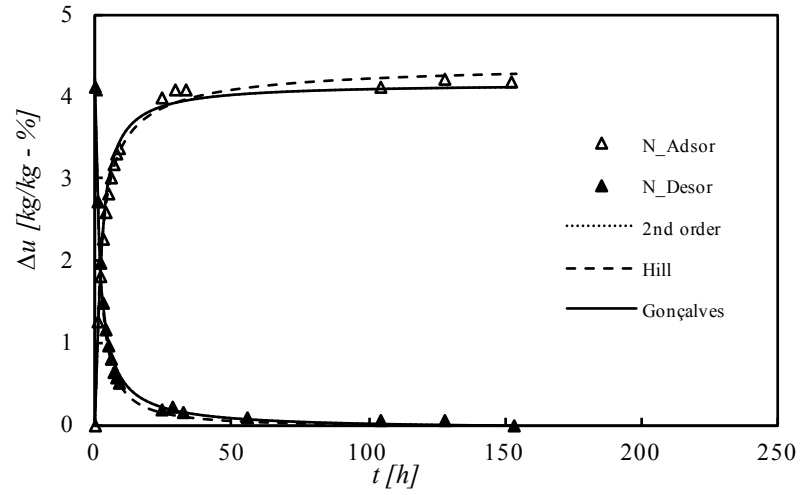

Figure 5.16 – All equations of sorption kinetic applied to response time test, for projected cellulose coating (N)

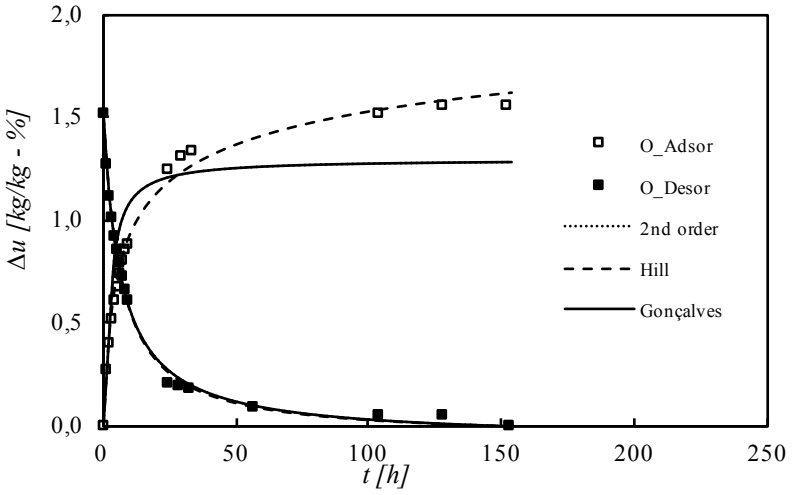

Figure 5.17 – All equations of sorption kinetic applied to response time test, for wood wool cement board (O)

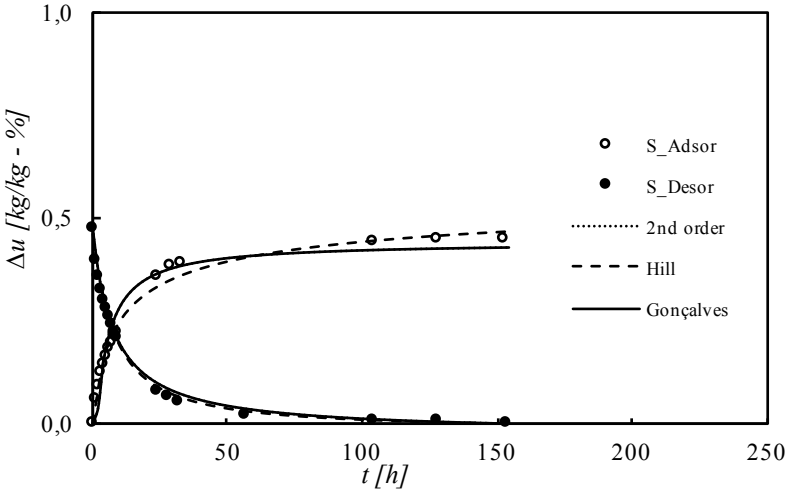

Figure 5.18 - All equations of sorption kinetic applied to response time test, for clayish earth plaster (S)

Following the conclusions of previous works [80] [105] [106], also in the present work, Hill's model to sorption kinetics, applied to experimental results of response time, is the one with the best fitting to all materials. This model is able to produce really good results to both adsorption and desorption phases, in function of time. This model may produce the best results since it does not achieve an earlier horizontal curve section, as it happens to the other two models, for all materials.

It is important to refer that for experiment of response time it was not presented the values of coefficient of determination (R^2) because, as it is shown in Table 5-13, all non-linear regressions for adsorption phase do not consider the initial moisture content and then the adsorption equations start from zero. Therefore, the coefficient of determination for adsorption phase for all equations of Table 5-13 is near to zero and it was chosen to not present them because those values do not represent the good fitting of all equations.

Chapter 6: Hygrothermal Simulation

6.1. General considerations

All analytic methods allow to obtain some materials' characteristics in a quick and considerably easy way. However, the analytic analysis is usually made considering some simplifications that let to do the hygrothermal calculations in a sensible mode. The analytic methods are usually made in steady state, that means that the analysis is normally made independently of the time, and those analytic analysis normally consider that there is not heat or moisture generation, and they are typically made in only one direction. Therefore, all simplifications of analytic methods can imply in lower the precision of the calculations, but it is compensated by the facility that they bring to calculations. However, there are some analytic methods that do not have low precision, since the output can be as simple as the equilibrium moisture content, like it happens in experiments of adsorption/desorption isotherm or response time.

To compensate the lack of precision of the analytic methods, an analysis of the hygrothermal behavior of a building is normally made in a transient regime, that allows to make a hygrothermal analysis in function of time and in the three orthogonal directions. The transient regime belongs to variable regime, at it considers a transition to a permanent regime, which simplifies considerably the hygrothermal analysis, without compromise a lot the accuracy of the calculations. However, even a transient analysis can be made analytically, it is little viable to do it analytically, since it takes a long time to complete the analysis. Therefore, it is easier to make the analysis with recourse to a simulation program, that can provide the results in a more sensible and fast way.

The main goals of the present hygrothermal simulation are to compare the experimental results of MBV with the same parameter achieved by simulation, as well as doing a sensivity study to assess the influence of thermal and hygric parameters of materials in the control of indoor climate. It was also chosen to make a hygrothermal simulation with some of the studied materials in the present dissertation placed as coating materials, with all the characteristics calculated in the present work, and understand their impact in interior environment.

To make all hygrothermal simulations in the present chapter it was chosen to use the software *Wufi Plus*, developed by *Fraunhofer Institut fur Bauphysic*, which is better described in section 6.2

6.2. Wufi Plus

The software *Wufi Plus* is a holistic model of simulation of elements behavior in dynamic regime, and it is able to quantify the thermal and hygric transfers of an element or building. This software considers many hygrothermal effects and parameters, like the following ones:

- Sources of indoor moisture;

- Moisture in envelope, coming from capillary action, water vapor diffusion or adsorption/desorption of moisture from interior or exterior climate;
- Sources of indoor heat;
- Heat from envelope;
- Solar energy that crosses the windows and opaque elements of enclosures;
- Natural or forced ventilation

All parameters, described above, that affect the thermal and hygric characteristics of indoor climate and that are considered by *Wufi Plus,* are represented in Figure 6.1.

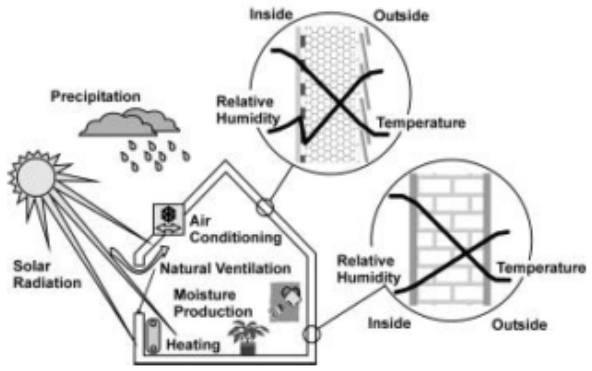

Figure 6.1 – Indoor and outdoor climate parameters considered by Wufi Plus [108]

The software *Wufi Plus* is able to make unidirectional analysis of heat and mass transfer and it represents all elements by a mesh that contains as many nodes as more refined is the analysis. These nodes have a certain volume of the element associated to them and each node have equations of heat and mass transfer.

The program chosen to use in present work was *Wufi Plus* due to it is able to make a transient analysis of the hygrothermal behavior of a building, and it was the chosen to use on the present wok since it is capable to produce reliable and accurate results [68] [73] [109] [110] [111].

6.3. Verification of MBV of studied materials

In order to validate both experimental trial of MBV and software *Wufi Plus*, it was made a comparison between the MBV achieved by experimental trials, presented in 3.3.5, and a MBV simulated by *Wufi Plus.*

To achieve a MBV from software, it is only necessary to extract the moisture content of the coating material, in function of time, and then apply those moisture content values to MBV formula. To condition that all mass transfer was only made between indoor climate and the coating materials, all surfaces of the building had a layer of a theoretical material, with a thickness of 0,001 m, with the minimum accepted value of porosity, and the highest possible value of moisture resistance factor. The building is a cube, with an internal volume of 1 m^3, and five of the six surfaces are composed only by the theoretical material, described before. Only one surface had a constructive system composed by the theoretical material (in outside) and the coating material to be tested (inside), and none of the six surfaces of the building had any type of window. The exterior climate was considered to have constant

temperature, since all surfaces were considered to have adiabatic behavior. All the considerations, explained before, were taken to ensure that the mass transfer would occur only between interior climate and the coating material intended to be analyzed.

As wood wool cement board (O) was not tested in experiment of moisture permeability, its value of moisture resistance factor is unknown. However, it was made five simulations of MBV varying the moisture resistance factor of wood wool cement board. Thus, it was achieved a curve of MBV in function of moisture resistance factor, by making a polynomial regression of the data achieved by simulation, and it is represented in Figure 6.2.

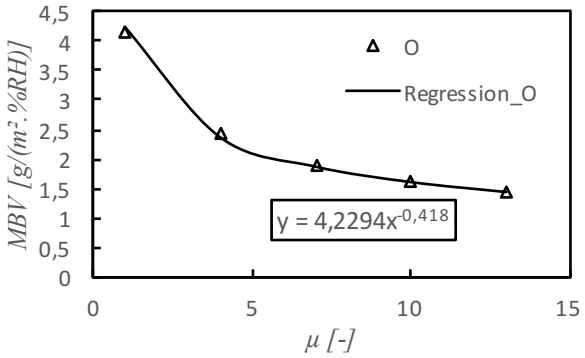

Figure 6.2 – Variation of MBV with moisture resistance factor, for wood wool cement board (O)

As it is possible to understand by Figure 6.2 the Moisture Buffering Value is strongly affected by variations of moisture resistance factor. To be possible to choose an ideal value of moisture resistance factor, it was considered the experimental MBV of the range of 33%-75% RH, which is placed in Table 4-9, and from the equation of Figure 6.2 it originated the ideal moisture resistance factor of 3,23 [-].

As the test of MBV assume that the relative humidity of indoor has the values of 33%, for 8 hours, and 75%, for 16 hours, so the simulation also had those values of relative humidity, during the same periods of time. It is important to refer that the MBV of the simulation was made in the last day of a 31 days' period (01/01/2017 to 31/01/2017), and the comparison between MBV obtained from software and from tests are represented by Figure 6.3

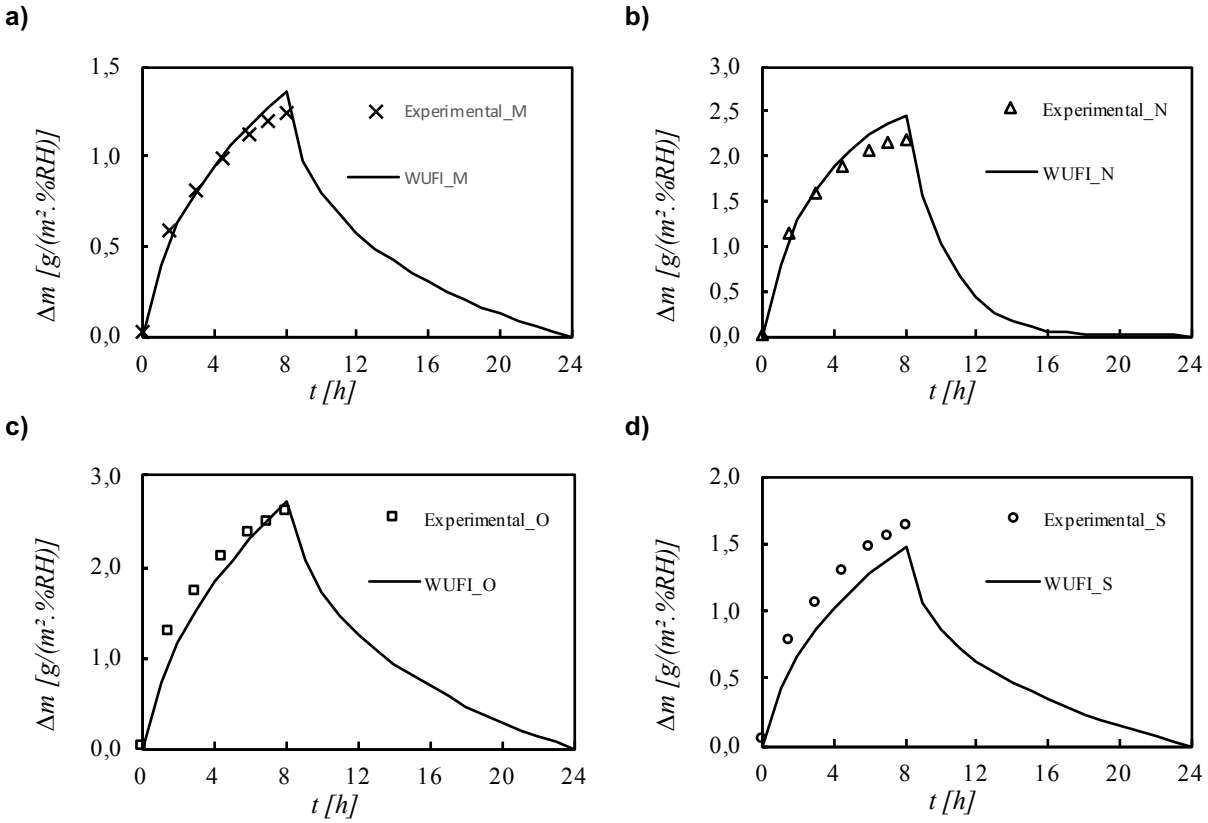

Figure 6.3 – Comparison between MBV obtained from tests and *Wufi Plus*, of all materials

The values of Moisture Buffering Value, that can be determined by Equation(3-13), achieved from experimental trials and from software are placed in Table 6-1, as well as the absolute value of variation between each other, in percentage.

Table 6-1 – MBV obtained from experimental trials and *Wufi Plus*

		M	**N**	**O**	**S**
MBV [g/(m².%RH)]	**Experimental**	1,2	2,2	2,6	1,6
	Wufi Plus	1,4	2,5	2,7	1,5
Variation [%]		9,0%	11,3%	4,2%	10,8%

M – Recycled cellulose board; **N –** Projected cellulose coating; **O –** Wood wool cement board; **S –** Clayish earth plaster

As it is possible to see by Figure 6.3 and Table 6-1, all materials have similar values of their experimental and simulated MBV and the small difference between them are justified by the MBV obtained by *Wufi Plus* is not susceptible to some problems inherent to experimental trials, like lack of climatic chamber's tightness, problems with the ventilation or inaccuracy of the scale, beyond many other factors. Even knowing that the moisture permeability was not determined experimentally for wood wool cement board, as explained earlier in the present chapter, it was possible to predict moisture resistance factor μ [-] of it and it produced similar values of MBV from test and from software, being the material with lower difference between them, as described in Table 6-1.

From Figure 6.3 it is possible to validate both experimental procedure of Nordtest [38] and the software *Wufi Plus*, since both produced similar values of MBV.

6.4. Sensivity study

A sensivity study has been made in order to understand which parameters affect more the hygrothermal conditions of the indoor climate of an old building. This sensivity analysis was made independently of the materials used on the present dissertation, since the main goal was to understand which coating materials' parameters affect the hygrothermal conditions of the interior climate of buildings, in a general form, without any climate control systems and with natural ventilation of the building.

6.4.1. Building characterization

The used building to make the hygrothermal simulation is composed by only one division and one floor and it intends to represent the geometry of a room of National Museum of Ancient Art of Portugal, like it has been made in previous work [112] . The used exterior climate was of Lisbon, provided by a file that belongs to *EnergyPlus*, with the data of temperature and relative humidity represented on Figure 6.4. It was not considered to exist incident rain, in order to condition that the moisture content of the elements of building be only consequence of the hygroscopicity of the materials-

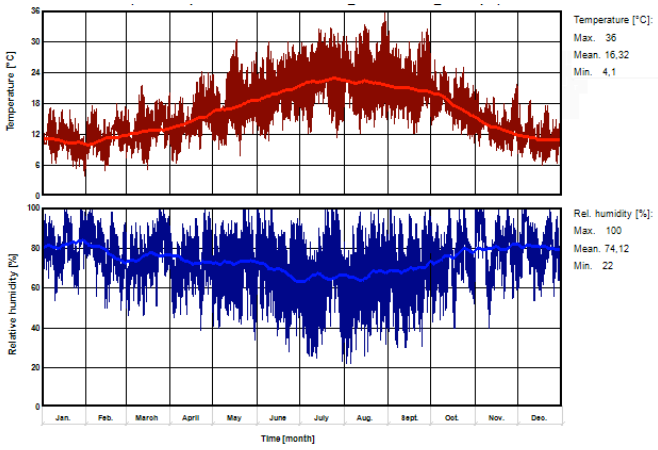

Figure 6.4 – Temperature and relative humidity of exterior climate of Lisbon

In order to ensure that the changes of interior environment of building was strongly affected by the thermal and hygroscopic behavior of the coating materials placed on all interior surfaces of the walls, all surfaces were considered to have adiabatic behavior, except the south wall, which have exchanges of mass and heat with the exterior. The south wall is the one which have windows, that represent 10% of the floor area, while all other surfaces, including the floor and ceiling, are totally opaque. The ceiling had no type of attic and it is totally horizontal, as it is the floor of the building.

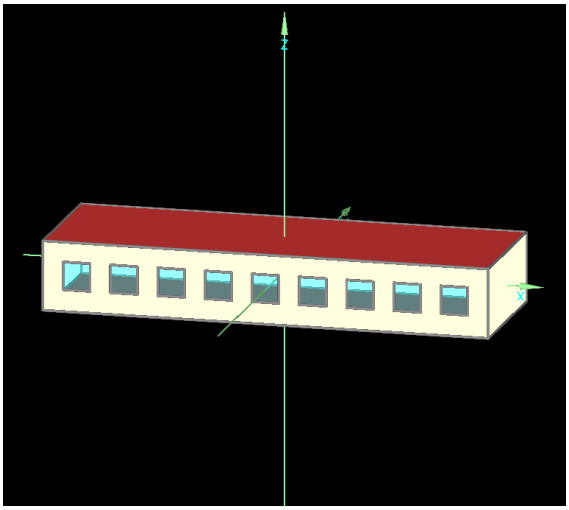

Figure 6.5 – Building used to sensivity study

Knowing that the only surface that have windows is the south wall, it is easy to identify the orientation of all the remaining elements, by Figure 6.5. The dimensions of all elements of the used building are presented on Table 6-2, knowing that they are made by the interior of the building.

Table 6-2 – Dimensions of all elements of the building used to sensivity study

Element	Width [m]	Height [m]	Area [m^2]
Floor	22,5	7,5	168,75
Ceiling	22,5	7,5	168,75
North wall	22,5	3,5	78,75
South wall	22,5	3,5	78,75
East wall	7,5	3,5	26,25
West wall	7,5	3,5	26,25
Windows (one/all)	1,35/12,15	1,4/12,6	1,89/17,01

The elements of the building, with the respective dimensions placed in Table 6-2, originated an interior volume of the building of 590,63 m^3.

As it is possible to see by Figure 6.5, there are nine windows on the building, all in south wall, with a heat transfer coefficient U of 3,3 W/(m^2.ºC) and a short-wave radiation average of 0,1 [-].

The composition of all walls consists in a limestone covered, in both sides, by a lime mortar fine. The floor was composed by concrete with a coating made of oak old placed above. The ceiling was composed by concrete, coated in exterior by oak old and by the tested coating material in interior surface. All dimensions and main characteristics of the opaque elements are placed on Table 6-3, and they were obtained in a previous work [112].

Table 6-3 – Main characteristics of building's opaque elements

Element	Materials	Thickness [m]	λ [W/(m.ºC)]	U [W/(m^2.ºC)]
Wall	Lime mortar fine	0,03	0,7	1,8
	Limestone	0,54	1,76	
	Lime mortar fine	0,03	0,7	
Ceiling	Oak old coating	0,02	0,15	Variable
	Concrete	0,25	1,7	
	Coating	0,03	Variable	
Floor	Concrete	0,25	1,7	2,0
	Oak old coating	0,02	0,15	

The tested coating materials were placed in interior surface of ceiling due to aesthetic reason and also to diminish its impact in thermal inertia of envelope, since the ceiling has a lower area than the sum of all walls, as it can be seen in Table 6-2.

It was considered a production of both moisture and heat inside the building, in order to reproduce better the real activity of people and presence of equipment inside buildings. It was considered the presence of 12 people inside the building and a air exchange rate of 0,3 h^{-1}, caused by natural infiltration. The building did not have any type of equipment inside, neither to control relative humidity, temperature or air exchange ratio.

6.4.2. Study's procedure

A previous work developed by Ferreira, C. [53] made two similar sensivity studies to the one made in the present dissertation. In that work, it was tested the influence of the air exchange rate, position of coating materials and position and exposition of the studied room in the control of indoor relative humidity. One of the main conclusions obtained on that work was that air exchange rate influences considerably the quantity of moisture that the hygroscopic materials applied as interior coatings adsorb and release. Another main conclusion was that the position and orientation of the studied room have almost no effect in indoor temperature and relative humidity and that the difference between having hygroscopic materials only on ceiling or place hygroscopic materials on ceiling and walls is considerably low. Therefore, the orientation of the studied room on the sensivity study of the present work was considered to be non-variable and the hygroscopic materials were only applied on ceiling.

From the previous work [53] it was possible to affirm that hygric materials affect positively the control of indoor RH but their influence on the control of indoor temperature was not assessed. For the sensivity study of the present work, the main goal was to understand which materials' characteristics influence more the temperature and relative humidity of building interior environment. For that, it would be necessary to choose parameters of materials that can vary significantly, among different type of materials, and also those parameters had to be able to influence the relative humidity and temperature of indoor. First of all, in the previous work [53] it was chosen to use the air exchange rate as one of the variables once it showed to affect significantly the stabilization of indoor relative humidity. Then it was decided to choose one parameter capable to improve the hygric behavior of buildings and another parameter able to improve the thermal behavior. As so, the chosen thermal parameter was thermal conductivity λ and the hygric parameter was MBV. Therefore, as shown in 6.3 the moisture resistance factor μ highly affects the MBV and it was the best way to vary MBV. As it was intended to have the three MBV in each one of the classes of "Moderate", "Good" and "Excellent" of Figure 3.33, then with the correct variation of μ were obtained the values of MBV placed in Figure 6.6. The values of thermal

conductivity were chosen in order to be significantly different between each other, in order to represent three different types of construction materials.

The first column of the tree diagram of Figure 6.6 contains the air exchange rates. The second column of the diagram contains the three chosen values of thermal conductivity, while in its third column are placed the values of MBV.

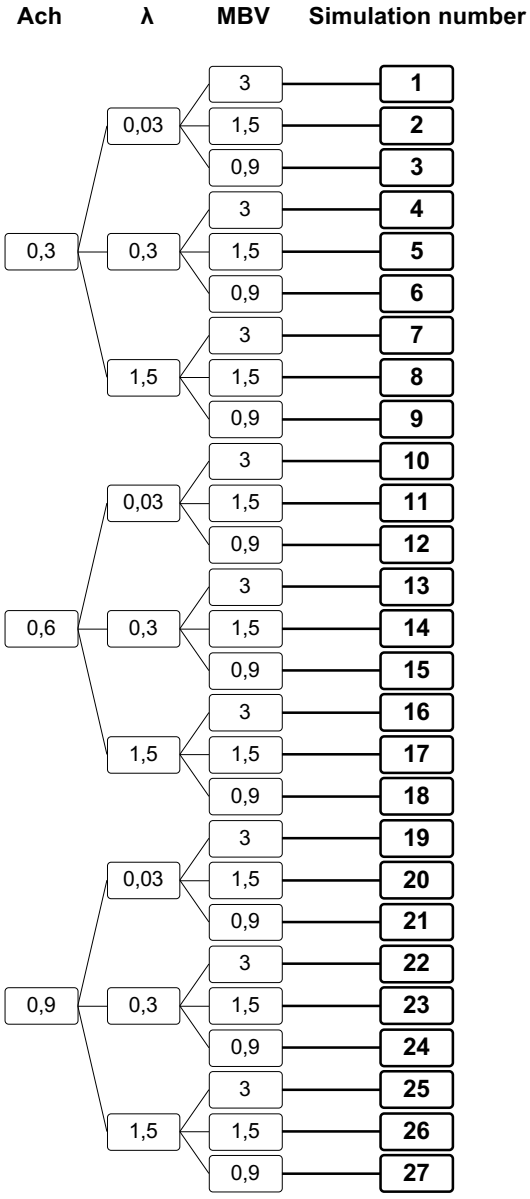

Figure 6.6 – Tree diagram of sensivity study

It was chosen to use only one sorption isotherm, and it was made a selection of three curves that, two of those represent two materials used in the present work and all three are placed in Figure 6.7. The chosen adsorption/desorption isotherm was the B curve of Figure 6.7.

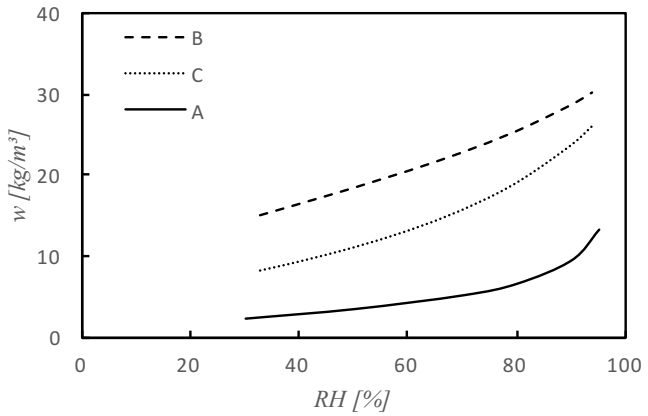

Figure 6.7 – Soprtion isotherms of sensivity study

It is important to refer that the only variable characteristics of coating materials were the air exchange rate, thermal conductivity and MBV, while all other characteristics maintained constant, like specific heat capacity c_p [J/kg.K)], porosity [m^3/m^3] and density [kg/m^3], which were always equal to 1000, 0.3 and 1000, respectively.

The period of the analysis, for each of twenty-seven simulations, were over three years. This long duration of the analysis is justified by the need of understand how the coating materials respond to long cycles of relative humidity and temperature and, as so, understand how they can improve the thermal and hygric inertia, and also to exposed them to all year season, which have different values of relative humidity and temperature of the exterior environment.

6.4.3. Analysis of results

The present sensivity study looks to understand how the coating materials can influence the temperature and relative humidity of interior climate, even knowing that there are many parameters that can be extracted from software. To make the analysis more explicit, the impact of the coating materials in temperature and relative humidity of indoor is not made in absolute values, because the graphs would be imperceptible, with the different curves almost overlapped, since the impact of the coating materials on temperature and RH is not high enough to put way all the curves. For that, the parameters that were chosen to understand the impact of the different simulations in relative humidity and temperature were Relative Humidity Stabilizations (RHS) [53] and Temperature Stabilization (TS), represented by Equation(6-1) and Equation(6-2), respectively.

$$RHS = \sum_{i=1}^{8760} \left| \overline{RH_{i,seas}} - RH_i \right| \quad (6\text{-}1)$$

$$TS = \sum_{i=1}^{8760} \left| \overline{T_{i,seas}} - T_i \right| \quad (6\text{-}2)$$

Both Equation(6-1) and Equation(6-2) are made to one year, which have 8760 hours, and is the absolute value of the difference between a seasonal dynamic mean and the values of each hour of relative humidity and temperature, respectively. Both seasonal dynamic means are achieved, for each hour, by making the arithmetic mean of the 15 days or 360 hours before and the 15 days or 360 hours after the hour which is being analyzed, as it is described in other works [113] [114].

It was chosen to use the percentiles of 1% and 99% to both temperature and relative humidity and it represents the value that is higher than 1% and 99% of all measurements, respectively. These percentiles are used to exclude atypical values of temperature or RH, which does not represent the acceptable values of the parameter.

To make an embracing analysis of the sensivity study, there were chosen to fix all of the three variable parameters, one at a time, that originated 24 graphs on total, 12 for RHS and another 12 for TS, as explained on Table 6-4.

Table 6-4 – Description of sensivity study's graphs

Fixed parameter		**RHS**	**TS**
Name	**Value**		
Thermal conductivity	**0,03**	Graph a1) and a2)	Graph j1) and j2
	0,3	Graph b1) and b2)	Graph k1) and k2)
	1,5	Graph c1) and c2)	Graph l1) and l2)
MBV	**0,9**	Graph d1) and d2)	Graph m1) and m2)
	1,5	Graph e1) and e2)	Graph n1) and n2)
	3,0	Graph f1) and f2)	Graph o1) and o2)
Air exchange rate (ach)	**0,3**	Graph g1) and g2)	Graph p1) and p2)
	0,6	Graph h1) and h2)	Graph q1) and q2)
	0,9	Graph i1) and i2)	Graph r1) and r2)

By Equation(6-1) and Equation(6-2) is easy to conclude that lower values of RHS and TS implies that the value of relative humidity or temperature, at a certain hour, is closer to the mean of the 30 days around that hour. Therefore, it is correct to affirm that lower values of RHS and TS are associated to higher hygroscopic and thermal inertia, respectively.

The graphs a), b) and c) of Figure 6.8 represent the variation of RHS with MBV of the materials and with the air exchange rate of the room, at constant values of thermal conductivity. The graphs a1), b1) and c1) show that the stabilization of relative humidity, over one year, increases with higher values of MBV of the coating material, since it indicates that the coating material has better capacity to buffer the humidity of indoor and, as so, it provides a higher hygric inertia to the room, with the increment of its MBV. The graphs a2), b2) and c2) shows that the air exchange rate of the room has significant influence in the stabilization of indoor relative humidity, since the increment of air exchange rate of the room causes an increment of RHS, which means that the hygric inertia takes lower values with higher values of air changes per hour. Therefore, it is correct to affirm that the reduction of air exchange rate of a room increases the ability of coating materials to control indoor relative humidity and it just confirms the same conclusions of previous works [53].

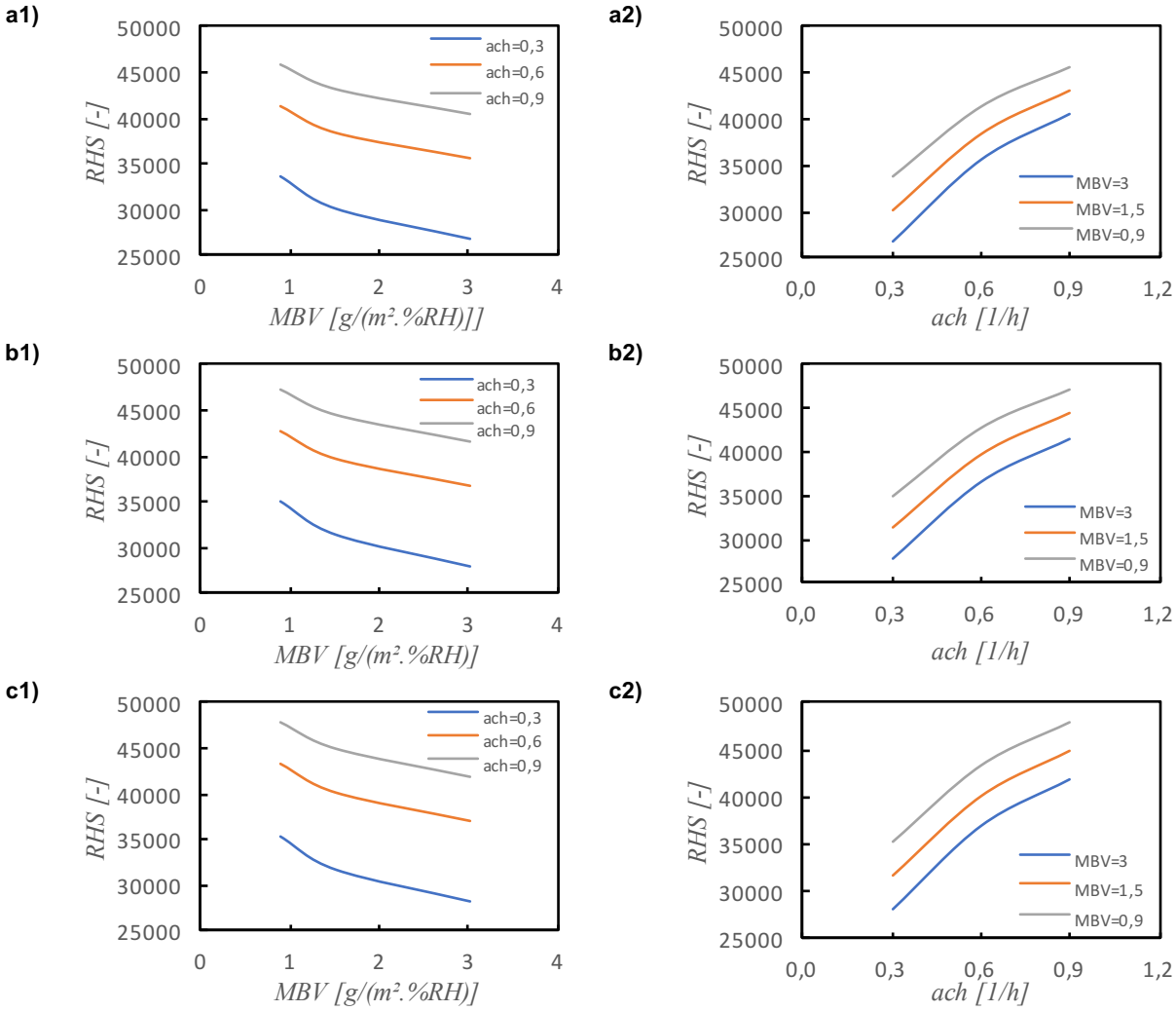

Figure 6.8 – Variation of RHS with MBV and air exchange rate, at fixed values of thermal conductivity

The graphs d), e) and f) of Figure 6.9 represent the impact that thermal conductivity and air exchange rate have in the stabilization of relative humidity of indoor climate, at fixed values of the MBV of the coating materials. By graphs d1), e1) and f1) it is possible to understand that the increment of thermal conductivity of coating materials leads to a few decreasing of the hygric inertia of a building or room, once this increment of thermal conductivity causes, equally, higher values of RHS. This is justified by the fact that higher thermal conductivity is inversely related with the porosity of materials, once the smaller is the porosity, then higher thermal conductivity will be. Therefore, if higher values of thermal conductivity imply less porosity of the coating material, then lower will be its ability to adsorb and release moisture from environment, what will lead to lower hygric inertia of the room. However, the increment of RHS with higher values of thermal conductivity only happens to low values of thermal conductivity and from about 0,25 W/(m.ºC) beyond the effect of thermal conductivity on hygric inertia is negligible. Form the same reasons of the graphs of Figure 6.8, the graphs d2), e2) and f2) of Figure 6.9 shows that the increment of air exchange rate of the room decreases significantly the hygric inertia of a room, since it raises a lot the RHS.

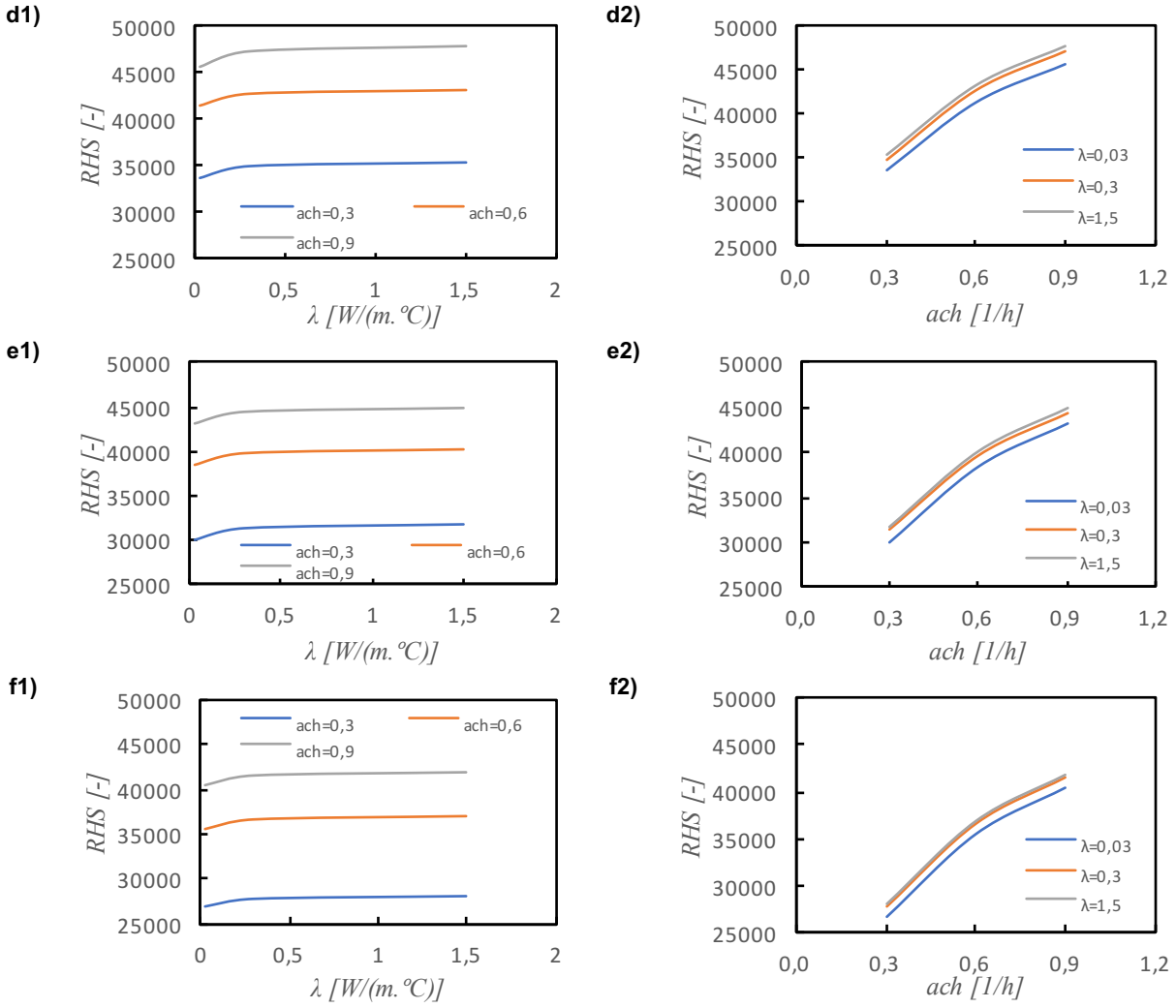

Figure 6.9 – Variation of RHS with thermal conductivity and air exchange rate, at fixed values of MBV

All graphs of Figure 6.10 are obtained by fixing the values of air exchange rate of the room and understand how RHS varies with the increment of thermal conductivity and MBV. It is possible to see by graphs g1), h1 and i1) that RHS increases with thermal conductivity, by the same reasons of the graphs d1), e1) and f1), and it is explained before. However, it is possible to see that the curves of graphs g1), h1) and i1) are less spaced than the curves of d1), e1) and f1), because the curves of Figure 6.10 are made by putting together the values of MBV and the curves of Figure 6.9 are organized by joining the simulations with the same air exchange rate, what revealed to have a huge impact on RHS, unlike the MBV that even having a big influence on RHS it still being lower than the influence of air exchange rate in hygric inertia, as it is possible to see by Figure 6.8. The graphs g2), h2) and i2) show that, for a constant value of air exchange rate, the increment of MBV leads to a decreasing of RHS, due to a higher ability of the coating material to buffer the moisture of indoor climate. It is important to refer that the curve of thermal conductivity equals to 0,03 W/(m.ºC), of graphs g2), h2) and i2), produces a higher hygric inertia to the room once it causes lower values of RHS than the other two ranges of thermal conductivity, because it has the smallest value of thermal conductivity and then it must have higher porosity than the others, which is directly proportional to its capability to stabilize RH of indoor.

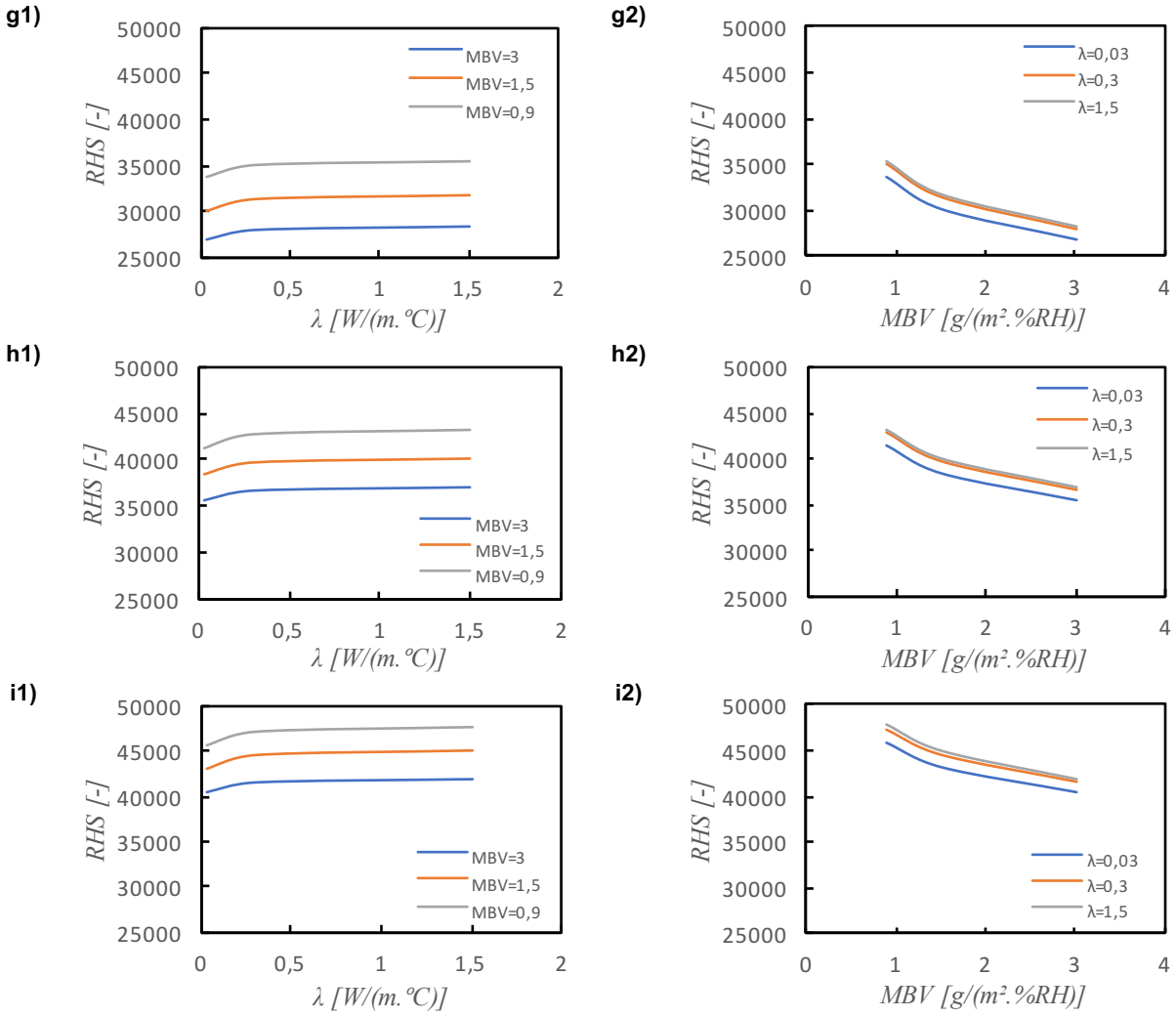

Figure 6.10 – Variation of RHS with thermal conductivity and MBV, at fixed values of air exchange rate

All graphs of Figure 6.11 were obtained by fixing the vales of thermal conductivity and varying both MBV and air exchange rate of the coating materials.

The main formula used to explain the variations of the thermal inertia of a building and also the parameter TS, is Equation(6-3), which relates the stored energy E_{st} [W] by some element with its density ρ [kg/m^3] and the quantity of temperature that through the element by unit of time.

$$\dot{E_{st}} = \rho * c_\rho * \frac{\partial T}{\partial t} dxdydz \qquad (6\text{-}3)$$

MBV is not directly related with any parameter of Equation(6-3) once is depends significantly of the porosity of materials, which does not have a strong relation with any parameter of this equation. Therefore, this is the reason why graphs k1) and l1) of Figure 6.11 shows no increment or reduction of TS with the increment of MBV.

The increment of air changes per hour causes a decreasing of thermal inertia of a building, as it is described by graphs j2), k2) and l2) of Figure 6.11. This is easily justified by the fact that over the year the outdoor temperature is usually different of the indoor temperature and, with the increment of air changes per hour there will be more air infiltrating inside with different temperature, which causes higher fluctuations of indoor temperature and then raises TS and diminishes thermal inertia. And this

is also the justification to the increment of TS with the increment of air exchange rate of graphs m2), n2) and o2) of Figure 6.12.

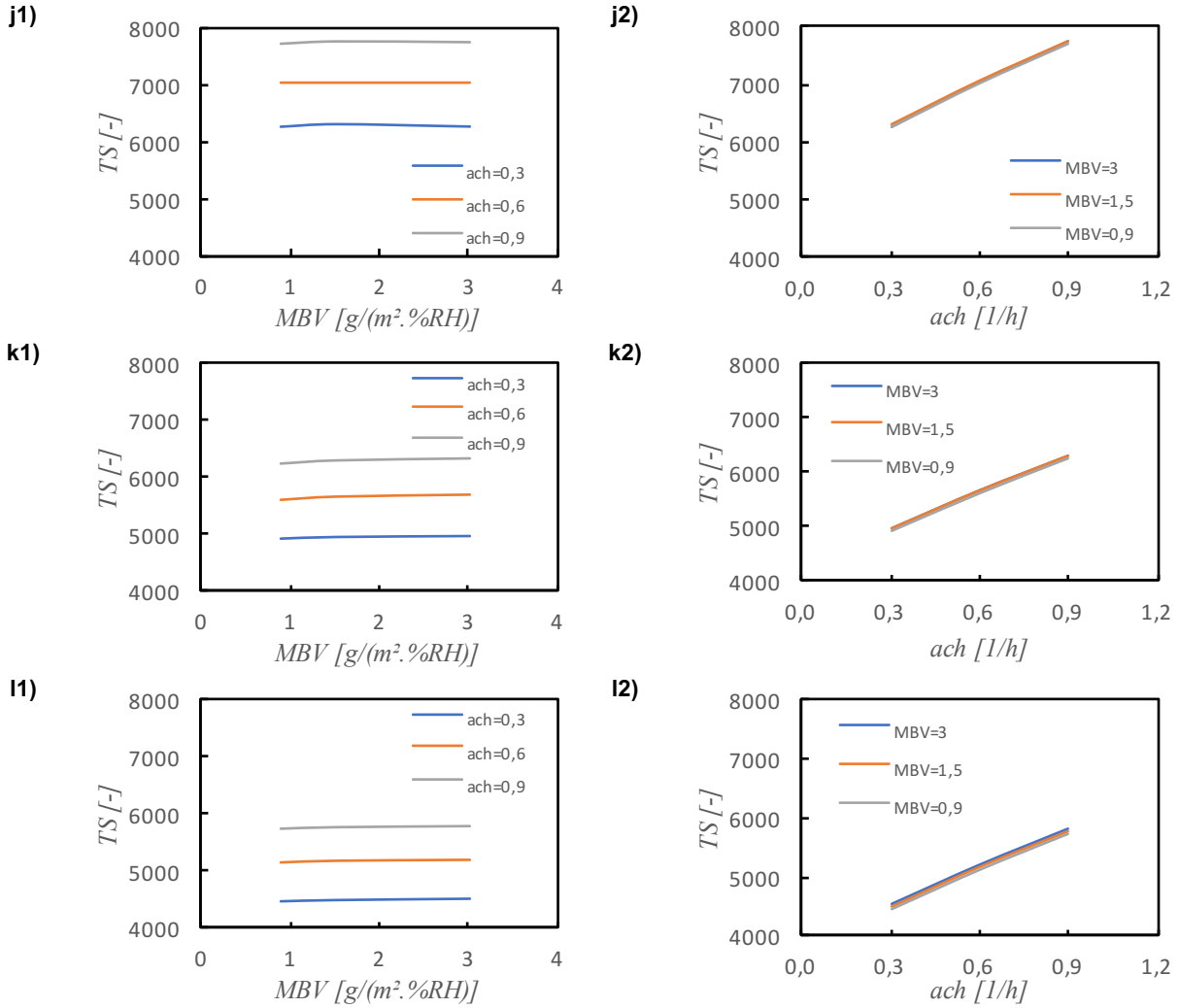

Figure 6.11 – Variation of TS with MBV and air exchange rate, at fixed values of thermal conductivity

All graphs of Figure 6.12 relate TS with the variation of thermal conductivity of coating materials and air exchange rate of the room. It is easy to understand that the increment of thermal conductivity will originate higher thermal inertia and lower values of TS, as it occurs in graphs m1), n1) and o1) of Figure 6.12, because it increases the quantity of temperature that through the element, per unit of time and also increases its stored energy, as it is possible to see by Equation(6-3).

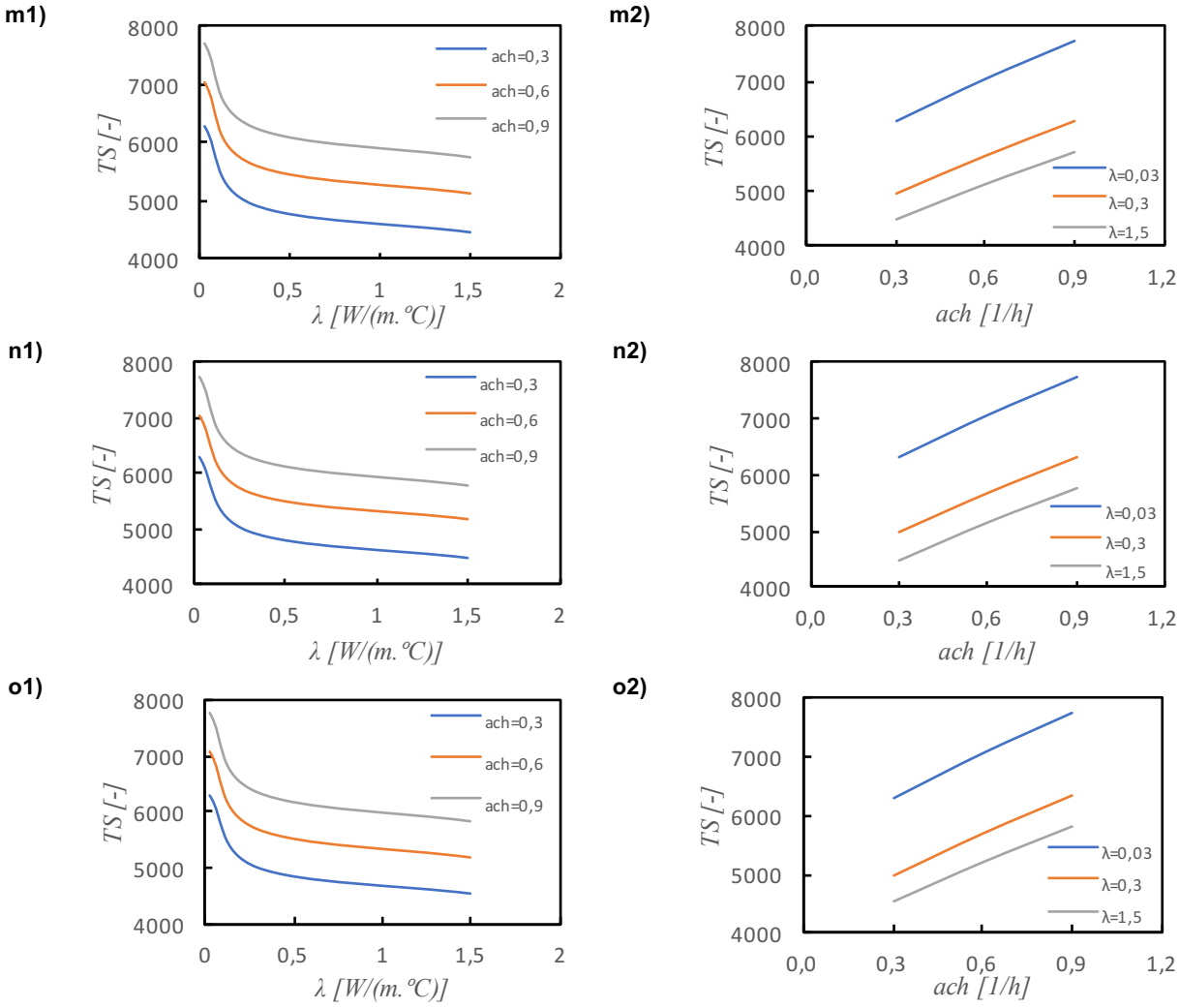

Figure 6.12 – Variation of TS with thermal conductivity and air exchange rate, at fixed values of MBV

All graphs of Figure 6.13 represent the variations of TS with the increment of thermal conductivity and MBV of coating materials, at constant values of air exchange rate.

The graphs p1), q1) and r1) of Figure 6.13 show that the increment of thermal conductivity of coating materials causes a decreasing of TS and then an increment of thermal inertia of a room. This can be easily justified by Equation(6-3), since it shows that higher values of thermal conductivity originate higher values of temperature that crosses the element per unit of time, which increases the stored energy by the element. Therefore, if the element is capable to store more heat then it will provide higher thermal inertia to the studied room. It is important to refer that all curves of graphs p1), qu1) and r1) are almost overlapped because even they represent different ranges of MBV, it has been proved already, by graphs j1), k1) and l1) of – Variation of TS with MBV and air exchange rate, at fixed values of thermal conductivity that MBV has almost no effect of thermal behavior of a certain room. The graphs p2), q2) and r2) show that MBV has no effect on thermal inertia of a room and it has the same justification of graphs j1), k1) and l1), described before.

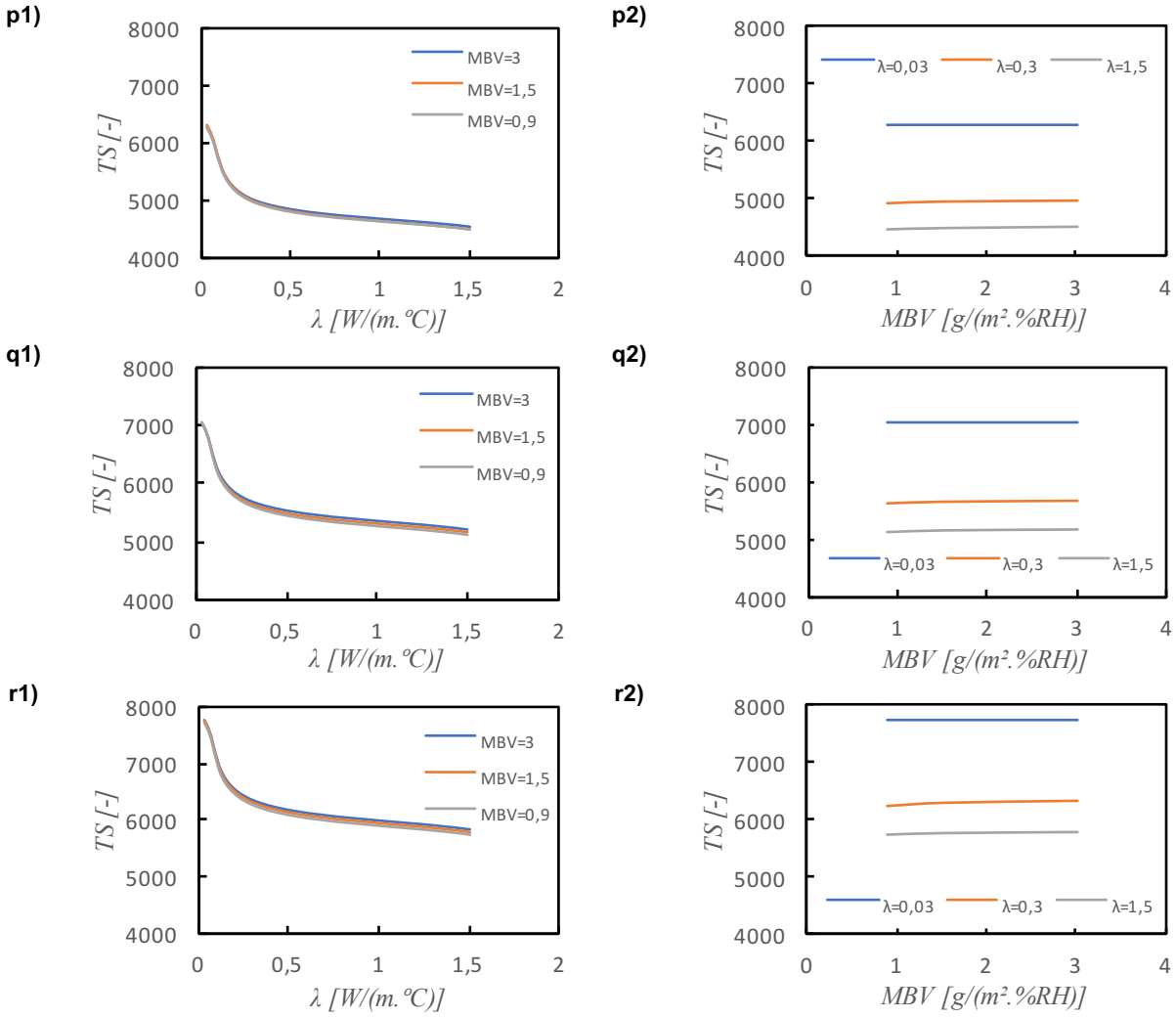

Figure 6.13 – Variation of TS with thermal conductivity and MBV, at fixed values of air exchange rate

The values of RHS and TS that caused all graphs of Figure 6.8 to Figure 6.13 are placed in Table 6-5, respectively, as well as the mean values of RH and temperature and the percentiles for each simulation.

Table 6-5 – Relative humidity and temperature results of all simulations of sensivity study

Sim.	Relative Humidity				Temperature			
	RHS [-]	Mean [%]	$RH_{1\%}$ [-]	$RH_{99\%}$ [-]	TS [-]	Mean [ºC]	$T_{1\%}$ [-]	$T_{99\%}$ [-]
1	26861,9	57,6	43,8	71,4	6281,4	22,7	15,6	30,5
2	30147,7	57,6	43,4	72,5	6298,0	22,7	15,6	30,5
3	33688,9	57,6	42,7	73,5	6280,1	22,7	15,6	30,5
4	27869,1	57,7	43,9	71,8	4991,9	22,7	15,8	30,1
5	31312,7	57,7	43,7	72,3	4974,9	22,7	15,8	30,1
6	34953,6	57,7	43,0	74,0	4945,6	22,7	15,8	30,1
7	28230,2	57,7	44,0	71,9	4527,1	22,7	15,9	30,5
8	31700,6	57,7	43,6	73,0	4500,7	22,7	15,9	29,9
9	35353,5	57,7	43,0	74,0	4476,0	22,7	15,9	29,9
10	35572,5	57,9	42,1	74,0	7050,7	21,4	14,1	29,4
11	38399,4	57,9	41,9	74,8	7061,3	21,4	14,1	29,4
12	41388,0	57,8	41,4	75,7	7040,4	21,4	14,2	29,5
13	36650,2	57,9	42,2	74,4	5691,6	21,4	14,4	29,0
14	39697,4	57,9	42,0	75,4	5667,6	21,4	14,4	29,0
15	42839,8	57,9	41,4	76,3	5629,1	21,4	14,4	29,0
16	37024,1	57,9	42,2	74,6	5197,8	21,4	14,5	28,8
17	40128,6	57,9	41,9	75,5	5175,3	21,4	14,5	28,8
18	43302,8	57,9	41,4	76,4	5134,3	21,4	14,5	28,8
19	40429,8	59,4	42,2	76,6	7740,7	20,5	13,2	28,8
20	43075,7	59,4	42,0	77,4	7748,4	20,5	13,2	28,8
21	45719,6	59,4	41,6	78,2	7725,3	20,5	13,2	28,8
22	41540,3	59,5	42,3	77,3	6325,1	20,5	13,4	28,3
23	44467,1	59,5	42,1	78,1	6299,3	20,5	13,4	28,3
24	47258,1	59,5	41,6	79,1	6258,7	20,5	13,4	28,3
25	41912,4	59,5	42,3	77,5	5810,1	20,5	13,5	28,2
26	44928,9	59,5	42,2	78,4	5778,9	20,5	13,5	28,1
27	47783,9	59,5	41,7	79,2	5733,6	20,5	13,5	28,1

Both daily hygroscopic index and hygric capacity have always the same value between each range of MBV. Therefore, values of daily hygroscopic index and hygric capacity only have three different values, one for each MBV of each simulation, and they are placed in Table 6-6. It is possible to see in this table that the increment of MBV causes an increment of both daily hygroscopic inertia and hygric capacity factors, what mean that it originates a raising of hygric inertia of the room. It is important to refer that to achieve the factor of daily hygroscopic inertia and hygric capacity it was needed to have the MBV of oak old coating and of lime mortar fine. Both MBV were determined by the same

procedure of 6.3, and the MBV of oak old is 0,67 g/(m^2.%RH) while the MBV of lime mortar fine is placed in the first line of Table 6-10.

Table 6-6 – Daily hygroscopic inertia index and hygric capacity of sensivity study

Simulation	MBV [g/(m^2.%RH)]	$I_{h,d}$ [g/(m^3.%RH)]	$Hygric_{cap.}$ [g/(m^3.%RH)]
3,6,9,12,15,18,21,24,27	0,9	0,11	0,82
2,5,8,11,14,17,20,23,26	1,5	0,14	1,01
1,4,7,10,13,16,19,22,25	3,0	0,20	1,45

The same work that defined the concept of daily hygroscopic inertia [29] also defined four classes of hygric inertia of a room/building, based on its values of daily hygroscopic inertia index. These classes of hygric inertia are defined on Table 6-7.

Table 6-7 – Classes of hygroscopic inertia

Class	$I_{h,d}$ [g/(m^3.%RH)]
I	$0 \leq I_{h,d} < 0,06$
II	$0,06 \leq I_{h,d} < 0,17$
III	$0,17 \leq I_{h,d} < 0,45$
IV	$0,45 \leq I_{h,d}$

From Table 6-7 and Table 6-8 it is shown that if the MBV of coating materials is increased to 3,0, then the class of hygroscopic inertia that was so far equal to II will be improved and will pass to class III. Even the increment of MBV from 0,9 to 1,5 does not affect the class of hygroscopic inertia, since it remains in class II, it even increases the value of hygroscopic inertia.

6.5. Influence of studied materials in interior climate

In order to understand how four of the studied materials in the present work affect the interior climate of an old building, they were placed as coating materials of the same building studied in 6.4 (Figure 6.5). The main goal of the present analysis was to understand how the studied materials in present work can control and damp the relative humidity and temperature of indoor, trying, as so, to discover how they can improve the thermal and hygric inertia of old buildings. The procedure was equal to the same used in 6.4 but, in this case, the coating materials were recycled cellulose board (M), projected cellulose coating (N), wood wool cement board (O) and clayish earth plaster. Therefore, the building's elements continued to have the same main characteristics of Table 6-3, as well as the windows, that continued to be equal to the ones of previous chapter.

6.5.1. Materials' characterization

The analysis of the present section considered that the coating materials would be applied with the same thickness of the studied samples in the present dissertation, described in Table 3-5. In order to replicate better the studied materials all characteristics that were calculated in the present work were utilized on software. Therefore, all moisture resistance factor, adsorption isotherm and thermal conductivity depending of moisture, achieved in the present work, were used as properties of coating materials in *Wufi Plus*. As the experimental trials were only made at limited number of relative humidity levels, so the materials' properties used in software had to be the one achieved by numerical analysis of tests, placed in Chapter 5. Thus, there were chosen the non-linear regressions that have best fitting to experimental results, one for each characteristic used on software.

The best non-linear regression of moisture permeability, used on the present analysis, was equation 3 of Table 5-4 (graph c) of Figure 5.7 to Figure 5.9). However, as wood wool cement board (O) was not tested in the present dissertation, it was determined its ideal moisture resistance factor in 6.3, and it take a constant value of 3,23 [-]. The parameter that can be extracted from moisture permeability test to software, is moisture resistance factor μ [-], which can be easily calculated by Equation(3-5). Therefore, the values of moisture resistance factor depending of relative humidityare represented by Figure 6.14.

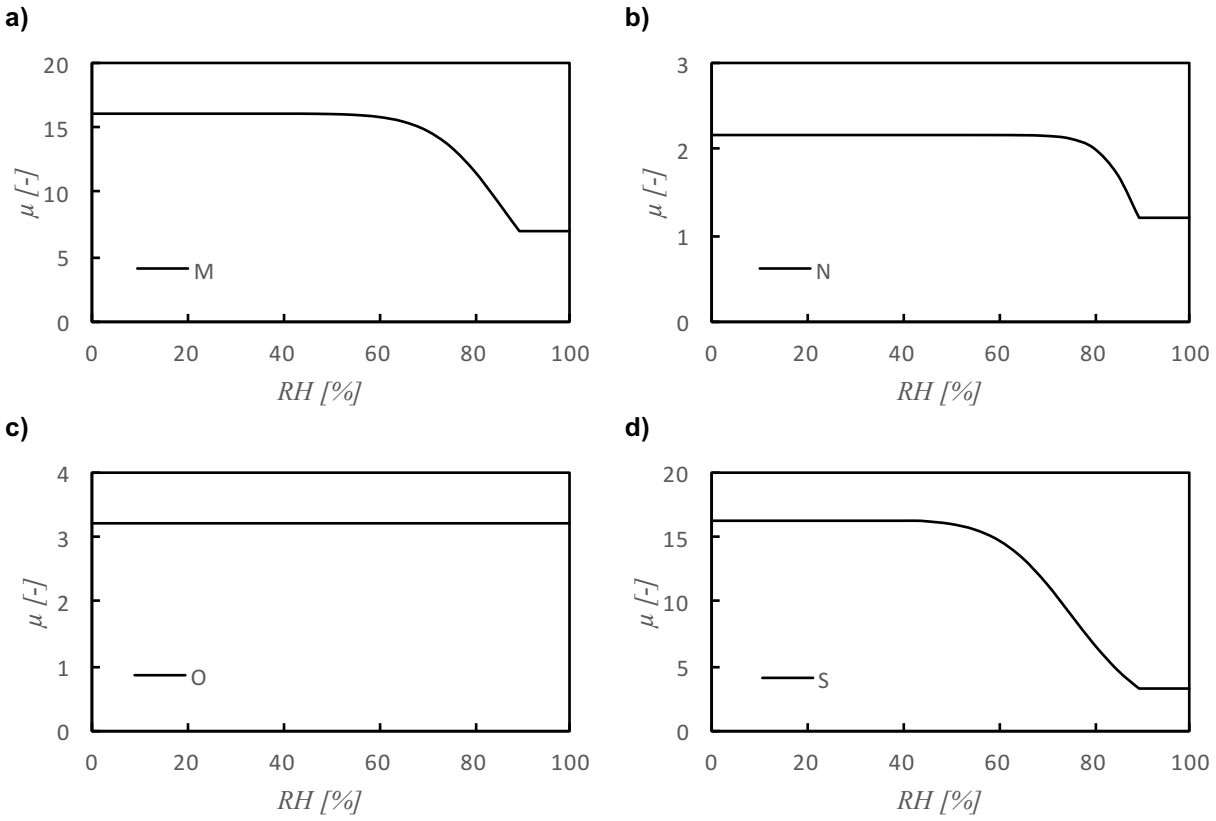

Figure 6.14 – Moisture resistance factor used on *Wufi Plus*, of all materials

The best non-linear regression obtained to experimental data of adsorption/desorption isotherm test was Hansen (1) (placed in Table 5-1 and represented by graph e) of Figure 5.1 to Figure 5.4). It is important to refer that the non-linear regressions were made in *u* [kg/kg - %], while the software demands that the values are presented in *w* [kg/m^3]. The values of moisture content can be related between *u* and *w*, by Equation(2-9). In 5.1, there were accomplished two different equations for both adsorption and desorption phase, for each material. However, *Wufi Plus* does not allow to input one

curve for adsorption phase and another for desorption one, once it only let to associate one curve of moisture content in function of relative humidity, for each material. To fulfil this lack of software, its manual [115] advices to use the mean curve between the adsorption and desorption isotherms, whenever the hysteresis is highly pronounced. Therefore, the mean values of adsorption and desorption isotherms were used and originated the graphs of Figure 6.15.

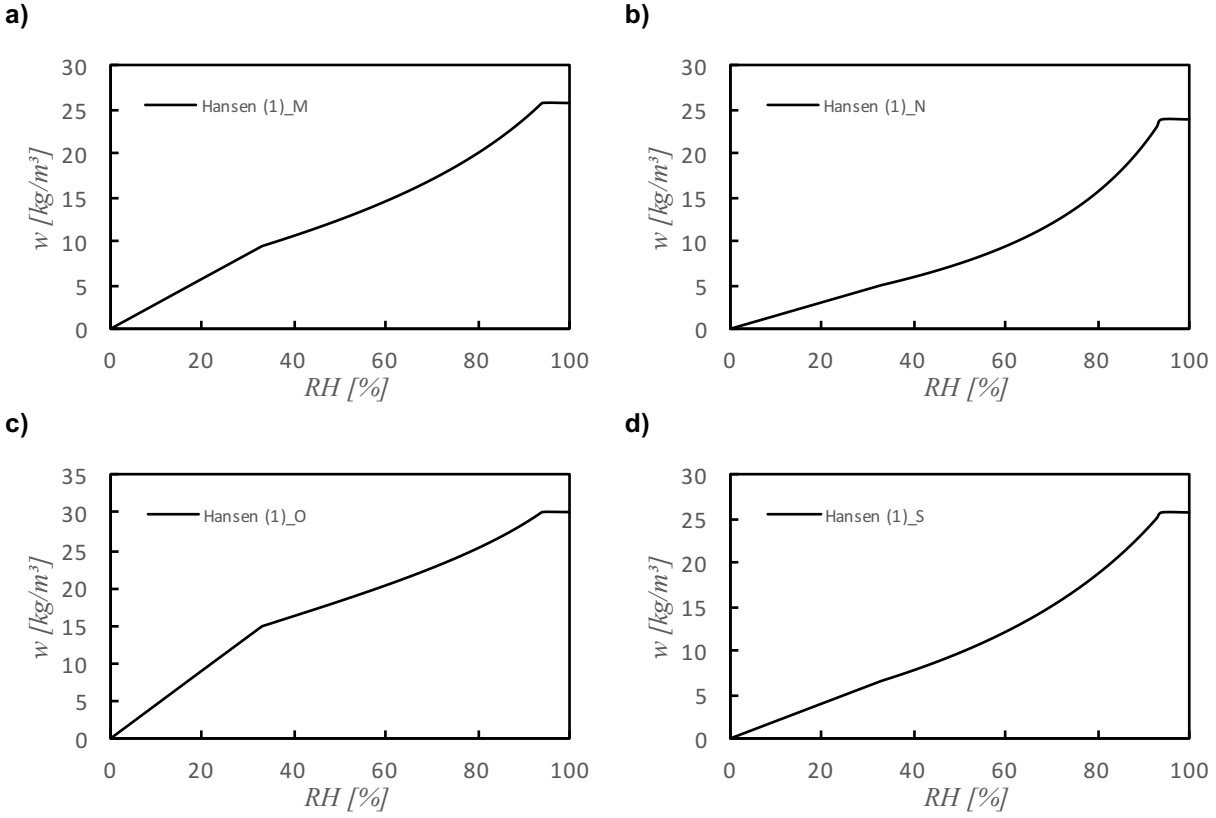

Figure 6.15 – Adsorption isotherms used on *Wufi Plus,* of all materials

The best non-linear regression of the experimental data of thermal conductivity was equation 3 of Table 5-7 (graph c) of Figure 5.10 to Figure 5.13). The non-linear regressions of the data, obtained experimentally, were made with thermal conductivity in function of moisture content *u* [kg/kg - %] of materials. However, the software only accepts inputs of thermal conductivity depending of *w* [kg/m^3]. The values of *u* and *w* can be related by Equation(2-9), which allows to input the values of thermal conductivity depending of moisture content, in *w* [kg/m^3].

Therefore, the graphs of materials thermal conductivity depending of its moisture content, are represented by Figure 6.16.

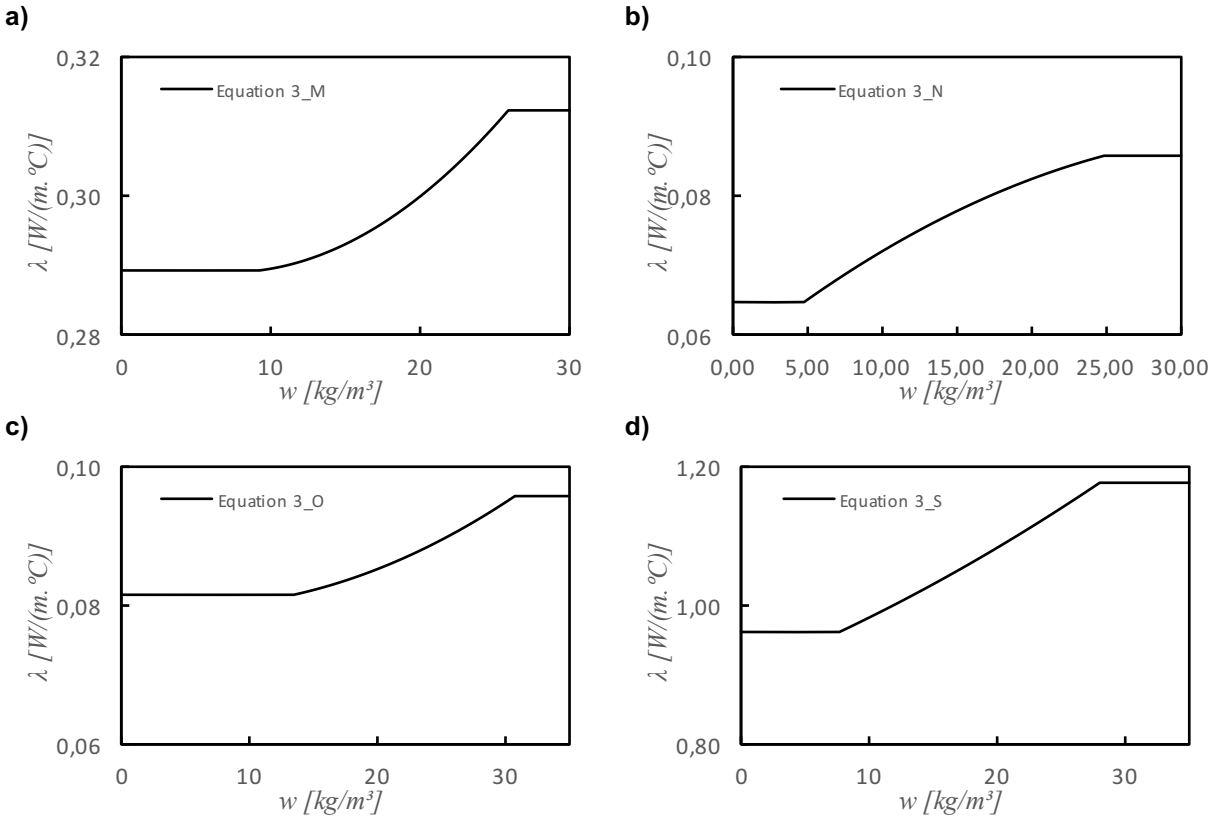

Figure 6.16 – Thermal conductivity depending of RH used on *Wufi Plus,* of all materials

6.5.2. Analysis of results

In order to understand the real impact of the studied materials in temperature and relative humidity of old buildings interior climate, a simulation between a usual constructive system of old buildings with and without the studied coating materials was made. All assumptions, building's dimensions, exterior climate, beyond all other, as well as the constructive system of building, were the same of the used in 6.4. The only different point to the sensivity study, made in 6.4, is that the simulations made with the four studied coating materials are compared with a base case, which the only different to the simulations with the studied coating materials is that the used coating is a lime mortar, with its main characteristics placed in Table 6-8.

Table 6-8 – Main characterisitics of lime mortar fine, used on *Wufi Plus*

	Density [kg/m^3]	**Thickness [m]**	**Porosity [-]**	**λ [W/(m.ºC)]**	**c_ρ [J/(kg.K)]**	**μ [-]**
Lime mortar, fine	1785	0,03	0,28	0,7	850	15

All four materials, that were chosen to be part of this study, were selected due to their good hygroscopic potential behavior. Therefore, it was analyzed their influence in both temperature and relative humidity of climate of indoor, that originated Figure 6.17. It is important to refer that each material is characterized by its MBV obtained by *Wufi Plus*, in 6.3, that is placed in Table 6-1, for recycled cellulose board (M), projected cellulose coating (N), wood wool cement board (O) and clayish earth plaster (S). The MBV of the coating of the base case, which is lime mortar fine, was calculated by the same procedure of the one made 6.3, and it originated a MBV equals to 1,0 W/(m^2.%RH).

From Figure 6.17, it is easy to understand that higher values of MBV causes higher hygroscopic inertia of a certain room or building, since the value of RHS has a reduction with the increment of MBV, because if MBV takes higher values, it means that the coating material is capable to adsorb and release more moisture from environment, which gives to it a better capacity to buffer the moisture of interior climate. It is also correct to affirm that, as MBV grows with porosity, then higher values of material's porosity will cause lower values of RHS of environment, which provides a higher hygric inertia to buildings. From Figure 6.17, it is correct to affirm that any increment of the hygroscopic behavior of the coating materials, represented by their MBV, has almost always a negative impact in thermal inertia of buildings, since the increment of MBV cause almost always an increment of Temperature Stabilization, as seen in Figure 6.17. Therefore, it is right to affirm that the ideal hygroscopic material must have a MBV equals to 1,5, since it lower RHS significantly but it does not harm the thermal inertia of buildings, since the TS remains equal to the one of MBV equals to 1,0.

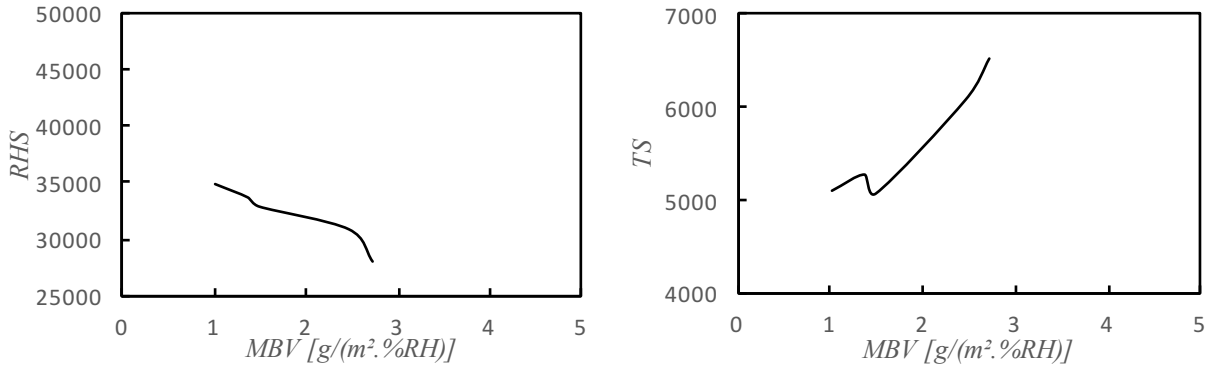

Figure 6.17 – Variation of RHS and TS with MBV of studied materials and base case

The values of RHS, TS, mean relative humidity and temperature and their percentiles, that are result of the simulation with the studied materials of the present dissertation are placed in Table 6-9.

Table 6-9 – Relative humidity and temperature results for all simulations with studied materials

Material	Relative Humidity				Temperature			
	RHS [-]	Mean [%]	$RH_{1\%}$ [-]	$RH_{99\%}$ [-]	TS [-]	Mean [ºC]	$T_{1\%}$ [-]	$T_{99\%}$ [-]
Lime mortar	34741,4	58,9	44,2	74,7	5110,0	22,3	15,5	29,7
M	33576,8	58,9	44,3	74,4	5284,2	22,3	15,5	29,7
S	32770,1	58,9	44,5	74,0	5080,3	22,3	15,5	29,7
N	30781,8	58,9	44,3	73,36	6090,4	22,3	15,4	30,0
O	27954,3	58,9	45,2	72,81	6536,0	22,3	15,3	30,1

M – Recycled cellulose board; **N –** Projected cellulose coating; **O –** Wood wool cement board; **S –** Clayish earth plaster

To better characterize the impact of coating materials on hygric inertia of a building, previous works defined an index of hygric inertia, that is represented by Equation(2-23) [29], while posterior work defined a concept of hygric capacity, that is achieved by Equation(2-24) [53]. Knowing that the air exchange rate had a constant value of 0,3 h^{-1}, the volume of the room was 590,63 m^3 and that the time of moisture production was equal to 24 hours, the values of daily hygroscopic inertia index for all five materials studied in the present section, are placed on Table 6-10, as well as the experimental MBV of M, N, O and S and the MBV obtained by software to lime mortar.

Table 6-10 – Daily hygroscopic inertia index and hygric capacity of studied materials

Coating Material	MBV [g/(m^2.%RH)]	$I_{h,d}$ [g/(m^3.%RH)]	$Hygric_{cap.}$ [g/(m^3.%RH)]
Lime mortar fine (Sim_0)	1,0	0,11	0,81
Recycled cellulose board (M)	1,2	0,13	0,91
Clayish earth plaster (S)	1,6	0,13	0,94
Projected cellulose coating (N)	2,2	0,17	1,22
Wood wool cement board (O)	2,6	0,18	1,29

As the Table 6-10 has the materials ordered by their value of MBV, growing from top to bottom of the table, it is easy to conclude that MBV is directly related with hygric inertia of a building, once higher values of MBV cause higher daily hygroscopic inertia and hygric capacity of a building or room, which means that the increment of MBV causes higher hygric inertia to the room.

From Table 6-7 and Table 6-10 it is possible to understand that the hygroscopic materials, placed as covering of ceiling, can improve the hygric inertia of a building because they increase both daily hygroscopic index and hygric capacity, as it is possible to see on Table 6-10. Both projected cellulose coating (N) and wood wool cement board (O) are capable to improve the class of hygric inertia of the room because they increase the class from II to III. However, all other coating materials are incapable to increase the class of hygric inertia of the studied building, once it remained in class II, but they still increase the parameter of daily hygroscopic inertia.

Chapter 7: Conclusions

7.1. Final conclusions

The relative humidity of indoor climate can cause some severe problems to the comfort of people and to the integrity of building materials. The relative humidity can be buffered by changing the ventilation, changing the heat transfer coefficient of enclosures, or lower the moisture of environment, beyond other many techniques. The decreasing of moisture of climate can be provoked by a mechanical dehumidification of it or, in other hand, by installing coating materials that are able to control it. Therefore, the main goal of the present work was to understand the impact of these coating materials on relative humidity of indoor. At the same way, it was also intended to understand how do these hygroscopic materials affect the thermal inertia of buildings, once the studied case was in old buildings, and see how does the increment of hygric inertia can damage the high thermal inertia of these old buildings.

For better understanding of how coating materials affects the hygric and thermal inertia of old buildings, it was chosen to make many experiments that were able to totally characterize the response of materials to climate changes. First of all, it is correct to affirm that porosity of materials are the main materials' characteristic that affect their behavior towards to controlling the relative humidity of indoor. Therefore, higher values of porosity imply that the velocity of material's response to climate changes will also increase but at similar values of porosity the pores' dimensions may influence more their response time. In this way, projected cellulose coating (N) is the coating material that has higher velocity of response to climate's changings, and clayish earth plaster (S) is the one with lower velocity of response. However, the materials with higher velocity of response are not always the best once if the cycles of relative humidity are long then the ideal coating material to buffer humidity should have a slow response to climate's variations. The quantity of moisture that a certain coating material can adsorb or release affects its ability to control the moisture from environment, and it showed to be directly proportional to porosity. However, this last parameter is not enough to define the behavior of materials to buffer humidity of indoor, since if the coating materials have ability to adsorb moisture from environment, but they do not have the capability to transfer the excess of moisture to the masonry, that is typically applied in old buildings, then their ability to reduce RH of indoor ends quickly. Therefore, it is important that the coating materials have high values of moisture permeability that allows them to transfer the moisture to other element of enclosures, and this is one of the reasons to clayish earth plaster (S) provides higher values of daily hygric inertia and hygric capacity than recycled cellulose board (M) does, even knowing that M has much bigger values of porosity than S.

The concept of MBV, which has a directly proportional relation with the velocity of response of materials, revealed to be, for buildings with high thermal inertia, a really good parameter to characterize the ability of materials to buffer the relative humidity of indoor since higher values of MBV always caused higher values of daily hygric inertia and hygric capacity, what means that the materials with higher MBV will control better the relative humidity of indoor. This makes that with a simple test as the MBV it is possible to understand what will be the impact of some material in the control of relative humidity of the interior climate of a certain building or room. It is important to refer that wood wool cement board (O) revealed to have higher MBV than projected cellulose coating (N), even the porosity of the second one is much bigger than the porosity of the first one, justified by the fact that O has about the double of thickness of N. This happened because both materials were prefabricated and the present work was susceptible to what the companies decided to provide.

The ability to control the temperature of indoor by coating materials is directly related with thermal conductivity of materials since the increment of this parameter causes higher thermal inertia of the building. This is justified by the quantity of energy that can be stored by any element be proportional to specific heat capacity, density and the quantity of temperature that through the material per unit of time. It was proved that it is possible to increment the stabilization of indoor RH and does not harms the thermal inertia of a building, if the increment of MBV be until about 1,5 g/(m^2.%RH).

The hygrothermal simulation, made in Chapter 6, allowed to confirm which parameters affect more the thermal and hygric inertia of buildings. The software *Wufi Plus* which already has been validated by previous works was also validated in the present work, since it produced similar values of MBV to the ones obtained by experiments. The hygrothermal simulation allowed to conclude that thermal conductivity of coating materials increases the thermal inertia of buildings and the air exchange rate of the room has an inversely relation of proportionality with thermal inertia of buildings. The MBV of coating materials has an almost non-significant impact on thermal inertia of buildings even having a slightly bad impact on it. Therefore, the Moisture Buffering Value of coating materials has a significant impact on hygric inertia of buildings since higher values of MBV causes higher hygric inertia and of a room and both projected cellulose coating (N) and wood wool cement board (O) are capable to raise the class of hygric inertia of a room. The thermal conductivity revealed to have a considerable bad effect on hygric inertia since the increment of thermal conductivity leads to a substantial reduction of hygric inertia of the building/room. Lastly, it was proved that the increment of air changes per hour of a room causes a reduction of both thermal and hygric inertia.

The ideal coating material is the one that is capable to increase both thermal and hygric inertia. However, the increment of hygric inertia is strongly affected by the increasing of materials' porosity, which normally implies lower values of thermal conductivity. These low values of thermal conductivity of coating materials can damage the thermal inertia of an old building since they do not allow the heat to achieve the thickest element of enclosures, which is usually masonry, not allowing it to store the heat to later release it back to environment. Therefore, it is necessary to be very careful during the prescription of coating material of old buildings. However, it is possible to choose coating materials capable to improve both thermal and hygric inertia, if they have high values of porosity, that increment their ability to buffer the relative humidity of indoor, and also have high values of density, which causes higher values of its stored energy and this way they do not damage the high values of thermal inertia, provided by the thick and heavy elements of enclosures.

To be possible to know the behavior of materials at any range of relative humidity or at any time, in Chapter 5 many analyses of the fitting of different equations to the data obtained experimentally were made, for all tests made in the present dissertation. The equation of Hansen (1) is the best equation that allows to know the adsorption and desorption behavior of moisture of coating materials, at any range of relative humidity. Equation 3 of both moisture permeability and thermal conductivity concepts revealed to be the best equations that represents the moisture permeability and thermal conductivity of coating materials at any value of relative humidity of indoor. For understanding the adsorption/desorption behavior of materials in function of time the best equation of non-linear regression to the experimental results was Hill's one, and it is capable to determine not only the maximum quantity of moisture that a material can adsorb or release, but also at what velocity it does.

Lastly, it is important to refer that the ability of coating materials to control both relative humidity and temperature of old buildings' indoor could be reasonably quantified by experiments, however their real response to climate changes of indoor cannot be reached by these experimental methods since they do not consider all possible variables that may exist in real environment. It is also important to highlight that the RH and temperature are not only dependent of the ability of coating materials to control them, but they are also dependent of the constructive system of enclosures, the exposition of the building to exterior climate and other parameters like the presence of people, equipment and illumination of indoor.

7.2. Future work

Although the present dissertation had covered many tests, and many variations inside them, there are still other tests to made or to repeat, in order to verify or correct some results obtained on the present work.

First of all, it would be important to make the test of intrusion of mercury to obtain the dimension of pores of materials, which is one of the main materials' parameters that affect its ability to adsorb and release moisture.

It would be important to repeat the test of MBV to wood wool cement board (O), in order to verify if its value of MBV at the range of 33%-75% of RH, due to the discrepancy, obtained in the present work, between MBV from test and from software (*Wufi Plus*). Also for wood wool cement board (O), it would be interesting to subject it to the test of moisture permeability, to quantify its permeability to moisture at various ranges of relative humidity, which would allow to calculate its ideal MBV.

Clayish earth plaster (S) should be subjected again to the test of adsorption/desorption isotherm, once its values of moisture content in equilibrium of desorption phase, obtained in present work, originated lower values than the ones of adsorption phase, which gave rise to negative hysteresis, and that does not represent the real behavior of materials.

It should be interesting to quantify the thermal inertia of materials also in desorption phase of adsorption/desorption isotherm test, once, in the present dissertation, it was only made in adsorption phase. Therefore, it should be important to determine the influence of materials' hysteresis in thermal conductivity, in order to understand the real thermal behavior of materials with variation relative humidity of indoor and, as so, with the variation of its moisture content.

Once the only response time test made in the present work was made at the range of 33% and 75% of relative humidity, it would be interesting to make the same test to other ranges of relative humidity, like 50% - 75% or 60% - 75%, in order to determine the velocity of response of materials to more ranges of relative humidity.

It would be interesting to make a similar sensivity study to one made on present dissertation, perhaps with the same software (*Wufi Plus*), but with the variation of other coating materials' parameters. This will allow to understand the impact of other characteristics of materials, like pores' dimensions, porosity, thickness of coating or permeability to moisture, in both thermal and hygric inertia of buildings.

Lastly, it is important to assess the durability of materials once they are frequently filled with moisture, which can harm their durability.

References

[1] F. M. A. Henriques, *Comportamento higrotérmico de edifícios (Book)*. 2011.

[2] *DIN, Deutsches Institut für Normung, "DIN 4108-2 Wärmeschutz und Energie-Einsparung in Gebäuden - Teil 2: Mindestanforderungen an den Wärmeschutz."* 2013.

[3] *ISO, International Standard Organization, "ISO 12571 Hygrothermal performance of building materials and products — Determination of hygroscopic sorption properties."* 2013.

[4] I. E. Agency, "Catalogue of Material Properties - Report Annex XIV, Volume 3," 1991.

[5] K. Kumaran, *IEA ANNEX 24 - Heat, Air and Moisture Transfer in Insulated Envelope Parts - Final Report Volume 3 - Task 3: Material Properties*. 1996.

[6] K. K. Hansen, *Sorption Isotherms - A Catalogue*. 1986.

[7] S. C. Chang and N. B. Hutcheon, "Dependence of water vapor permeability on temperature and humidity," *Heating, Pip. Air Cond.*, 1956.

[8] R. C. Mclean, G. H. Galbraith, and C. H. Sanders, "Moisture transmission testing of building materials and the presentation of vapour permeability values," *Build. Res. Pract.*, vol. 18, no. 2, pp. 82–91, 1990.

[9] G. H. Galbraith, J. S. Guo, and R. C. Mclean, "The effect of temperature on the moisture permeability of building materials," *Build. Res. Inf.*, vol. 28, no. 4, pp. 245–259, 2000.

[10] S. Brunauer, P. H. Emmett, and E. Teller, "Adsorption of Gases in Multimolecular Layers," vol. 407, no. 1, 1938.

[11] R. Peuhkuri, "Moisture Dynamics in Building Envelopes (PHD thesis)," Technical University of Denmark, 2003.

[12] D. Boer and D. Boer, "Experimental Confirmation of Different Mechanisms of Evaporation from Ink-Bottle Type Pores : Equilibrium , Pore Blocking, and Cavitation," no. 10, pp. 9830–9837, 2002.

[13] J. Correia, "Avaliação da higroscopicidade de materiais correntes (Master's thesis)," Faculdade de Ciências e Tecnologia - Nova University of Lisbon, 2013.

[14] J. H. Page, J. Liu, B. Abeles, H. W. Deckman, and D. A. Weitz, "Pore-Space Correlations in Capillary Condensation in Vycor," vol. 71, no. 8, pp. 6–9, 1993.

[15] J. Kwiatkowski, M. Woloszyn, and J. Roux, "Modelling of hysteresis influence on mass transfer in building materials," vol. 44, pp. 633–642, 2009.

[16] G. H. Galbraith, R. C. Mclean, and Z. Tao, "Vapour permeability: Suitable and consistency of current test procedures," *Build. Serv. Eng. Res. Technol.*, vol. 14, no. Figure 1, pp. 67–70, 1993.

[17] *ISO, International Standard Organization, "ISO 12572 Hygrothermal performance of water vapour transmission properties."* 2015.

[18] G. H. Galbraith and R. C. McLean, "Realistic vapour permeability values," *Batim. Int. Build. Res. Pract.*, vol. 14, no. 2, pp. 98–103, 1986.

[19] G. H. Galbraith and R. C. Mclean, “Interstitial Condensation and the Vapour Permeability of Building Materials,” *Energy Build.*, vol. 14, pp. 193–196, 1990.

[20] G. H. Galbraith, R. C. Mclean, and J. Guo, “Moisture permeability data presented as a mathematical function applicable to heat and moisture transport models,” *Build. Res. Inf.*, vol. 26, no. 3, 1997.

[21] G. H. Galbraith, R. C. Mclean, and J. S. Guo, “Moisture permeability data presented as a mathematical relationship,” pp. 157–168, 2017.

[22] G. H. Galbraith, C. Mcibse, Z. Tao, R. C. Mclean, and M. C. Minste, “Separation of moisture flow through porous building materials into vapour and liquid components,” *Build. Serv. Eng. Res. Technol.*, vol. 14, no. 3, pp. 107–113, 1993.

[23] P. G. H. Galbraith and D. J. Kelly, “Alternative Methods for Measuring Moisture Transfer Coefficients of Building Materials,” *Res. Build. Phys.*, pp. 249–254, 2003.

[24] G. H. Galbraith, R. C. Mclean, J. Guo, D. Kelly, C. Lee, and G. G. Oba, “The use of differential permeability in moisture transport modelling,” *Proc. Build. Simulations 99’*, pp. 2–7, 1999.

[25] G. H. Galbraith, R. C. Mclean, and D. Kelly, “Moisture permeability measurements under varying barometric pressure,” *Build. Res. Inf.*, vol. 25, no. 6, pp. 348–353, 1997.

[26] W. M. Haynes, *CRC Handbook of Chemistry and Physics (Book)*. 2016.

[27] A. Worch, “The Behaviour of Vapour Transfer on Building Material Surfaces : The Vapour,” vol. 28, no. 2, pp. 187–200, 2004.

[28] *BSI, British Standard Institute, “BS EN 15026 Hygrothermal performance of building components and building elements — Assessment of moisture transfer by numerical simulation.”* 2007.

[29] N. M. M. Ramos, “A importância da inércia higroscópica no comportamento higrotérmico dos edifícios (PHD thesis),” Faculdade de Engenharia da Universidade do Porto, 2007.

[30] H. S. L. C. Hens, “The vapor diffusion resistance and air permeance of masonry and roofing systems,” vol. 41, pp. 745–755, 2006.

[31] K. Svennberg and L. Wadsö, “A modified cup-method for lightweight and highly permeable materials.,” *Res. Build. Phys.*, pp. 177–182, 2003.

[32] NORDTEST, “Intercomparison on measurement of water vapour permeance,” p. 30, 2003.

[33] B. Time, “Hygroscopic Moisture Transport in Wood,” 1998.

[34] T. Padfield, “Humidity buffering of the indoor climate by absorbent walls,” pp. 1–8, 1998.

[35] J. Arfvidsson, “Moisture penetration depth for periodically varying relative humidity at the boundary (CIB report),” 1999.

[36] T. Mitamura, C. Rode, and J. Schultz., “Full Scale Testing of Indoor Humidity and Moisture Buffering in Building Materials”. ASHRAE Conference, IAQ 2001 – Moisture, Microbes and Health Effects: Indoor Air Quality and Moisture in Buildings,” 2001.

[37] “Workshop on moisture buffer capacity - Summary report (Technical University of Denmark),” 2003.

[38] NORDTEST, “Moisture Buffering of Building Materials,” 2005.

[39] S. Roels and H. Janssen, “Is the moisture buffer value a reliable material property to

characterise the hygric buffering capacities of building materials ?," 2005.

[40] *Japanese Standards Association. JIS A 1470-1 "Test method of adsorption/desorption efficiency for building materials to regulate an indoor humidity – Part 1: Response method of humidity."* 2002.

[41] S. Roels and H. Janssen, "A comparison of the Nordtest and Japanese test methods for the moisture buffering performance of building materials," *Build. Phys.*, 2006.

[42] S. Dubois, F. Mcgregor, A. Evrard, A. Heath, and F. Lebeau, "An inverse modelling approach to estimate the hygric parameters of clay-based masonry during a Moisture Buffer Value test," *Build. Environ.*, vol. 81, pp. 192–203, 2015.

[43] S. Verbeke and A. Audenaert, "Thermal inertia in buildings : A review of impacts across climate and building use," *Renew. Sustain. Energy Rev.*, pp. 1–19, 2017.

[44] H. Hens, *Applied Building Physics - Boundary Conditions, Building Performance and Material Properties*. 2011.

[45] "'http://www.netgreensolar.com' Visited on 10/08/2017"." .

[46] M. D. Isola, F. R. Ambrosio, and G. G. E. Ianniello, "Experimental Analysis of Thermal Conductivity for Building Materials Depending on Moisture Content," pp. 1674–1685, 2012.

[47] M. Rahim, O. Douzane, A. D. T. Le, and T. Langlet, "Effect of moisture and temperature on thermal properties of three bio-based materials," *Constr. Build. Mater.*, vol. 111, pp. 119–127, 2016.

[48] E. Troppová, M. Svenhlík, J. Tippner, and R. Wimmer, "Influence of temperature and moisture content on the thermal conductivity of wood-based fibreboards," *Mater. Struct.*, vol. 18, no. 2, pp. 4077–4083, 2014.

[49] D. Medjelekh, L. Ulmet, and S. Abdou, "A field study of thermal and hygric inertia and its effects on indoor thermal comfort : Characterization of travertine stone envelope," *Build. Environ.*, vol. 106, pp. 57–77, 2016.

[50] N. Mendes, C. Fernandes, P. C. Philippi, and R. Lamberts, "Moisture content influence on thermal conductivity of porous building materials," *Build. Simul.*, vol. 1, no. 2, pp. 957–964, 2001.

[51] A. Ronzino and V. Corrado, "The influence of coatings on the environmental hygric inertia of plastered rooms .," *Energy Procedia*, vol. 78, pp. 1507–1512, 2015.

[52] N. M. M. Ramos and V. P. De Freitas, "A simple method for hygroscopic inertia impact assessment," *IEA Annex 41 Proj.*, vol. 2, no. 2, pp. 2–8, 2005.

[53] C. Ferreira, "Inércia higroscópica em museus instalados em edifícios antigos (PDH thesis)," Faculdade de Engenharia da Universidade do Porto, 2015.

[54] "Condensation in Buildings - Handbook," 2014.

[55] W. H. Organization, *WHO guidelines for indoor air quality: Dampness and mould (Book)*. 2009.

[56] F. Henriques, *Humidade em paredes (Book)*. 1994.

[57] A. V Arundel, E. M. Sterling, J. H. Biggin, and T. D. Sterling, "Indirect Health Effects of Relative Humidity in Indoor Environments," *Environ. Health Perspect.*, vol. 65, no. 3, pp. 351–361, 1986.

[58] H. Viitanen and T. Ojanen, "Improved Model to Predict Mold Growth in Building Materials,"

2007.

[59] *BSI, British Standard Institute, "BS 5250 Standards Publication Code of practice for control of condensation in buildings."* 2011.

[60] *Decree-law n. 118/2013 de 20th August, "Regulamento de Desempenho Energético dos Edifícios de Habitação (REH)." pp. 4988–5005, 2013.* .

[61] *IPQ, Instituto Português da Qualidade "NP 1037-1 Ventilação e evacuação dos produtos da combustão dos locais com aparelhos a gás Parte 1: Edifícios de habitação. Ventilação natural" 2015.* .

[62] H. E. Silva, "Análise microclimática de um edifício histórico em clima temperado: limites sustentáveis para a correta conservação dos materiais," *Ambient. Construído*, vol. 15, no. 2, pp. 65–77, 2015.

[63] C. J. Simonson, *Moisture, Thermal and Ventilation Performance of Tapanila Ecological House (Book)*. 2000.

[64] O. F. Osanyintola and C. J. Simonson, "Moisture buffering capacity of hygroscopic building materials : Experimental facilities and energy impact," *Energy Build.*, vol. 38, pp. 1270–1282, 2006.

[65] I. Air, B. Munksgaard, and I. A. I. R. Issn, "The effect of structures on indoor humidity – possibility to improve comfort and perceived air quality," *Blackwell Munksgaard*, pp. 243–251, 2002.

[66] C. J. Simonson, M. Salonvaara, and T. Ojanen, *Improving Indoor Climate and Comfort with Wooden Structures (Book)*. 2001.

[67] T. Padfield, "Exploring the limits for passive indoor climate control," pp. 1–12, 2008.

[68] F. Antretter, C. Mitterer, S. Jung, and A. Holm, "Use of moisture buffering tiles for indoor climate stability under different climatic requirements," *HVAC Res.*, vol. 18, pp. 275–282, 2012.

[69] N. M. M. Ramos, J. M. P. Q. Delgado, and V. P. De Freitas, "Influence of finishing coatings on hygroscopic moisture buffering in building elements," *Constr. Build. Mater.*, vol. 24, no. 12, pp. 2590–2597, 2010.

[70] T. Padfield and L. A. Jensen, "Humidity buffering by absorbent materials," pp. 1–11, 2010.

[71] H. Yoshino, T. Mitamura, and K. Hasegawa, "Moisture buffering and effect of ventilation rate and volume rate of hygrothermal materials in a single room under steady state exterior conditions," *Build. Environ.*, vol. 44, no. 7, pp. 1418–1425, 2009.

[72] H. Hens, "Impact of hygric inertia on indoor climate : simple models," *IEA Annex 41 Proj.*, no. 3, 2003.

[73] C. Ferreira, V. P. De Freitas, and N. M. M. Ramos, "Quantifying the Influence of Hygroscopic Materials in the Fluctuation of Relative Humidity in Museums Housed in Old Buildings," *NSB 2014*, pp. 600–607, 2014.

[74] H. Janssen and S. Roels, "The dependable characterisation of the moisture buffer potential of interior elements," *Build. Phys.*, pp. 669–676, 2008.

[75] H. Janssen and S. Roels, "Qualitative and quantitative assessment of interior moisture buffering by enclosures," *Energy Build.*, vol. 41, no. 4, pp. 382–394, 2009.

[76] M. Salonvaara and A. Holm, “Moisture Buffering Effects on Indoor Air Quality — Experimental and Simulation Results,” 2004.

[77] S. Cerolini, M. D. Orazio, C. Di Perna, and A. Stazi, “Moisture buffering capacity of highly absorbing materials,” *Energy Build.*, vol. 41, pp. 164–168, 2009.

[78] K. Svennberg, “Moisture Buffering in the Indoor Environment,” 2006.

[79] L. Fang, G. Clausen, and P. O. Fanger, “Impact of Temperature and Humidity on the Perception of Indoor Air Quality,” *Indoor Air*, pp. 80–90, 1998.

[80] D. Rocha, “Análise das potencialidades de utilização da inércia higroscópica em edifícios (Master’s thesis),” Faculdade de Ciências e Tecnologia - Nova University of Lisbon, 2016.

[81] “Technical data sheet of fermacell Firepanel A1.” .

[82] “Technical data sheet of projected cellulose coating.” .

[83] J. Grilo, “Carcterização de argamassas de cal hidráulica natura NHL3.5 de fabrico nacional |(Master’s thesis),” Faculdade de Ciências e Tecnologia - Nova University of Lisbon, 2013.

[84] “http://www.celenit.com/en/about-us/what-is-celenit/what-is-celenit, visited on 03/02/2017.” .

[85] “Thechnical data sheet of Celenit.”

[86] J. Lima, P. Faria, and A. Santos Silva, “Earthen Plasters Based on Illitic Soils from Barrocal Region of Algarve: Contributions for Building Performance and Sustainability,” *Key Eng. Mater.*, vol. 678, pp. 64–77, 2016.

[87] “Technical data sheet of Aralab FITOCAL 300.” .

[88] H. E. Silva and F. M. A. Henriques, “Manual de caracterização higrotérmica do património cultural: Monitorização, caracterização dos materiais e simulação (documento interno não publicado) Caparica, Portugal: FCT-UNL.” 2017.

[89] “Technical data sheet of KERN PLJ1200-3A.” .

[90] “Thecnical data sheet of AFP Precision Balances - Adam.” .

[91] “Techcnical data sheet of TA35 Thermal Anemometer.” .

[92] *CEN, European Committe for Standarization “EN 1946-1 Thermal performance of building products and components - Specific criteria for assessment of laboratories measuring heat transfer properties - Part 1: Common criteria.”* 1999.

[93] *CEN, European Comitte for Standarization “ EN 1946-3 Thermal performance of building products and components - Specific criteria for the assessment of laboratories measuring heat transfer properties - Part 3 : Measurements by heat flow meter method.”* 1999.

[94] *ISO, International Standard Organization, “ISO 8301 Thermal insulation - Determination of steady-state thermal resistance and related properties - Heat flow meter apparatus.”* 1991.

[95] “ISO, International Standard Organization, ‘ISO 8301 Thermal insulation - Determination of steady-state thermal resistance and related properties - Heat flow meter apparatus - Amendment 1,’” 2010.

[96] J. R. Philip, “The theory of infiltration: 4 sorptivity and algebraic infiltration equations,” *Comonwealth Sci. Ind. Res. Organ.*, vol. 84, no. 3, pp. 257–264, 1956.

[97] I. Langmuir, *Journal of the American Chemical Society*. 1918.

[98] A. W. Lykow, “Transporterscheinugen in kapillarporosen Korpern,” *Akademie-Verlag*, 1958.

[99] F. Hansen, “Coupled Moisture/Heat Transport in Cross Sections of Structures,” *Bet. og Konstr.*, 1985.

[100] H. Hens, *Building Physics Heat, Air and Moisture - Fundamentals and Engineering Method with Examples and Exercises*. 2012.

[101] J. M. P. Q. Delgado, N. M. M. Ramos, and V. P. De Freitas, “Can Moisture Buffer Permormance be Estimated from Sorption Kinetics?,” *J. Build. Phys.*, vol. 29, no. 4, 2005.

[102] S. Lagergren, “Zur Theorie der Sogenannten Adsorption Geloster Stoffe,” *K. Sven. Vetenskapsakademiens Handl.*, vol. 24, no. 4, pp. 1–39, 1898.

[103] I. Langmuir, “The Adsorption of Gases on Plane Surfaces of Glass, Mica and Platinum,” *J. Am. Chem. Soc.*, vol. 40, no. 9, pp. 1361–1403, 1918.

[104] A. Ben Lamine and Y. Bouazra, “Application of statistical thermodynamics to the olfaction mechanism,” *Chem. Senses*, vol. 22, pp. 67–75, 1997.

[105] Y. Ben Torkia, M. Khalfaoui, and A. Ben Lamine, “On the use of the Hill’s model as local isotherm in the interpretation of the behaviour of the adsorption energy distributions,” *J. Appl. Phys.*, vol. 6, no. 3, pp. 62–73, 2014.

[106] C. Chen, “Evaluation of Equilibrium Sorption Isotherm Equations,” *Open Chem. Eng. J.*, vol. 7, pp. 24–44, 2013.

[107] Y. S. Ho and G. Mckay, “Pseudo-second order model for sorption processes,” *Elsevier*, vol. 34, pp. 451–465, 1999.

[108] A. Holm, H. M. Kuenzel, K. Sedlbauer, and F. Bauphysik, “The hygrothermal behaviour of rooms: combining thermal building simulation and hygrothermal envelope calculation,” *Build. Simul.*, pp. 499–506, 2003.

[109] F. Antretter, F. Sauer, T. Schöpfer, and A. Holm, “Validation of a hygorthermal whole building simulation software,” *Build. Simul.*, pp. 1694–1701, 2011.

[110] M. Barclay, N. Holcroft, M. Patten, and A. Shea, “Modelling and testing methods to determine whole building hygrothermal performance with natural fibre building materials,” *Build. Environ.*, 2014.

[111] S. P. Casey, M. R. Hall, S. C. E. Tsang, and M. A. Khan, “Energetic and hygrothermal analysis of a nano-structured material for rapid-response humidity buffering in closed environments,” *Build. Environ.*, vol. 60, pp. 24–36, 2013.

[112] H. E. Silva and F. Henriques, “Análise e classificação microclimática de edifícios históricos: Capela das Albertas, Museu Nacional da Arte Antiga (Lisboa),” *Construção Mag.*, 2017.

[113] *CEN, European Committe for Standarization “EN 15757 Conservation of cultural property. Specifications for temperature and relative humidity to limit climate-induced machanical damage in organic hygroscopic materials.”* 2010.

[114] H. E. Silva and F. M. A. Henriques, “Microclimatic analysis of historic buildings : A new methodology for temperate climates,” *Build. Environ.*, vol. 82, pp. 381–387, 2014.

[115] S. Stadler, “WUFI ® Plus 3.1 Manual,” 2017.